PALLADIUM-CATALYZED ALKOXYCARBONYLATION AND AMINOCARBONYLATION OF TERMINAL ALKYNES: SYNTHESIS AND APPLICATIONS OF α,β-UNSATURATED ESTERS AND AMIDES. COMPUTATIONAL STUDY OF THE REACTION MECHANISM

BY

RAMI SULEIMAN

A Dissertation Presented to the

DEANSHIP OF GRADUATE STUDIES

KING FAHD UNIVERSITY OF PETROLEUM & MINERALS

DHAHRAN, SAUDI ARABIA

In Partial Fulfillment of the

Requirements for the Degree of

DOCTOR OF PHILOSOPHY

In

CHEMISTRY

MARCH 2010

KING FAHD UNIVERSITY OF PETROLEUM & MINERALS

DHAHRAN, SAUDI ARABIA

DEANSHIP OF GRADUATE STUDIES

This dissertation, written by **Mr. RAMI KHALID MOHAMMAD SULEIMAN** under the direction of his dissertation advisor and approved by his thesis committee, has been presented to and accepted by Dean of Graduate Studies, in partial fulfillment of the requirements for the degree of **DOCTOR OF PHILOSOPHY IN CHEMISTRY**.

Dissertation Committee

Prof. Bassam El Ali
Dissertation Advisor

Prof. Shaikh A. Ali
Member

Prof. Basel Abu Sharkh
Member

Dr. Abdullah J. Al-Hamdan
Department Chairman

Dr. Mohammed Fettouhi
Member

Dr. Salam Zummo
Dean of Graduate Studies

Dr. Abdullatif Ibdah
Member

26/4/10
[Date]

Dedicated to Father, Rana, Osama and Raghad

ACKNOWLEDGMENT

Gratitude and praise be to Almighty Allah for making it possible for me to accomplish this work successfully and blessing and peace be upon prophet Mohammad (SAW).

The work enclosed within this dissertation would not have been possible if it were not for my mentor and advisor Prof. Bassam El-Ali, who gave me the seed to propagate this scientific project that has blossomed into a tree of many fruitful ideas to come. In many respects he has taught me more about teaching others, perseverance and an appreciation for homogeneous catalysis. Thanks to prof. El Ali for teaching me more than just chemistry and that great things are accomplished only by the perfection of minor details.

I wish to also thank my dissertation committee members, Prof. S. A. Ali, Prof. B. Abu-Sharkh, Dr. M. B. Fettouhi, and Dr. Abdullatif Ibdah for their constructive contribution toward the success of the work. Also, my deep thanks to Dr. Abdullah Hamdan, the chairman of chemistry department, for his kind professional support. I am highly in debt for all faculty members for showing their concern and help in my studies.

I am grateful for all departmental stuff members for their technical and endless support. I must express my gratitude to my colleague whom I spent with them very nice and priceless times.

A special thank to Dr. Mohammad Semreen, University of Sharja, for his support in one way or another.

I am highly grateful to my parents, brothers and sisters for their deep concern, love and encouragement. I must thank from my deep hart my parents in law family for their continuous support and encouragement before and during my study.

My deep recognition to King Fahd University of Petroleum & Minerals for providing the sponsorship and the material support for my thesis project.

To my wife Rana, thank you for being there when I needed you and when I did not. I cannot really give you the thank you deserve for your selfless sacrifices, and for supporting me in everyway possible.

TABLE OF CONTENTS

Chapter 2

Palladium-DPPB-Borate-Catalyzed Regioselective Synthesis of Cinnamate Esters by Alkoxycarbonylation of Phenylacetylene

Chapter 3

Palladium(II)-Catalyzed Catalytic Aminocarbonylation and Alkoxycarbonylation of Terminal Alkynes: Regioselectivity Controlled by the Nucleophiles

Chapter 4

Palladium-Catalyzed Selective Alkoxycarbonylation of *Gem*-α,β-enamides: A Novel Approach towards new ω-Amido Esters and *N*-Substituted Cyclic Succinimides

Chapter 5

Synthesis, Characterization, and Catalytic Applications of New Binuclear Pd(II) Diimine and Phosphine Mixed-Ligand Complexes

Chapter 6

A DFT Study on the Mechanism of Palladium-Catalyzed Alkoxycarbonylation and Aminocarbonylation of Alkynes: Hydride Versus Alkoxy Pathways

Chapter 7

LIST OF FIGURES

LIST OF TABLES

LIST OF SCHEMES

DISSERTATION ABSTRACT

NAME OF STUDENT: **RAMI KHALID MOHAMMAD SULEIMAN**

TITLE OF STUDY: PALLADIUM-CATALYZED ALKOXYCARBONYLATION AND AMINOCARBONYLATION OF TERMINAL ALKYNES: SYNTHESIS AND APPLICATIONS OF α,β-UNSATURATED ESTERS AND AMIDES. COMPUTATIONAL STUDY OF THE REACTION MECHANISM

MAJOR FIELD: **CHEMISTRY**

DATE OF THE DEGREE: MARCH 2010

Palladium–catalyzed carbonylation reactions, carried out in the presence of various nucleophiles like amines and alcohols, belong to the most widely used homogeneous catalytic reactions in synthetic chemistry. The α,β-unsaturated amides and esters produced from the above reactions are important intermediates in a wide range of organic reactions. In the present study, we have successfully developed a catalyst system for the alkoxycarbonylation of phenylacetylene using palladium-dppb-salicylborate catalyst system with high regioselectivity towards the formation of *trans* isomer under mild reaction conditions. Milder reaction conditions for the alkoxycarbonylation and aminocarbonylation of terminal mono and dialkynes have been obtained using the catalyst system $Pd(OAc)_2$/dppb/*p*-TsOH/CH_3CN/CO in acetonitrile. Results showed significant disparity in the conversion of terminal alkynes and in the selectivity towards the *gem* or *trans* unsaturated esters or amides by changing the type of nucleophile. The catalyst systems have been optimized by screening various reaction parameters (catalyst precursor, ligand, CO pressure, solvent and temperature).

Furthermore, an effective synthesis of mono and dicyclic succinimides has been achieved via palladium-catalyzed alkoxycarbonylation of *gem*-enamides followed by ring closure.

New palladium-binuclear complexes based on chelating diimines and bridging diphosphine or diimine ligands have been successfully synthesized and characterized. The new complexes showed a promising activity in the coupling of arylboronic compounds to various electron-rich and deficient olefins.

We have carried out computational investigation of mechanisms proposed for alkoxycarbonylation and aminocarbonylation reactions in order to account for the interesting activity and regioselectivity of the developed palladium catalyst systems.

DOCTOR OF PHILOSPHY DEGREE
KING FAHD UNIVERSITY OF PETROLEUM & MINERALS
DHAHRAN, SAUDI ARABIA

الخلاصة

الإسم: رامي خالد محمد سليمان

عنـوان الرسـالة: الألكوكسيكاربونيليـشين و الأماينوكاربونيلـشين المحفـز بـالبلاديوم للألكاينـات الطرفية: تصنيع و تطبيقات الإسترات و الأميدات الغير مشبعة و الدراسة الحاسوبية لآلية التفاعل

التخصص: الكيمياء

تاريخ التخرج: آذار 2010

إن تفاعلات الألكوكسيكاربونيليشن و الأمـاينو كاربونيليشن المحفزة بـالبلاديوم التـي تجرى بوجـود الأمينـات و الكحـولات تنتمـي إلـى التفـاعلات المحفـزة المتجانـسة الأوسـع إسـتخداما فـي الكيميـاء التصنيعية، حيث ان الأميدات و الإسترات الناتجة من التفاعلات السابقة هـي وسـائط مهمـة فـي عدد كبير من التفاعلات العضوية.
لقد قمنا في هذه الدراسة بتطوير نظام محفز لتفاعل الالكوكسيكاربونيليشن لمادة فنيل أستيلين مكون من palladium-dppb-salicylborate و يتميز بإنتقائية عالية لإنتاج الإستر الطـولي فـي ظـروف تفاعل معتدلة.
كمـا تـم الحـصول علـى ظـروف معتدلـة جـدا لتفـاعلي الألكوكسيكاربونيليـشن و الأماينوكاربونيليـشن للألكاينات الطرفية باستخدام نظام تحفيز مكـون مـن $Pd(OAc)_2$/dppb/*p*-TsOH/CH_3CN/CO فـي مـذيب الأسيتونايترايل، حيث أظهـرت النتـائج إختلافا واضـحا فـي تحولية الألكاينـات الطرفيـة و انتقائية التفاعلين نحو تكوين إسترات و أميدات طولية و متفرعة عند تغير نـوع النيوكلوفايل . لقد تم تطـوير النظـام المحفز الأكثـر فعاليـة بدراسـة عوامل التفاعل المختلفة (المحفز الإبتدائي، المتصل، ضغط اول أكسيد الكربون، المذيب و درجة الحرارة).
لقـد تـم أيـضا تحـضير مركبـات السكـسينامايد الحلقيـة الأحاديـة و الثنائيـة عـن طريـق تفاعـل الألكوكسيكاربونيليشن المحفز بالبلاديوم للإينياميدات متبوعة بتحلق الناتج.
تم تحضير و وتوصيف معقدات بلاديوم ثنائية النواة جديدة تعتمد علـى متصلات ثنائية الأمين و أخرى جسرية واصلة بين ذرتـي البلاديوم مكونـة من متصلات ثنـائي الفوسفين او ثنـائي الأمين، حيـث أظهـرت المعقـدات الجديـدة فعاليـة مـشجعة فـي تفـاعلات الـربط الكيميـائي بـين مركبـات الأريلبورونيك أسيد مع الألكينات مشبعة و غير مشبعة الإلكترونات.
لقد أجرينـا أبحاثـا حاسـوبية لآليـات التفاعـل المقترحـة لتفـاعلات الألكوكسيكاربونيليـشن و الأمـاينو كاربونيليشن من أجل وصـف سبب الفعاليـة و الإنتقائيـة المميزة لأنظمـة البلاديوم المحفزة التـي تـم تطويرها في هذه الدراسة.

درجة الدكتوراة في الفلسفة

جامعة الملك فهد للبترول و المعادن

الظهران-المملكة العربية السعودية

CHAPTER 1

INTRODUCTION AND LITERATURE REVIEW

1.1 Introduction

Homogeneous catalysis has played an important role in the development of chemical industry, which includes the development of new technologies as well as solving environmental problems. Particularly, the advances in conversion of cheaper feedstock to value-added chemical products, new synthetic routes for pharmaceuticals, fine and specialty chemicals to replace stoichiometric routes, waste minimization, pollutants removal and global preservation, have been significant. Homogeneous catalysis by metal complexes has some unique features of high activity and selectivity at milder operating conditions, which lead to major breakthrough in reactions such as carbonylation, hydroformylation, oxidation, hydrogenation, oligomerization and metathesis etc (1).

Palladium complexes are among the most extensively used in catalysis, and are best known for their excellent performance in C-C (and C-heteroatom) bond forming reactions and are utilized as versatile synthetic tool in many research laboratories (2). Palladium catalyzes efficiently the carbonylation reactions of allene, alkenes and alkynes. The palladium-catalyzed carbonylation of alkynes represents an important and attractive route for the production of α,β-unsaturated carboxylic acids and their derivatives (3). The α,β-unsaturated amides or esters produced from the above reactions are important intermediates in a many industries and can be also employed in a wide range of organic reactions.

1.2 Literature background

The term “carbonylation” was coined by W. Reppe during the thirties and is generally used to refer to those reactions in which CO alone or CO combined with other compounds (especially nucleophiles with mobile H-atom) are introduced into particular substrates (saturated or unsaturated). ‘Carbonylation’, used here as a generic term, includes reactions such as formylation, hydroformylation, carboxylation, and homologation, which involve the introduction of a carbonyl group into an organic substrate. Group VIIIB metals, especially Fe, Co, Ni, in the form of metal carbonyls or other derivatives catalyze these reactions. More recently Ir, Rh, Ru, Os, Pt, and Pd complexes have been widely used as catalysts (4,5).

Carbonylation reactions rank among the most useful transformations homogeneously catalyzed by transition-metal complexes, forming the basis for industrial and laboratory processes currently in practice (6). Some of the initial scientific discoveries in this field gradually evolved into large-scale commercial carbonylation processes. Noteworthy among the commercial carbonylation processes are the ‘oxo’ process (olefin hydroformylation), the Reppe process (hydrocarboxylation of acetylene to acrylic acid) and Monsanto process (carbonylation of methanol to acetic acid) (6-8). These processes are employed worldwide to prepare millions of tones of commodity chemicals each year. In addition, it has been predicted that the importance of carbonylation reactions in the total chemical output will continue to grow as several new carbonylation processes are expected to reach commercialization. The basic reason is that the feedstock i.e. syngas (carbon monoxide & hydrogen) are versatile and inexpensive (7).

The carbonylation of alkenes and alkynes with CO and water is known as hydrocarboxylation reaction. If alcohol is used in place of water it is referred to as hydroesterification. While, addition of CO and amines or CO and thiols to unsaturated compounds are referred to as aminocarbonylation and thiocarbonylation, respectively (4) (Scheme 1.1).

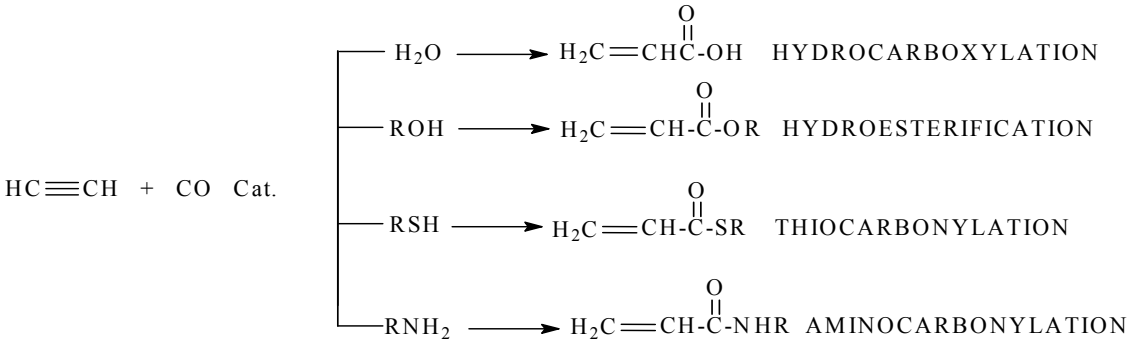

Scheme 1.1. Different carbonylation reactions of alkynes.

1.2.1 Carbonylation of alkenes

The synthesis of carboxylic acids or their ester derivatives, by the reaction of an olefinic substrate with CO and water or alcohol, catalyzed by phosphoric acid or other Lewis acids has been known since 1931 (9); branched aliphatic acids and esters are obtained. In the presence of H_2SO_4, the reaction may be carried out under milder conditions (10). This synthesis, however, has a serious limitation due to the experimental conditions and the complex mixture of products. Much more interesting, is the carbonylation of olefinic substrates conducted in the presence of metal carbonyls or metal compounds which under the reaction conditions may be transformed into metal complexes containing carbonyls groups. This reaction, discovered by Reppe and Kroper around 1940 (11, 12), consists of

the addition of hydrogen and carboxyalkyl, thiocarboxyalkyl, amide, or similar group to an olefinic substrate (eq. 1.1).

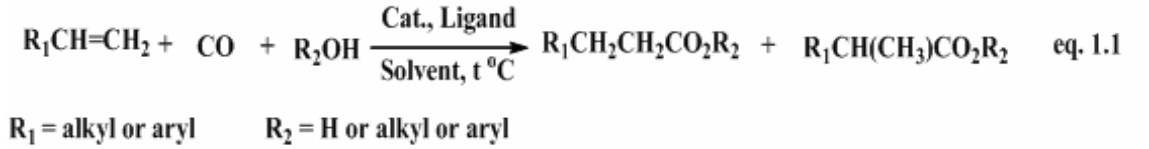

The standard carbonylation catalysts such as $Co_2(CO)_8$ and $Ni(CO)_4$ have been used to prepare fatty-acid esters (13). Other catalysts based on Pd, Pt, Rh, and Ru found widespread use because of their better performance under milder reaction conditions (4,6). Molecules containing both olefinic unsaturations at suitable distance and a group having active hydrogen (**1.1**) may react with CO to give cyclic compounds (**1.2**) (14-16) (eq. 1.2).

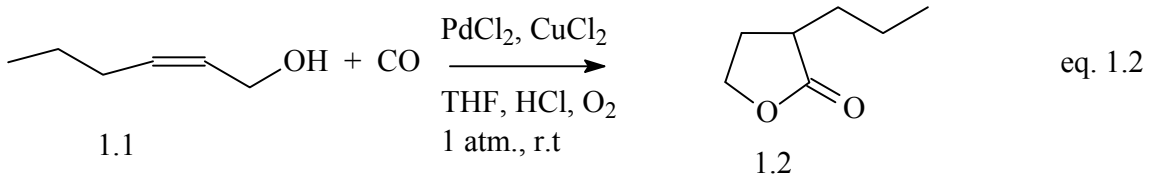

1.1 1.2

The regioselectivity of linear versus branched products is an important issue, because mixtures of isomeric carboxylic acids or esters are usually obtained, owing to Markovnikov and anti-Markovnikov addition of the metal hydride to the alkene. In fatty acids synthesis linear isomer is preferred (15) **(1.4)** (eq. 1.3), whereas the converse is the case in carbonylation of pro-chiral styrene related compounds to give chiral arylpropionic acids **(1.5)**, an important class of non-steroidal anti-inflammatory agents (17-20). The regioselectivity in palladium-catalyzed reactions, involving phosphine ligands, are largely controlled by the variation of the ligands (eq. 1.3). PPh_3 promotes

preferential carbonylation of alkenes toward the branched acid **(1.3)**, whereas bidentate phosphine ligands give linear products **(1.4)** overwhelmingly (21-24).

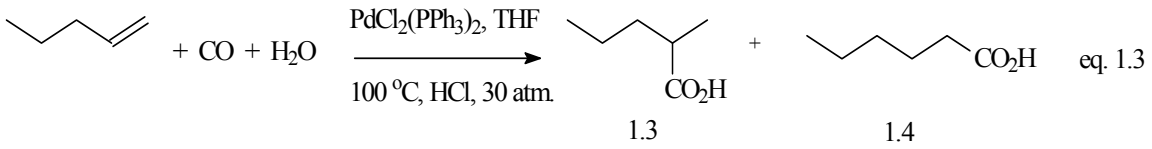

1.3 1.4 eq. 1.3

The steric and electronic effects of the chiral phosphine ligands exert a dramatic influence on the yield and selectivity of the reaction. In fact, the hydrocarboxylation reaction of 6-methoxynaphthalene under mild experimental conditions in the presence of (S)-(+)-binaphthyl-2,2'-diyl hydrogen phosphate (BNPPA) gave optically active naproxen **(1.5)** (72-91% ee) in good chemical yields (46-71 %) (eq. 1.4) (19,25).

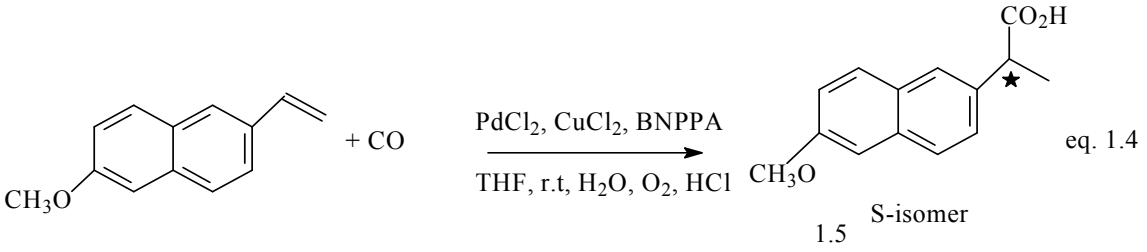

1.5 S-isomer eq. 1.4

The development of two-phase catalysis processes, where the catalyst can be separated from the products and recycled, is an important step toward economical and friendly environmental processes. For example, the catalytic system composed of water-soluble triphenylphosphine trisulfonate (TPPTS), Pd complex as a catalyst, and acid as a promoter (26) gave very high yield and selectivity of carboxylic acids (eq. 1.5).

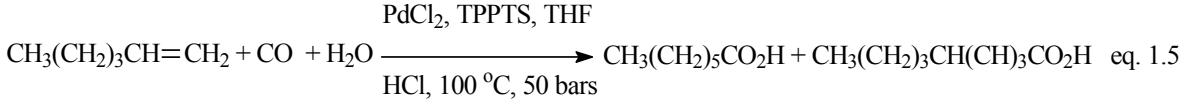

eq. 1.5

The methoxycarbonylation of styrene has been studied using $Pd(OAc)_2$/L/acid catalytic systems with L being chiral ferrocene- and biphosphole-based ligands. Good activities are obtained in mild conditions. The Chemoselectivities and regioselectivities (up to 98 % in favor of the branched isomer) are excellent but the enantioselectivities remain moderate (ee up to 17 %) (27). Very recently, hydroesterfication and hydroformylation-acetalization of 1-hexene in ethanol catalyzed by rhodium complexes immobilized on poly(4-vinylpyridine) were achieved. The reaction products distribution depends on the nature of the coordinate amine to the rhodium center (28). Recently, Alper et al. reported a highly regioselective anti-Markovnikov palladium-borate-catalyzed methoxycarbonylation of terminal alkyl and aryl olefins (eq. 1.6). Very good yields (up to quantitative) and excellent regioselectivities towards the linear ester were obtained (29).

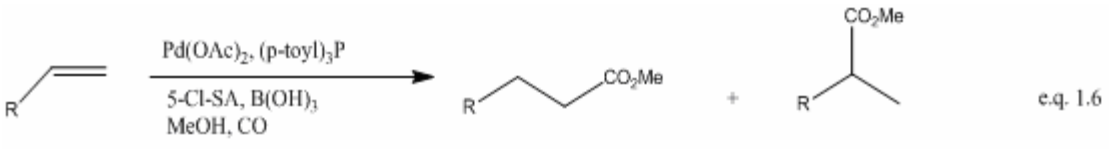

e.q. 1.6

Linear esters were also obtained as major product when [BMM][PF_6] ionic liquid was applied in the palladium-catalyzed hydroalkoxycarbonylation of styrene (30).

1.2.2 Carbonylation of alkynes

The high reactivity of the acetylenic compounds with CO in the presence of transition metals, particularly group VIII, including the great industrial importance of the products obtained, led to a significant scientific and industrial activity in this field since these discoveries. The scope of the reaction of the carbonylation of alkynes was extended to

obtain a large variety of derivatives of mono- and dicarboxylic acids, keto acids, esters of aldehydo-acids, cyclic ketenes and hydroquinones (5).

The first research on addition of CO to acetylene in the presence of transition metal compounds or metal carbonyls was carried out in Germany between 1938 and 1940 by two different industrial research groups, working under the supervision of Reppe (31) and Roelen (32). Reppe was investigating new aspects of acetylene chemistry when he reacted acetylene with $Ni(CO)_4$ and water (eq. 1.7) and obtained acrylic acid (eq. 1.8) instead of the expected aldehydes. As a logical extension, Roelen was investigating the hydroformylation of olefins in the presence of cobalt catalysts. He tried to carry out the hydroformylation of acetylene. He obtained, however, high-molecular-weight products containing only traces of acrolein, which was the intended product (31, 32).

$$CH{\equiv}CH + CO \xrightarrow{Ni(CO)_4} CH_2{=}CH{-}CHO \qquad \text{eq. 1.7}$$

$$CH{\equiv}CH + CO \xrightarrow[H_2O]{Ni(CO)_4} CH_2{=}CHCO_2H \qquad \text{eq. 1.8}$$

The most widely used catalysts for commercial alkynes carbonylation were the $Ni(CO)_4$ and $Co_2(CO)_8$, or their precursors. In general, these catalytic systems require high temperature (100-200 ^oC) and pressure (30-200 atm); milder conditions (25-100 ^oC, 1-10 atm) usually were used in stoichiometric reactions (33). Attempts to decrease the $Ni(CO)_4$ consumption have led to "semi-catalytic" processes in which CO gas was used in addition to the $Ni(CO)_4$ (5). An important disadvantage of using this catalyst was the formation of the volatile and highly toxic $Ni(CO)_4$ during the reaction. PPh_3 ligand, has

been used to counteract this problem (34), but the presence of the ligand reduced the catalytic activity.

Other cobalt compounds were used in the stoichiometric and catalytic carbonylation of alkynes under milder conditions. In general, however, the stoichiometric carbonylation of alkynes with $Co_2(CO)_8$ and $HCo(CO)_4$ is rather unsuccessful, because these compounds form very stable and unreactive complexes with alkynes (5). In contrast, under more severe conditions (100-200 ^oC, 200-300 atm. of CO), cobalt compounds show high catalytic activity for carbonylation of alkynes.

The reactivity of iron, ruthenium, rhodium and osmium have not yet been investigated systematically, but the existing reports indicate that products such as quinines, hydroquinones (eq. 1.9) and lactones are formed, in the reactions of these metals with alkynes. In general, the catalytic reactions are sluggish and the product distributions are poor (5).

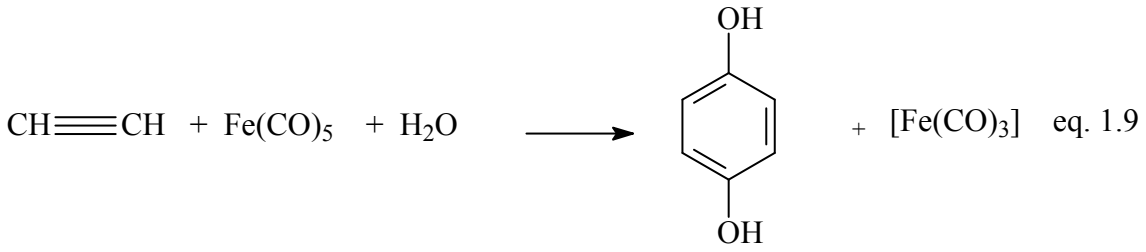

eq. 1.9

Synthesis of Maleimides **(1.6)** was recently achieved by the Rh-Catalyzed carbonylation of alkynes with pyridin-2-ylmethylamine (35).

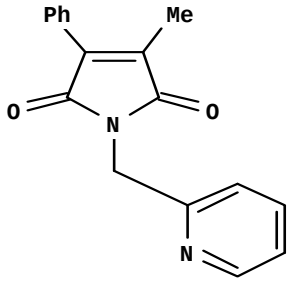

1.6

The use of palladium-catalysts in carbonylation of alkynes was first reported in 1962 (36,37). Tsuji and co-worker were the first to study the carbonylation of alkynes with palladium complexes involving the catalytic system $PdCl_2/CuCl_2/HCl/O_2$ to produce mainly products of dicarbonylation (eq. 1.10) (38-42).

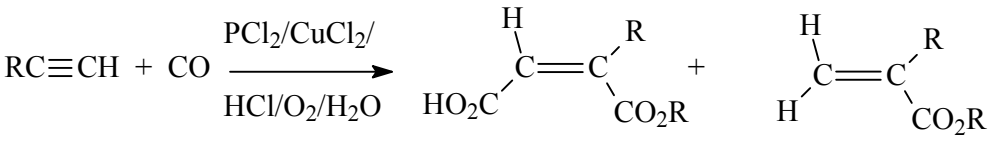

eq. 1.10

R = alkyl or aryl

(Z)-3-Haloacrylates were also synthesized successfully via palladium-catalyzed carbonylation of terminal alkynes in the presence of a catalytic amount of PdX_2 and equivalent amount of CuX_2 (X = Cl and Br) (43).

1.2.3 Thiocarbonylation of alkynes

The transition-metal-catalyzed carbonylation of organic sulfur compounds has been the subject of few investigations (44). It was previously considered that many transition metals, including palladium, have strong affinity to thiols, which make the catalytic reactions ineffective. A series of transition-metal-catalyzed addition and carbonylation/addition reactions of organic disulfides and thiols to acetylenes has been

developed (45); $Pd(PPh_3)_4$ and $PdCl_2(PPh_3)_2$ gave a complex mixture of products (eq. 1.11) in carbonylative addition of thiophenol with 1-octyne (46).

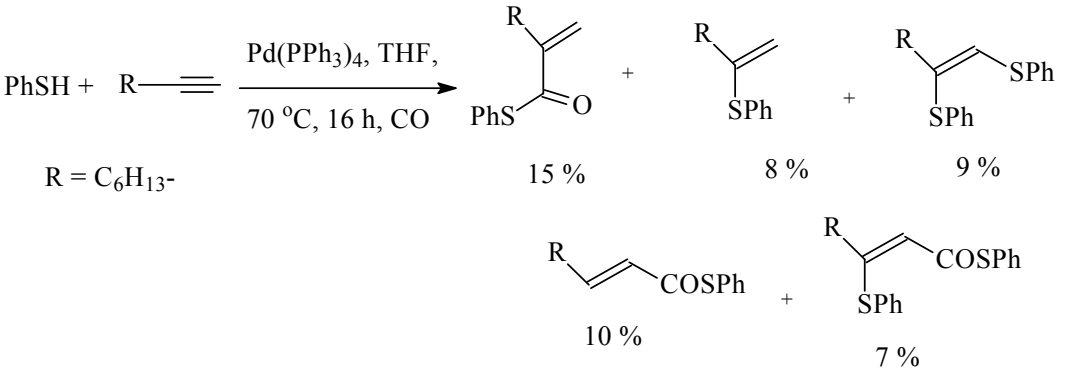

eq. 1.11

$Pt(PPh_3)_4$ gave predominately branched isomer thioester *via* carbonylation acetylene with benzothiol (47). Alper and coworkers have introduced new interesting methods of palladium-catalyzed thiocarbonylation of propargylic alcohols (48) (eq. 1.12), allylic alcohols (49) allenes (50), and enynes (51).

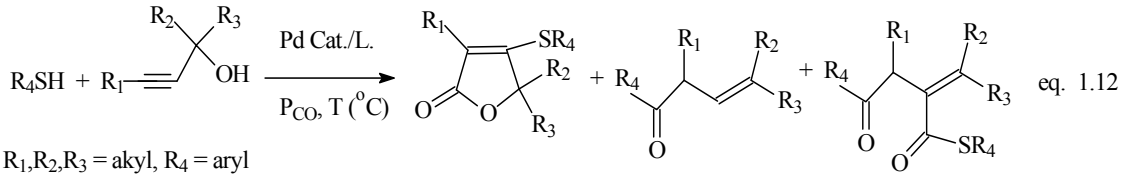

eq. 1.12

The control of the regioselective thiocarbonylation of RC≡CH [R = Pr, pentyl, Me_3C, $(CH_2)_3NC$, Ph] with 4-$R_1C_6H_4SH$ (R1 = H, Me) was successfully achieved by using $Pd(OAc)_2$ and 1,4-bis(diphenylphosphino)butane (dppb) or 1,3-bis(diphenylphosphino)propane (dppp) as catalyst systems. The formation of the corresponding thioesters **1.7** and **1.8** depends mainly on the type of ligand (dppp or dppb) and the type of solvent (THF or CH_2Cl_2) under CO/H^+ or syngas mixture (52) (eq. 1.13).

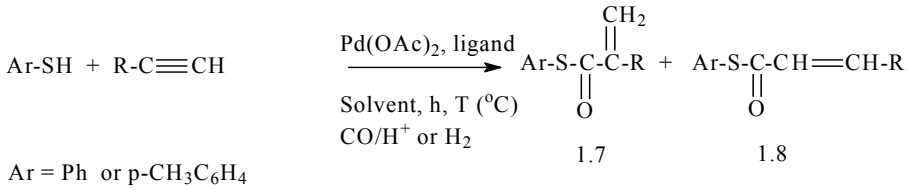

eq. 1.13

1.2.4 Aminocarbonylation of alkynes

Reppe was the first to synthesize substituted acrylamides from acetylene and various amines in the presence of $Ni(CO)_4$. He prepared many acrylamides by reacting acetylene or phenyl acetylene with carbon monoxide in the presence of primary or secondary amines, aniline, urea, pyrolidone or acetamide. Stoichiometric quantities of $Ni(CO)_4$ were employed along with polymerization inhibitors such as hydroquinine (53). Similarly, the use of nickel halides as catalyst has also been reported in xylene or benzene as a solvent at 100-190 ^oC to give isolated yield of amides ranging between 20-50 % (54) (eq. 1.14).

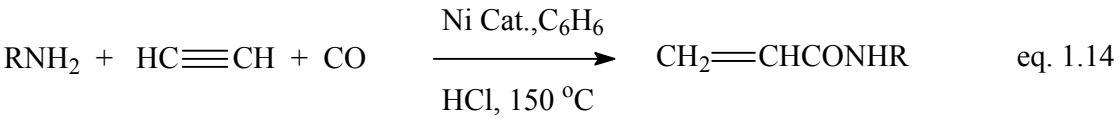

eq. 1.14

Naher et al. reported in 1956 the first semi-catalytic synthesis of acrylamides. They reacted acetylene and $Ni(CO)_4$ in acrylic acid and then successively added CO, HCl, and excess ammonia, at 50-90 ^oC (55). The highest yields were obtained with aniline and secondary amines; however, with primary amines, secondary reactions sometimes occurred to yield bisacryloylamines (eq.1.15).

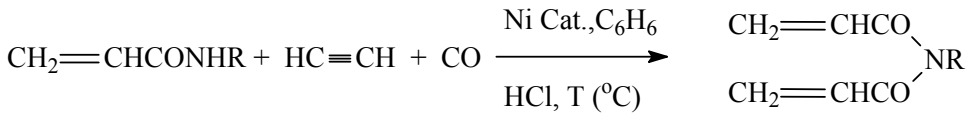

eq. 1.15

Acetylene reacted with diethylamine to form succinic acid and diethyl acrylamide with 12 % and 66 % yield, respectively, by using $Ni(CN)_2$ catalyst. $Co_2(CO)_8$ was found to catalyze the reaction of aniline, CO and acetylene to giving succinic acid dianiline **(1.9)** (56) (eq. 1.16).

$$CH{\equiv}CH + 2PhNH_2 + 2CO \xrightarrow[\text{Tol. T } (^oC)]{Co_2(CO)_8} \underset{\textbf{1.9}}{PhNHCOCH_2CH_2CONHPh} \quad \text{eq. 1.16}$$

Palladium-complexes were also used in the synthesis of 2-substituted acrylamides *via* carbonylation of various terminal alkynes with diethyl amine in the presence of organic iodides or HI salt (57). Similarly, palladium-catalyzed carbonylation of allylamines **(1.10)** under CO (50 atm) at 110 ^oC proceeded efficiently to give the corresponding β,γ-unsaturated amides **(1.11)**. The carbonylation occurred at the less substituted carbon of the allyl units to give linear amides with high regioselectivity (58) (eq. 1.17).

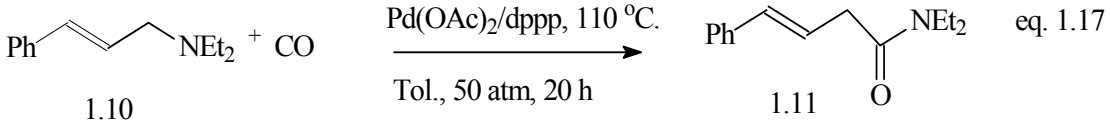

1.10 1.11 eq. 1.17

The selective synthesis of α,β-unsaturated amides **(1.13)** has been achieved via palladium (0)-catalyzed insertion of carbon monoxide into an unactivated carbon-nitrogen bond of propargylamines (52) **(1.12)** (eq. 1.18) and 2,3- dienylamines (60).

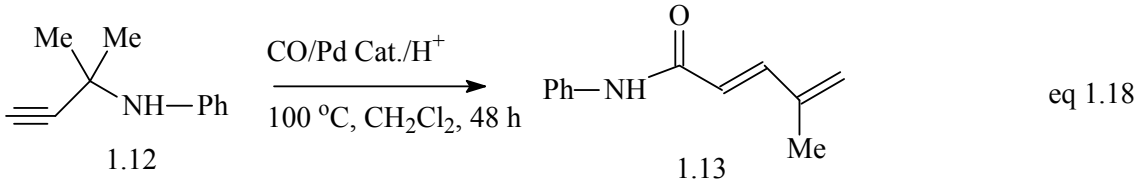

1.12 1.13 eq 1.18

Gem-α,β-unsaturated amides (**1.14**) were prepared as major isomers (82%) by regioselective carbonylative addition. of alkyl alkynes, to anilines, in the presence of $Pd(OAc)_2$/1,3-bis(diphenylphosphino)propane/p-toluenesulfonic acid/CO as the catalytic system. However, the reaction catalyzed by $Pd(OAc)_2$/1,4-bis(diphenylphosphino)butane/H_2/ CO in CH_2Cl_2 as a solvent affords *trans*-α,β-unsaturated amides, (**1.15**) as the major isomer (82 %) (3,61,62) (eq. 1.19).

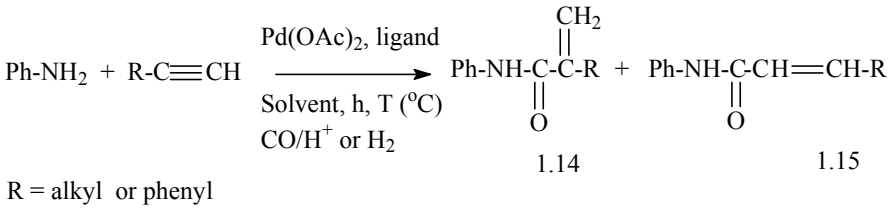

eq. 1.19

The aminocarbonylation of phenylacetylene has been studied in the presence of the catalytic system formed by palladium acetate in combination with (2-pyridyl)diphenylphosphine and methanesulfonic acid. The catalytic activity is strongly influenced by the nature of the amine. Good reaction rates are achieved using amines of low basicity such as aniline. The solvent influences both the activity and the selectivity of the catalyst. The highest reaction rates accompanied by complete regioselectivity towards the branched amide are obtained working in dichloromethane/N-methylpyrrolidinone mixtures. Also the acid to palladium molar ratio and the P(CO) affect to a lower extent the process. The highest catalyst activity is obtained operating at a methanesulfonic acid/Pd molar ratio of 30:1 and at P(CO) = 20 atm (63).

Very recently, Park et al reported the cobalt-rhodium heterobimetallic nanoparticle-catalyzed aminocarbonylation of internal alkynes (eq. 1.20) (64).

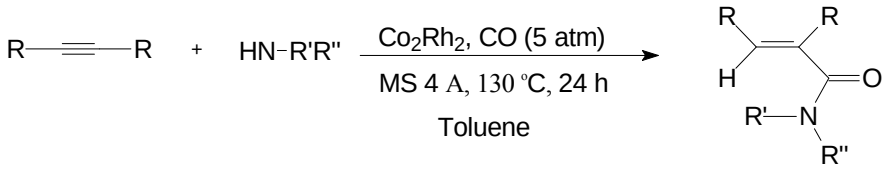

eq. 1.20

Recently, Alper et al. reported the $Pd(OAc)_2$/dppp-catalyzed aminocarbonylation of alkynes with amines in ionic liquid [bmim][Tf_2N] under mild conditions. However, their catalytic system is effective in the presence of relatively high CO pressure (200 psi) (eq. 1.21) (65).

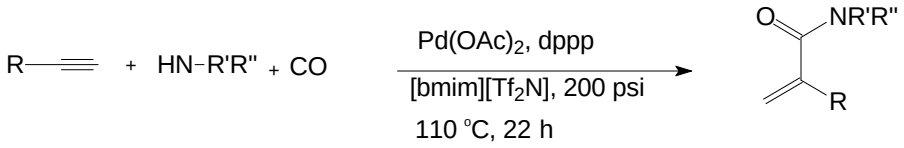

eq. 1.21

1.2.5 Hydrocarbonylation of alkynes

The synthesis of α,β-unsaturated acids is one of the most important of the acetylene carbonylation reactions and it has found practical application in laboratory and industrial scale. Unsubstituted and substituted acrylic and succinic acids are the main products prepared from acetylenic substrates, CO, and water; moreover, other mono- and polycarboxylic acids were obtained in smaller amount (31, 32). The reactions can be carried out either at 90-200 ^oC under CO pressure (30-200 atm) in the presence of metal carbonyl (group VIII), or milder conditions with stoichiometric amount of $Ni(CO)_4$ (5).

Most of the hydrocarboxylation reactions were carried out in acidic medium; however, Sternberg and coworkers reported the hydrocarboxylation of diphenylacetylene in alkaline medium using $Ni(CO)_4$ (66). Alkynes are hydrocarboxylated with formic acid in the presence of $Pd(OAc)_2$ and suitable phosphine ligand to give both linear and branched unsaturated carboxylic acids (eq. 1.22).

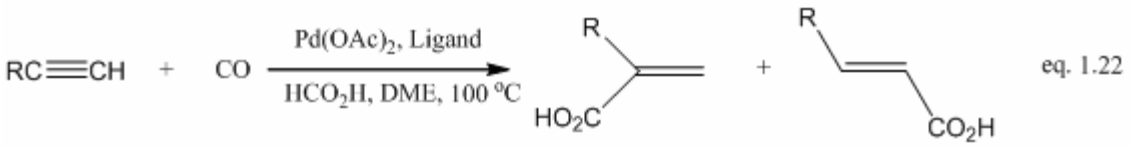

eq. 1.22

The reagent generated in situ in THF was used also for the regio and stereoselective hydrocarboxylation of terminal and internal alkynes (67).

In hydrocarboxylation of substituted diphenylacetylene, electron-donating substituents (methoxy, methyl, etc) in para-position favored the carbonylation of the acetylenic carbon atom adjacent to the *para*-substituent (eq. 1.23), opposite behavior was observed with electron-withdrawing groups (Cl, NO_2, etc). The presence of a substituent in the *ortho*-position induces carbonylation of the carbon adjacent to the substituted phenyl group (4,6-8,68).

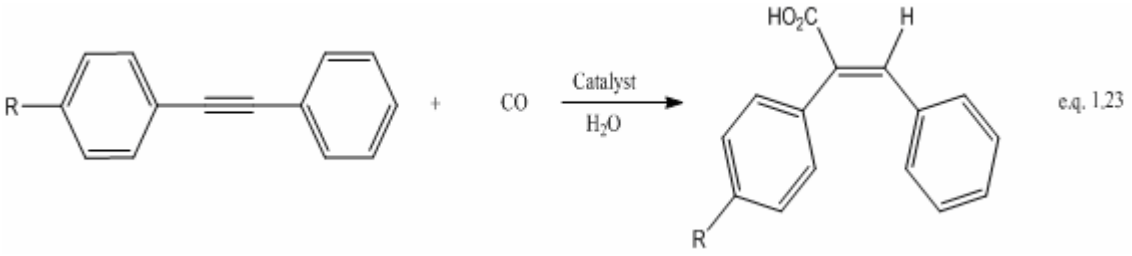

eq. 1.23

Anomalous results occur when hydrogen of the acetylenic carbon is replaced by a halogen **(1.16)** and propargylic halides **(1.17)**. The former gave hydrocarbons (eq. 1.24), whereas the later gave allenic acids **(1.18)** (eq. 1.25) (69). Cylocarbonylation of unsaturated alcohols, amines, and other suitable substrates, produce lactones, lactams or other cyclic compounds (70).

$$2CH_3C{\equiv}CI + 2Ni(CO)_4 + 2AcOH \longrightarrow 2CH_3C{\equiv}CH + NiI_2 + Ni(OAc)_2 + 8CO$$

1.16 eq. 1.24

$$HC{\equiv}CCH_2Cl + H_2O \xrightarrow[-HCl]{Ni(CO)_4} CH_2{=}C{=}CHCOOH$$

1.17 1.18 eq. 1.25

Yamamato et al. achieved the suppression of β-hydride elimination in the intramolecular hydrocarboxylation of alkynes leading to the formation of lactones (71).

1.2.6 Alkoxycarbonylation of alkynes

The transition-metal catalyzed carbonylation of alkynes known since the pioneering work of Reppe has been optimized for nickel carbonyls and variety of cobalt and iron carbonyl. Platinum complexes needed $SnCl_2$ as a promoter. Palladium-catalyzed hydroesterification of 1-alkynes normally gives rise to linear and branched α,β-unsaturated esters. The ratio depends on the reaction conditions employed (72) (eq. 1.26).

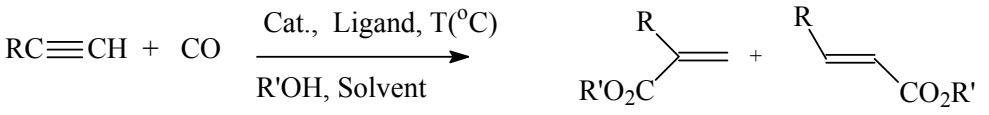

eq 1.26

R' = aryl, Ph, alkyl. Pd = $Pd(PPh_3)_4$ or $Pd(OAc)_2$/dppf

Usually, the regioselectivity for the formation of branched (acrylates) has been observed with the system comprising of palladium black and HI in the hydroesterification of phenylacetylene and propyne to afford the branched esters selectively (73). Similarly, the regioselective hydroesterification of terminal alkynes catalyzed by $Pd(dba)_2$/dppb gives branched esters (74), and the reaction occurred well even with tertiary alcohols. Aryl- and alkyl-acetylenes are carbonylated in the presence of $Pd(PPh_3)_4$ or $Pd(OAc)_2$/dppf using phenol as nucleophile to give branched esters in good selectivity and yield (75).

The hydroesterification of terminal alkynes with 1-butanol by the catalytic system $Pd(dba)_2/PPh_3$/*p*-TsOH also proceeds smoothly under the normal pressure of CO to afford branched esters selectively (76). The regioselective hydroesterification of alkynes and alkynols **(1.19)** using formate esters catalyzed by $Pd(OAc)_2$/dppb/ PPh_3/P-TsOH

have been reported (77) (eq. 1.27). $Pd(OAc)_2/PPh_2Py/MeSO_3H$ gives very active system, which catalyzes the hydroesterification of propyne with excellent selectivity toward branched ester (99.95 %) (78).

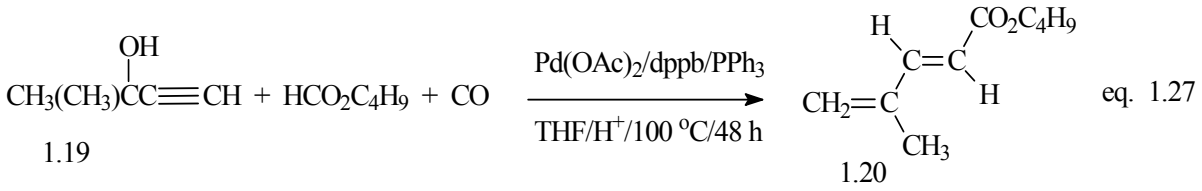

1.19 1.20 eq. 1.27

On the other hand, different catalytic systems capable of giving selectively the linear esters have been reported. For instance, Knifton reported the monophosphine-stabilized Pd(II)/Sn(II) system which catalyzed the hydroesterification of 1-heptyne at 80 °C and 240 atm with 81 % selectivity for the linear ester and 65 % combined yield (79). Thus, $Pd(dba)_2$/dppb catalyzed the regioselective conversion of terminal alkynes and formate esters into linear α,β-unsaturated esters (eq. 1.28) at 100 °C under CO pressure of 80 atm (80).

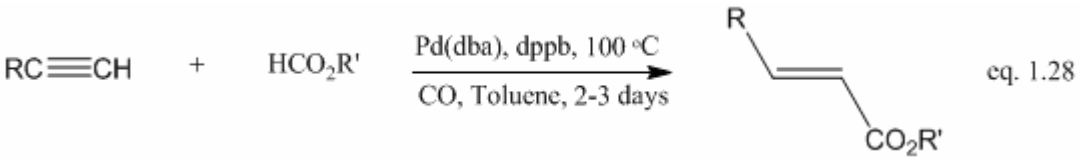

eq. 1.28

Similarly, $PtCl_2$(dppb) with $SnCl_2$ as a promoter were reported to give the linear isomer as a major product, however, the chemoselectivity of the reaction was poor due to the formation of high molecular mass by-products, and to partial polymerization of both substrate and carbonylation products (81).

Pd(II) regioselectively catalyzes the hydroesterification of terminal alkynes under syngas forming α,β-unsaturated esters in excellent yields under neutral conditions. A high selectivity for linear esters was obtained with the catalytic system that includes Pd(II),

1,4-bis(diphenylphosphino)butane (dppb), and CO/H_2 in CH_2Cl_2 as a solvent. The control of the regioselectivity depends strongly upon the type of ligand, the solvent, and the use of the syngas mixture (82).

Palladium complexes of 2-pyridyldiphenylphosphine anchored on polystyrene, poly(methylmethacrylate) and styrene-methylmethacrylate copolymer form highly active heterogeneous catalysts for the alkoxycarbonylation of terminal alkynes with activities approaching those obtained under homogeneous conditions (83).

1.2.7 Conventional methods for the synthesis of unsaturated amides

The classical synthesis of 2-substituted acrylamides, important intermediates for polymer synthesis (84), was mostly achieved by reacting substituted amines (or derivatives of aniline or acrylonitriles) (85) with acryloyl chlorides or substituted acrylic acids (86) (Scheme 1.2).

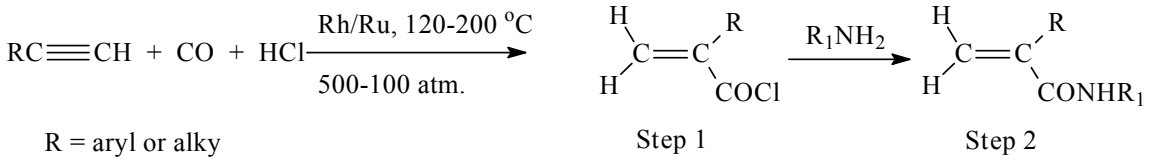

Scheme 1.2. Conventional method for the synthesis of unsaturated amides.

While α,β-unsaturated amides could be synthesized by the olefination of aldehyde with carbamidomethylene triphenylphosphorane **(1.21)** (87) (eq. 1.29).

$$PhCHO + \underset{\mathbf{1.21}}{Ph_3P{=}CHCONH_2} \longrightarrow \underset{\mathbf{1.22}}{PhCH{=}CHCONH_2} + Ph_3PO \qquad \text{eq. 1.29}$$

1.3 Objectives of this work

- To develop a catalyst system for the alkoxycarbonylation of terminal alkynes using various alcohols affording the *trans* α,β-unsaturated esters in high conversions and regioselectivities under mild reaction conditions.
- To develop a catalyst system for the aminocarbonylation of terminal alkynes using alkyl amines yielding the *gem* and *trans* α,β-unsaturated amides in high conversions and total control of regioselectivity under mild reaction conditions.
- To apply the optimal reaction conditions of the alkoxycarbonylation and aminocarbonylation catalyst systems on the carbonylation of di-acetylenes.
- To employ the products of the alkoxycarbonylation and aminocarbonylation reactions as substrates in alkoxycarbonylation reactions to produce ω-amido esters.
- To synthesize new palladium(II)-binuclear complexes based on chelating diimines ligands and bridging diphosphine or diimine ligands. The catalytic activity of the new complexes will be tested in the reaction of coupling of olefins.
- To address the origin of the activity and regioselectivity of the alkoxycarbonylation and aminocarbonylation reactions by carrying out a full DFT computational study on the proposed catalytic cycles of the above mentioned two reactions.

CHAPTER 2

PALLADIUM-DPPB-BORATE-CATALYZED REGIOSELECTIVE SYNTHESIS OF CINNAMATE ESTERS BY ALKOXYCARBONYLATION OF PHENYLACETYLENE

2.1 Introduction

The synthesis of carboxylic esters from easily available starting materials is one of the basic reactions in synthetic chemistry. The use of carbon monoxide as a 'carboxyl-source' in palladium-catalyzed hydroalkoxycarbonylation reaction is a widely known methodology for the synthesis of esters (88,89). Cinnamic acid and its derivatives are important intermediates for the production of pharmaceuticals, fragrances, light-sensitive, electrically conductive materials and agrochemicals (90). Cinnamate esters are made conventionally through Claisen condensation from benzaldehyde and alkylacetate in the presence of sodium alkoxide (91) or by esterification of cinnamic acid (92), or by using palladium acetate-tertiary phosphine as a catalyst in the reaction of phenyl bromide and an alkyl acrylate (93).

Many publications and patents disclose oxidative carbonylation of olefins to α,β-unsaturated esters by reacting an olefin with carbon monoxide, oxygen, and an alcohol in the presence of palladium and copper salts (90,94-96). The disadvantages of these methods are a large excess of oxidant (copper (II) salt) (97), and lack of selectivity due to many side products (90).

Alkoxycarbonylation of phenylacetylene with alcohols normally gives *gem*- and *trans*-α,β-unsaturated esters (**3** and **4)** (Equation 2.1). The ratio of these products strongly depends on the catalytic system and the reaction conditions employed (72,76,81,82). The regioselective synthesis of the *gem*-α,β-unsaturated ester **3** has been achieved by various methods (73,74,76). However, there is only one report that describes the regioselective alkoxycarbonylation of phenylacetylene into *trans*-α,β-unsaturated esters (89 %) using the cationic palladium complex [(Pd(dppf)(PhCN)]BF_4 (72).

The recent report on palladium-borate-catalyzed methoxycarbonylation of alkenes (98) encouraged us to investigate in this chapter the effect of salicylborate on the one step synthesis of cinnamic acid esters by palladium catalyzed regioselective alkoxycarbonylation of phenylacetylene (Equation 2.1).

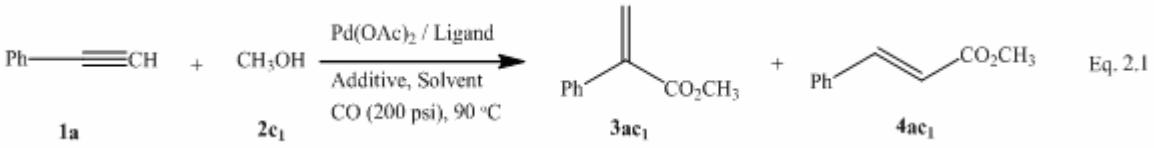

2.2 Results and discussion

The regioselective synthesis of *gem*- or *trans*-α,β-unsaturated ester was achieved by the direct carbonylation of phenylacetylene with methanol catalyzed by palladium (II) in the presence of a diphosphine ligand and suitable additives. The reaction conditions were optimized and the effect of various reaction parameters on the activity and selectivity were determined.

2.2.1 Effect of the type of palladium complex

The activity and the selectivity of various palladium catalysts and their effects on the selectivity of the catalytic alkoxycarbonylation of phenylacetylene with methanol were studied and the results are summarized in Table 2.1. The reaction is carried out by adding the required amount of the palladium complex, dppb, salicylic acid, boric acid and methanol in 10 ml acetonitrile under CO (200 psi) at 90 ^{o}C for 3 h. Conversions higher than 96 % were obtained with $Pd(OAc)_2$, $Pd(NO_3)_2$, $PdSO_4$ and Pd/C. However, palladium catalysts containing chloride ions gave no products under the reaction conditions, whereas $Pd(CN)_2$ gave only 12 %. It seems that the presence of ligands having higher binding ability such as chloride (Table 2.1, entries 6-8) reduces the availability of the coordination sites around palladium, hence leading to lower catalytic activity (99,100). This is probably related to the strong interaction of the chloride ion with the active center compared to the relatively easy replacement of NO_3^-, SO_4^{2-} and OAc^- anions by the bidentate phosphine ligand. A salicylborate complex (BSA) is probably formed in-situ between boric and salicyclic acid (Equation 2.2) (98).

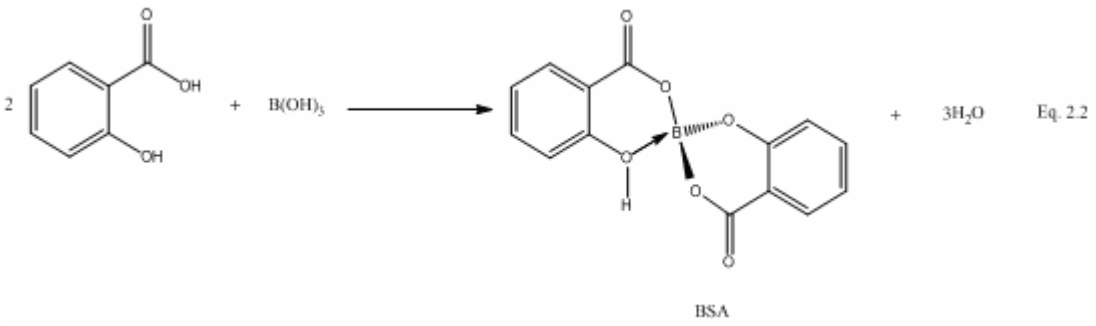

Table 2.1. Alkoxycarbonylation of phenylacetylene by [Pd] / dppb / BSA.

Effect of the type of palladium catalyst.[a]

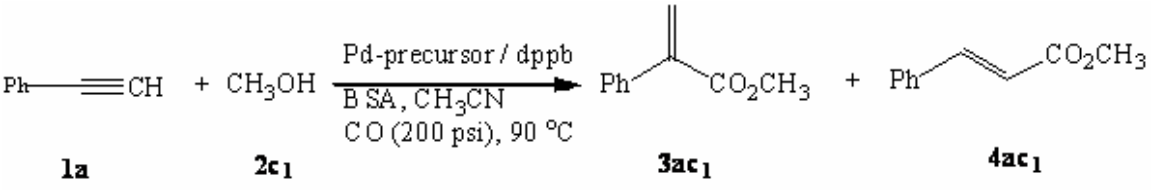

Entry	Palladium Catalyst	Conversion[b] (%)	$4ac_1$ / $3ac_1$[c] (%)
1	$Pd(OAc)_2$	99	92 / 8
2	$Pd(NO_3)_2$	99	84 / 16
3	$PdSO_4$	98	91 / 9
4	Pd/C (5%)	97	90 / 10
5	$Pd(CN)_2$	12	97 / 3
6	$PdCl_2$	Traces	-
7	$Pd(PhCN)_2Cl_2$	0	-
8	$Pd(PPh_3)_2Cl_2$	0	-

a. Reaction conditions: [Pd] (0.02 mmol), dppb (0.08 mmol), phenylacetylene (2.0 mmol), $B(OH)_3$ (0.30 mmol); salicylic acid (0.60 mmol), methanol (8.0 mmol), CH_3CN (10.0 ml), CO (200 psi), 90 ^oC, 3 h.

b. Determined by GC.

c. Determined by GC and ^1H NMR.

2.2.2 Effect of the type of ligand

The effect of the type of ligand on the conversion and the selectivity toward both *trans*- and *gem*-α,β-unsaturated ester were investigated. Different bidentate phosphine ligands with wide range of bite angles and also monodentate phosphine ligands were used in the study. The results, summarized in the Table 2.2, showed an increase in the conversion of phenylacetylene and in the selectivity toward *trans*-α,β-unsaturated ester (methyl cinnamate) with the increase in the bite angle of the ligands. A correlation between diphosphine ligand bite angle, rate and selectivity has been observed. Dppe, [1,2-bis(diphenylphosphino)ethane], with the bite angle of 85^{o} gave only 3 % conversion of phenylacetylene into mainly styrene, while dppf, [1,1'-bis-(diphenylphosphino)ferrocene], and dppp, [1,3-bis(diphenylphosphino)propane], with bite angles 96^{o} and 91^{o} gave conversions of 99 % and 88 % and selectivities in the *trans* isomer **4** of 86 % and 76 %, respectively. A further increase in the bite angle to 98^{o} in dppb, [1,4-bis(diphenylphosphino)butane], led to a total conversion and a selectivity of 92 % in methyl cinnamate. The only exception was observed with BINAP, [2,2'-bis(diphenylphosphino)methyl)1,1'-binaphthyl], and BIPHEN, [2,2'-bis-(diphenylphosphino)methyl)1,1'-biphenyl], which is probably related to the narrow flexibility range and more rigid backbone that reduces the range of bite angle (61). A similar correlation between the increase in bite angles of diphosphine ligands and the rate or selectivity were also reported in the hydrocarboxylation of styrene (101) and carbonylative coupling of aniline with 1-heptyne (61).

The major reasons for these variations in the conversion and selectivity toward the *trans* isomer **4** are related to both steric and electronic effects of the ligands, with the steric

effect to be the major determinant in this catalytic system. The steric nature of the catalytic intermediate ensures that the hydropalladation process exhibits high regioselectivity, resulting in *cis*-addition of Pd complex to a less hindered carbon atom, which finally yields the *trans* isomer **4**. With dppp and dppb, the organic backbone is bent out of the plane of coordination and that in contrast, a skew conformation observed for dppe. In complexes with dppp and dppb, the phenyl groups can bend away from the remaining two coordination sites (102,103). Flexible backbones also impose low-energy barriers for the variation of the P-Pd-P angle and Pd-P distances. Moreover, theoretical calculations indicate such flexibility may enhance migration reactions (104,105).

Extended Huckel calculations indicate that in the diphosphine complexes with small ligand bite angles, the electron density is shifted to the hydride ligand. Therefore, the increase of the bite angle of the ligand increases the hydride ligand acidity, hence the basicity of the following ligands increases in the order: dppe > dppp > dppb. This order suggests a possible reason for the reduced activity of dppe (106).

It was suggested that availability of two coordination sites is crucial to the possible formation of active cationic palladium complex in the alkoxycarbonylation of phenylacetylene (**1a**) (107). Another key to the formation of *trans* isomer may be the ability of dppb to coordinate to palladium through one or both phosphine atoms depending on the circumstances inferring the result that dppb is effective, whereas dppe is almost ineffective for this carbonylation process (108-110).

Basic monophosphine ligand such as PBu_3 show less catalytic activity with 11 % conversion and 80 % selectivity in *gem* isomer **3** (Table 2.2, entry 7).

Table 2.2. Alkoxycarbonylation of phenylacetylene by $Pd(OAc)_2$ / ligand / BSA. Effect of the type of ligand.[a]

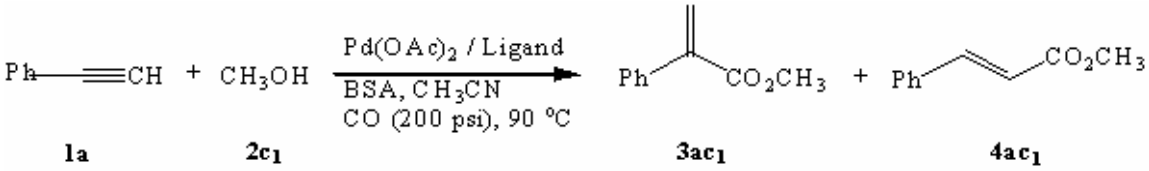

1a **2c$_1$** **3ac$_1$** **4ac$_1$**

Entry	Ligand	Bite angle	Conversion[b] (%)	4ac$_1$ / 3ac$_1$[c] (%)
1	dppb	98	100	92 / 8
2	dppf	96	99	86 / 14
3	dppp	91	88	76 / 24
4	BIPHEN	92	100	46 / 54
5	BINAP	92	99	34 / 66
6[d]	dppe	85	3	-
7[e]	Bu_3P	-	11	20 / 80
8	PPh_3	-	24	14 / 86

[a] Reaction conditions: $Pd(OAc)_2$ (0.02 mmol), ligand (0.08 mmol), phenylacetylene (2.0 mmol), $B(OH)_3$ (0.30 mmol); salicylic acid (0.60 mmol), methanol (8.0 mmol), CH_3CN (10.0 ml), CO (200 psi), 90 ^oC, 3 h.

[b] Determined by GC.

[c] Determined by GC and ^1H NMR.

[d] 3 % Styrene

[e] 6 % Styrene

Similarly, low conversion (24 %) of phenylacetylene and higher selectivity (86 %) for the *gem* isomer **3** was observed when triphenylphosphine was used as a ligand, (Table 2.2, entry 8).

2.2.3 Effect of the ratio of dppb / $Pd(OAc)_2$

The ratio of dppb / $Pd(OAc)_2$ is also found to have a significant role on the catalyst activity and the selectivity of the reaction (Figure 2.1). The conversion increases from 66 % (dppb / [Pd] = 1), to 100 % (dppb / [Pd] = 2) and the total conversion was maintained up to a ratio of dppb / [Pd] of 5 after which the conversion decreased significantly (51 %). The selectivity in *trans* ester **4** increases from 70 % to 90 % then to 92 % and finally remains 92 % at dppb / [Pd] ratio of 1, 2, 4 and 5, respectively. Substantial decomposition of the active catalyst into palladium metal was observed only with ratio dppb / [Pd] =1. The use of excess ligand increased probably the steric and electronic density around the palladium center so that the equilibrium shifts towards the direction of *pro-trans* intermediate.

2.2.4 Effect of the type and the amount of additives

Table 2.3 shows the effect of the type and the amount of additives on the catalytic alkoxycarbonylation of phenylacetylene with methanol. The presence of acid is necessary to form the catalytically active species. The results show no reaction in the absence of salicylborate (BSA) (Table 2.3, entry 1). The catalytic activity is considerably low (10 %) with 0.03 mmol of salicylborate, and complete conversions were obtained when the amounts of salicylborate were increased to 0.30 mmol and 0.45 mmol (Table

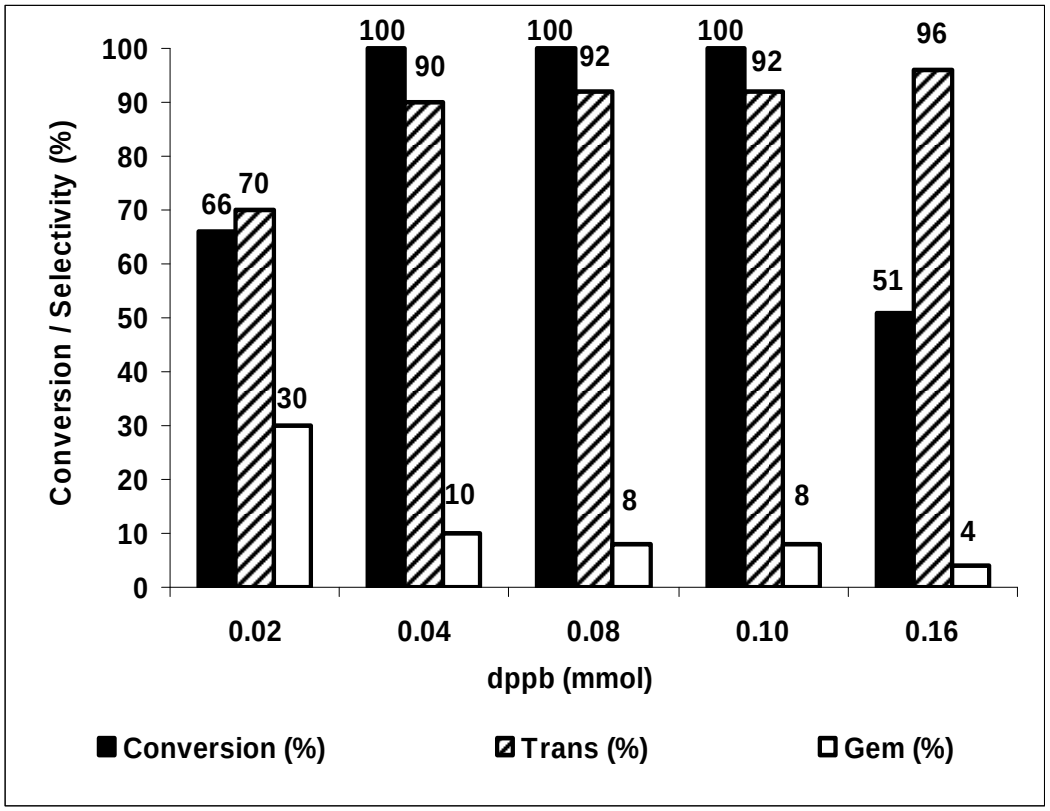

.

Reaction Conditions: $Pd(OAc)_2$ (0.02 mmol), phenylacetylene (2.0 mmol), methanol (8.0 mmol), $B(OH)_3$ (0.30 mmol); salicylic acid (0.60 mmol), CH_3CN (10.0 ml), CO (200 psi), 90 ^oC, 3 h.

(*trans* + *gem* = 100 %)

Figure 2.1. Alkoxycarbonylation of phenylacetylene with methanol by $Pd(OAc)_2$ / dppb / BSA.

Effect of the amount of ligand

2.3, entries 2-5). The results indicate that the acid should be present in significant excess to achieve maximum activity and selectivity (Table 2.3, entries 1-5). At lower acid concentrations and in the presence of excess of methanol, lower activities were observed (111, 112).

A decrease in both conversion and selectivity towards the *trans* isomer was observed when salicyclic acid alone was used as promoter (Table 2.3, entry 6). The total conversions obtained with sulfonic acid derivatives such as methanesulfonic and *p*-toluenesulfonic acid (Table 2.3, entries 8-9) have encouraged us to pursue further these systems in order to improve both conversions and selectivities using a variety of alkyl and aryl alkynes.

The basic question concerns the role of the acid in this carbonylation reaction. The acid may react forming metal hydride species through protonation of the electron-rich Pd(0) species which is formed from in situ reduction of Pd(II) when heated in the presence of CO (113). These species are electron-rich and known to form Pd-H in the presence of strong acid. The salicylborate anion can either coordinate to the metal center forming neutral complex, or act as a counter-ion to the cationic palladium species. The later is more plausible in the present system for three reasons: firstly, the coordination of the salicylborate anion would render it prone to hydrogenation of the alkynes to alkenes and alkanes (114), the second reason is the displacement of weakly coordinating labile anions from the sphere of metals by less labile ligands (115), and finally, the weakly coordinating anions, because of their easier dissociation from ion-pair, generate a more electrophilic palladium center (13,116).

Table 2.3. Alkoxycarbonylation of phenylacetylene by $Pd(OAc)_2$ / dppb. Effect of the type of additives.[a]

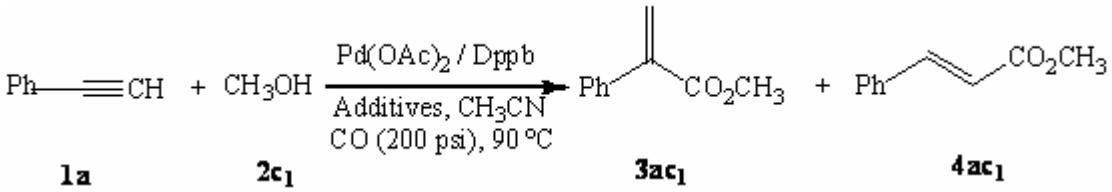

1a **2c$_1$** **3ac$_1$** **4ac$_1$**

Entry	Additive mmol / mmol	Conversion[b] (%)	4ac$_1$ / 3ac$_1$[c] (%)
1	-	0	-
2	$B(OH)_3$ / Salicylic acid 0.03 / 0.06	10	88 / 12
3	$B(OH)_3$ / Salicylic acid 0.10 / 0.20	91	85 / 15
4	$B(OH)_3$ / Salicylic acid 0.30 / 0.60	100	92 / 8
5	$B(OH)_3$ / Salicylic acid 0.45 / 0.90	100	91 / 9
6	Salicylic acid 0.60	22	47 / 53
7	$B(OH)_3$ 0.30	0	-
8	*p*-TSOH 0.30	100	86 / 14
9	CH_3SO_3H 0.30	100	89 / 11

[a] Reaction conditions: $Pd(OAc)_2$ (0.02 mmol), dppb (0.08 mmol), phenylacetylene (2.0 mmol), methanol (8.0 mmol), CH_3CN (10.0 ml), CO (200 psi), 90 °C, 3 h.

[b] Determined by GC.

[c] Determined by ^1H NMR and GC.

2.2.5 Effect of type of solvent

Table 2.4 contains the results of the effect of various solvents on the catalytic alkoxycarbonylation of phenylacetylene with methanol. No clear correlation was found between the conversion, the selectivity and the dielectric constant of the solvents. Non-coordinating solvent, such as n-hexane, dichloromethane and toluene gave conversions of 35 %, 43 %, and 89 % with the corresponding selectivities in *trans* isomer **4** of 39 %, 41 % and 24 %, respectively (Table 2.4, entries 5-7).

Almost complete conversions were obtained with polar coordinating solvents such as acetonitrile, benzonitrile, DMF, and DMSO (Table 2.4, entries 1-4). However, when methanol was used alone as a solvent and a nucleophile under similar conditions, only 32 % conversion was obtained after 3 hours of reaction (Table 2.4, entry 9). This may be due to the formation of less active palladium carbomethoxy complex (111,112). As described earlier, the coordination of the anions to the cationic palladium center may depend strongly on the polarity of the reaction medium (13). Solvation of the ion-pair by the polar solvents is expected to facilitate cation-anion dissociation and, therefore, renders the metal center more electrophilic and more easily accessible by the substrate molecules (13).

Among all used solvents, only acetonitrile and benzonitrile gave complete conversions and with the *trans*-α,β-unsaturated ester **4** formed as the major product. The reason for the high selectivity for the *trans* isomer exclusively in these solvents is not yet totally clear. It could be explained by the fact that acetonitrile is acting as both solvent and co-ligand (90,117). In cationic complexes the fourth coordination position could be occupied by acetonitrile that probably plays an active role in the migratory insertion

Table 2.4. Hydroesterification of phenylacetylene by $Pd(OAc)_2$ / dppb / BSA.Effect of the type of solvent.[a]

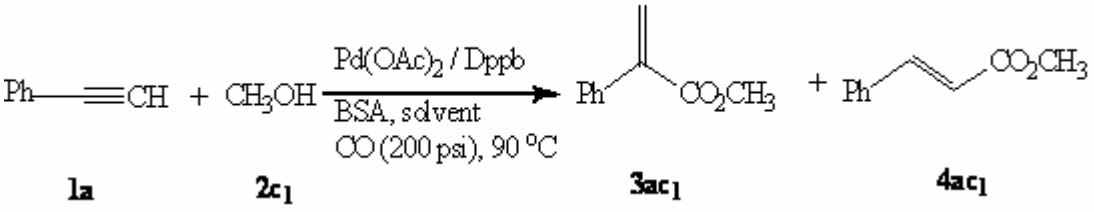

Entry	Solvent	Conversion[b] (%)	$4ac_1$ / $3ac_1$[c] (%)
1	CH_3CN	100	92 / 8
2	PhCN	100	86 / 14
3	DMSO	100	18 / 82
4	DMF	96	12 / 88
5	Toluene	89	24 / 76
6	CH_2Cl_2	43	41 / 59
7	Hexane	35	39 / 61
8	THF	8	24 / 76
9	CH_3OH	32	30 / 70

[a] Reaction conditions: $Pd(OAc)_2$ (0.02 mmol), dppb (0.08 mmol), phenylacetylene (2.0 mmol), $B(OH)_3$ (0.30 mmol); salicylic acid (0.60 mmol), methanol (8.0 mmol), solvent (10.0 ml), CO (200 psi), 90 °C, 3 h.

[b] Determined by GC.

[c] Determined by GC and ^1H NMR.

(118). It is apparent that the nucleophilic character of the co-ligand may remarkably affect the rate of conversion of $[Pd(P\text{-}P)H]^+$ into $[Pd(P\text{-}P)OMe]^+$ and hence promote the products of carbonylation whose formation required Pd-H bond (116).

The influence of the co-ligand on the stability of the hydride metal initiator and hence on product selectivity has previously been reported for palladium-catalyzed enantioselective carbonylation of styrene (119).

2.2.6 Effects of the temperature

A systematic study on the influence of the temperature on the regioselectivity and the catalytic activity in the alkoxycarbonylation of phenylacetylene with methanol was achieved at a variety of temperatures ranging from 70 ^oC to 110 ^oC (Figure 2.2). The formation of the *trans-*α,β-unsaturated esters prevailed in all temperatures. An increase in the temperature, however, increased the amount of the *trans-*α,β-unsaturated ester up to 90 ^oC above which the selectivity in *trans* ester **4** started dropping.

At higher temperature (110 ^oC), complete conversion was obtained while the selectivity for the *trans* isomer decreased to 78 %; this decrease could be related to the displacement of phosphine by CO which is favored at higher temperature (120). This makes the palladium center less crowded and therefore less selective for the trans isomer. Similarly, the lower temperature (80 ^oC) resulted in lower selectivity in *trans* isomer **4** with conversion remain the same (100 %). The conversion of phenylacetylene and the selectivity toward the *trans-*α,β-unsaturated ester were deteriorated as the reaction temperature decreased to 70 ^oC.

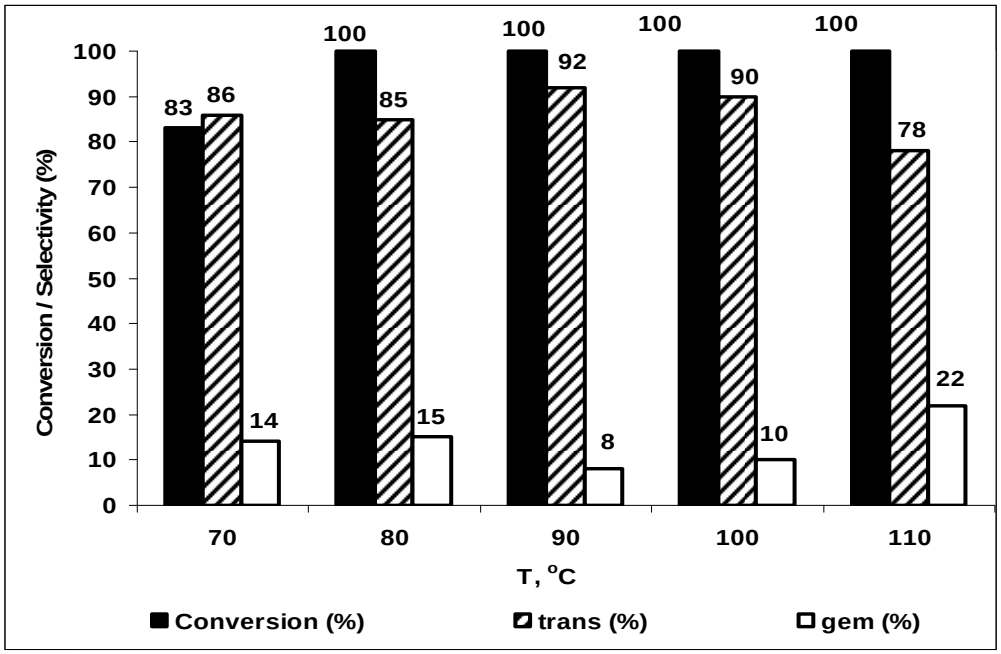

Reaction conditions: $Pd(OAc)_2$ (0.02 mmol), dppb (0.08 mmol), phenylacetylene (2.0 mmol), methanol (8.0 mmol), $B(OH)_3$ (0.30 mmol); salicylic acid (0.60 mmol), CH_3CN (10.0 ml), CO (200 psi), 3 h.

(*trans* + *gem* = 100 %).

Figure 2.2. Alkoxycarbonylation of phenylacetylene with methanol by $Pd(OAc)_2$/dppb/BSA.

Effect of the temperature.

2.2.7 Alkoxycarbonylation of Phenylacetylene with different Alcohols

The effect of different alcohols as esterifying reagents were studied and the results are presented in Table 2.5. The conversions and selectivities remained fairly constant with increasing numbers of carbons in the alcohol. This shows that the alkoxy mechanism is playing a minor role in this process because the initial formation of palladium carboalkoxy will be expected to decrease with the increase in the number of carbons of alcohols (111,112,121).

2.2.8 Proposed Mechanisms

There are two main mechanisms that have been proposed for alkoxycarbonylation of alkynes with alcohols: the hydride and alkoxy mechanisms (72,99,101,121,122). It was reported that the insertion of styrene into metal acyl bond led to *gem* products, while insertion into hydrides led to *trans* products (123). Based on the analysis of the literature and the present experimental results we tentatively proposed two possible schemes, where the hydride mechanism represents the major route towards the *trans* product (Scheme 2.1). This was clear from the promoting effect of a hydride source observed with acid (Table 2.3) (99,123).

The first step in the proposed mechanism was the formation of palladium hydride species **A** by the reaction of $Pd(OAc)_2$, dppb, CO and acid (61). The coordination of alkyne to palladium center will give intermediate **B** which depends on the nature of the palladium center, polarity of the solvent, steric and electronic effect of the ligand.

Table 2.5. Alkoxycarbonylation of phenylacetylene by [Pd] / dppb / BSA in the presence of different alcohols.[a]

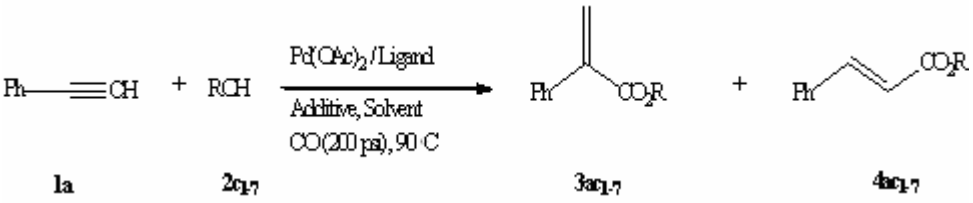

1a 2c1-7 3ac1-7 4ac1-7

Entry	Alcohol ROH	Conversion[b] (%)	trans / gem[c] (%)
1	**CH_3OH** **$2c_1$**	100	92 / 8
2	**CH_3CH_2OH** **$2c_2$**	99	91 / 9
3	**$CH_3(CH_2)_2OH$** **$2c_3$**	99	92 / 8
4	**$(CH_3)_2CHOH$** **$2c_4$**	99	91 / 9
5	**$CH_3(CH_2)_3OH$** **$2c_5$**	99	91 / 9
6	**$CH_3(CH_2)_4OH$** **$2c_6$**	99	90 / 10
7	**$CH_3(CH_2)_6OH$** **$2c_7$**	100	89 / 11

[a] Reaction conditions: $Pd(OAc)_2$ (0.02 mmol), dppb (0.08 mmol), phenylacetylene (2.0 mmol), ROH (8.0 mmol), $B(OH)_3$ (0.30 mmol); salicylic acid (0.60 mmol), CH_3CN (10.0 ml), 200 psi of CO, 90 ^oC, 3 h.

[b] Determined by GC.

[c] Determined by GC and ^1H NMR.

A literature precedent describes that the regiochemistry can be attributed to mainly steric effects (114). Thus (dppb)Pd-H bond tends to add preferentially to the less crowded carbon, i.e., to the terminal carbon forming intermediate **C**.

With the monodentate phosphine, the lower conversion and selectivity is related to the lower steric crowdeness and preference for the *trans* orientation of the monodentate phosphine ligand due to both steric and electronic reasons. It is well known that the *gem*-*trans* ratio is rapidly changed at high temperature and affected by the use of excess of ligand (Table 2.2, entries 7 and 8) (13).

The charge distribution in phenylacetylene indicates that the terminal carbon is more nucleophilic than the internal carbon, because of the electron withdrawing effect of the phenyl group. Theoretical calculations (using Gaussian 03) gave the charge distribution as -0.452 for the terminal carbon and 0.094 for the internal carbon, therefore, it is expected that the terminal carbon of the triple bond will have more affinity for the cationic palladium than the internal; hence more trans isomer will be expected with cationic palladium species.

Solvation by the polar solvents is expected to facilitate and stabilize cation-anion dissociation and therefore render the metal center more electrophilic and more easily accessible by the substrate molecules (13). Claver and co-wokers have proposed that high *gem* selectivity proceed through a neutral catalytic cycle, while the *trans* preference follows a cationic catalytic cycle (101). Carboalkoxy mechanism can also play a major role in forming the *gem* isomer. The assumption of the formation of the two isomers regioselectively through different catalytic cycles could be valid for our system, where

the product distribution percent can be explained by the difference in thermodynamic stability of the regioselectivity key intermediates in the same catalytic cycle.

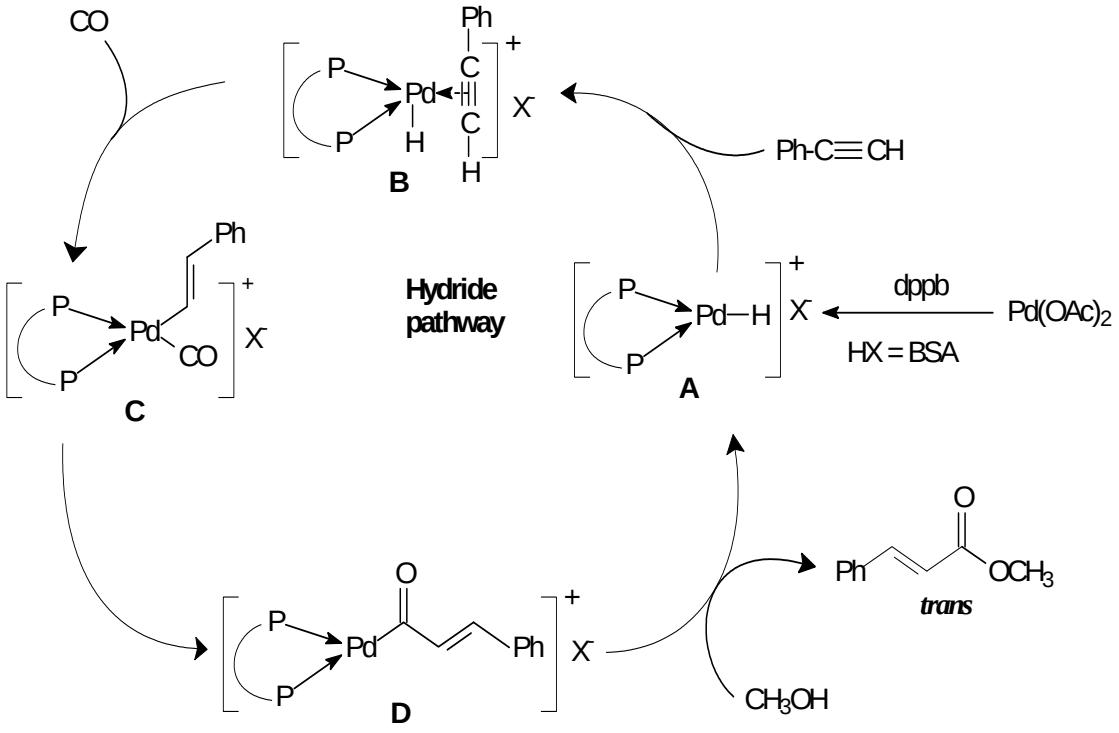

Scheme 2.1. Proposed mechanism for the formation of the *trans* products.

The presence of coordinating acetonitrile solvent molecules can in principle affect the stability of palladium acyl intermediates. However, literature data prove the absence of this effect. In complex [Pd(^{13}C(O)Me)(P-P')MeCN](OTf) (P=PPh_2, P'=$(toly)_2$), no displacement of MeCN by ^{13}CO was observed at 1 atm (13). A similar result was already found for the complex [Pd(^{13}COMe)(BINAPHOS)CD_3CN](OTf) (124). Thermodynamic consideration may explain the stability of these palladium acyl complexes without the displacement of acetonitrile.

The reactions in DMF and DMSO gave *gem*-α,β-unsaturated ester selectively (Table 2.4 entries 3, 4). The *gem* isomer was also produced when other alcohols such as 1-butanol and 2-propanol were used in place of methanol. Also the *gem*-α,β-unsaturated ester was produced as the major product when neat methanol was used in the absence of any other solvent. As already described in the literature, the formation of *gem* isomer was explained by the initial formation of carboalkoxy species (alkoxy mechanism). CO insertion into the palladium-oxygen bond affords acylpalladium, and finally methanolysis of the acyl yields the final product (Scheme 2.2) (110).

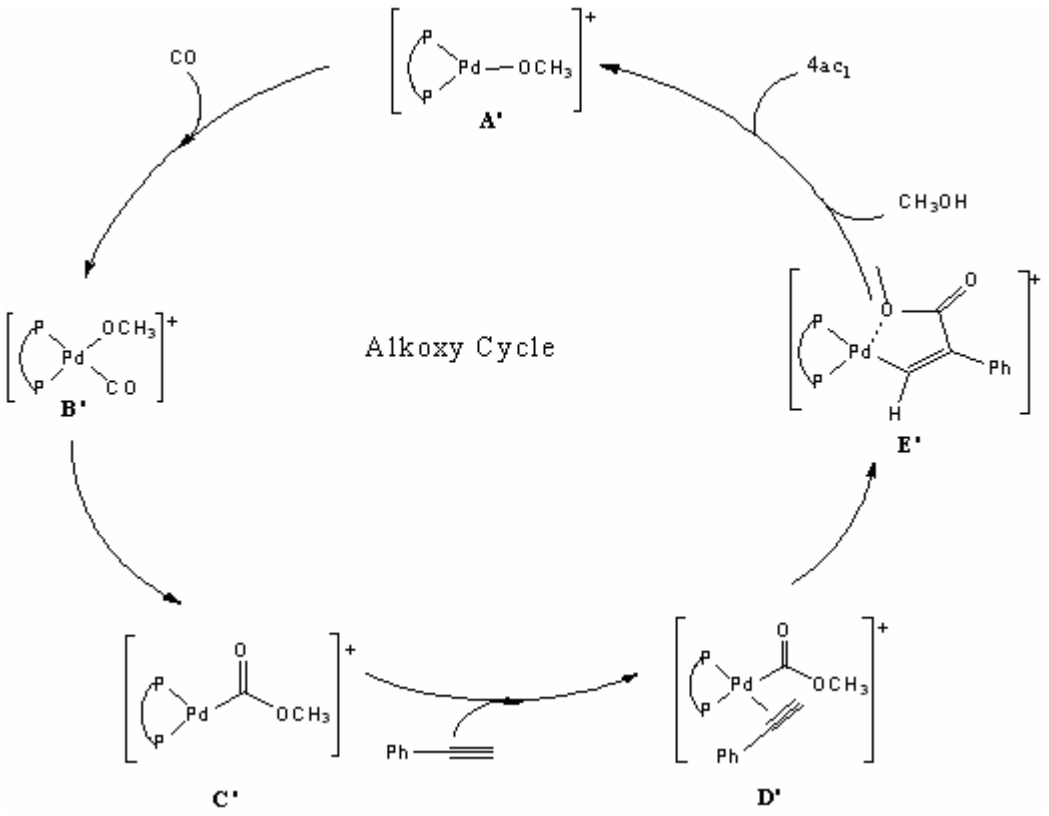

Scheme 2.2. Proposed mechanism for the formation of the *gem* products.

2.3 Conclusions

Palladium (II) and 1,4-bis(diphenylphosphino)butane in the presence of a mixture of salicylic and boric acids (BSA) and in acetonitrile was an effective and selective catalyst system for the regioselective alkoxycarbonylation of phenylacetylene into *trans*-α,β-unsaturated ester (*trans*-methyl cinnamate). Polar coordinative solvents were found to be more active compared the non-polar solvents or polar non-coordinative solvents. Acetonitrile was the most effective solvent for high selectivity toward the formation of *trans* isomer. This is may be due to its ability to act as co-ligand with low binding affinity and also to stabilize palladium cationic species, which may be responsible for high selectivity towards *trans* isomers. Monophosphines as ligands in acetonitrile gave low conversion with *gem*-α,β-unsaturated ester as the major product. It was found that the suitable conditions for the formation of the *trans*-α,β-unsaturated ester appear to be the combined use of bulky diphosphines, acetonitrile and palladium cationic species as a catalyst. It was observed that the selectivity towards *trans* isomer increases with the increase in bite angles of the diphosphine ligands.

2.4 Experimental section

2.4.1 Materials

Phenylacetylene, palladium catalysts, phosphine ligands and acids were purchased from Aldrich Company and were used without further purification. The alcohols and the solvents were distilled under N_2 and dried before use.

^{1}H and ^{13}C NMR spectra were recorded on 500 MHz Joel 150 NMR machine. Chemical shifts were reported in ppm relative to tetramethyl silane (TMS) using $CDCl_3$. The

products of the reactions were analyzed on gas chromatography (Agilent GC 6890 plus Series) equipped with a split–splitless injector (split ratios of 20:1). The temperature of the injector was 250 ^{o}C, with 10 psi constant pressure. The column was an HP-5 column (30 m × 0.25 mm i.d., 0.25 μm film thickness). Helium was the carrier gas with a flow rate of 1.5 mL/min, and programmed temperature was applied to obtain the separation of the compounds; precisely the initial temperature was 50 °C, hold 2 min, then ramped at 10 °C/min to 140 °C (hold time 0 min), then finally ramped at 20 °C/min to 250 °C (hold time 20 min). The detector was flame ionization detector (FID), with hydrogen and air flow of 40.0 and 450.0 ml/min, respectively. Makeup flow was on with 45.0 ml/min of helium.

The products of the reactions were also analyzed on GC-MS (Varian Saturn 2000) equipped with HP-5 MS column (30 m × 0.25 mm i.d., 0.25 μm film thickness). Helium was the carrier gas at a flow rate of 1.0 mL/min and programmed temperature was applied to obtain the separation of the compounds; precisely the initial temperature was 50 °C, hold 2.0 min, then ramped at 10 °C/min to 140 °C (hold time 0 min), then finally ramped at 20 °C/min to 250 °C (hold time 20 min). The temperatures of injector, transfer line and ionization source were 250, 225 and 270 °C, respectively. NIST MS search was used for compound identification.

2.4.2 General procedure for the alkoxycarbonylation of phenylacetylene with alcohols

A mixture of $Pd(OAc)_2$ (0.02 mmol), 1,4-bis(diphenylphosphino)butane (0.08 mmol), boric acid (0.3 mmol), salicyclic acid (0.6 mmol), phenylacetylene (2.0 mmol), and

alcohol (8.0 mmol) in 10 ml of acetonitrile was placed in the glass liner, equipped with a stirring bar, fitted in a 45 ml Parr autoclave. The autoclave was purged three times with carbon monoxide, pressurized with 200 psi of CO. The mixture was stirred and heated for the required time (Appendix A1). After cooling the pressure was released, the mixture was diluted with ethyl ether, washed with water, dried with anhydrous $MgSO_4$, and analyzed by GC.

CHAPTER 3

PALLADIUM (II)-CATALYZED CATALYTIC AMINOCARBONYLATION AND ALKOXYCARBONYLATION OF TERMINAL ALKYNES: REGIOSELECTIVITY CONTROLLED BY THE NUCLEOPHILES

3.1 Introduction

Palladium–catalyzed carbonylation reactions, carried out in the presence of various nucleophiles like amines and alcohols, belong to the most widely used homogeneous catalytic reactions in synthetic chemistry (125). α,β-Unsaturated amides or esters can be prepared by a direct carbonylation of alkynes in the presence of appropriate nucleophiles such as amines (aminocarbonylation) or alcohols (alkoxycarbonylation).

Aminocarbonylation plays a special role in synthesizing carboxamides which are difficult to prepare via conventional carboxylic acid/carboxylic halide-carboxamide route (e.g., with bulky substituents at the amide nitrogen) from easily available starting materials (13). The acrylic esters derivatives produced by the above reaction are employed in a wide of organic reactions such as nucleophilic additions and cycloaddition reactions (126). They are also extensively used in the synthesis of polymeric materials (127). Cinnamic acids and their esters are important intermediates for the production of pharmaceuticals, fragrances, light-sensitive materials, electrically conductive materials, and agrochemicals (90). The development of more efficient aminocarbonylation and alkoxycarbonylation catalytic systems in terms of conversion, selectivity and diversity of synthesized products is still a challenging area. It is well-known that the ratio of products

from aminocarbonylation and alkoxycarbonylation reactions depends strongly on the catalytic system and the reaction conditions employed (61,72). The regioselective synthesis of the *gem*-α,β-unsaturated esters has been achieved easily by various methods (52,74,82). However, the research reports that describe the regioselective synthesis of the *trans*-α,β-unsaturated esters are still limited (72). Many aminocarbonylation reactions of alkynes have been reported in the literature (62,64,65). Nevertheless, only limited work has been done towards the selective aminocarbonylation of terminal alkynes using primary and secondary alkylamines; high regioselectivities and yields for the aimed products were achieved under relatively mild conditions (63,65,128). The use of the same catalytic system for the aminocarbonylation and alkoxycarbonylation of terminal alkynes has been reported (13,99). However, no apparent change on the selectivity of the reaction was observed by changing the type of nucleophile. In the present chapter, we wish to report the results of the comparative study of the aminocarbonylation and alkoxycarbonylation of terminal alkynes using the same catalyst system $Pd(OAc)_2$/dppb/*p*-TsOH/CH_3CN/CO. A careful screening of the various reaction conditions including the type of catalyst, the type and amount of ligand, the amount of additive, the type of solvent, and the type of amines or alcohols has been considered.

3.2 Results and discussion

The aminocarbonylation and alkoxycarbonylation of phenylacetylene (**1a**), adopted as a model alkyne, using diisobutylamine (**2b$_1$**) and methanol (**2c$_1$**) was carried out using the system $Pd(OAc)_2$/dppb/*p*-TsOH/CO/CH_3CN (Table 3.1). Excellent conversion and regioselectivity towards the formation of *gem* isomer **3ab$_1$** (2-acrylamide) were obtained

with the alkylamine **2b$_1$**, while *trans* isomer **4ac$_1$** (cinnamate ester) was the predominant product with methanol (**2c$_1$**) as a nucleophile. The reaction conditions were optimized and the effect of various reaction parameters on the activity and selectivity were determined.

3.2.1 Effect of the type of palladium complexes

The presence of metal catalyst is essential for the catalytic carbonylation of alkynes. No reaction was observed in the absence of palladium catalysts. We have considered various palladium complexes in the aminocarbonylation and alkoxycarbonylation of phenylacetylene (**1a**) using diisobutylamine (**2b$_1$**) and methanol (**2c$_1$**). The results are summarized in Table 3.1. No significant change on the selectivity of the reaction was observed in the aminocarbonylation experiments by changing the type of palladium catalysts (Table 3.1, entries 1-7), where the *gem* isomers **3ab$_1$** were obtained as major products. Different ratios of products (**3ac$_1$ / 4ac$_1$**) were obtained in the alkoxycarbonylation experiments using different palladium catalysts (Table 3.1, entries 1-7). It seems that the presence of ligands having higher binding ability such as chloride or cyanide (Table 3.1, entries 2-5) reduces the availability of the coordination sites around palladium, hence leading to lower catalytic activity in alkoxycarbonylation of terminal alkynes (99,100). With methanol as a nucleophile, low yields (7-27 %) were obtained with $PdCl_2$, $PdCl_2(PPh_3)_2$, $Pd(PhCN)_2Cl_2$, and $Pd(CN)_2$. While lower selectivity (**3ac$_1$/4ac$_1$=** 62/38) was observed with $PdSO_4$.

Table 3.1. Palladium(II)-catalyzed aminocarbonylation and alkoxycarbonylation of phenylacetylene (**1a**) using diisobutylamine (**2b$_1$**) and methanol **(2c$_1$**). Effect of the type of palladium catalysts.[a]

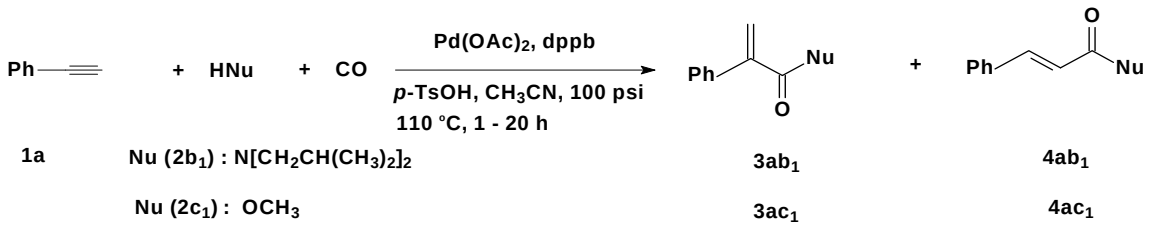

Entry	Catalyst	Conversion 1a (%)[b]		Product Distribution[c] (%)	
		2b$_1$	**2c$_1$**	**3ab$_1$ / 4ab$_1$**	**3ac$_1$ / 4ac$_1$**
1	$Pd(OAc)_2$	99	99	97 / 3	12 / 88
2	$PdCl_2$	100	27	95 / 5	25 / 75
3	$PdCl_2(PPh_3)_2$	91	7	97 / 3	10 / 90
4	$Pd(PhCN)_2Cl_2$	88	4	97 / 3	11 / 89
5	$Pd(CN)_2$	38	22	97 / 3	35 / 65
6	$PdSO_4$	56	99	96 / 4	62 / 38
7	Pd/C (5%)	34	97	97 / 3	13 / 87

[a] Reaction conditions: catalyst (0.02 mmol), dppb (0.08 mmol), phenylacetylene (2.0 mmol), diisobutylamine (**2b$_1$**) (2.0 mmol) or methanol (**2c$_1$**) (8.0 mmol), CO (100 psi), *p*-TsOH (0.3 mmol), CH_3CN (10 ml), 110 °C, 20 h (**1a**+**2b$_1$**) and 1 h (**1a**+**2c$_1$**).

[b] Determined by GC based on phenylacetylene.

[c] Determined by GC and ^{1}H NMR

3.2.2 Effect of the type of ligand

The effect of the type of the ligand on the carbonylative coupling of phenylacetylene (**1a**) with diisobutylamine (**1b$_1$**) and methanol (**2c$_1$**) was investigated. Different bidentate phosphine ligands with wide range of bite angles, and also monodentate phosphine ligands were used in the study. The results, summarized in Table 3.2, showed no catalytic activity in the aminocarbonylation reaction of phenylacetylene and an excellent activity in alkoxycarbonylation reaction when monodentate ligand PPh_3 was used (Table 3.2, entry 1). The use of $P(OPh)_3$ ligand inhibits completely both reactions, which may be due to the formation of stable complexes (Table 3.2, entry 2). A correlation between diphosphine ligand bite angle, rate and selectivity has been observed for the two studied reactions. For example, an increase in the bite angle of the diphosphine ligand used resulted in an increase in both activity and selectivity to produce selectively **3ab$_1$** and **4ac$_1$** in the aminocarbonylation and alkoxycarbonylation reactions, respectively (Table 3.2, entries 3-6). A similar correlation between diphosphine ligand bite angle, catalytic efficiency and selectivity were also observed in palladium-catalyzed alkoxycarbonylation of phenylacetylene (see section 2.2.2), and palladium-catalyzed cross coupling reactions of Grignard reagents with organic halides (129). Extended Huckel calculations indicate that in the diphosphine complexes with small ligand bite angles, the electron density is shifted to the hydride ligand (106). Therefore, the increase of the bite angle of the ligand increases the hydride ligand acidity, hence the basicity of the following ligands increases in the order: dppe > dppp > dppb. This order suggests a possible reason for the reduced activity of dppe in alkoxycarbonylation of (**1a**) (106). In the alkoxycarbonylation mechanism, the hydropalladation process exhibits high regioselectivity, resulting in *cis*-

addition of Pd hydride complex to a less hindered carbon atom, which finally yields the *trans* isomer **4ac$_1$** (102,103). Our postulation about the early coordination of amine and diphosphine ligand to the active palladium center can be used to explain the insensitivity for the type of phosphine ligands on the selectivity of the aminocarbonylation reaction (Table 3.2, entries 3-6).

The study of the effect of different dppb/Pd ratios is found to have significant effect on the catalytic activity and product distribution of the alkoxycarbonylation reaction (Figure 3.1), while only significant improvement in catalytic activity was observed for the aminocarbonylation catalyst system (Figure 3.2). No change in the activity and the selectivity for both reactions were observed at the ratios of dppb / Pd = 3-4. However, in the aminocarbonylation experiments, the use of excess amounts of dppb ligand (> 0.08 mmol) resulted in lowering the rate of the reaction, which could be explained by competing dppb ligand with the reactant molecules for co-ordination, causing decrease in the activity, but with no effect on the product distribution.

3.2.3 Effect of the solvent

The study of the effect of solvent is extremely important in the aminocarbonylation and alkoxycarbonylation reactions of alkynes (Table 3.3). The results showed no clear correlation between the dielectric constant of the solvent and the outcome of the reactions. Various polar and non-polar solvents tested with alkoxycarbonylation of phenylacetylene led to excellent conversions (except *n*-hexane) producing mainly the *gem* isomer as predominant product, except with acetonitrile where *trans*-α,β-unsaturated ester **4ac$_1$** was the major product. This lower activity with *n*-hexane (Table

Table 3.2. Palladium(II)-catalyzed aminocarbonylation and alkoxycarbonylation of phenylacetylene (**1a**) using diisobutylamine (**2b$_1$**) and methanol **(2c$_1$**). Effect of the type of ligand.[a]

Entry	Ligand	Conversion 1a (%)[b]		Product Distribution[c] (%)	
		2b$_1$	**2c$_1$**	**3ab$_1$ / 4ab$_1$**	**3ac$_1$ / 4ac$_1$**
1	PPh_3	0	99	-	14 / 86
2	$P(OPh)_3$	0	0	-	-
3	dppe	12	0	85 / 15	-
4	dppp	59	0	97 / 3	-
5	dppf	78	12	97 / 3	62 / 38
6	dppb	99	99	97 / 3	11 / 89

[a] Reaction conditions: $Pd(OAc)_2$ (0.02 mmol), Ligand (0.08 mmol) except PPh_3, and $P(OPh)_3$ (0.16 mmol), phenylacetylene (2.0 mmol), diisobutylamine (**2b$_1$**) (2.0 mmol) or methanol (**2c$_1$**) (8.0 mmol), CO (100 psi), *p*-TsOH (0.3 mmol), CH_3CN (10 ml), 110 °C, 20 h (**1a+2b$_1$**) and 1 h (**1a+2c$_1$**).

[b] Determined by GC based on phenylacetylene.

[c] Determined by GC and ^1H NMR.

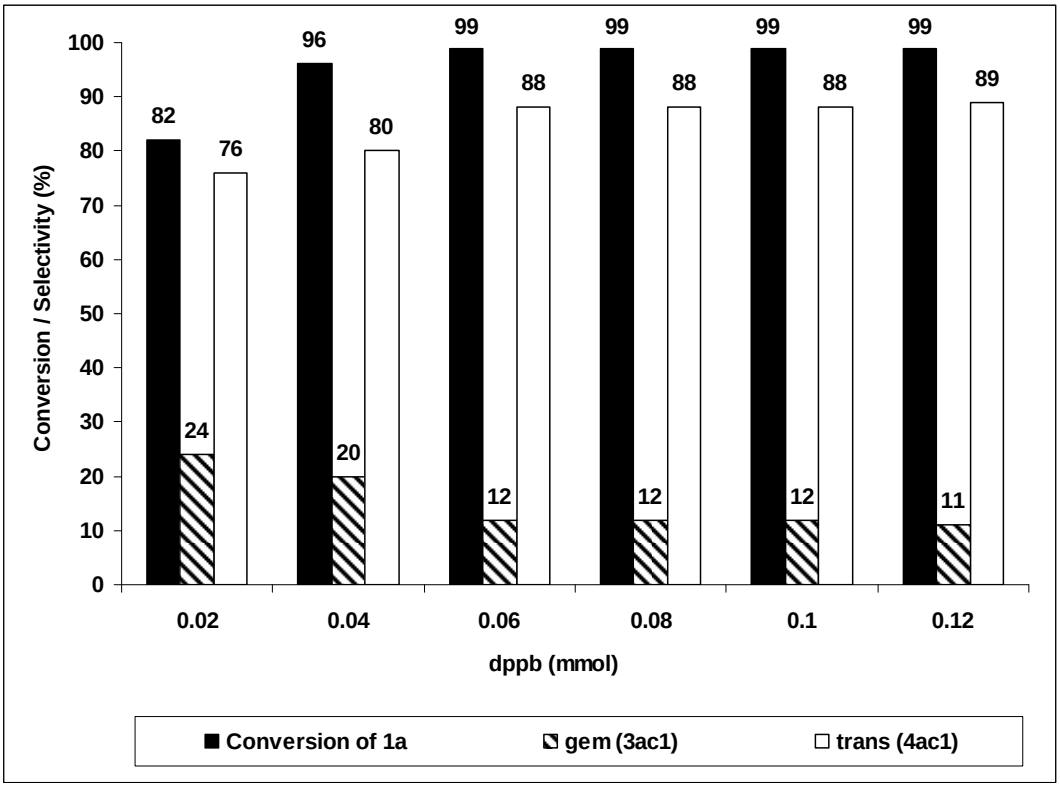

Reaction conditions: $Pd(OAc)_2$ (0.02 mmol), **1a** (2.0 mmol), **$2c_1$** (8.0 mmol), CO (100 psi), *p*-TsOH (0.30 mmol), CH_3CN (10 ml), 110 °C, 1 h.

Figure 3.1. Alkoxycarbonylation of phenylacetylene (**1a**) using methanol (**$2c_1$**) by $Pd(OAc)_2$/dppb/*p*-TsOH.

Effect of the amount of dppb.

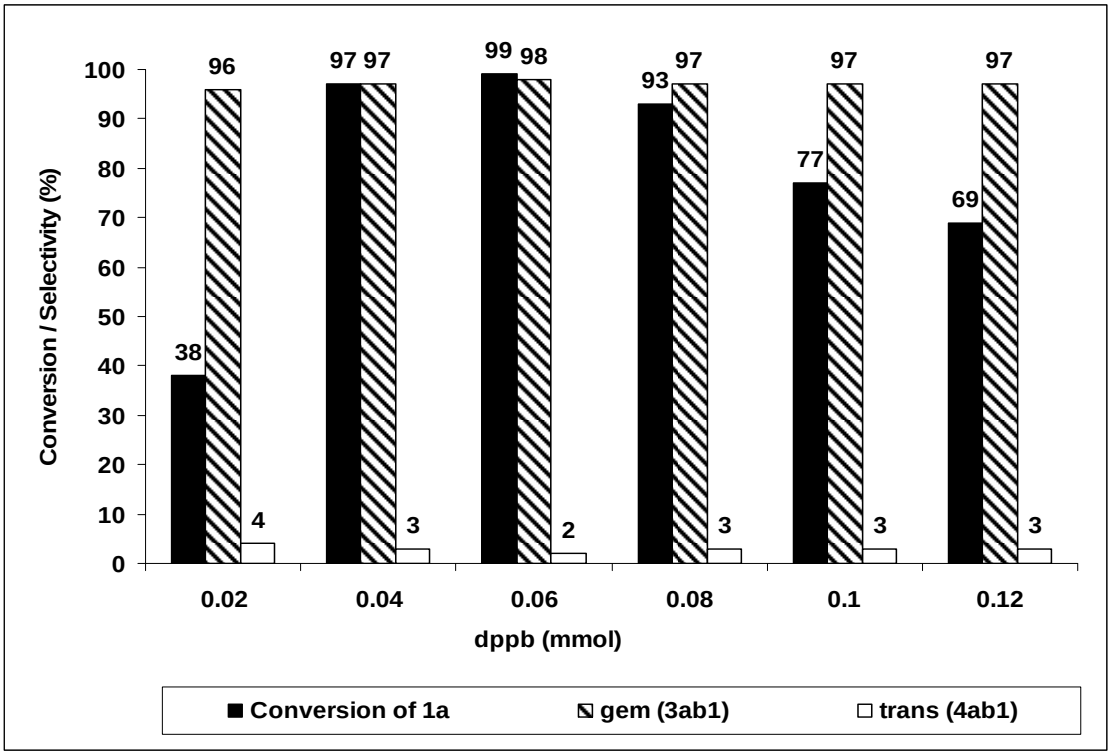

Reaction conditions: $Pd(OAc)_2$ (0.02 mmol), **1a** (2.0 mmol), **$2b_1$** (2.0 mmol), CO (100 psi), *p*-TsOH (0.30 mmol), CH_3CN (10 ml), 110 °C, 20 h.

Figure 3.2. Aminocarbonylation of phenylacetylene (**1a**) using diisobutylamine (**$2b_1$**) by $Pd(OAc)_2$/dppb/*p*-TsOH.

Effect of the amount of dppb.

3.3, entry 5) compared to other solvents is due probably to the fact that this non-polar solvent favors the coordination of the counter ion to the complex cation, so that it competes with the reacting molecules (99).

The opposite regioselectivity of the alkoxycarbonylation reaction was only achieved when CH_3CN was used as solvent (Table 3.3, entry 7). The reason for the high selectivity for the *trans* isomer **4ac$_1$** exclusively in acetonitrile as a solvent is not yet very clear, but it is possible that acetonitrile acts both as a solvent and a co-ligand (90).

The drastic increase in the catalytic activity in the aminocarbonylation reaction was only observed with acetonitrile as a solvent. The change in the reaction rate was also accompanied with excellent selectivity of the reaction (Table 3.3, entry 7).

3.2.4 Effect of the amount of *p*-TsOH additive

The reaction of carbonylative coupling of phenylacetylene (**1a**) with diisobutylamine (**2b$_1$**) and methanol (**2c$_1$**) catalyzed by Pd/dppb in acetonitrile was carried out in the presence of different amount of *p*-TsOH additive. The results of the aminocarbonylation reaction (Figure 3.3) clearly showed that the presence of acid additive is not crucial for the reaction, since a conversion of 27 % of phenylacetylene was obtained in the absence of *p*-TsOH. This yield was increased to 44 % by elongating reaction time to 36 hours. However, the addition of *p*-TsOH led to a significant increase in the activity (93 %) and a slight increase in the selectivity of the reaction towards *gem* isomer **3ab$_1$** (97 %). It seems that acid as additive is not an essential part of the active starting catalytic species, and its role appears as a promoter in the process of formation of the active catalytic species, or in the successive transformation of catalytic intermediates in the catalytic

Table 3.3. Palladium(II)-catalyzed aminocarbonylation and alkoxycarbonylation of phenylacetylene (**1a**) using diisobutylamine (**$2b_1$**) or methanol **($2c_1$**). Effect of the type of solvent.[a]

Entry	Solvent	Conversion 1a (%)[b]		Product Distribution[c] (%)	
		$2b_1$	**$2c_1$**	**$3ab_1$ / $4ab_1$**	**$3ac_1$ / $4ac_1$**
1	DMF	Traces	93	-	82 / 18
2	DMSO	28	99	67 / 33	87 / 13
3	DCM	19	99	94 / 6	75 / 25
4	THF	Traces	99	-	90 / 10
5	*n*-Hexane	22	72	89 / 11	69 / 31
6	Toluene	14	100	42 / 58	79 / 21
7	CH_3CN	93	99	97 / 3	12 / 88

[a] Reaction conditions: $Pd(OAc)_2$ (0.02 mmol), dppb (0.08 mmol), phenylacetylene (2.0 mmol), diisobutylamine (**$2b_1$**) (2.0 mmol) or methanol (**$2c_1$**) (8.0 mmol), CO (100 psi), *p*-TsOH (0.3 mmol), Solvent (10 ml), 110 °C, 20 h (**1a+$2b_1$**) and 1 h (**1a+$2c_1$**).

[b] Determined by GC based on phenylacetylene.

[c] Determined by GC and ^{1}H NMR

cycle. Also, the acid can create a free site at the metal center by the acid-base equilibrium with acetate ion on the metal center (90).

Unlike aminocarbonylation, the presence of acid additive in the alkoxycarbonylation reactions is absolutely necessary to form the active species; no reaction occurred in the absence of *p*-TsOH. The effect of the concentration of *p*-TsOH on the catalytic activity and the selectivity is shown on Figure 3.4. The acid may react forming metal hydride species through protonation of the electron-rich Pd(0) species, which is formed in situ from the reduction of Pd(II) (113). These species are electron-rich and known to form Pd-H in the presence of strong acid. The selectivity is not affected by change in *p*-TsOH concentration, which suggests that OTs^- may not be very strongly coordinated to the Pd center (99).

3.2.5 Effect of the reaction temperature

The effect of temperature was also carefully studied. Similar reaction conversions were obtained with the aminocarbonylation and the alkoxycarbonylation reactions at 90 °C (Table 3.4, entry 1). The 10 °C increment in the reaction temperature resulted in almost complete conversion for alkoxycarbonylation system, and doubling the activity for the aminocarbonylation reaction (Table 3.4, entry 2). Maximum conversion of the aminocarbonylation reaction was obtained at 120 °C (Table 3.4, entry 4), but the catalyst partially decomposed and Pd black precipitated was formed. The selectivity of both reactions was not almost affected by the change of the reaction temperature.

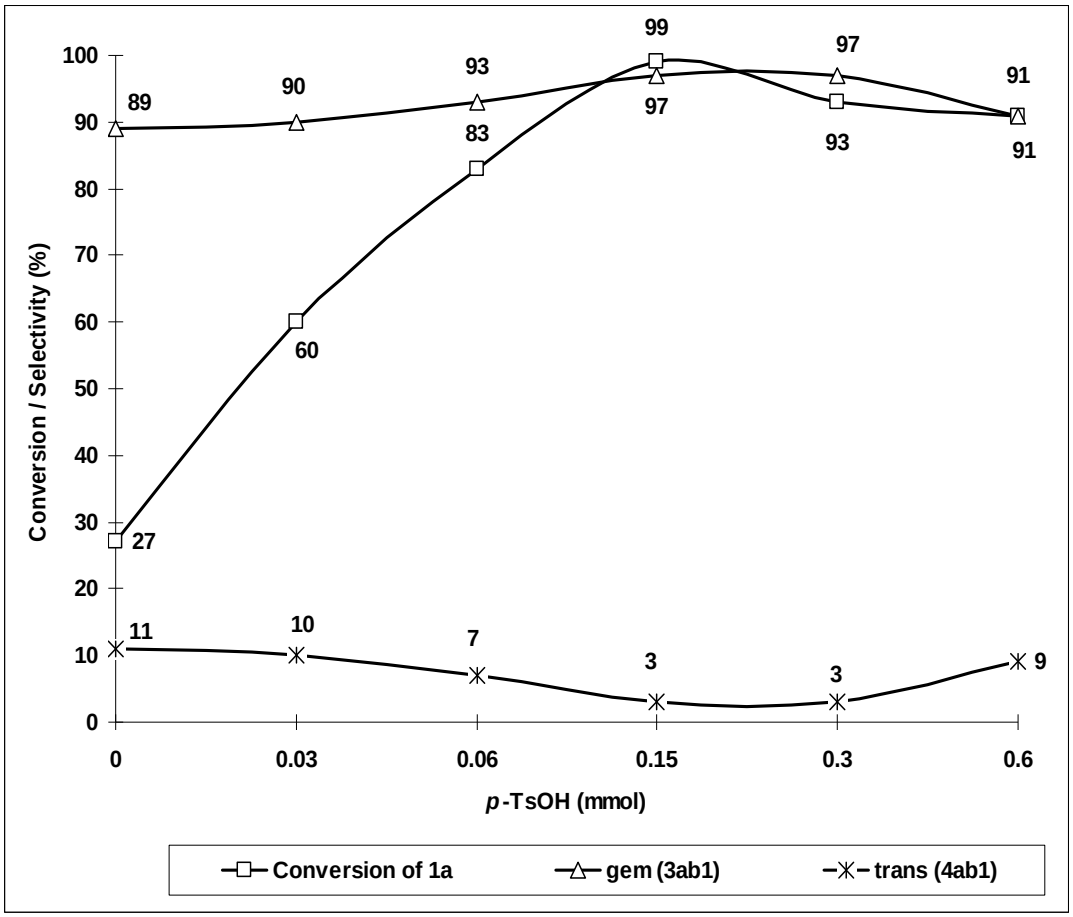

Reaction conditions: $Pd(OAc)_2$ (0.02 mmol), dppb (0.08 mmol), **1a** (2.0 mmol), **$2b_1$** (2.0 mmol), CO (100 psi), CH_3CN (10 ml), 110 °C, 20 h.

Figure 3.3. Aminocarbonylation of phenylacetylene (**1a**) using diisobutylamine (**$2b_1$**) by $Pd(OAc)_2$/dppb/*p*-TsOH.

Effect of the amount of *p*-TsOH.

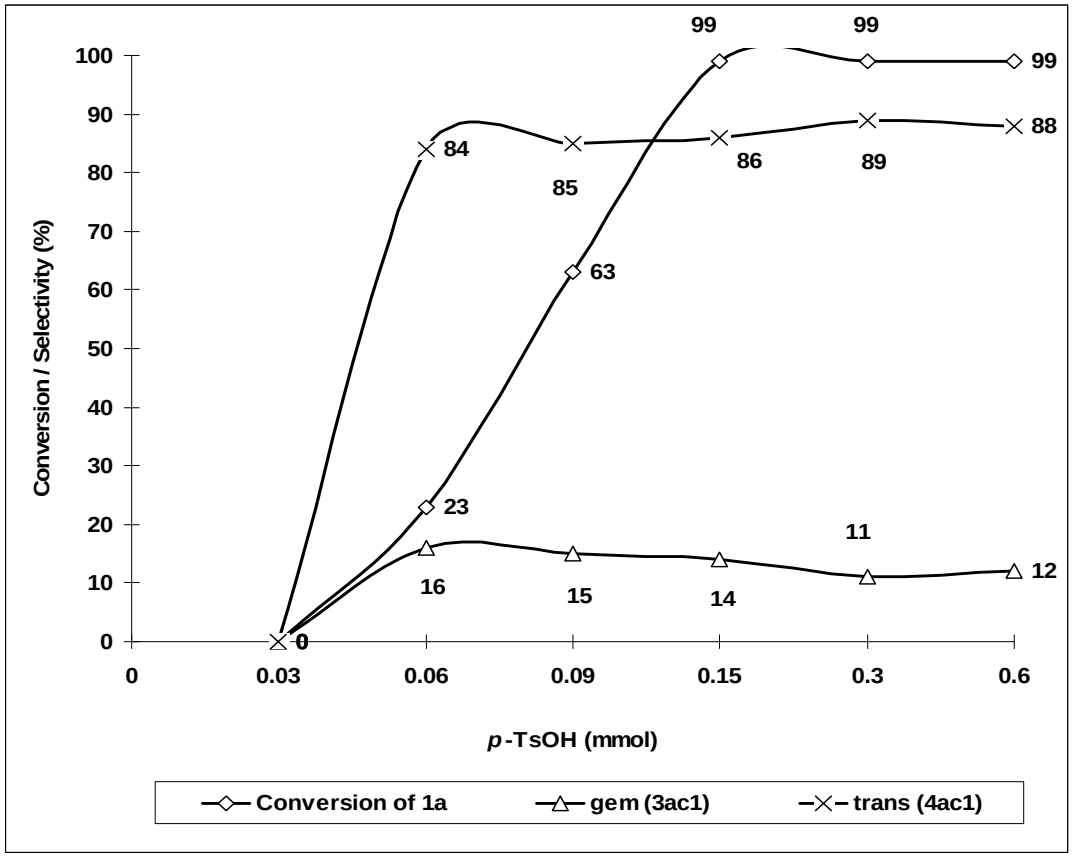

Reaction conditions: $Pd(OAc)_2$ (0.02 mmol), dppb (0.08 mmol), **1a** (2.0 mmol), **2c$_1$** (8.0 mmol), CO (100 psi), CH_3CN (10 ml), 110 °C, 1 h.

Figure 3.4. Alkoxycarbonylation of phenylacetylene (**1a**) to methanol (**2c$_1$**) by $Pd(OAc)_2$/dppb/*p*-TsOH.

Effect of the amount of *p*-TsOH.

Table 3.4. Palladium(II)-catalyzed aminocarbonylation and alkoxycarbonylation of phenylacetylene (**1a**) using diisobutylamine (**$2b_1$**) and methanol (**$2c_1$**). Effect of the temperature.[a]

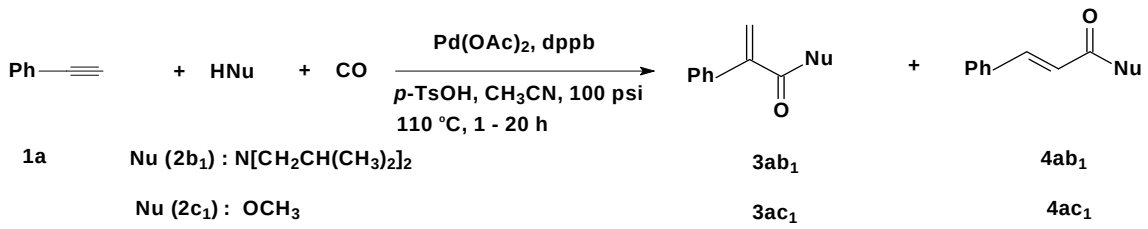

Entry	Temperature (°C)	Conversion 1a (%)[b]		Product Distribution[c] (%)	
		$2b_1$	**$2c_1$**	**$3ab_1$ / $4ab_1$**	**$3ac_1$ / $4ac_1$**
1	90	30	30	88 / 12	10 / 90
2	100	57	99	97 / 3	11 / 89
3	110	93	99	97 / 3	12 / 88
4	120	99	99	96 / 4	14 / 86

[a] Reaction conditions: $Pd(OAc)_2$ (0.02 mmol), dppb (0.08 mmol), phenylacetylene (2.0 mmol), diisobutylamine (**$2b_1$**) (2.0 mmol) or methanol (**$2c_1$**) (8.0 mmol), CO (100 psi), *p*-TsOH (0.3 mmol), CH_3CN (10 ml), 20 h (**1a+$2b_1$**) and 1 h (**1a+$2c_1$**).

[b] Determined by GC based on phenylacetylene.

[c] Determined by GC and ^1H NMR

3.2.6 Effect of the type of nucleophile

The carbonylative coupling of phenylacetylene (**1a**) with a variety of primary and secondary amines **2b$_{1-6}$** and alcohols **2c$_{1-4}$** was studied. The results are presented in Tables 3.5 and 3.6.

In the aminocarbonylation reaction, no correlation was found between the catalytic activity and the basicity of the amines employed in the carbonylative reactions. Moderate to complete conversions were obtained with different alkyl amines affording the *gem* isomers **3ab$_{1-4}$** in excellent regioselectivity (Table 3.5, entries 1-4). Surprisingly, the employment of aromatic amines **2b$_{5-6}$** with the same catalytic system afforded the *trans* isomer **4ab$_{5-6}$** as a major product**.** Reversing the selectivity of the reaction by changing the type of amine is now reported for the first time for the aminocarbonylation of alkynes. The results obtained with aromatic amines **2b$_{5-6}$** leading to the regioselectively formation of *trans* isomer **4ab$_{5-6}$** were similar to already published data by our laboratory (130).

For alkoxycarbonylation reaction, neither conversion nor selectivity were significantly changed by modifying the type of alcohol used (Table 3.6). Complete conversion and excellent selectivity towards the *trans* isomer **4ac** were obtained with alcohols **2c$_{1-4}$** with different number of carbon atoms. This method provides advantages in terms of both catalytic activity and regioselectivity compared to the systems described in the literature (72). It seems that the alkoxy mechanism is playing a minor role in this process because the initial formation of palladium carboalkoxy decreases with the increase in the number of carbons of alcohols (111,112).

Table 3.5. Aminocarbonylation of phenylacetylene (**1a**) using various amines **2b$_{1-6}$**.[a]

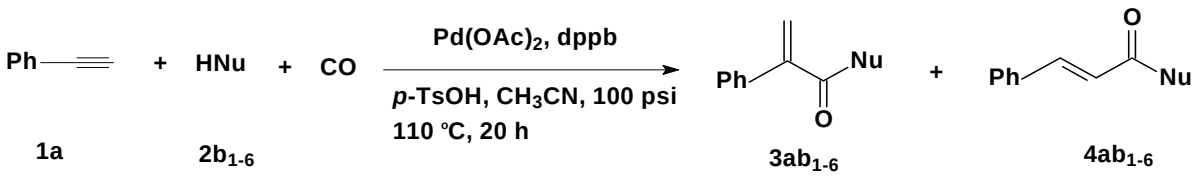

Entry	Amine **2b**	Conversion 1a (%)[b]	Product Distribution[c] (%)	
			3ab	**4ab**
1	Diisobutylamine **2b$_1$**	93	97 **3ab$_1$**	3 **4ab$_1$**
2	*n*-Hexylamine **2b$_2$**	56	95 **3ab$_2$**	5 **4ab$_2$**
3	Cyclohexylamine **2b$_3$**	63	96 **3ab$_3$**	4 **4ab$_3$**
4	Benzylamine **2b$_4$**	100	88 **3ab$_4$**	12 **4ab$_4$**
5	Aniline **2b$_5$**	100	34 **3ab$_5$**	66 **4ab$_5$**
6	N-methylaniline **2b$_6$**	100	44 **3ab$_6$**	56 **4ab$_6$**

[a] Reaction conditions: $Pd(OAc)_2$ (0.02 mmol), dppb (0.08 mmol), amine (2.0 mmol), phenylacetylene (2.0 mmol), *p*-TsOH (0.3 mmol), CH_3CN (10 ml), CO (100 psi), 110 °C, 20 h .

[b] Determined by GC based on phenylacetylene.

[c] Determined by GC and ^1H NMR

Table 3.6. Alkoxycarbonylation of phenylacetylene (**1a**) using various alcohols **2c$_{1-4}$**.[a]

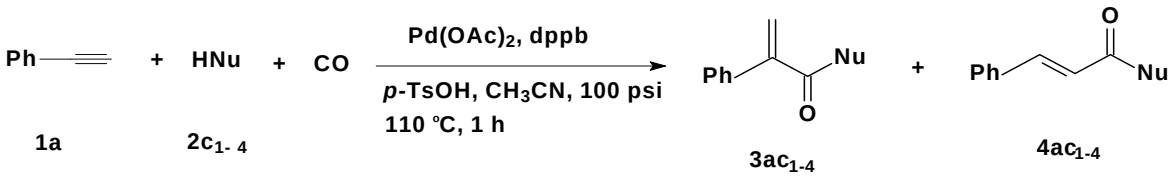

1a **2c$_{1-4}$** **3ac$_{1-4}$** **4ac$_{1-4}$**

Entry	Alcohol 2c	Conversion 1a (%)[b]	Product Distribution[c] (%)	
			3ac	4ac
1	MeOH **2c$_1$**	100	11 **3ac$_1$**	89 **4ac$_1$**
2	EtOH **2c$_2$**	100	11 **3ac$_2$**	89 **4ac$_2$**
3	*n*-PrOH **2c$_3$**	100	15 **3ac$_3$**	85 **4ac$_3$**
4	*i*-PeOH **2c$_4$**	100	13 **3ac$_4$**	87 **4ac$_4$**

[a] Reaction conditions: $Pd(OAc)_2$ (0.02 mmol), dppb (0.08 mmol), alcohol (8.0 mmol), phenylacetylene (2.0 mmol), *p*-TsOH (0.30 mmol), CH_3CN (10 ml), CO (100 psi), 110 °C, 1 h.

[b] Determined by GC based on phenylacetylene.

[c] Determined by GC and ^1H NMR.

It is also important to note that the aminocarbonylation and alkoxycarbonylation reactions take place not only with terminal aromatic alkynes but also selectively with terminal alkyl alkynes such as 1-heptyne **1b** (equation 3.1).

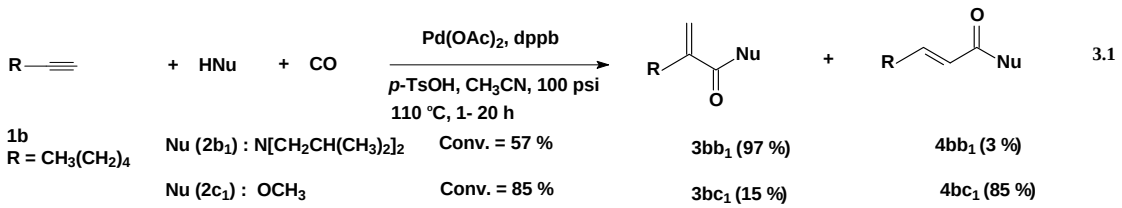

3.2.7 Proposed Mechanisms

The mechanism of the aminocarbonylation and alkoxycarbonylation reactions of terminal alkynes catalyzed by $Pd(OAc)_2$ / dppb / *p*-TsOH / CO is not yet well understood. Based on the literature and the present experimental observations, we tentatively propose two mechanisms for the alkoxycarbonylation and aminocarbonylation of terminal alkynes using different amines and alcohols (Schemes 2.1 and 3.1).

On the basis of the promoting effect of a hydride source such as *p*-TsOH, it is likely that this mechanism plays a major role with alcohol nucleophile (see section 2.2.8). The first step in the proposed mechanism is the formation of active cationic palladium hydride species **A** (Scheme 2.1). This intermediate is formed by the reaction of $Pd(OAc)_2$, dppb and acid (61). The tosylate, in comparison with acetate, seems to be preferable for the formation of such species because it is a less coordinating ligand compared to acetate, so that the subsequent incorporation of alkynes proceeds smoothly (76). Thus, the next proposed step is the coordination of alkyne on **A** to yield **B**. The formation of intermediate **C** includes the insertion of the coordinated alkyne into a Pd-H bond to give a (σ-vinyl) palladium complex followed by the coordination of CO molecule.

Experimental results obtained in this study suggest three factors that control hydride addition to the triple bond to produce *trans* isomer: the nature of the catalyst precursor [$PdCl_2$; $Pd(OAc)_2$], nature of the solvent, and steric and electronic effect of the ligand. Migratory insertion of CO into the palladium-vinyl bond leads to the formation of intermediate **D**. Finally, the methanolysis of the acyl complex produces the *trans* isomer **4** and regenerating the hydride species **A**.

The results of the aminocarbonylation of phenylacetylene are totally different in the presence of the same catalyst system and at the same experimental conditions. The *gem* α,β-unsaturated amides are formed as the major products. We believe that this reaction proceeds via a mechanism similar to alkoxy mechanism we already proposed for the formation of *gem* ester in the alkoxycarbonylation reaction (Scheme 2.2). While we proposed a plausible reaction mechanism (Scheme 3.1), the stepwise details for this aminocarbonylation process are still open to debate and remain subject to further experimental and computational investigations. The key of our suggested mechanism will be the formation of active cationic species **AM'** via the reaction of amine with $Pd(OAc)_2$ and dppb. The experimental results for the effect of type of amine obtained in this study supported the assumption of early coordination of amine nucleophile. This type of coordination makes the electronic effect as predominant factor in determining the activity and selectivity of the reaction. Experimental results for the effect of ligand suggests also an important role of this effect in determining the conversion and selectivity of the aminocarbonylation reaction, and hence the formation of the active species **AM'**.

The next step will involve the coordination of CO molecule forming the intermediate **BM'**. Insertion of CO into Pd-N bond will produce intermediate **CM'** with amide group on palladium center (64). The isolation of traces amount of urea derivatives as byproducts in aminocarbonylation reaction gives more support for the existence of **CM'**. Coordination of alkyne on metal center and then alkyne insertion in Pd-C bond will lead to the formation of intermediate **EM'**. The final step will be the protonolysis of intermediates **EM'** yielding the final *gem* product and the active startup species **AM'**. The role of *p*-TsOH in enhancing the catalytic activity of the aminocarbonylation reaction can be explained by its utility in promoting the protonolysis step.

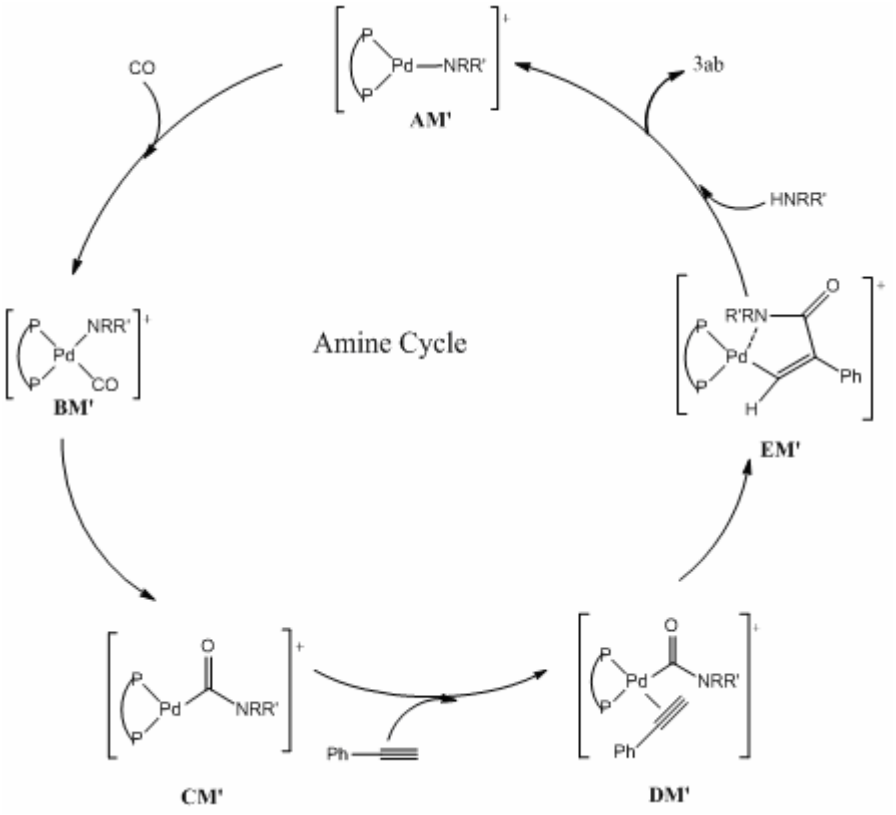

Scheme 3.1. Palladium-catalyzed aminocarbonylation of phenylacetylene. Palladium-amine pathway leading to 2-acrylamides

3.3 Conclusions

The regioselective control in the synthesis of 2-acrylamides **3ab** and cinnamate esters **4ac** was achieved by the aminocarbonylation and alkoxycarbonylation of phenylacetylene (**1a**) using various amines and alcohols, respectively. A simple catalytic system $Pd(OAc)_2$/ dppb / *p*-TsOH / CH_3CN / CO under relatively mild experimental conditions was used. The selectivity of the reactions depends strongly on the type of nucleophile. However, the nature of the catalyst precursor, the type of solvent, and the steric and electronic effects of the ligand play also a significant role. The results obtained showed great advantages in terms of both catalytic activity and regioselectivity in producing the 2-acrylamides **3ab** and cinnamate esters **4ac** compared to other systems reported in the literature.

3.4 Experimental section

3.4.1 Materials and instruments

Alkynes, amines, alcohols, palladium catalysts, phosphine ligands, and *p*-toluenesulphonic acid (*p*-TsOH) are highly pure commercially available materials and were used without any purification. Dry solvents have been used in all experiments. ^{1}H and ^{13}C NMR spectra were recorded on 500 MHz Joel 1500 NMR machine. Chemical shifts (δ) were reported in ppm relative to tetramethyl silane (TMS) using $CDCl_3$. IR spectra were recorded on Perkin-Elmer 16F PC FT-IR spectrometer and reported in wave numbers (cm^{-1}). Gas chromatography (GC) analyses were realized on Agilent GC 6890. The products of the reactions were also analyzed on GC-MS Varian Saturn 2000

equipped with 30 m capillary column (HP-5). Thin-layer chromatography (TLC) analyses were performed on silica gel Merck 60 F254 plates (250 μm layer thickness).

3.4.2 General procedure for the carbonylative coupling of phenylacetylene (1a) with amines or alcohols

A mixture of $Pd(OAc)_2$ (0.02 mmol), 1,4-bis(diphenylphosphino)butane (dppb; 0.08 mmol), *p*-toluenesulphonic acid (*p*-TsOH; 0.3 mmol), alkyne (2.0 mmol) and amine (2.0 mmol) or alcohol (8.0) in 10 ml acetonitrile was placed in the glass liner, equipped with a stirring bar, fitted in 45 ml parr autoclave. The autoclave was vented three times with CO and then pressurized at room temperature with 100 psi CO. The mixture was stirred and heated at 110 ºC for the required time. After cooling, the pressure was released, the reaction mixture was filtered and a sample of this solution was immediately analyzed by GC and GC-MS. The solvent was then removed and the products were separated by preparative TLC (30% EtOAc/petroleum ether 40-70 ^oC). The products were identified by ^1H and ^{13}C NMR, FT-IR and GC-MS analyses. Compounds **3ab$_{1-4}$** prepared in this study are new amides and their spectral data are given below, while the other products (**3ab$_{5-6}$** (62), **4ac$_{1-4}$** (131)) are known compounds. Representative NMR spectra for compound **3ab$_1$** are given in appendix AII.

3.4.3 Spectral and analytical data for some α,β-unsaturated amides

N,N-Diisobutyl-2-phenylpropeneamide (3ab$_1$)

Oil, IR ($CHCl_3$) *v* (cm^{-1}) 1633 (CO); ^1H NMR δ ($CDCl_3$): 0.71 (d, 6H, $CH(\underline{CH_3})_2$, *J* = 5.00 Hz), 0.91 (d, 6H, $CH(\underline{CH_3})_2$, *J* = 5.00 Hz), 1.82 (m, 1H, $\underline{CH}(CH_3)_2$), 2.10 (m, 1H,

CH$(CH_3)_2$), 2.99 (d, 2H, NCH_2, *J* = 7.50 Hz), 3.31 (d, 2H, NCH_2, *J* = 7.50 Hz), 5.28 (d, 1H, $=CH_2$, *J* = 1.50 Hz), 5.64 (d, 1H, $=CH_2$, *J* = 1.50 Hz), 7.22-7.45 (m, 5H arom.); ^{13}C NMR δ ($CDCl_3$): 19.0 $(CH_3)_2$, 19.4 $(CH_3)_2$, 25.4 (CH), 26.0 (CH), 50.4 (NCH_2), 54.9 (NCH_2), 113.6 ($=CH_2$), 125.0 (C4'), 127.6 (C3', C5'), 127.8 (C2', C6'), 135.5 (C1'), 145.4 (C$=CH_2$), 170.4 (C=O); GC-Ms *m/z* 259 (M^+); Analysis calculated for $C_{17}H_{25}NO$ (259.38): C, 78.72; H, 9.71; N, 5.40. Found: C, 78.69; H, 9.83; N, 5.54.

N-Hexyl-2-phenylpropenamide ($3ab_2$)

Oil, IR ($CHCl_3$) *v* (cm^{-1}) 1657 (CO), 3299 (NH); ^1H NMR δ ($CDCl_3$): 0.83 (t, 3H, CH_3CH_2, *J* = 7.72 Hz), 1.21-1.48 (m, 6H, -$(CH_2)_3$-), 2.31 (m, 2H, NCH_2CH_2), 3.28 (t, 2H, NCH_2, *J* = 6.40 Hz), 5.56 (s, 1H, $=CH_2$), 5.98 (s, 1H, $=CH_2$), 6.30 (s, 1H, NH), 7.11-7.72 (m, 5H arom.); ^{13}C NMR δ ($CDCl_3$): 14.0 (CH_3), 22.5 (CH_3CH_2), 26.5 ($CH_3CH_2CH_2CH_2$), 29.3 ($CH_3CH_2CH_2CH_2$), 31.4 (NCH_2CH_2), 39.9 (NCH_2), 120.8 ($=CH_2$), 125.9 (C4'), 127.9 (C3', C5'), 128.6 (C2', C6'), 137.0 (C1'), 145.1 (C$=CH_2$), 167.8 (C=O); GC-Ms *m/z* 231 (M^+); Analysis calculated for $C_{15}H_{21}NO$ (231.33): C, 77.88; H, 9.15; N, 6.05. Found: C, 78.02; H, 9.04; N, 6.17.

N-Cyclohexyl-2-phenylpropenamide ($3ab_3$)

White solid, m.p 102-104 °C; IR ($CHCl_3$) *v* (cm^{-1}) 1641 (CO), 3279 (NH); ^1H NMR δ ($CDCl_3$): 0.83-2.33 (m, 10H, -$(CH_2)_5$-), 3.88 (m, 1H, NCH), 5.58 (d, 1H, $=CH_2$, *J* = 1.60 Hz), 5.79 (s, 1H, NH), 6.03 (d, 1H, $=CH_2$, *J* = 1.60 Hz), 6.98-7.48 (m, 5H arom.); ^{13}C NMR δ ($CDCl_3$): 24.7 ($2CH_2$), 25.7 (CH_2), 32.8 ($2CH_2$), 48.5 (NCH), 121.2 ($=CH_2$), 125.9 (C4'), 127.9 (C3', C5'), 128.6 (C2', C6'), 137.0 (C1'), 145.1 (C$=CH_2$), 166.6 (C=O);

GC-Ms *m/z* 229 (M^+); Analysis calculated for $C_{15}H_{19}NO$ (229.32): C, 78.56; H, 8.35; N, 6.11. Found: C, 78.69; H, 8.41; N, 5.97.

N-Benzyl-2-phenylpropenamide (3ab$_4$)

Oil, IR ($CHCl_3$) *v* (cm^{-1}) 1652 (CO), 3403 (NH); ^{1}H NMR δ ($CDCl_3$): 4.14 (s, 1H, NH), 4.37 (s, 2H, NCH_2), 5.50 (s, 1H, $=CH_2$), 5.90 (s, 1H, $=CH_2$), 6.79-7.62 (m, 10H arom.); ^{13}C NMR δ ($CDCl_3$): 43.1 (NCH_2), 120.7 (C4'), 125.4 (C4 benzyl), 126.5 (C3', C5'), 126.8 (C3, C5 benzyl), 127.4 (C2', C6'), 127.8 (C2, C6 benzyl), 136.2 (C1'), 137.8 (C1 benzyl), 144.3 ($\underline{C}=CH_2$), 167.6 (C=O); GC-Ms *m/z* 237 (M^+); Analysis calculated for $C_{16}H_{15}NO$ (237.29): C, 80.98; H, 6.37; N, 5.90. Found: C, 80.86; H, 6.45; N, 5.98.

CHAPTER 4

PALLADIUM-CATALYZED SELECTIVE ALKOXYCARBONYLATION OF *GEM* α,β-ENAMIDES: A NOVEL APPROACH TOWARDS NEW ω-AMIDO ESTERS AND N-SUBSTITUTED CYCLIC SUCCINIMIDES

4.1 Introduction

N-substituted cyclic succinimides represent a group of imide derivatives that have good antifungal, antidepressant and antituberculosis activities (132,133). Numerous methods have been reported for the synthesis of cyclic succinimides (134-136). However, the availability of simple routes for their synthesis is still limited. Moreover, carbonylation methodology has never been reported as a route for the synthesis of such compounds. The alkoxycarbonylation of enamides represents a potential method for the synthesis of ω-amido esters, which can be converted into *N*-substituted cyclic succinimides. The synthesis of a variety of ω-amido ester precursors in high yields and regioselectivity using carbonylation methodology represents a significant advantage for the synthesis of N-substituted cyclic succinimides. The alkoxycarbonylation of enamides with alcohols normally leads to γ-amido esters and ω-amido esters. Catalytic systems developed for the alkoxycarbonylation of enamides have focused on the production of α,γ-amido esters, since these products are good precursors for the synthesis of amino acids (137-139). To the best of our knowledge, there are no reports describing the production of ω-amido esters regioselectively *via* the alkoxycarbonylation of enamides. Moreover, the

carbonylation of a double bond conjugated to carbonyl and phenyl groups in enamides has not been reported.

Considering the synthetic importance of the alkoxycarbonylation of enamides for the preparation of α,ω-amido esters, we report here in this chapter the palladium-catalyzed synthesis of mono and di-α,ω-amido esters in high yields and regioselectivity. In addition, the synthesized mono and di-ω-amido esters undergo elimination of an alcohol group to yield the corresponding *N*-substituted cyclic succinimides.

4.2 Results and discussion

The alkoxycarbonylation of *N*-cyclohexyl-2-phenylpropenamide (**3b$_3$**, R=Ph**;** R'=cyclohexyl), adopted as a model substrate, using palladium–phosphine systems was studied by varying the reaction parameters (Equation 4.1) in order to optimize the reaction conditions. ω-Amido ester **6b$_3$c$_1$** was the desired product, while the hydrogenation product **5ab$_3$** was considered a by-product of the reaction. It is worth mentioning that the branched isomeric ester that normally results from carbonylation of an internal olefin was not detected in this reaction.

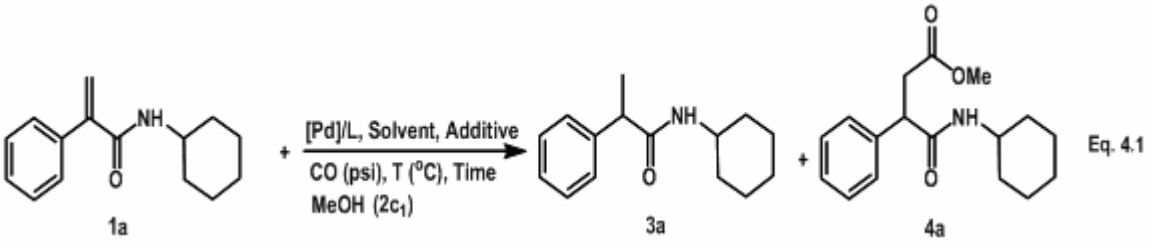

Since varying the solvent had a noticeable influence on both the conversion and the regioselectivity of the catalytic reactions, we carried out the alkoxycarbonylation of **3ab$_3$**

using $Pd(PPh_3)_2Cl_2$ as catalyst in the presence of different solvents and the results are summarized in Table 4.1. No conversion of **3ab$_3$** in *n*-hexane and dichloromethane was observed (Table 4.1, entries 1 and 2), while THF led to moderate conversion, but mainly to formation of the hydrogenation product **5ab$_3$** (Table 4.1, entry 3). Promising regioselectivity in the formation of ω-amido ester **6b$_3$c$_1$** was obtained when acetonitrile was used as the solvent (Table 4.1, entry 4). Our attempts to increase the conversion and the regioselectivity of the alkoxycarbonylation reaction forming **6b$_3$c$_1$** were successful using neat methanol which acts as both the solvent and trapping agent (Table 4.1, entry 5), and also by adding an optimum amount of H_2O (8 mmol) (Table 4.1, entry 6). The addition of water may be necessary to improve the reactivity of the enamide; perhaps a water molecule remains in close proximity to the palladium throughout the catalytic cycle (140).

In order to better understand of the nature of the active palladium catalytic species involved in the alkoxycarbonylation of *gem* enamides, we studied the alkoxycarbonylation of **3ab$_3$** using different palladium complexes (Table 4.2). A preliminary experiment with $Pd(PhCN)_2Cl_2$ as the catalyst precursor showed no catalytic activity in the absence of any added ligand (Table 4.2, entry 1). The crucial role of a phosphine ligand in enhancing the activity of the catalyst system was proved with the addition of monodentate or bidentate phosphine ligands. In these cases, good conversions and complete regioselectivity for the ω-amido ester **6b$_3$c$_1$** were achieved (Table 4.2, entries 2-4). The good conversions obtained with PPh_3 as the ligand (Table 2, entry 4) encouraged us to examine the $Pd(PPh_3)_2Cl_2$ complex for the alkoxycarbonylation of **3ab$_3$** (Table 4.2, entries 5-7); excellent conversions and regioselectivities were obtained

Table 4.1. Palladium-catalyzed alkoxycarbonylation of **3ab$_3$** by $Pd(PPh_3)_2Cl_2$. The effect of the type of solvent.[a]

Entry	Solvent	Conversion **3ab$_3$** (%)[b]	Products Distribution (%)[c]	
			5ab$_3$	**6b$_3$c$_1$**
1	n-hexane	0	-	-
2	CH_2Cl_2	0	-	-
3	THF	64	93	7
4	CH_3CN	40	38	62
5	CH_3OH	84	1	99
6[d]	CH_3OH	100	0	100

[a] Reaction conditions: $Pd(PPh_3)_2Cl_2$ (0.04 mmol), **3ab$_3$** (0.50 mmol), CH_3OH (8.0 mmol), Solvent (8 ml), CO (100 psi), 110 °C, 6 h.

[b] Determined by GC

[c] Determined by GC and ^{1}H-NMR spectroscopy

[d] H_2O = 8 mmol

even in the absence of any added phosphines (Table 4.2, entry 6). The use of $PdCl_2/PPh_3$ as the catalyst system produced comparable activity and regioselectivity as that obtained with $Pd(PPh_3)_2Cl_2$ (Table 4.2, entry 8). Again, the presence of the phosphine ligand was crucial for the reaction since no catalytic activity towards forming **6b$_3$c$_1$** was observed with $PdCl_2$ alone as the catalyst (Table 4.2, entry 9). No catalytic activity was observed in the absence of chloride; $Pd(OAc)_2$ gave no reaction even in the presence of different monophosphine ligands in the alkoxycarbonylation of **3ab$_3$** (Table 4.2, entries 11-13).

The use of $Pd(PPh_3)_2Cl_2$ as the catalyst has been reported before in the alkoxycarbonylation of *N*-vinylphthalimide (141). However, our proposed method showed opposite regioselectivity under milder reaction conditions.

Furthermore, we carried out the alkoxycarbonylation of different enamides, prepared by aminocarbonylation of terminal alkynes (see chapter 3), using various alcohols and the results are presented in Table 4.3. In the majority of cases, the reactions proceeded cleanly to give the desired products **6bc** in high yields (Table 4.3, entries 1-4,6). Surprisingly, the alkoxycarbonylation of enamide precursor **3ab$_5$** was accompanied by formation of the corresponding cyclic product **7b$_5$** in moderate yield (Table 4.3, entry 5). This result encouraged us to pursue this system further to improve the selectivity for the formation of *N*-substituted cyclic succinimide products. It was interesting to observe that the activity and selectivity of the alkoxycarbonylation of enamides was not affected by the type of alcohol (Table 4.3, entries 1-3). On the other hand, the catalyst system promoted alkoxycarbonylation of the geminal bond in **3ab$_7$** selectively, and not the other olefinic bond present in the same molecule (Table 4.3, entry 6).

Table 4.2. Palladium-catalyzed alkoxycarbonylation of **3ab$_3$**. The effect of different palladium complexes and phosphine ligand.[a]

Entry	Catalyst	Ligand	Conversion **3ab$_3$** (%)[b]	Products Distribution (%)[c]	
				5ab$_3$	**6b$_3$c$_1$**
1	$Pd(PhCN)_2Cl_2$	-	0	-	-
2	$Pd(PhCN)_2Cl_2$	t-Bu$(Ph)_2$P	64	0	100
3	$Pd(PhCN)_2Cl_2$	dppb	64	0	100
4	$Pd(PhCN)_2Cl_2$	PPh_3	69	1	99
5	$Pd(PPh_3)_2Cl_2$	t-Bu$(Ph)_2$P	98	0	100
6	$Pd(PPh_3)_2Cl_2$	-	100	0	100
7[d]	$Pd(PPh_3)_2Cl_2$	-	84	1	99
8	$PdCl_2$	PPh_3	89	3	97
9	$PdCl_2$	-	15	100	0
10	$PdCl_2$	t-Bu$(Ph)_2$P	46	10	90
11	$Pd(OAc)_2$	t-Bu$(Ph)_2$P	0	-	-
12	$Pd(OAc)_2$	PPh_3	0	-	-
13	$Pd(PPh_3)_4$	-	0	-	-

[a] Reaction conditions: Catalyst (0.04 mmol), Ligand (0.08 mmol), **3ab$_3$** (0.50 mmol), CH_3OH (8.0 ml), H_2O (8.0 mmol), CO (100 psi), 110 °C, 6 h.

[b] Determined by GC

[c] Determined by GC and ^{1}H-NMR spectroscopy

[d] No H_2O added

Table 4.3. Alkoxycarbonylation of different enamides **3ab** using various alcohols **2c**.[a]

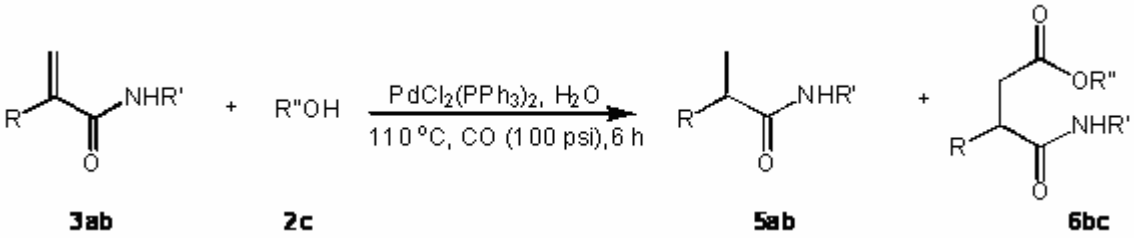

Entry	Enamide 3ab	Alcohol 2c	Conversion 3ab (%)[b]	Product Distribution[c] (%)	
				5ab	6bc
1	**3ab$_3$** R= Ph, R' = Cy	**2c$_1$** R"= Me	100	0	100 **6b$_3$c$_1$**
2	**3ab$_3$**	**2c$_2$** R"= Et	99	3	97 **6b$_3$c$_2$**
3	**3ab$_3$**	**2c$_4$** R"= *i*-pr	93	4	96 **6b$_3$c$_3$**
4	**3ab$_4$** R= Ph, R' = Bnz	**2c$_1$**	100	0	100 **6b$_4$c$_1$**
5[d]	**3ab$_5$** R= Ph, R' = Ph	**2c$_1$**	97	0	100 **6b$_5$c$_1$**
6	**3ab$_7$** R= Cyclohexenyl, R' = Cy	**2c$_1$**	89	0	100 **6b$_7$c$_1$**

[a] Reaction conditions: $Pd(PPh_3)_2Cl_2$ (0.04 mmol), enamide (0.50 mmol), CH_3OH (8.0 ml), H_2O (8.0 mmol), CO (100 psi), 110 °C, 6 h.

[b] Determined by GC and ^{1}H-NMR spectroscopy

[c] Determined by GC

[d] A 56 % yield of cyclic product **7b$_5$** was obtained

It is also important to note that the alkoxycarbonylation reaction takes place selectively with *N*,*N*-disubstituted *gem*-enamides also, e.g. **3ab$_8$** (equation 4.2).

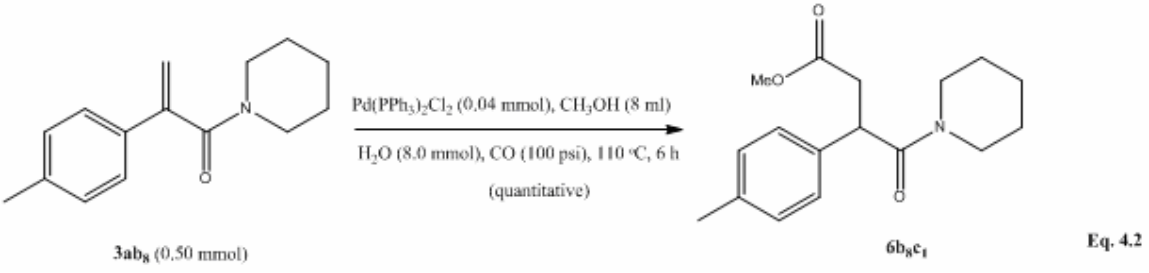

3ab$_8$ (0.50 mmol) **6b$_8$c$_1$** Eq. 4.2

The successful preparation of the ω-amido esters **6bc** encouraged us to examine the cyclization of these compounds to afford the corresponding *N*-substituted cyclic succinimides **7b** (Equation 4.3). The cyclic products were obtained in moderate to excellent yields by reacting **6bc** with CaH as a base in DMF at 50 °C. Addition of the base was essential for this cyclization step, since simple heating gave no product. DMF was the only solvent that led to good conversions compared to other polar and non-polar solvents.

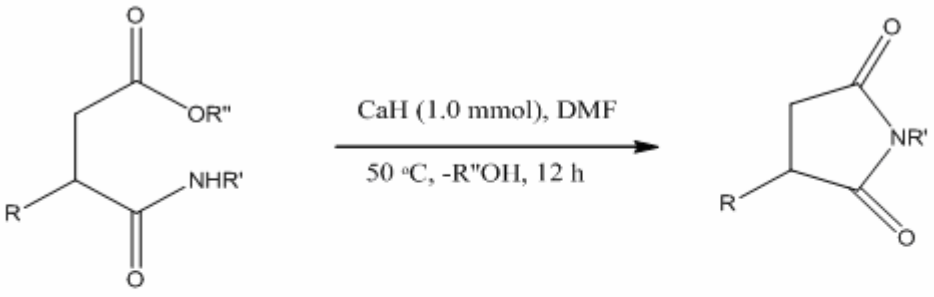

Eq. 4.3

(0.50 mmol)

6b$_3$c$_1$	61%	**7b$_3$**
6b$_4$c$_1$	91%	**7b$_4$**
6b$_7$c$_1$	51 %	**7b$_7$**

Using a similar strategy, novel *N*-substituted di-cyclic succinimides **11** were synthesized in good yields via alkoxycarbonylation of *N*-substituted diacrylate amides **9**, followed by ring closure of the resulting ω-di-amido esters **10** (Scheme 4.1). To the best of our knowledge, the alkoxycarbonylation of diacrylate amides has not been reported in the literature. It is worth noting that compounds **9ab$_3$** and **9bb$_3$** have been successfully synthesized in high yields and regioselectivity via palladium-catalyzed aminocarbonylation of diacetylenes **8a,b** with cyclohexylamine (**2b$_3$**).

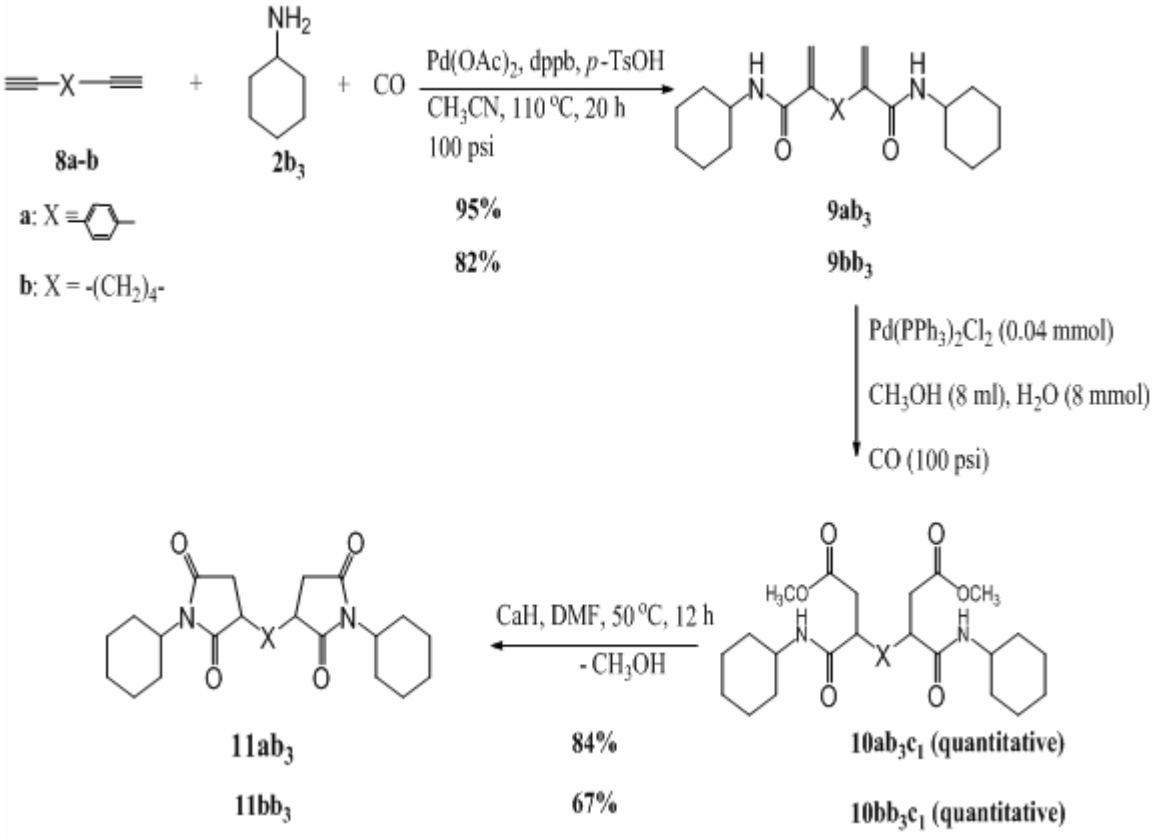

Scheme 4.1. The synthesis of N-substituted di-cyclic succinimides **11** starting from diacetylenes **8** and cyclohexylamine (**2b$_3$**).

4.3 Proposed mechanism

The results reported in Tables 4.1 and 4.2 encouraged us to propose a mechanism for this reaction (Scheme 4.2).

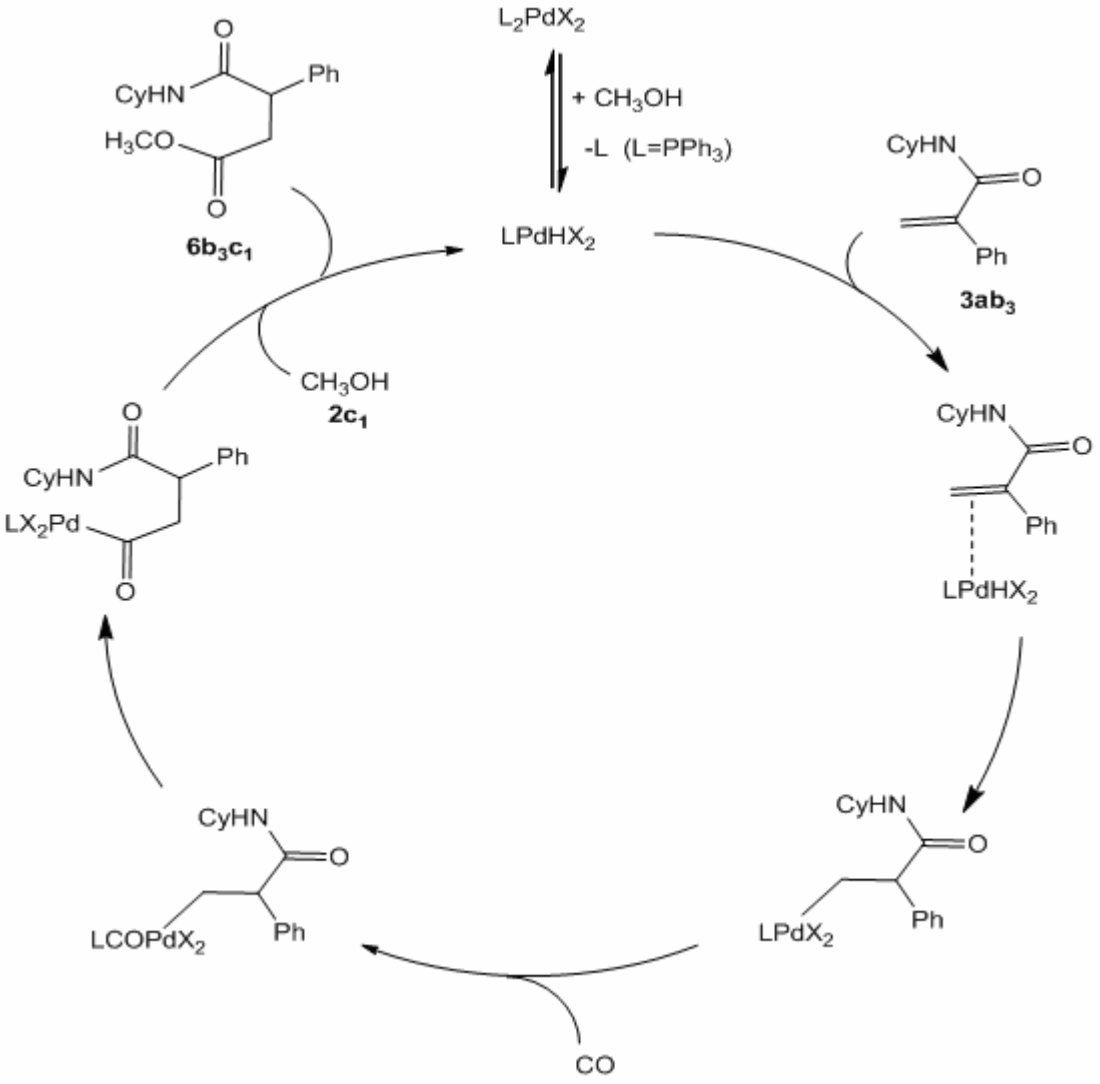

Scheme 4.2. Possible mechanism for alkoxycarbonylation of enamide **3ab$_3$** with **2c$_1$**.

The mechanism suggests the formation of the palladium hydride species from palladium catalyst and methanol. There is a crucial need for chloride and PPh_3 ligands on the palladium center throughout the cycle.

4.4 Conclusions

The synthesis of mono and di-*N*-substituted cyclic succinimides has been successfully achieved via alkoxycarbonylation of enamides followed by ring closure. The alkoxycarbonylation of enamides proceeds smoothly and effectively to afford the corresponding ω-amido esters using the catalyst $Pd(PPh_3)_2Cl_2$ under mild experimental conditions. This method tolerates a variety of enamides and alcohols. This carbonylation methodology also represents an attractive and effective procedure for the synthesis of N-substituted cyclic succinimides.

4.5 Experimental section

4.5.1 Materials and instruments

Alkynes, amines, alcohols, palladium catalysts, phosphine ligands, and *p*-toluenesulphonic acid (*p*-TsOH) are highly pure commercially available materials and were used without any purification. Dry solvents have been used in all experiments. ^{1}H and ^{13}C NMR spectra were recorded on 500 MHz Joel 1500 NMR machine. Chemical shifts (δ) were reported in ppm relative to tetramethyl silane (TMS) using $CDCl_3$. IR spectra were recorded on Perkin-Elmer 16F PC FT-IR spectrometer and reported in wave numbers (cm^{-1}). Gas chromatography (GC) analyses were realized on Agilent GC 6890. The products of the reactions were also analyzed on GC-MS Varian Saturn 2000 equipped with 30 m capillary column (HP-5). Thin-layer chromatography (TLC) analyses were performed on silica gel Merck 60 F254 plates (250 μm layer thickness).

4.5.2. General procedure for the synthesis of enamides and diacrylate amides

Enamides **3ab$_{3,4,7,8}$** were synthesized according to procedure in section 3.4.2, while enamide **3ab$_5$** was prepared using the reference literature method (62). **3ab$_7$** and **3ab$_8$** are novel enamides while enamides **3ab$_{3\text{-}5}$** are known and their spectral data are reported in section 3.4.2 and reference 62.

The method reported in section 3.4.2 was adopted for the synthesis of diacrylate amido esters **9ab$_3$** and **9bb$_3$**, but with a slight modification:

A mixture of $Pd(OAc)_2$ (0.02 mmol), 1,4-bis(diphenylphosphino)butane (dppb, 0.08 mmol), *p*-toluenesulfonic acid (*p*-TsOH, 0.3 mmol), dialkyne (1.0 mmol) and cyclohexylamine (2.0 mmol) in acetonitrile (10 ml) was placed in a glass liner, equipped with a stirrer bar, and then placed in a 45 ml Parr autoclave. The autoclave was vented three times with CO and then pressured at room temperature with CO (200 psi). The mixture was stirred and heated at 110 ºC for 24 h. After cooling, the pressure was released, and the products were collected on a filter paper, washed with methanol and dried under vacuum. The products were identified by ^1H and ^{13}C NMR, FT-IR and EI-MS analyses.

2-Cyclohexenyl-N-cyclohexylacrylamide (**3ab$_7$**):

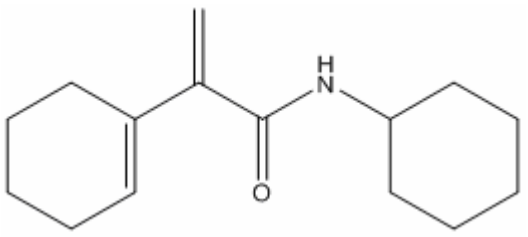

White solid, m.p 120-121 °C; IR (KBr) *v* (cm^{-1}): 1637 (CO), 3287 (NH); ^{1}H NMR δ ($CDCl_3$): 1.14-2.34 (m, 18H, -$(CH_2)_5$- amine and -$(CH_2)_4$- alkyne moiety), 3.84 (m, 1H, NCH), 5.18 (s, 1H$_\alpha$, =CH_2), 5.29 (s, 1H$_\beta$, =CH_2), 5.69 (t, 1H, =CH, *J* = 6.20 Hz), 5.99 (brs, 1H, NH); ^{13}C NMR δ ($CDCl_3$): 21.8, 22.4, 24.7, 25.5, 33.0, 47.9, 48.1, 112.6, 129.3, 133.0, 147.9, 168.8; GC-Ms *m/z* 233 (M^+); Analysis calculated for $C_{15}H_{23}NO$ (233.35): C, 77.21; H, 9.93; N, 6.00. Found: C, 77.25; H, 9.77; N, 5.84.

1-(Piperidin-1-yl)-2-p-tolylprop-2-en-1-one **(3ab$_8$)**:

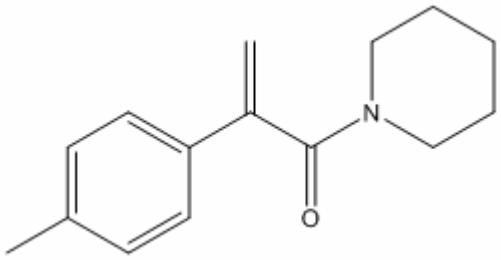

Oil, IR ($CHCl_3$) *v* (cm^{-1}) 1631 (CO); ^{1}H NMR δ ($CDCl_3$): 1.59 (m, 2H, CH_2 piperidinyl ring), 2.31 (s, 3H, CH_3 tolyl), 2.33 (m, 4H, CH_2 piperidinyl ring), 3.27 (t, 2H, NCH_2, *J* = 4.85 Hz), 3.65 (t, 2H, NCH_2, *J* = 4.85 Hz), 5.25 (s, 1H, =CH_2), 5.65 (s, 1H, =CH_2), 7.14 (d, 2H arom., *J* = 7.30), 7.37 (d, 2H arom., *J* = 7.30); ^{13}C NMR δ ($CDCl_3$): 21.1, 24.4, 25.6, 26.2, 42.3, 47.9, 112.2, 125.5, 129.4, 132.7, 138.4, 145.0, 169.3; GC-Ms *m/z* 229 (M^+); Analysis calculated for $C_{15}H_{19}NO$ (229.14): C, 78.62; H, 8.36; N, 6.11. Found: C, 78.55; H, 8.29; N, 6.22.

2,2'-(1,4-Phenylene)bis(N-cyclohexylacrylamide) (**9ab$_3$**):

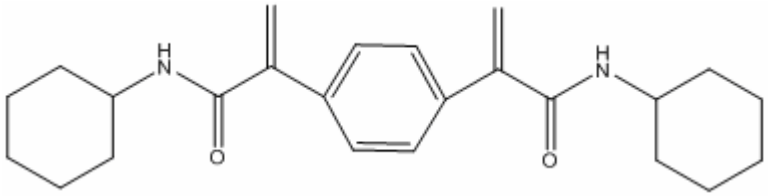

White solid, m.p 215-216 °C; IR (KBr) *v* (cm^{-1}): 1636 (CO), 3263 (NH); ^{1}H NMR δ ($CDCl_3$): 1.10-1.97 (m, 20H, -$(CH_2)_5$-), 3.91 (m, 2H, NCH), 5.63 (br s, 2H, NH), 5.65 (s, $2H_\alpha$, =CH_2), 6.02 (s, $2H_\beta$, =CH_2), 7.40 (s, 4H arom.); ^{13}C NMR δ ($CDCl_3$): 24.8, 25.4, 32.9, 48.5, 121.1, 128.1, 137.0, 144.7, 166.5; EI-Ms *m/z* 380 (M^+); Analysis calculated for $C_{24}H_{32}N_2O_2$ (380.64): C, 75.73; H, 8.47; N, 7.39. Found: C, 75.66; H, 8.43; N, 7.33.

N^1,N^8-Dicyclohexyl-2,7-dimethyleneoctanediamide (**$9bb_3$**):

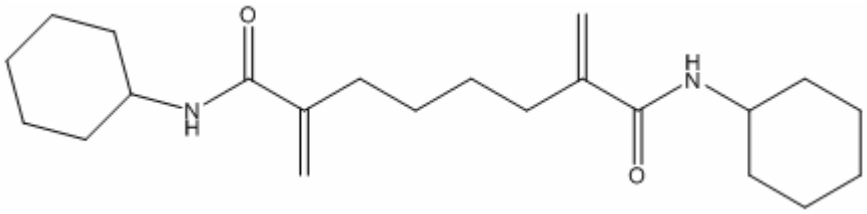

White solid, m.p 153-154 °C; IR (KBr) *v* (cm^{-1}): 1615 (CO), 3286 (NH); ^{1}H NMR δ ($CDCl_3$): 1.15-2.31 (m, 28H, CH_2 in amine and alkyne moeity), 3.81 (m, 2H, NCH), 5.21 (s, $2H_\alpha$, =CH_2), 5.51 (s, $2H_\beta$, =CH_2), 5.71 (brs, 2H, NH); ^{13}C NMR δ ($CDCl_3$): 24.9, 25.5, 27.5, 32.1, 33.1, 48.2, 116.8, 146.0, 168.1; EI-Ms *m/z* 360 (M^+); Analysis calculated for $C_{22}H_{36}N_2O_2$ (360.53): C, 73.29; H, 10.06; N, 7.77. Found: C, 73.52; H, 9.96; N, 7.84.

4.5.3 General procedure for the alkoxycarbonylation of mono and diacrylate amides

A mixture of $Pd(PPh_3)_2Cl_2$ (0.04 mmol), enamide (0.5 mmol) and H_2O (8.0 mmol) in methanol (8 ml) was placed in glass liner, equipped with a stirring bar, and placed in a 45 ml Parr autoclave. The autoclave was vented three times with CO and then pressurized at room temperature with CO (100 psi). The mixture was stirred and heated at 110 ºC for 6 h. After cooling, the pressure was released, the reaction mixture was filtered after adding anhydrous Na_2SO_4 and a sample of the filtrate was immediately analyzed by GC and GC-MS. The solvent was removed and the products were separated by preparative TLC (30 % EtOAc/petroleum ether 40-70 ^oC). The products were identified by ^1H and ^{13}C NMR, FT-IR and GC-MS analyses. All the ω-amido esters obtained in this study are new compounds and their spectral data are given below, while the hydrogenation byproduct **5ab$_3$** is a known compound (142).

Methyl 4-(cyclohexylamino)-4-oxo-3-phenylbutanoate (**6b$_3$c$_1$**):

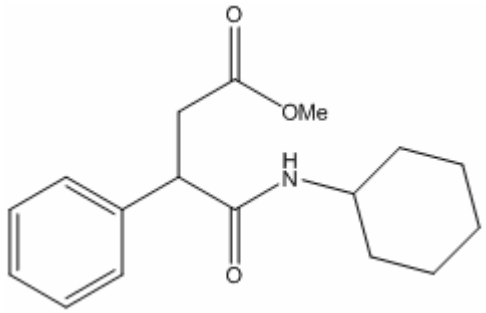

White solid, m.p 98-99 °C, IR (KBr) *v* (cm^{-1}): 1637 (CO amide), 1729 (CO ester), 3272 (NH); ^1H NMR δ ($CDCl_3$): 0.90-1.81 (m, 10H, -$(CH_2)_5$-), 2.26 (m, 1H$_\alpha$, $\underline{CH_2}$COOMe), 3.12 (m, 1H$_\beta$, $\underline{CH_2}$COOMe), 3.57 (s, 3H, OCH_3), 3.60 (m, 1H, Ph$\underline{CH}$), 3.85 (m, 1H, NCH), 5.65 (brs, 1H, NH), 7.24-7.87 (m, 5H arom.); ^{13}C NMR δ ($CDCl_3$): 24.6, 25.2, 32.4, 32.6, 37.6, 48.2, 48.3, 51.5, 127.4, 127.7, 128.8, 131.9, 139.0, 171.1, 172.4; GC-Ms

m/z 289 (M^+); Analysis calculated for $C_{17}H_{23}NO_3$ (289.36): C, 70.56; H, 8.01; N, 4.84. Found: C, 70.71; H, 7.97; N, 5.03.

Ethyl 4-(cyclohexylamino)-4-oxo-3-phenylbutanoate (**6b$_3$c$_2$**):

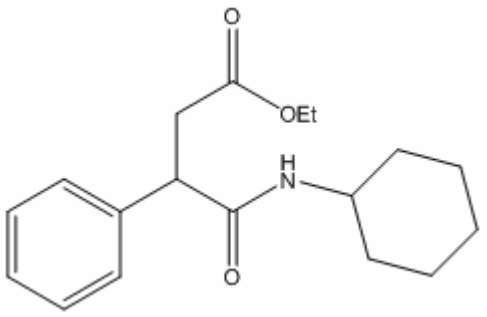

Oil, IR, ($CHCl_3$) *v* (cm^{-1}): 1649 (CO amide), 1730 (CO ester), 3273 (NH); ^{1}H NMR δ ($CDCl_3$): 0.90-1.95 (m, 13H, -$(CH_2)_5$- and CH_3), 2.28 (m, 1H$_\alpha$, $\underline{CH_2}$COOEt), 3.18 (m, 1H$_\beta$, $\underline{CH_2}$COOEt), 3.64 (m, 1H, Ph$\underline{CH}$), 3.84 (m, 1H, NCH), 4.03 (brs, 2H, OCH_2), 5.58 (brs, 1H, NH), 7.09-7.90 (m, 5H arom.); ^{13}C NMR δ ($CDCl_3$): 13.9, 24.1, 24.5, 25.2, 32.4, 32.5, 37.8, 48.3, 48.5, 50.5, 60.4, 127.3, 128.7, 132.4, 139.0, 171.1, 172.0; GC-Ms *m/z* 303 (M^+); Analysis calculated for $C_{18}H_{25}NO_3$ (303.38): C, 71.25; H, 8.31; N, 4.62. Found: C, 70.91; H, 8.22; N, 4.71.

Isopropyl 4-(cyclohexylamino)-4-oxo-3-phenylbutanoate (**6b$_3$c$_3$**):

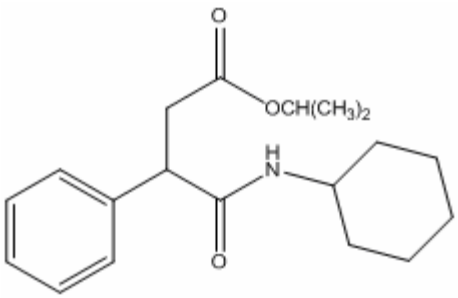

Oil, IR, ($CHCl_3$) *v* (cm^{-1}): 1650 (CO amide), 1720 (CO ester), 3272 (NH); ^1H NMR δ ($CDCl_3$): 0.93-1.97 (m, 16H, -$(CH_2)_5$- and CH_3), 2.33 (m, 1H$_\alpha$, $\underline{CH_2}$COOi-pr), 3.21 (m, 1H$_\beta$, $\underline{CH_2}$COOi-pr), 3.69 (m, 1H, Ph$\underline{CH}$), 3.88 (m, 1H, NCH), 4.94 (brs, 2H, OCH), 5.59 (brs, 1H, NH), 7.14-7.75 (m, 5H arom.); ^{13}C NMR δ ($CDCl_3$): 21.5, 21.6, 24.1, 24.6, 25.3, 30.5, 32.6, 32.7, 38.1, 48.3, 48.6, 50.5, 67.7, 126.9, 127.7, 128.7, 130.4, 132.5, 139.0, 171.2, 171.5; GC-Ms *m/z* 303 (M^+); Analysis calculated for $C_{19}H_{27}NO_3$ (317.41): C, 71.89; H, 8.57; N, 4.41. Found: C, 71.85; H, 8.42; N, 4.45.

Methyl 4-(benzylamino)-4-oxo-3-phenylbutanoate (**6b$_4$c$_1$**):

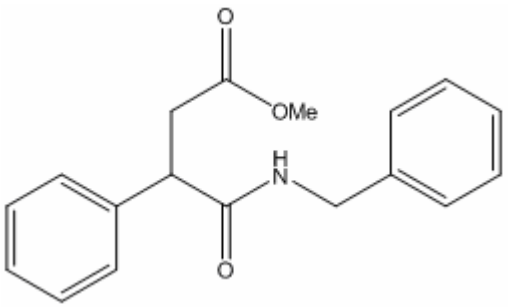

Oil, IR, ($CHCl_3$) *v* (cm^{-1}): 1681 (CO amide), 1722 (CO ester), 3402 (NH); ^1H NMR δ ($CDCl_3$): 2.55 (m, 1H$_\alpha$, $\underline{CH_2}$COOMe), 3.22 (m, 1H$_\beta$, $\underline{CH_2}$COOMe), 3.50 (s, 3H, OCH_3), 4.27 (m, 1H, Ph$\underline{CH}$), 4.62 (s, 2H, NCH_2), 6.70 (brs, 1H, NH), 7.01-7.73 (m, 10H arom.); ^{13}C NMR δ ($CDCl_3$): 37.2, 43.3, 48.0, 51.3, 126.8, 127.0, 127.2, 127.5, 127.7, 128.1, 128.4, 128.5, 128.8, 130.1, 138.1, 138.7, 172.1, 172.2; GC-Ms *m/z* 297 (M^+); Analysis calculated for $C_{18}H_{19}NO_3$ (297.33): C, 72.71; H, 6.44; N, 4.71. Found: C, 72.49; H, 6.53; N, 4.85.

Methyl 4-oxo-3-phenyl-4-(phenylamino)butanoate (**6b$_5$c$_1$**):

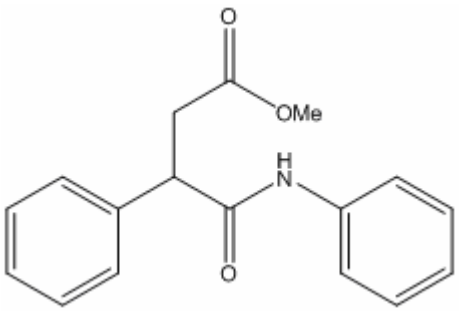

Oil, IR, ($CHCl_3$) *v* (cm^{-1}): 1681 (CO amide), 1711 (CO ester), 3402 (NH); ^{1}H NMR δ ($CDCl_3$): 2.67 (m, 1H$_\alpha$, $\underline{CH_2}$COOMe), 3.00 (m, 1H$_\beta$, $\underline{CH_2}$COOMe), 3.61 (s, 3H, OCH_3), 4.20 (m, 1H, Ph$\underline{CH}$), 6.95 (brs, 1H, NH), 7.15-7.69 (m, 10H arom.); ^{13}C NMR δ ($CDCl_3$): 37.1, 45.7, 51.7, 119.5, 123.6, 126.2, 127.1, 127.7, 128.3, 128.6, 128.9, 131.7, 136.7, 137.8, 138.2, 170.3, 172.1; GC-Ms *m/z* 283 (M^+); Analysis calculated for $C_{17}H_{17}NO_3$ (283.32): C, 72.07; H, 6.05; N, 4.94. Found: C, 69.96; H, 6.18; N, 4.86.

Methyl 3-cyclohexenyl-4-(cyclohexylamino)-4-oxobutanoate (**6b$_7$c$_1$**):

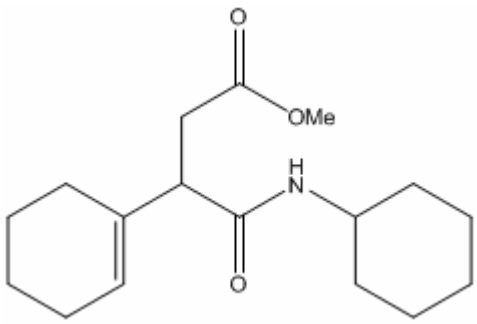

Oil, IR, ($CHCl_3$) *v* (cm^{-1}): 1632 (CO amide), 1733 (CO ester), 3268 (NH); ^{1}H NMR δ ($CDCl_3$): 0.99-2.27 (m, 18H, -$(CH_2)_5$- amine and -$(CH_2)_4$- alkyne moiety), 2.28 (m, 1H$_\alpha$, $\underline{CH_2}$COOMe), 2.80 (m, 1H$_\beta$, $\underline{CH_2}$COOMe), 3.17 (m, 1H, $\underline{CH}CH_2COMe$), 3.50 (s, 3H, OCH_3), 3.59 (m, 1H, NCH), 5.53 (t, 1H, =CH, *J* = 6.26 Hz), 5.76 (brs, 1H, NH); ^{13}C NMR δ ($CDCl_3$): 21.7, 22.4, 24.4, 24.9, 25.1, 32.4, 33.8, 47.7, 50.2, 51.1, 125.6, 128.0,

131.6, 135.4, 170.6, 172.6; GC-Ms *m/z* 293 (M^+); Analysis calculated for $C_{17}H_{27}NO_3$ (293.40): C, 69.59; H, 9.28; N, 4.77. Found: C, 69.66; H, 9.12; N, 4.75.

Methyl 4-oxo-4-(piperidin-1-yl)-3-p-tolylbutanoate (**6b$_8$c$_1$**):

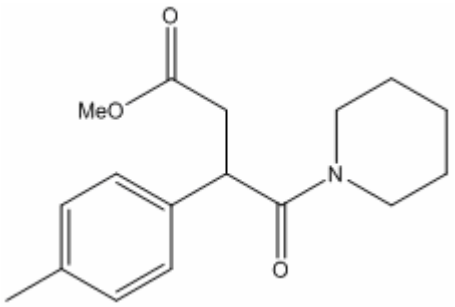

Oil, IR, ($CHCl_3$) *v* (cm^{-1}): 1637 (CO amide), 1736 (CO ester); ^{1}H NMR δ ($CDCl_3$): 1.46 (m, 2H, CH_2 piperidinyl ring), 1.82 (m, 4H, CH_2 piperidinyl ring), 2.54 (s, 3H, CH_3 tolyl), 2.88 (m, 1H$_\alpha$, $\underline{CH_2}$COOMe), 3.04 (m, 1H$_\beta$, $\underline{CH_2}$COOMe), 3.27 (t, 4H, NCH_2, *J* = 4.85 Hz), 3.65 (s, 3H, OCH_3), 4.32 (m, 1H, Ph$\underline{CH}$), 7.14 (d, 2H arom., *J* = 7.30), 7.37 (d, 2H arom., *J* = 7.30); ^{13}C NMR δ ($CDCl_3$): 19.4, 19.7, 20.9, 27.4, 28.1, 39.5, 44.8, 51.2, 52.6, 125.6, 127.2, 136.5, 139.4, 171.9, 172.3; GC-Ms *m/z* 289 (M^+); Analysis calculated for $C_{17}H_{23}NO_3$ (289.16): C, 70.61; H, 8.01; N, 4.84. Found: C, 69.92; H, 8.14; N, 4.95.

Dimethyl 3,3'-(1,4-phenylene)bis(4-(cyclohexylamino)-4-oxobutanoate) (**10ab$_3$c$_1$**):

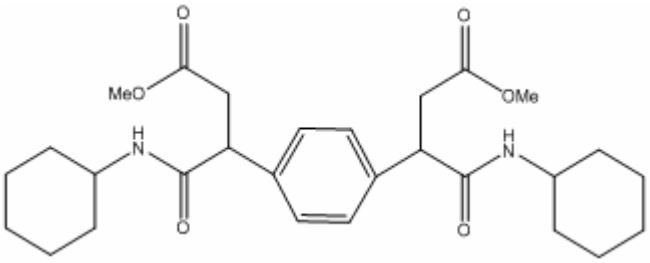

White solid, m.p 175-176 °C, IR (KBr) *v* (cm^{-1}): 1639 (CO amide), 1738 (CO ester), 3324 (NH); ^{1}H NMR δ ($CDCl_3$): 0.95-1.89 (m, 20H, -$(CH_2)_5$-), 2.61 (m, $2H_\alpha$, $\underline{CH_2}$COOMe), 3.22 (m, $2H_\beta$, $\underline{CH_2}$COOMe), 3.63 (s, 6H, OCH_3), 3.69 (m, 2H, Ph$\underline{CH}$), 3.89 (m, 2H, NCH), 5.80 (brs, 2H, NH), 7.37 (s, 4H arom.); ^{13}C NMR δ ($CDCl_3$): 24.5, 25.2, 32.5, 37.5, 48.0, 48.2, 51.5, 128.0, 138.2, 170.9, 172.3; EI-Ms *m/z* 500 (M^+); Analysis calculated for $C_{28}H_{40}N_2O_6$ (500.62): C, 67.18; H, 8.05; N, 5.59. Found: C, 67.24; H, 7.89; N, 5.64.

Dimethyl 3,8-bis(cyclohexylcarbamoyl)decanedioate (**$10bb_3c_1$**):

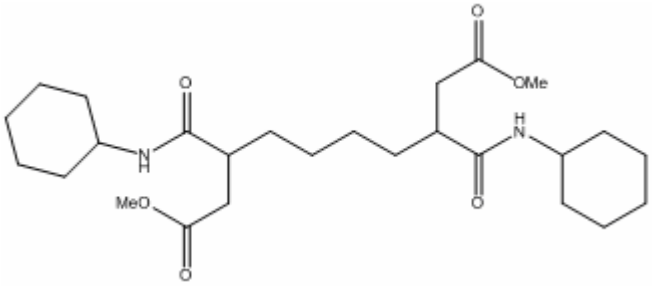

White solid, m.p 139-140 °C, IR (KBr) *v* (cm^{-1}): 1636 (CO amide), 1732 (CO ester), 3284 (NH); ^{1}H NMR δ ($CDCl_3$): 1.14-1.87 (m, 28H, CH_2), 2.37 (m, $2H_\alpha$, $\underline{CH_2}$COOMe), 2.72 (m, $2H_\beta$, $\underline{CH_2}$COOMe), 3.64 (s, 6H, OCH_3), 3.73 (m, 4H, NCH and $\underline{CH}CH_2$COOMe), 6.00 (brs, 2H, NH); ^{13}C NMR δ ($CDCl_3$): 24.7, 25.3, 26.7, 31.9, 32.8, 36.6, 42.7, 47.9, 51.4, 172.8, 173.1; EI-Ms *m/z* 480 (M^+); Analysis calculated for $C_{26}H_{44}N_2O_6$ (480.63): C, 67.18; H, 8.05; N, 5.59. Found: C, 67.24; H, 7.89; N, 5.64.

4.5.4 General procedure for the ring closure of ω-amido esters

In a 50 ml round bottom flask, ω-amido ester (0.50 mmol) and CaH (1.0 mmol) were dissolved in DMF (30 ml) and the mixture heated at 50 °C with stirring for 12 h. The mixture was filtered, poured onto water (30 ml), extracted with dichloromethane (50 ml), concentrated to dryness and purified by preparative TLC plate eluting with a mixture of EtOAc-petroleum ether (2:8) to afford pure products. The cyclic succinimides **7b$_3$**, **7b$_4$** and **7b$_6$** are known compounds (143,133,136), while the other cyclic sccinimides are new products and their spectral data are given below:

3-Cyclohexenyl-1-cyclohexylpyrrolidine-2,5-dione (**7b$_7$**):

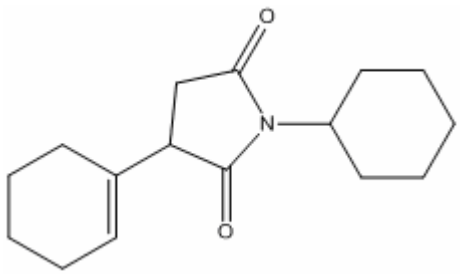

Oil, IR, ($CHCl_3$) *v* (cm^{-1}): 1698 (CO); ^{1}H NMR δ ($CDCl_3$): 1.23-2.17 (m, 18H, -$(CH_2)_5$- amine and -$(CH_2)_4$- alkyne moiety), 2.48 (m, 1H$_\alpha$, $\underline{CH_2}CON$), 2.81 (m, 1H$_\beta$, $\underline{CH_2}CON$), 3.30 (m, 1H, NCH), 3.97 (m, 1H, $\underline{CH}CH_2CON$), 5.63 (t, 1H, =CH, *J* = 6.26 Hz); ^{13}C NMR δ ($CDCl_3$): 21.9, 22.4, 25.0, 25.1, 25.8, 27.7, 28.6, 28.9, 29.4, 33.9, 34.1, 51.8, 126.5, 133.2, 176.8, 178.3; GC-Ms *m/z* 261 (M^+); Analysis calculated for $C_{16}H_{23}NO_2$ (261.17): C, 73.58; H, 8.88; N, 5.36. Found: C, 73.45; H, 8.69; N, 5.44.

3,3'-(1,4-Phenylene)bis(1-cyclohexylpyrrolidine-2,5-dione) (**11ab$_3$**):

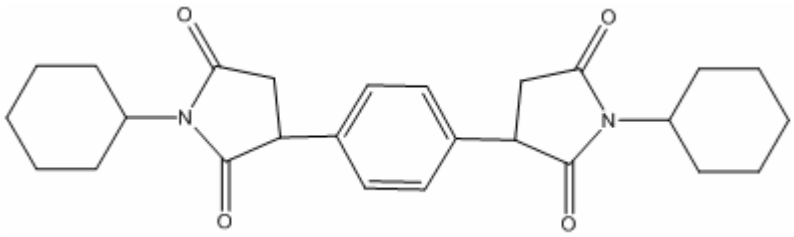

White solid, m.p 185-186 °C; IR, (KBr) *v* (cm^{-1}): 1696 (CO); ^{1}H NMR δ ($CDCl_3$): 1.05-1.76 (m, 20H, -$(CH_2)_5$-), 2.68 (m, 2H$_\alpha$, $\underline{CH_2}CON$), 3.15 (m, 2H$_\beta$, $\underline{CH_2}CON$), 3.60 (m, 2H, Ph$\underline{CH}$), 3.89 (m, 2H, NCH), 7.37 (m,4H arom.); ^{13}C NMR δ ($CDCl_3$): 24.9, 25.7, 28.7, 30.9, 36.8, 45.1, 51.9, 128.4, 131.9, 176.0, 177.5; EI-Ms *m/z* 436 (M^+); Analysis calculated for $C_{26}H_{32}N_2O_4$ (436.54): C, 71.53; H, 7.39; N, 6.41. Found: C, 71.67; H, 7.54; N, 6.22.

3,3'-(Hexane-1,6-diyl)bis(1-cyclohexylpyrrolidine-2,5-dione) (**11bb$_3$**):

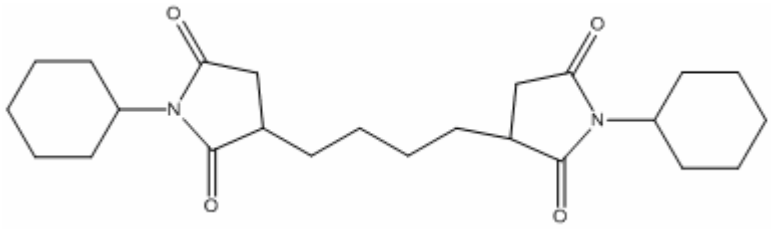

Oil, IR, ($CHCl_3$) *v* (cm^{-1}): 1697 (CO); ^{1}H NMR δ ($CDCl_3$): 1.04-1.84 (m, 28H, CH_2), 2.28 (m, 2H$_\alpha$, $\underline{CH_2}CON$), 2.88 (m, 2H$_\beta$, $\underline{CH_2}CON$), 3.65 (m, 2H, CO$\underline{CH}$), 3.86; (m, 2H, NCH); ^{13}C NMR δ ($CDCl_3$): 24.6, 24.8, 25.7, 28.6, 32.4, 34.1, 39.1, 48.6, 176.4, 179.8; EI-Ms *m/z* 444 (M^+); Analysis calculated for $C_{26}H_{40}N_2O_4$ (444.60): C, 70.24; H, 9.07; N, 6.30. Found: C, 70.47; H, 8.85; N, 6.33.

CHAPTER 5

SYNTHESIS, CHARACTERIZATION, AND CATALYTIC APPLICATIONS OF NEW BINUCLEAR Pd(II) DIIMINE AND PHOSPHINE MIXED-LIGAND COMPLEXES

5.1 Introduction

Palladium complexes based on pyridine-containing ligands have been used effectively as catalysts in different organic and polymeric reactions for the last years. For example, $PdCl_2$(bpy) complex shows high efficiency as a catalyst for Heck reaction in glycerol-organic biphasic medium (144). Pd(II)-catalyzed intramolecular addition of vinylpalladium species to the nitrile groups was achieved in the presence of 2,2'-bipyridine (bpy) as a ligand (145). Pd-2,2'-bipyridyl complex also catalysed the oxidative carbonylation of phenol to diphenyl carbonate (146). Palladium complexes containing bulky dinitrogen ligands (**5.1** – **5.3**) have been used in the olefin-methyl acrylate copolymerization (147).

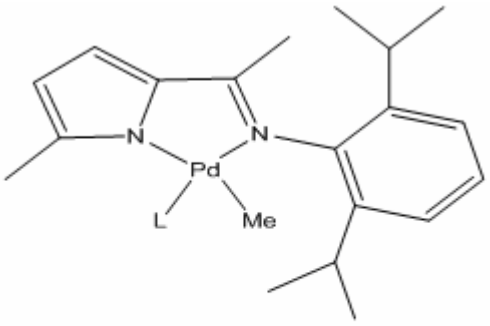

5.1: L = PPh_3

5.2: L = PMe_3

5.3: L = Pyridine

Polynuclear palladium-dinitrogen complexes are receiving more interest nowadays. One of the shortcomings in this research is the lack of versatile and general precursors that allow di- and polynuclear complexes to be constructed from mononuclear sources. Square planar Pd(II) complexes have been used in conjugation with a range pyridine-containing ligands to generate two- or three-dimentional arrays via self-assembly (148). Palladium dinitrogen-diphosphine complexes have been synthesized successfully (**5.4** and **5.5**) and they showed high catalytic activity in CO-ethylene polymerization (149). However, reports on palladium dinitrogen-diphosphine bridged complexes are limited in the literature (150).

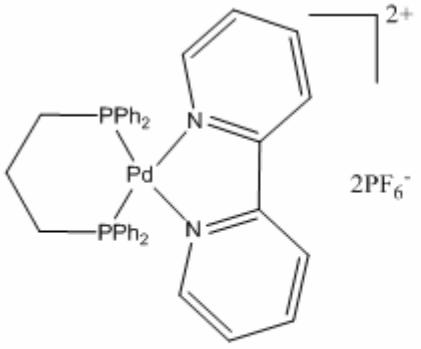

5.4

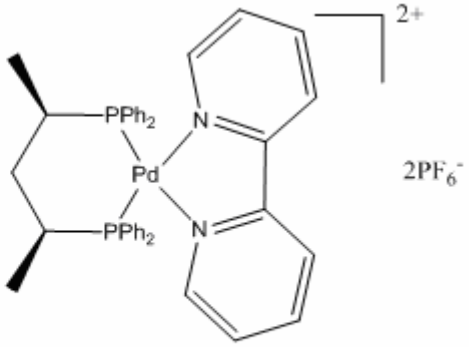

5.5

This chapter consists of the results of the synthesis, characterization and catalytic application of new Pd(II) bimetallic mixed ligand complexes based on chelating diimines and having bridging diphosphines or dimines ligands (Figure 5.1).

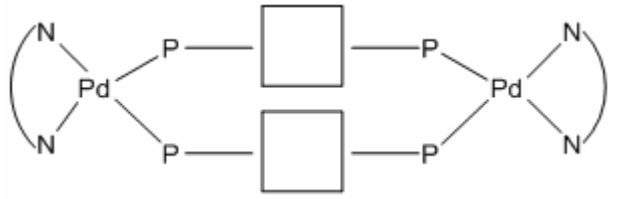

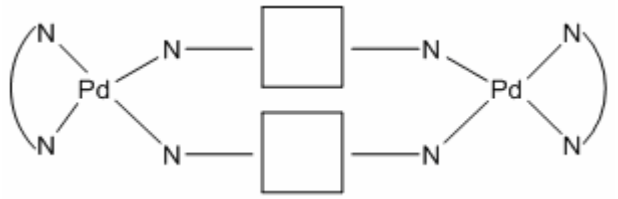

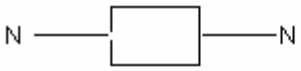

Dinitrogen bridging ligands

4,4'-bipyridine

trans-1,2-bis(4-pyridyl)ethylene

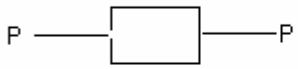

Diphosphine bridging ligands

1,2-bis(diphenylphosphino)acetylene-(DPA)

trans 1,2-bis(diphenylphosphino)ethylene-(DPE)

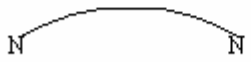

Diimine ligands

4,4'-dimethyl-2,2'-bipyridine

5,5'-dimethyl-2,2'-bipyridine

Figure 5.1. Pd(II) bimetallic mixed ligand complexes.

5.2 Synthetic strategy

- The precursor for the Pd(II) binuclear complexes based on diphosphines and diimines bridging ligands were $[Pd(X)(OTf)_2]$ (OTf = trifluroacetate , X = 2,2'-bipyridine, 4,4'-dimethyl-2,2'-bipyridine, 5,5'-dimethyl-2,2'-bipyridine) which were prepared by mixing 1:1 ratio of $Pd(OAc)_2$ and X ligand, and then adding an excess amount of 100 % HOTf.

- Pd(II) binuclear complexes based on chelating diimines and bridging diphosphines ligands were prepared by reacting Pd-precursor with the bridging diphosphines ligands (DPA or DPE) in 1:1 ratio to produce $[Pd_2(X)_2(DPA)_2](OTf)_4$ and $[Pd_2(X)_2(DPA)_2](OTf)_4$. The triflate ion was converted to hexafluorophosphate by reacting the resulted complexes with an excess amount of NH_4PF_6 (Scheme 5.1).

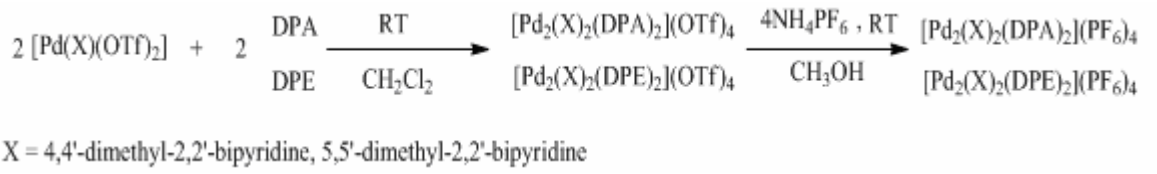

Scheme 5.1. General synthetic strategy for Pd(II) binuclear complexes based on chelating diimines and bridging diphosphine ligands

- In order to produce Pd(II) binuclear complexes based on chelating diimine and bridging diimine ligands, the same Pd-precursor was allowed to react with diimine bridging ligands Y (Y = 4,4'-bipyridine or trans 1,2-bis(4-pyridyl)ethylene) in 1:1 ratio. The resulting complexes $[Pd_2(X)_2(Y)_2](OTf)_4$ were converted into hexafluorophosphate salts form by reacting with an excess amount of NH_4PF_6 (Scheme 5.2).

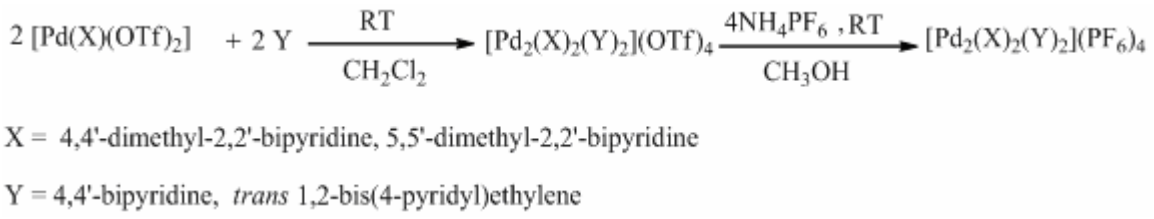

Scheme 5.2. General synthetic strategy for Pd(II) binuclear complexes based on chelating and bridging diimine ligands.

5.3 Results and Discussion

5.3.1 Synthesis of Palladium(II) 4,4'-2,2'-bipyridine bridged diphosphine and diimine ligands complexes

5.3.1.1 (4,4'-Dimethyl-2,2'-bipyridyl)bis(trifluroacetato)palladium(II); [Pd11]

To prepare Pd11, a modified method of Milani et al (151) was used. In 250 mL Erlenmeyer flask, 6.000 mmol (1.347 g) palladium acetate were dissolved in 100 mL of anhydrous methanol. After stirring for 30 minutes, the orange-red mixture was filtered off to remove undissolved palladium acetate. After that 7.200 mmol (1.326 g) 4,4'-dimethyl-2,2'-bipyridine were added to the filtrate under nitrogen with constant stirring. The mixture was then stirred for 30 minutes. The solution turned intense red. Subsequently, 12.3 mL of 100 % trifluroacetic acid were added slowly to the solution to precipitate the trifluroacetate salt (Scheme 5.3). Immediately after the addition of trifluroacetic acid, a light green creamy suspension was obtained. Stirring was continued for another 30 minutes. The mixture was thoroughly washed with cold methanol to remove excess of trifluroacetic acid. The yellow precipitate was dried under vacuum (yield: 2.581 g, 83.2 %).

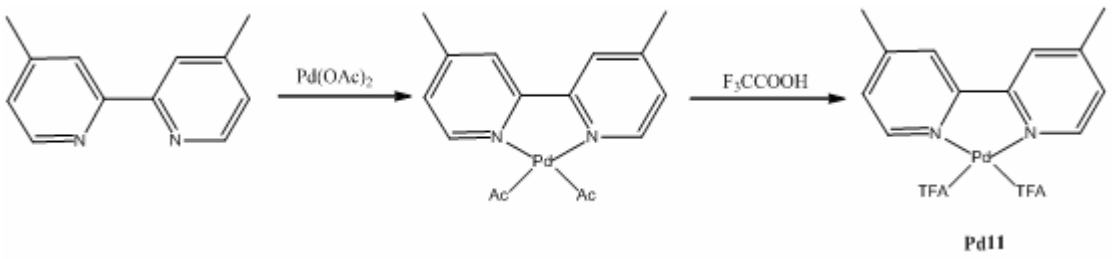

Scheme 5.3. Synthesis of [Pd11]

5.3.1.2 Bis(4,4'-Dimethyl-2,2'-bipyridyl)bis(μ_2-bis(diphenylphosphino)acetylene) palladium(II) hexafluorophosphate; [Pd111]

0.500 mmol (0.257 g) of Pd11 were dissolved in 50 ml acetonitrile in 125 ml Erlenmeyer flask. Separately, 0.500 mmol (0.197 g) of bis(diphenylphosphino)acetylene (DPA) were dissolved in 10 ml methanol. The two solutions were mixed and stirred for 16 h at room temperature. The color of the mixed solution changed from light orange to dark orange and finally it became light yellow. The volume of the later solution was reduced to 50 mL in vacuum, then a solution of NH_4PF_6 (3.0 mmol, 0.49 g) in 5 ml methanol was added. The resulted solution was stirred at room temperature for 30 minutes. A light green precipitate was formed, which was next washed with methanol and dried under vacuum (yield: 0.514 g, 52.7 %).

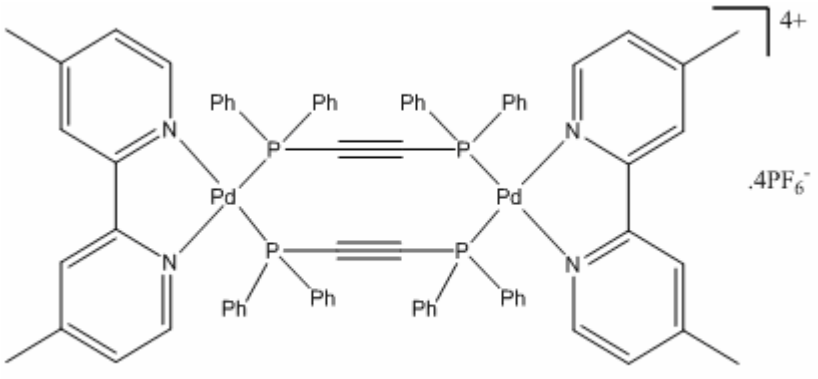

5.3.1.3 Bis(4,4'-Dimethyl-2,2'-bipyridyl)bis(μ_2-1,2-bis(diphenylphosphino)ethylene) palladium(II) hexafluorophosphate; [Pd112]

0.500 mmol (0.257 g) of Pd11 were dissolved in 50 ml acetonitrile in 125 ml Erlenmeyer flask. Separately, 0.500 mmol (0.198 g) of *trans*-1,2-bis(diphenylphosphino)ethylene (DPE) were dissolved in 10 ml methanol. The two solutions were mixed and stirred for 16 h at room temperature. The color of the mixed solution changed from light orange to dark green. The volume of the later solution was reduced to 50 mL in vacuum, then a solution of NH_4PF_6 (3.0 mmol, 0.49 g) in 5 ml methanol was added. The resulted solution was stirred at room temperature for 30 minutes. A light yellow precipitate was formed. It was then washed with methanol and dried under vacuum (yield: 0.965 g, 98.9 %).

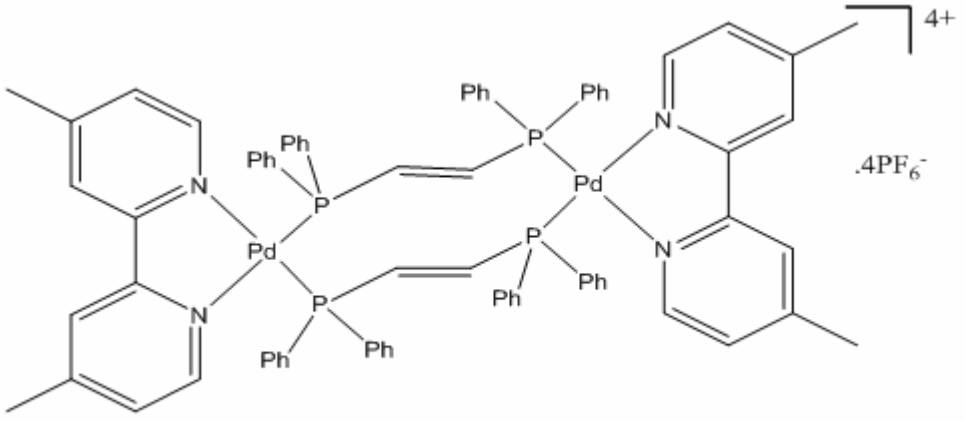

Pd112

5.3.1.4 Bis(4,4'-Dimethyl-2,2'-bipyridyl)bis(μ_2-4,4'-bipyridine)palladium(II) hexafluorophosphate; [Pd113]

0.500 mmol (0.257 g) of Pd11 were dissolved in 50 ml acetonitrile in 125 ml Erlenmeyer flask. Separately, 0.500 mmol (0.078 g) of 4,4'-bipyridine were dissolved in 10 ml methanol. The two solutions were mixed and stirred for 16 h at room temperature. The

color of the mixed solution turned light green. The volume of this solution was reduced to 50 mL in vacuum, then a solution of NH_4PF_6 (3.0 mmol, 0.49 g) in 5 ml methanol was added. The resulted light green creamy solution was stirred at room temperature for 30 minutes. A light green precipitate was formed, which was next washed with methanol and dried under vacuum (yield: 0.725 g, 98.4 %).

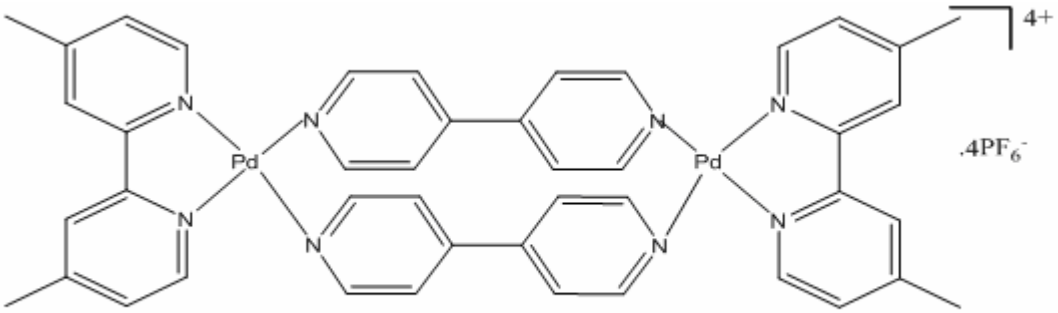

Pd113

5.3.1.5 Bis(4,4'-Dimethyl-2,2'-bipyridyl)bis(μ_2-*trans*-1,2-bis(4-pyridyl)ethylene) palladium(II) hexafluorophosphate; [Pd114]

0.500 mmol (0.257 g) of Pd11 were dissolved in 50 ml acetonitrile in 125 ml Erlenmeyer flask. Separately, 0.500 mmol (0.0911 g) of *trans*-1,2-bis(4-pyridyl)ethylene were dissolved in 10 ml methanol. The two solutions were mixed and stirred for 16 h at room temperature. The color of the mixed solution is light yellow. The volume of this solution was reduced to 50 mL in vacuum, then a solution of NH_4PF_6 (3.0 mmol, 0.49 g) in 5 ml methanol was added. The resulted light green creamy solution was stirred at room temperature for half an hour. A light green precipitate was formed. It was then washed with methanol and dried under vacuum (yield: 0.758 g, 99.4 %).

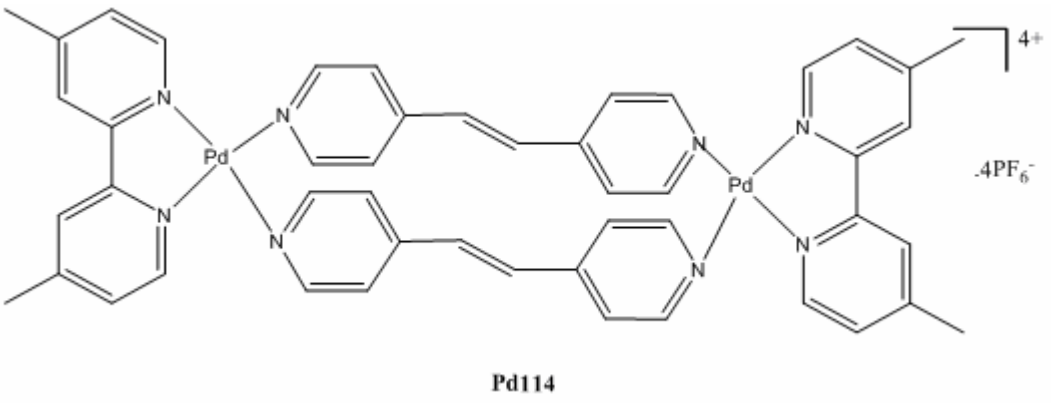

Pd114

5.3.2 (5,5'-Dimethyl-2,2'-bipyridyl)bis(trifluroacetato)palladium(II); [Pd12]

To prepare Pd12, the same method used for the preparation of Pd11 was followed (Scheme 5.4). The color of the final precipitate is light green (yield: 2.114 g, 68.2 %).

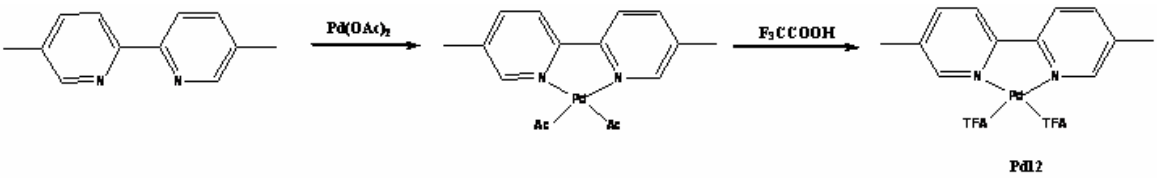

Pd12

Scheme 5.4. Synthesis of [Pd12]

5.3.2.1 Bis(5,5'-Dimethyl-2,2'-bipyridyl)bis(μ_2-bis(diphenylphosphino)acetylene) palladium(II) hexalfluorophosphate; [Pd121]

0.500 mmol (0.257 g) of Pd12 were dissolved in 50 ml acetonitrile/methanol (3:1) in 125 ml Erlenmeyer flask. Separately, 0.500 mmol (0.197 g) of bis(diphenylphosphino)acetylene (DPA) were dissolved in 10 ml methanol. The two solutions were mixed and stirred for 16 h at room temperature. The color of the mixed solution changed from light orange to dark orange and finally it became light yellow. The volume of the light yellow solution was reduced to 50 mL under vacuum, then a solution of NH_4PF_6 (3.0 mmol, 0.49 g) in 5 ml methanol was added. The resulting solution was

stirred at room temperature for half an hour. A light orange precipitate was formed, which was next washed with methanol and dried under vacuum (yield: 0.776 g, 79.6 %).

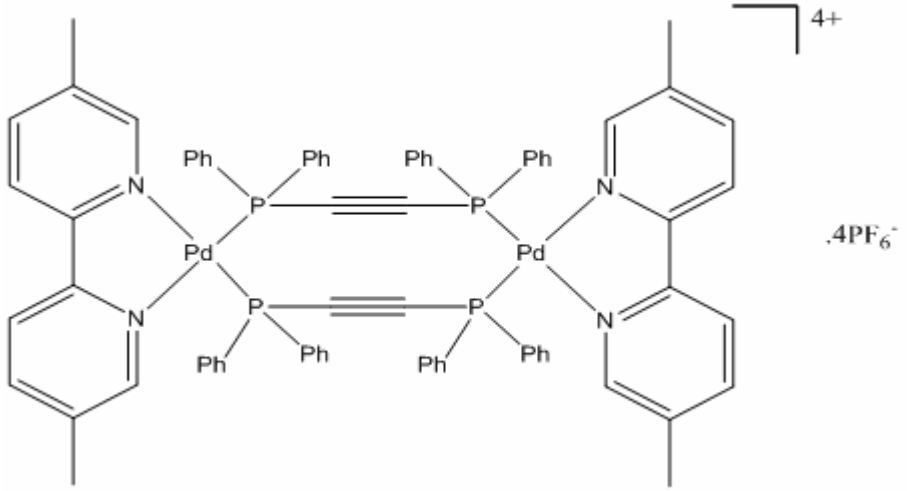

Pd121

5.3.2.2 Bis(5,5'-Dimethyl-2,2'-bipyridyl)bis(μ_2-1,2-bis(diphenylphosphino)ethylene) palladium(II) hexafluorophosphate; [Pd122]

0.500 mmol (0.257 g) of Pd12 were dissolved in 50 ml acetonitrile/methanol (3:1) in 125 ml Erlenmeyer flask. Separately, 0.500 mmol (0.198 g) of *trans*-1,2-bis(diphenylphosphino)ethylene (DPE) were dissolved in 10 ml methanol. The two solutions were mixed and stirred for 16 h at room temperature. The color of the mixed solution changed from light green to dark green. The volume of the light green solution was reduced to 50 mL under vacuum, then a solution of NH_4PF_6 (3.0 mmol, 0.49 g) in 5 ml methanol was added. The resulting solution was stirred at room temperature for 30 minutes. A light green precipitate was formed. It was then washed with methanol and dried under vacuum (yield: 0.964 g, 98.7 %).

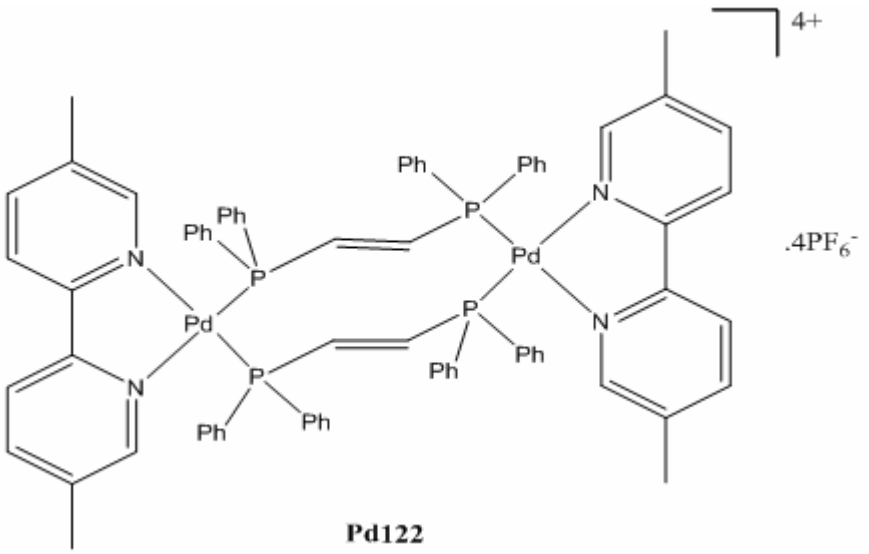

Pd122

5.3.2.3 Bis(4,5'-dimethyl-2,2'-bipyridyl)bis(μ_2-4,4'-bipyridine)palladium(II) hexafluorophosphate; [Pd123]

0.500 mmol (0.257 g) of Pd12 were dissolved in 50 ml acetonitrile/methanol (3:1) in 125 ml Erlenmeyer flask. Separately, 0.50 mmol (0.078 g) of 4,4'-bipyridine were dissolved in 10 ml methanol. The two solutions were mixed and stirred for 16 h at room temperature. The color of the mixed solution is light green. The volume of this solution was reduced to 50 mL under vacuum, then a solution of NH_4PF_6 (3.0 mmol, 0.49 g) in 5 ml methanol was added. The resulted light green creamy solution was stirred at room temperature for 30 minutes. A light green precipitate was formed, washed with methanol and dried under vacuum (yield: 0.720 g, 97.7 %).

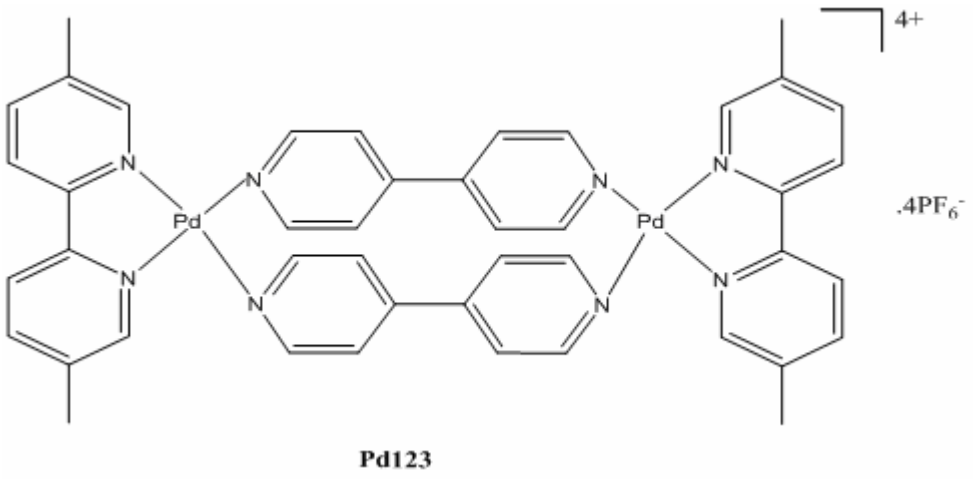

Pd123

5.3.2.4 Bis(5,5'-dimethyl-2,2'-bipyridyl)bis(μ_2-*trans*-1,2-bis(4-pyridyl)ethylene) palladium(II) hexafluorophosphate; [Pd124]

0.500 mmol (0.257 g) of Pd12 were dissolved in 50 ml acetonitrile/methanol (3:1) in 125 ml Erlenmeyer flask. Separately, 0.50 mmol (0.0911 g) of *trans*-1,2-bis(4-pyridyl)ethylene were dissolved in 10 ml methanol. The two solutions were mixed and stirred for 16 h at room temperature. The color of the mixed solution is light green. The volume of this solution was reduced to 50 mL under vacuum, then a solution of NH_4PF_6 (3.0 mmol, 0.49 g) in 5 ml methanol was added. The resulting light green creamy solution was stirred at room temperature for 30 minutes. A light green precipitate was formed, washed with methanol and dried under vacuum (yield: 0.755 g, 99.0 %).

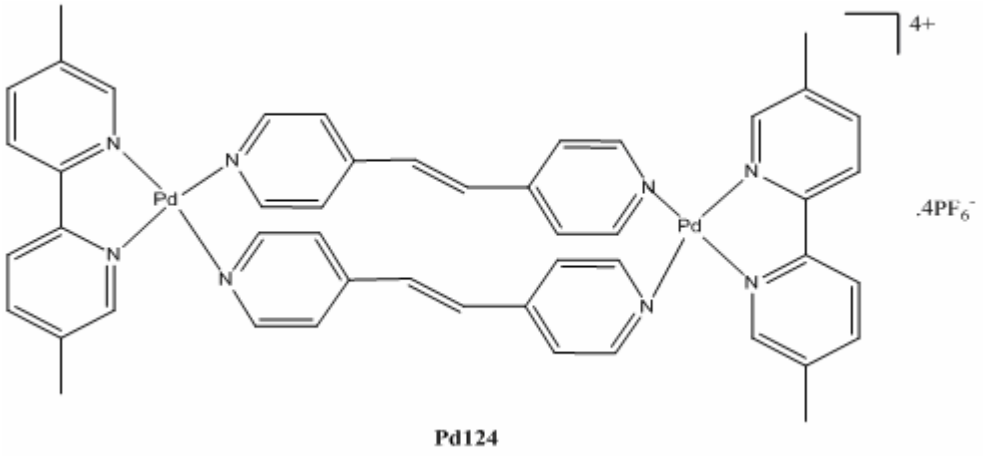

Pd124

5.3.3 Characterization of the complexes

5.3.3.1 Elemental Analysis and Melting points

The elemental analysis and melting point measurements were carried out for all complexes. The samples were dried under vacuum after washing with cold methanol to remove the free ligand and excess of trifluroacetate or ammonium hexaflurophosphate. The results of analysis of the complexes are given in Table 5.1.

Comparison of melting points of these complexes showed that complexes with diimines bridging ligands have slightly higher melting points than complexes containing diphosphines bridging ligands.

5.3.3.2 Ultraviolet and Visible Spectroscopy

The spectra of all complexes were recorded in a mixture of dimethylformamide and dichloromethane (1: 49).

5.3.3.2.1 Electronic spectra of the ligands

The absorption spectra of all chelating and bridging ligands used were recorded (Appendix AIV). The chelating 4,4'-dimethyl-2,2'-bipyridine ligand has two specific absorption bands, one at 283 nm with shoulder at 290 nm and the second one is at 246 nm. The 5,5'-dimethyl-2,2'-bipyridine ligand has similar specific absorption bands, at 290 nm with shoulder at 300 nm and at 247 nm. DPA and DPE as bridging ligands showed one absorption band at 246 nm and 244 nm, respectively, while 1,2-bis(4-pyridyl)ethylene ligand has 3 absorption bands at 300, 288 and 246 nm.

Table 5.1 Results of elemental analysis and melting points of complexes

Complex		C%	H%	N%	M.p (°C)
Pd111	***Calculated***	46.81	3.31	2.87	171-173
	Found	46.55	3.45	3.06	
Pd112	***Calculated***	46.72	3.51	2.87	170-173
	Found	46.44	3.59	2.98	
Pd113	***Calculated***	35.86	2.73	7.60	180-183
	Found	35.67	2.58	8.04	
Pd114	***Calculated***	37.79	2.91	7.34	181-184
	Found	37.88	3.06	7.65	
Pd121	***Calculated***	46.81	3.31	2.87	169-171
	Found	46.68	3.57	3.11	
Pd122	***Calculated***	46.72	3.51	2.87	175-176
	Found	46.83	3.76	3.12	
Pd123	***Calculated***	35.86	2.73	7.60	185-188
	Found	35.59	2.88	7.77	
Pd124	***Calculated***	73.79	2.91	7.34	182-184
	Found	73.96	3.09	7.64	

5.3.3.2.2 Electronic spectra of the complexes

The spectra of all complexes are given in Appendix AIV. The spectra showed absorption bands in the region of 240 – 250 nm similar to those in free ligands but with slight change in λ_{max} upon complexation. Most of the complexes absorb in the region of 350-300 nm with high absorption coefficient ε. These can be assigned to metal to ligand charge transfer (MLCT) transitions. For example, the MLCT transition of Pd123 was observed at 319 nm.

5.3.3.3 Fourier Transform Infrared Spectroscopy (FT-IR)

The FT-IR spectra were recorded using KBr pellets in the range of 4000 – 400 cm^{-1}. The spectra of free ligands and complexes are given in Appendix AIII.

All spectra showed a strong absorption range from 820 to 830 cm^{-1} corresponding to aromatic C-H out of plane bending modes. The spectra showed also a shift in the absorption in the range 1350-1600 cm^{-1} after complexation. These shifts are attributed to the change in electron density in the pyridine ring when the non-bonding pair of electrons on the nitrogen atom is donated to the metal ion (152). The aromatic C=C and C=N stretching absorptions are found in the range of 1400-1650 cm^{-1}.

5.3.3.4 ^{1}H and ^{31}P NMR Spectroscopy

NMR Techniques are highly useful techniques for assigning the complexation process especially for phosphorus-containing ligands. The complexation process for complexes Pd111, Pd112, Pd121 and Pd122 can be easily proved by observing the ^{31}P chemical shifts of free bridging diphosphines ligands and their related complexes, which are

reported in Table 5.2. A significant increase in the chemical shift of ^{31}P coordinating atom by more than 60 δ ppm have been observed for DPA complexes (Table 5.2, entries 1,3,5), while and DPE bridged complexes show an increase in the ^{31}P chemical shift by more than 40 δ ppm (Table 5.2, entries 2,4,6).

For bridging diimine complexes, the change in the ^{1}H NMR chemical shifts of protons in the chelating and bridging diimine ligands can be used to predict the formation of the new Pd-N bonds in complexes Pd113, Pd114, Pd123 and Pd124. The complexation process in the above complexes resulted in an increase in the chemical shifts of ligand protons by the order of 0.10 to 0.80 δ ppm.

A representative ^{1}H NMR spectrum for complex Pd124 is shown in Figure 5.2, while ^{1}H NMR spectra of free ligands and bridged diimines complexes are in appendix AV.

It is worth mentioning that X-ray analysis of the new complexes was not accomplished since trials to obtain good crystal growth in different solvents were not yet successful for any of these complexes.

5.3.4 Catalytic applications of the new complexes

5.3.4.1 Introduction

The use of mononuclear Pd(bpy) complexes as catalyst for the conjugate addition and Heck coupling of arylboronic acid to α,β-unsaturated esters (153), encouraged us to investigate the catalytic activity of the new binuclear Pd(II) complexes in the coupling reactions of arylboronic acid derivatives with various olefins. The conjugate addition of organometallic reagents to olefins represents an example of transmetalation between

Table 5.2 ^{31}P chemical shifts (δ) (in DMSO-d_6) relative to H_3PO_4 for phosphorus-containing free ligand and their complexes.

Entry	Compound	^{31}P Chemical shift (δ)
1	DPA	-33.58
2	DPE	-9.13
3	Pd111	32.13
4	Pd112	34.78
5	Pd121	32.18
6	Pd122	35.63

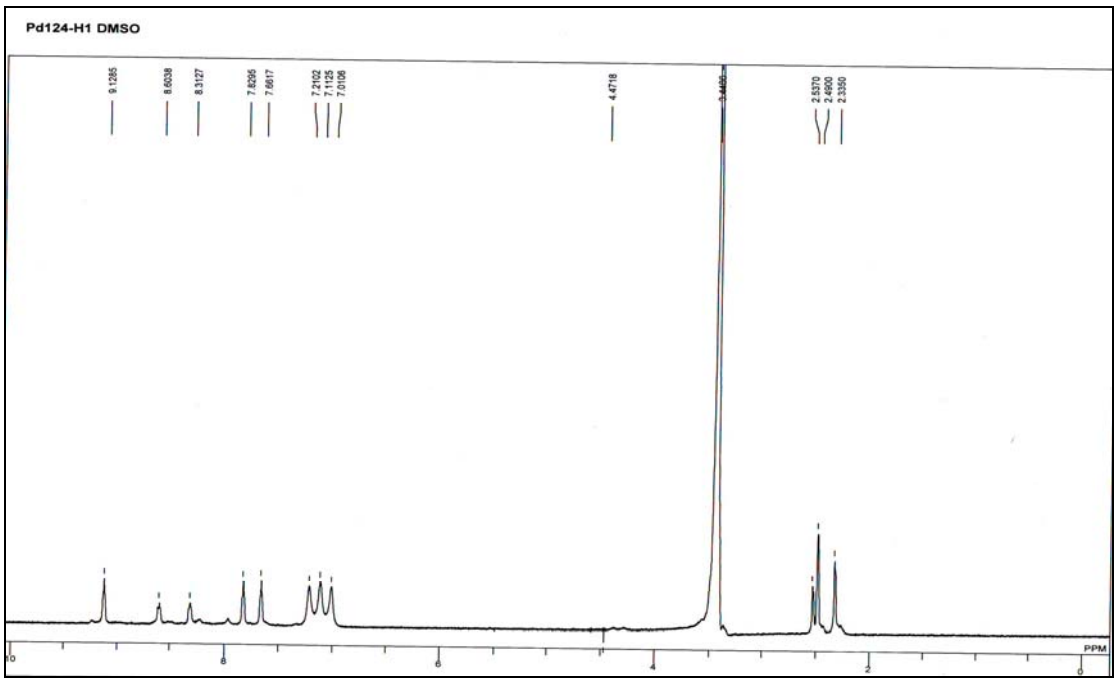

Figure 5.2. ^{1}H NMR spectrum of Pd124.

organometallic reagents and transition metals, which represents a powerful tool for the construction of C-C bonds (154).

After the first report of Heck (155) and further development by Uemura (156) and Mori (157), the transition metal-catalyzed coupling of organoboronic acids and olefins, known as the oxidative Heck reaction, had been extensively investigated (158), particularly by Jung (158c,d,m), Larhed (158b,e,h,i), Lautens (158j), and Brown (158f), mainly because boronic acids are stable, nontoxic, and easily available. The methods developed thus far require the presence of an oxidant to reoxidize Pd(0), for example, $Cu(OAc)_2$, quinone, or O_2, producing stoichiometric amounts of metal waste or being associated with potentially hazardous handling and not suitable for air-sensitive conditions. The development of efficient palladium catalysts for the conjugate addition and Heck coupling of arylboronic acid to olefins without adding any oxidant additives is still a challenging area for researchers.

With any binuclear-bridged synthetic strategy, a certain amount of rigidity is necessary to generate active catalyst in terms of selectivity and yield, although, in most cases, it is a mistaken strategy to target only the most rigid structures, since the proceeding of some elementary steps required in the catalytic cycle will not be possible with rigid catalysts (159).

5.3.4.2 Results and discussion

The coupling reaction of phenylboronic acid (**13a**) with *trans*-cinnamate ester (**4ac$_1$**), adopted as model substrate, was carried out using Pd113 as catalyst precursor in a solvent (Equation 5.1).

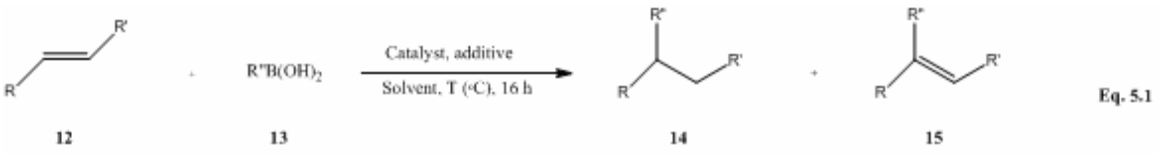

The effect of varying different types of solvent on the yield and chemoselectivity of the reaction was carefully studied and data are reported in Table 5.3. Low to moderate catalytic activities were obtained with all solvents when reaction carried out in 8 mL solvent (Table 5.3, entries 1-8). Although methanol showed the highest conversion of **4ac$_1$** (Table 5.3, entry 3), acetonitrile produced the Heck-coupling product (**15aa**) in higher chemoselectivity (Table 5.3, entry 5). The use of glacial acetic acid (reported in reference 153) mixed with tetrahydrofuran and in the presence of 8.0 mmol water gave a result comparable to acetonitrile experiment (Table 5.3, entries 7,8). Changing the reaction time to approach Pd(bpy) catalytic system reported previously (153) did not significantly enhanced the activity and selectivity of the reaction (Table 5.3, entries 9,10). When smaller volumes of solvent were used, significant improvements in the conversion of **4ac$_1$** were obtained, but surprisingly with increase in the yield of conjugate addition product **14aa** (Table 5.3, entries 11,12). The conversion of **4ac$_1$** reached 92 % by doubling the amount of palladium catalyst ((Table 5.3, entry 13). The addition of acid or base additive to the reaction mixture inhibited the reaction and produced also unexpected change on product distribution (Table 5.3, entries 15,16). The addition of acid additive enhanced the formation of **15aa**, while the addition of base allows the formation of **14aa** chemoselectively, which suggests that the formation of **14aa** and **15aa** takes place via two different catalytic pathways. Trials to increase the yield of **14aa** by adding H_2 or isopropanol were not successful since first additive produced the hydrogenated starting material (Table 5.3, entry 17), and the second one produced the Heck-coupling product

15aa in higher selectivity (Table 5.3, entry 18). As expected, the addition of *p*-benzoquinone oxidant increased the catalytic activity (Table 5.3, entry 19) which can be explained by the role of oxidant in regeneration of Pd(II) after the catalytic cycle (Scheme 5.5) (160).

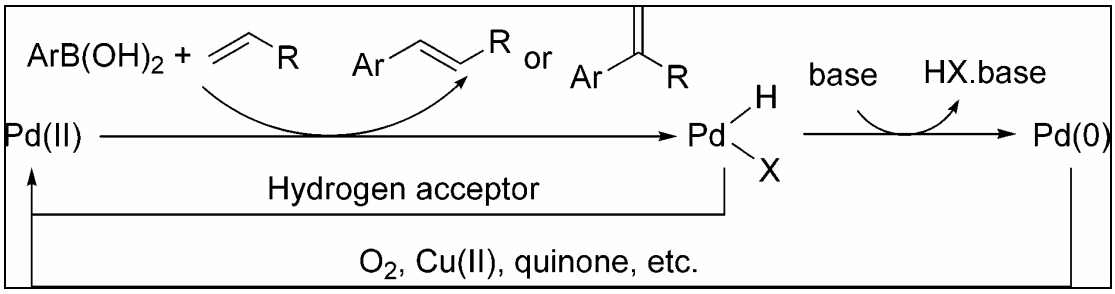

Scheme 5.5. Oxidative coupling of arylboronic acid to olefins.

Next, we examined the catalytic activity of the new binuclear palladium(II)-bridged complexes in the vinylation of arylboronic acid in acetonitrile (4 ml) and at 110 °C (Equation 5.1) and data are summarized in Table 5.4. The catalytic activity of the new complexes ranges from moderate for the bridging diphosphine palladium complexes Pd111 and Pd121 to very good and excellent activity with the other complexes.

It is important to note that the increase in the conversion of **4ac$_1$** was accompanied in most cases with an increase in the chemoselectivity of **14aa**, which encouraged us to conclude that the formation of the conjugate addition product **14aa** was by a thermodynamically controlled process, and the formation of **15a** was by a kinetically controlled process. Theoretical calculations using DFT (B3LYP/6-31G(d)) method have

Table 5.3. The coupling of arylboronic acid (**13a**) to **4ac$_1$** reaction. Effect of varying different solvents.[a]

Entry	Solvent	Additive mmol	Conversion 4ac$_1$ (%)[b]	Products Distribution (%)[c]	
				14aa	15aa
1	THF	-	19	-	100
2	CH_2Cl_2	-	14	6	94
3	CH_3OH	-	58	32	68
4	CH_3COOH	-	13	-	100
5	CH_3CN	-	48	-	100
6	CH_3CN /CH_3COOH (3:1)	H_2O 8.0	31	9	91
7	THF/CH_3COOH (3:1)	H_2O 8.0	48	6	94
8	THF/CH_3COOH (1:1)	H_2O 8.0	41	-	100
9[d]	CH_3CN	-	44	6	94
10[e]	CH_3CN	-	67	16	84
11[f]	CH_3CN	-	76	28	72
12[g]	CH_3CN	-	80	34	66
13[h]	CH_3CN	-	92	36	64
14[f]	CH_3OH	64	64	20	80
15[f]	CH_3CN	*p*-TsOH 0.50	65	8	92
16[f]	CH_3CN	K_2CO_3 0.50	20	100	-
17[i]	CH_3CN	H_2 (100 psi)	-	100	-
18[f]	CH_3CN/*i*-PrOH (1:1)	-	30	2	98
19	CH_3CN	1,4-benzoquinone	90	12	88

[a] Reaction conditions: Pd113 (0.02 mmol), **4ac$_1$** (0.50 mmol), **13a** (1.0 mmol) Solvent (8 ml), 110 °C, 16 h.

[b] Determined by GC

[c] Determined by GC and ^{1}H-NMR

[d] Temperature = 70 °C

[e] Reaction time = 3 days

[f] Solvent = 4 ml

[g] Solvent = 2 ml, [h] Catalyst = 0.04 mmol, [i] 93 % Hydrogenation product

been carried out for determining the most thermodynamically stable product and the results showed that **14aa** is more stable than **15aa** by 30.4 Kcal/mol.

Using the optimized conditions, we then examined the reaction of various arylboronic acids **13a-b** with different olefins. The results are summarized in Table 5.5.

Cinnamate esters **4ac$_{1-2}$** reacted efficiently with **13a** but with lower chemoselectivity in case of **4ac$_1$** (Table 5.5, entries 1,2) even in the absence of any base or oxidant as additives. Comparable reaction conversion and chemoselectivity were obtained when **1a** was allowed to react with phenyboronic acid derivative **13b** (Table 5.5, entry 3). Unsaturated esters containing *geminal* double bond reacted in moderate activity with **13a** (Table 5.5, entries 4,5). Excellent catalytic activity and chemoselectivity of the new palladium complex Pd113 with ketone **12e** is expected since palladium(II) catalysts promote 1,4-additions to unsaturated ketones more efficiently than to unsaturated esters (Table 5.5, entry 6). This is mainly due to a slow equilibration between C-enolate and water-sensetive O-enolate (see mechanism below) for ester derivatives (161). Surprisingly, aldehyde **12f** showed poor reactivity with phenylboronic acid **13a** using the optimized catalyst system (Table 5.5, entry 7). For more screening of different electron-rich and deficient olefins, we explored the reactivity of substrates **12g-i** with **13a** under optimized reaction conditions, where only **12g** was arylated effectively with higher chemoselectivity (72 %) forming the heck-coupling product **15fa** (Table 5.5, entries 8-10).

It is worth noting that compounds **14** and **15** are known compounds and their spectral data are available in literature.

Table 5.4. Coupling of arylboronic acid (**13a)** to **4ac$_1$** catalyzed by new binuclear palladium complexes Pd111-Pd124.[a]

Entry	Complex	Conversion **4ac$_1$** (%)[b]	Products Distribution (%)[c]	
			14aa	**15aa**
1	Pd111	48	20	80
2	Pd112	76	33	67
3	Pd113	76	28	72
4	Pd114	76	33	67
5	Pd121	53	14	86
6	Pd122	85	30	70
7	Pd123	86	38	62
8	Pd124	87	29	71

[a] Reaction conditions: Complex (0.02 mmol), **4ac$_1$** (0.50 mmol), **13**a (1.0 mmol), CH_3CN (4 ml), 110 °C, 16 h.

[b] Determined by GC

[c] Determined by GC and ^{1}H-NMR

Table 5.5. Reaction of arylboronic acids **13a-b** with various olefins.

Entry	Olefin 12	Boronic acid 13	Conversion 12 (%)[b]	Products Distribution (%)[c]	
				14	**15**
1	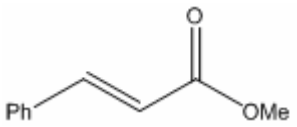 **4ac$_1$**	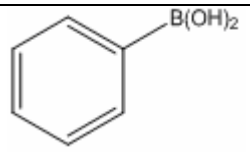 **13a**	76	28 **14aa**	72 **15aa**
2	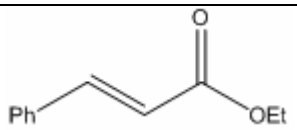 **4ac$_2$**	**13a**	75	40 **14ba**	60 **15ba**
3	**4ac$_1$**	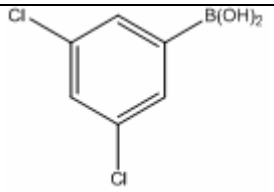 **13b**	72	32 **14ab**	68 **15ab**
4	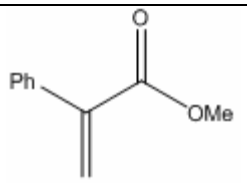 **3ac$_1$**	**13a**	60	36 **14ca**	64 **15ca**
5	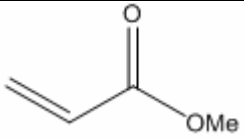 **12d**	**13a**	44	24 **14da**	76 **15da**

Table 5.5. Continued

6[d]	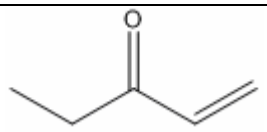 **12e**	**13a**	100	91 **14ea**	9 **15ea**
7	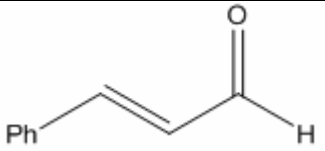 **12f**	**13a**	-	-	-
8	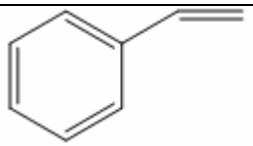 **12g**	**13a**	79	28 **14ga**	72 **15ga**
9	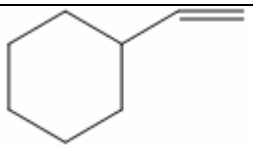 **12h**	**13a**	-	-	-
10	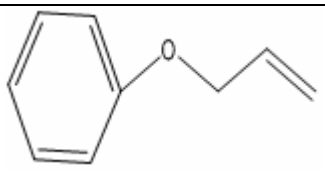 **12i**	**13a**	11	23 **14ia**	77 **15ia**

[a] Reaction conditions: Pd113 (0.02 mmol), **12** (0.50 mmol), **13** (1.0 mmol), CH_3CN (4 mL), 110 °C, 16 h.
[b] Determined by GC
[c] Determined by GC and ^{1}H-NMR
[d] 27 % double conjugate addition products
[e] 82 % Stilbene

5.3.4.3 Proposed mechanism

The coupling of organoboronic acids with alkenes in a Heck-type reaction has been extensively investigated (158). The reaction is known as “oxidative Heck reaction” and involves the use of a Pd(II) catalyst which transmetalates with the organoboron compound to form a Pd-aryl species. After the insertion in the olefinic double bond, the β-hydride elimination leads to the coupling product and to Pd(0) which is re-oxidated to Pd(II) by an additional oxidant. According to mechanistic studies, the presence of a base and water is necessary for the reaction to occur (160). The base leads, via the formation of OH^-, to the generation of a boronate species $[RB(OH)_3]^-$ which undergoes the transmetalation. Without the addition of a base, the energy barrier for the transmetalation process is too high (162).

The proposed general catalytic cycle for the conjugate addition of arylboronic acids is shown in Scheme 5.6 (163). The cationic palladium species **A'** transmetalates to the activated arylboronic acid, giving species **B'**. After coordination of the palladium complex to the carbon-carbon double bond of the enone, the aryl group is transferred to the β position forming α-palladate species **D'**, which is in equilibrium with the Pd-O enolate **E'**. Pd is known to be bounded mainly to the carbon atom in contrast to analogous Rh systems. If the electronic properties of the enolate and its geometry allow the Pd and the hydrogen next to it to be in a *syn* orientation, β-hydride elimination can occur affording the Heck product **15**. Alternatively, the protonolysis of species **D'** or **E'** leads to the conjugate addition product, **14** and the initial cationic species **A'.** Cationic palladium enolates are much more susceptible to hydrolytic Pd-C bond cleavage than neutral palladium species and this is essential to avoid competing β-hydride elimination (164).

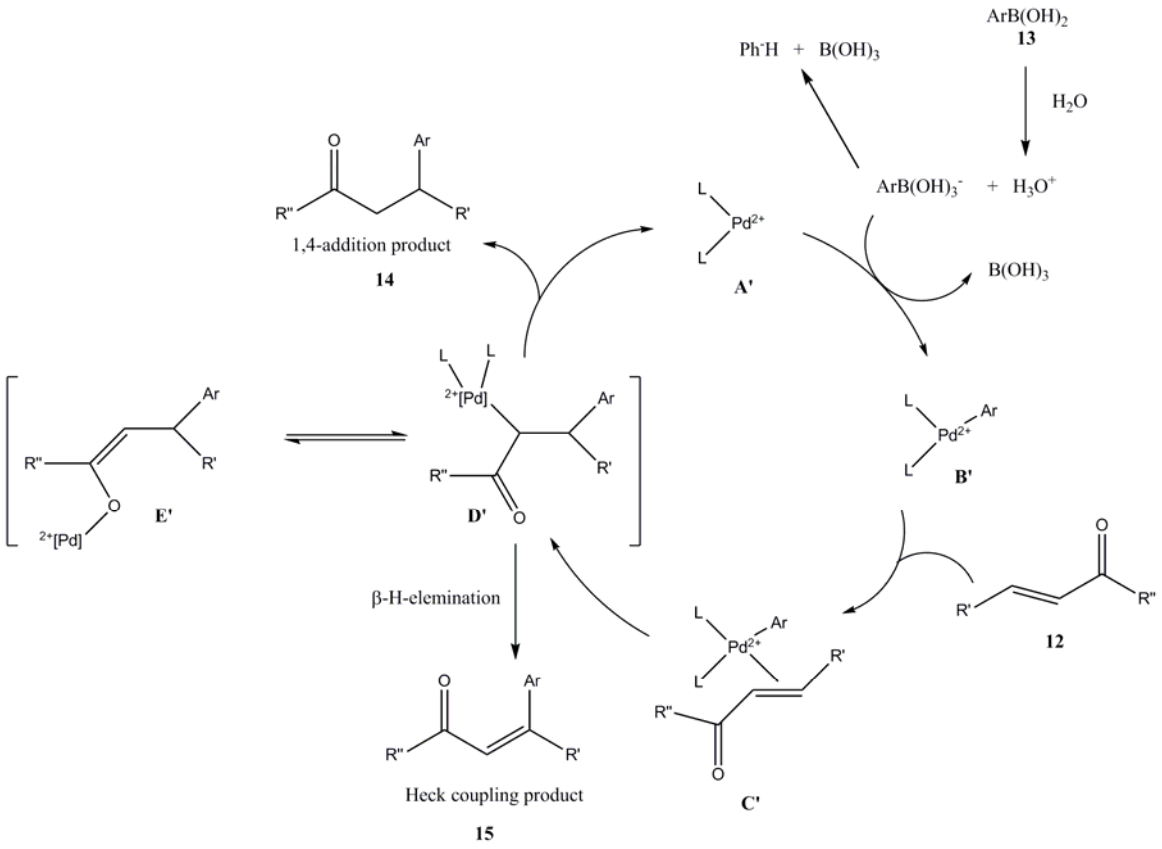

Scheme 5.6. Proposed catalytic cycle in literature for the Pd-catalyzed conjugate addition of arylboronic acids and formation of Heck coupling product.

The interesting catalytic activity of our new binuclear palladium complexes even in the absence of any base, water and oxidant additives suggests some modifications on the above proposed mechanism. Previous studies suggest that the regeneration of Pd(II) after each catalytic cycle is the key step for the Pd-catalyzed oxidative Heck reaction. Following the release of the coupling product from Pd(II), the X-Pd-H intermediate might be intercepted by a hydrogen acceptor, such as solvent or substrate, thus regenerating the Pd(II) without forming Pd(0) and so circumventing the need for traditional oxidants or base (Scheme 5.5) (160).

Since the new synthesized binuclear palladium complexes have two types of ligands: chelating and bridging; it is worth indicating the ligand type that played the crucial role in developing the assigned interesting catalytic activity. To achieve this, we have examined the catalytic activity of catalyst systems composed of $Pd(OAc)_2$ with chelating or bridging ligands or a mixture of both in our model reaction. The results are presented in Table 5.6. We can conclude easily based on these results that chelating ligands are essential for producing the catalytic activity, while bridging ligands are slightly influencing the chemoselectivity of the reaction by providing certain electronic properties and rigidity to the active palladium complexes.

5.4 Conclusions

In summary, the synthesis of various new binuclear palladium complexes with chelating diimines and bridging diphosphines and diimines has been acheived successfully. Their structures have been characterized using different elemental and spectral techniques. We have developed an efficient protocol for the conjugate addition and oxidative Heck coupling of arylboronic acids with both electron rich and electron deficient olefins using the new synthesized complexes. The method requires neither oxidant nor base to operate, broadening the scope of palladium-catalyzed coupling reactions.

Table 5.6. Coupling of arylboronic acid 13a to **4ac$_1$** catalyzed by Pd113. Effect of chelating and bridging ligand in Pd113 on the conversion and chemoselectivity.[a]

Entry	**Ligand**	**Conversion 4ac$_1$ (%)[b]**	**Products Distribution (%)[c]**	
			14aa	**15aa**
1	4,4'-dimethyl-2,2'-bipyridine	91	46	54
2[d]	4,4'-bipyridine	30	15	85
3	4,4'-dimethyl-2,2'-bipyridine/ 4,4'-bipyridine (1:1)	70	52	48

[a] Reaction conditions: $Pd(OAc)_2$ (0.04 mmol), Ligand (0.08 mmol), **4ac$_1$** (0.50 mmol), **13a** (1.0 mmol), CH_3CN (4 mL), 110 °C, 16 h.

[b] Determined by GC

[c] Determined by GC and ^{1}H-NMR

[d] 15 % Hydrogenation product

5.5 Experimental

5.5.1 Materials and instruments

$Pd(OAc)_2$, diimine ligands, diphosphine ligands, trifluroacetic acid (TFA), ammonium hexafluorophospate (NH_4PF_6), *trans*-cinnamate esters, and phenylboronic acid [$PhB(OH)_2$] are highly pure commercially available materials and were used without any purification. Dry solvents have been used in all experiments. ^1H and ^{13}C NMR spectra were recorded on 500 MHz Joel 1500 NMR machine. Chemical shifts (δ) were reported in ppm relative to tetramethyl silane (TMS) using $CDCl_3$ or DMSO-d_6. IR spectra were recorded on Perkin-Elmer 16F PC FT-IR spectrometer and reported in wave numbers (cm^{-1}). Melting points were determined using Büchi melting point apparatus. Elemental analysis was carried out using Euro Vector EA 3000. UV-vis of complexes was carried out using Perkin Elmer Lambda EZ 210 spectrometer. Appropriate sample was dissolved in dimethylformamide and then volume was adjusted to 25 ml with distilled dichloromethane. The screening of the reactants and products of the catalytic application part was carried out using Agilent GC 6890 Series gas chromatograph equipped with a split–splitless injector (split ratios of 20:1). The temperature of the injector was 250 ^oC, with 10 psi constant pressure. The column was an HP-5 column (30 m × 0.25 mm i.d., 0.25 μm film thickness). Helium was the carrier gas at a flow rate of 1.5 mL/min and programmed temperature (50 °C, hold 2 min, then ramped at 10 °C/min to 140 °C, then finally ramped at 20 °C/min to 250 °C ,hold time 20 min). The detector was flame ionization detector (FID), with hydrogen and air flow of 40.0 and 450.0 ml/min respectively. Makeup flow was on with 45.0 ml/min of helium. The products of the reactions were also analyzed on GC-MS Varian Saturn 2000 equipped with 30 m

capillary column (HP-5). Helium was the carrier gas at a flow rate of 1.0 mL/min and programmed temperature (50 °C, hold 2.0 min, then ramped at 10 °C/min to 140 °C, then finally ramped at 20 °C/min to 250 °C, hold time 20 min). The temperatures of injector, transfer line and ionization source were 250, 225 and 270 °C, respectively. NIST MS search was used for compound identification.

5.5.2 General procedure for the conjugate addition of phenylboronic acid to *trans*-cinnamate esters catalyzed by new Pd(II) bimetallic mixed ligand complexes:

To a 45 ml glass liner tube, phenylboronic acid (0.50 mmol), *trans*-cinnamate ester (0.50 mmol), palladium complex (0.02 mmol), and solvent (10 mL) were added under nitrogen. The mixture was stirred and heated at 110 °C for 24 h. After cooling, the reaction mixture was filtered and a sample of this solution was immediately analyzed by GC and GC-MS. The solvent was then removed and the products were separated by preparative TLC (30 % EtOAc/petroleum ether 40-70 ^{o}C). The products were identified by ^{1}H and ^{13}C NMR, FT-IR and GC-MS analyses.

CHAPTER 6

A DFT STUDY ON THE MECHANISM OF PALLADIUM-CATALYZED ALKOXYCARBONYLATION AND AMINOCARBONYLATION OF ALKYNES: HYDRIDE VERSUS ALKOXY PATHWAYS

6.1 Introduction

It is well-known that the ratio of products from aminocarbonylation and alkoxycarbonylation reactions depends strongly on the catalytic system and the reaction conditions employed (61,72,125). The development of more efficient catalyst systems in terms of conversion and regioselectivity is still a challenging area for these reactions. However, to achieve this goal it is paramount to determine which structural characteristics of reaction parameters are most influential in promoting the formation of highly reactive and stable catalysts (165). Furthermore, the understanding of regioselectivity profile of these reactions requires an insight on the structure and energy of species involved in these reactions.

Recent progress in computational chemistry has shown that many important chemical and physical properties of the species involved in these reactions can be predicted from first principles by various computational techniques (166). This ability is especially important in these reactions where experimental isolation of key intermediates is difficult to achieve.

Many catalytic cycles have been proposed for different catalytic systems that catalyze the alkoxycarbonylation (13,72,74) and aminocarbonylation (61,62,64,65) of alkynes. The support of these mechanisms was based primarily on the understanding of the influence

of different reaction parameters on the catalytic activity and regioselectivity. The use of theoretical calculations to model catalytic cycles has been reported for metal-catalyzed hydroformylation (167), hydrogenation (2), cross-coupling (168), etc… reactions. However, reports on computational studies on the alkoxycarbonylation and aminocarbonylation of alkynes are almost absent in the literature.

In this chapter, we present a theoretical study of alkyne alkoxycarbonylation and aminocarbonylation that developed in parallel with experimental results of which have already been reported in chapter 3. In these experimental studies, the aminocarbonylation and alkoxycarbonylation reactions of terminal alkynes took place smoothly and efficiently using a catalyst system $Pd(OAc)_2$/dppb/*p*-TsOH/CH_3CN/CO. The catalytic system was tested and optimized using two different nucleophiles: alcohols and amines. The alkoxycarbonylation reaction produced the *trans* ester **4** as predominant product (complete conversion of alkyne and 90 % selectivity) with excellent reaction rate, while *gem* isomer was the major amide product **3** (ca. 97 %) in aminocarbonylation reaction after 20 hours reaction period. The catalytic activity and regioselectivity of the two reactions proved to be highly sensitive to the type of solvent, where acetonitrile solvent was the best solvent to produce the highest yield and selectivity of the desired products. Furthermore, changing the type of solvent in alkoxycarbonylation reaction resulted in producing the *gem* ester **3** as major product.

Based on experimental findings; we proposed two different catalytic cycles for alkoxycarbonylation (hydride) and aminocarbonylation (amine) reactions in chapters 2 and 3. The aim of this DFT theoretical investigation is to validate the solution-based observation, predicting possible catalytic cycles, key intermediates and transition states

involved these reactions, and to address the origin of variation in rate and regioselectivity of the two reactions.

The DFT study employs chelating phosphines based on dhpb ($PH_2CH_2CH_2CH_2CH_2PH_2$). The validity of ligand simplification was tested by employing the real non-simplified DPPB ligand in some intermediates. The alkyne used in this study is propyne. Methanol is used as nucleophile in alkoxycarbonylation mechanisms, while dimethylamine is used in aminocarbonylation study. Results map appropriate transition states and associated energy barriers both in the gas phase and in acetonitrile (via a polarizable continuum model (PCM)).

6.2 Computational Details

All calculations were performed using the GAUSSIAN 03 series of programs (169), using the B3LYP functional (170,171). The structures of the reactants, intermediates, transition states, and products were fully optimized in the gas phase without any symmetry restrictions using an effective core potential (172) and its associated double-ζ LANL2DZ (169,173) basis set for the palladium atom. Hydrogen atoms where represented by the 6-31G basis set and extra series of p-polarization has been added for hydride atoms and H atoms involved in hydrogenation processes. C, N, and O atoms where represented by the 6-31G(d) basis set (174-176). The frequency calculations at the same level were also carried out to confirm that the optimized structures were ground states without imaginary frequency ($N_{Imag} = 0$) or transition states with one imaginary frequency ($N_{Imag} = 1$). Especially, the lone imaginary frequency of each transition state displayed the desired displacement orientation, and the validity of each reaction path was

further examined by the intrinsic reaction coordinate calculations (IRC). Zero-point energy corrections (ZPE), derived from the frequency calculations, were added to the total energies of each species in the catalytic cycles. The Gibbs energies (*G*) were also calculated at 298.15 K. In all cases the wave functions were found to be stable with respect to relaxing spin and symmetry constraints. Solvent effects were taken into account by means of PCM (177,178) (acetonitrile, $\epsilon = 36.64$) single-point calculations at the gas-phase optimized geometries.

6.3 Results and Discussion

6.3.1 Hydride cycle

The proposed hydride cycle for the alkoxycarbonylation of propyne is shown in Scheme 6.1. The proposed intermediates for *trans* isomer (major product in alkoxycarbonylation reaction) are shown only in this cycle for simplification.

6.3.1.1 Catalyst generation. The first key step in the mechanism of the alkoxycarbonylation of alkyne is the formation of the 14-electron active catalyst $[Pd(II)(P_2)(H)]^+$ (**1C**) via reaction of $Pd(OAc)_2$, P_2 and HX (*p*-TsOH) (61). Acetonitrile solvent can coordinate to this species forming intermediate **1C-S**, but this assumption was not considered since energy barrier to the next step will be endothermically high (18.0 kcal/mol).

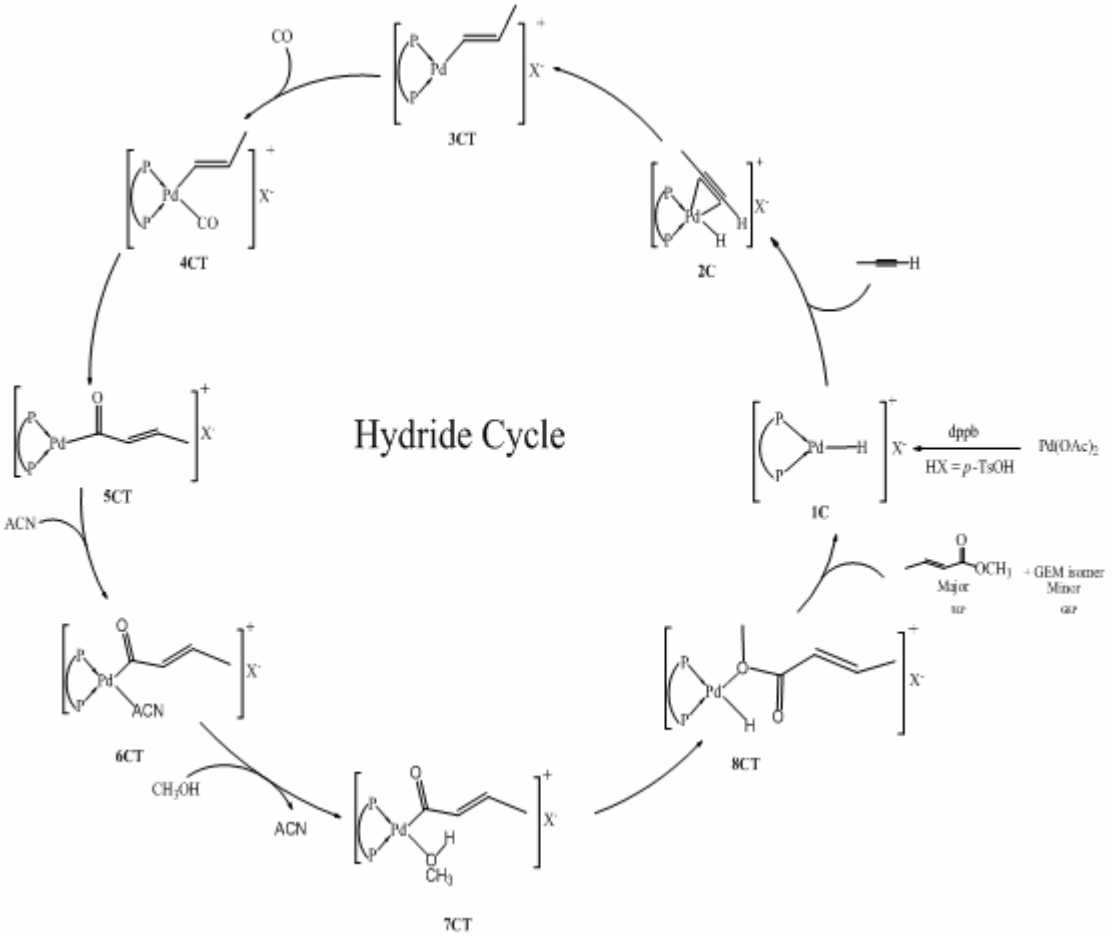

Scheme 6.1. DFT-derived scheme for alkoxycarbonylation of propyne by a hydride-cationic Palladium(II) bisphosphine complex.

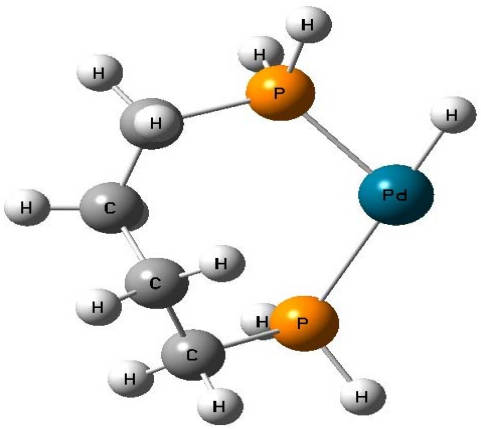

1C (0.0 kcal/mol)

6.3.1.2 Alkyne coordination. The optimized structure of **2C** (distorted square pyramidal) showed that the Pd-H bond occupies the equatorial position to the $PdP_2C{\equiv}C$. The Pd–C and C≡C bond lengths are 2.234/2.463 Å, and they are very close to those in the propyne complex. The C≡C bond length in **2C** (1.235 Å) is also longer than in the free form (1.207 Å), and this elongation can be explained by the donation and back donation interaction model of the frontier molecular orbital (2). The coordination of alkyne to the precursor **1C** is exothermic by a 25.6 kcal/mol.

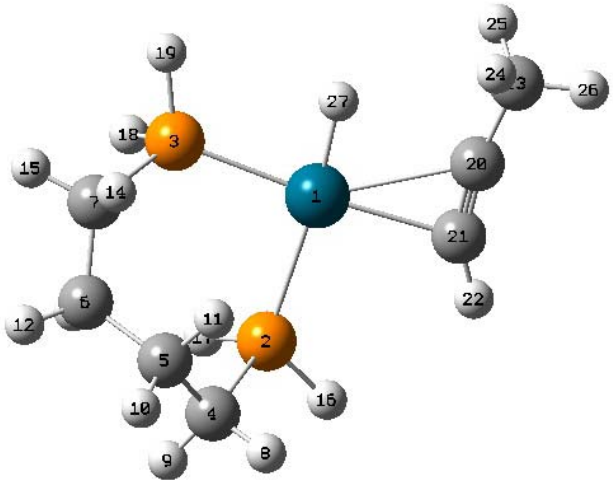

2C (-25.6 kcal/mol)

6.3.1.3 Alkyne insertion. The insertion of terminal alkynes, except for acetylene, into the Pd-H bond can occur in two ways, which are described as *anti*-Markovnikov and Markovnikov additions. Therefore, two types of vinyl complexes, *trans* and *gem* (therefore **T** and **G** notations are used in the text), can be formed. This alkylation reaction was considered as the key step for the regioselectivity (167). It is necessary to rotate the C≡C double bond into the parallel orientation to the H–Pd bond, which can facilitate the insertion.

The structures of the two transition states, **2C/3CT-TS** and **2C/3CG-TS**, are located, and their imaginary vibration modes (409i and 383i cm^{-1}) indicate the migratory insertion of hydrogen to the C≡C triple bond with the shortening of the H-C distances (1.848 and 1.849 Å). The skeleton of **2C/3CT-TS** and **2C/3CG-TS** around the palladium center has a distorted square planar geometry, and the H–Pd–C≡C torsion angles in **2C/3CT-TS** and **2C/3CG-TS** are -0.075° and -0.72°. Taking **2C** as the starting point, the computed activation free energies for both pathways are 0.4 and 1.7 kcal/mol, respectively. There is therefore no kinetic control over the regioselectivity, and this is in agreement with the findings for the olefin insertion process of the propene and acetamide complexes (138) and with our experimental results.

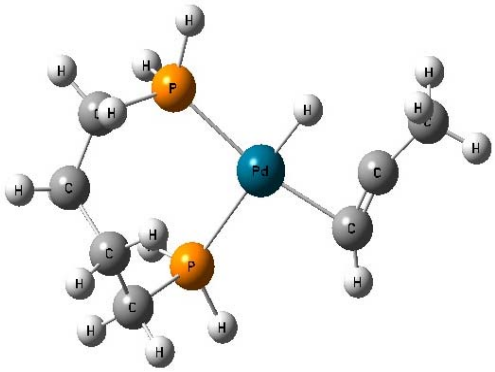

2C/3CT-TS (0.4 kcal/mol)

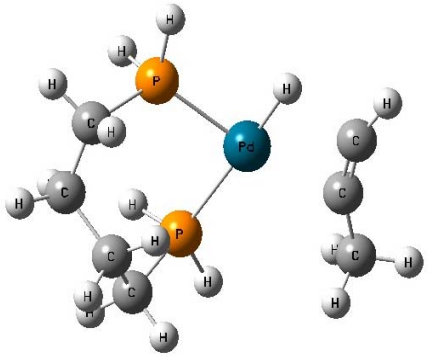

2C/3CG-TS (1.7 kcal/mol)

The optimized geometries of **3CT** and **3CG** are similar to **1C** where the PdP_2C forms a distorted triangle or a distorted square planar structure with vacant site on palladium center for further molecule coordination. The vinyl moieties in the two geometries are on same plane with dpph carbon atoms. The *trans* isomer **3CT** is isoenergetic with **3CG** (difference is 1.0 kcal/mol), which indicates no contribution of alkyne insertion step in accounting for the regioselectivity of the alkoxycarbonylation reaction.

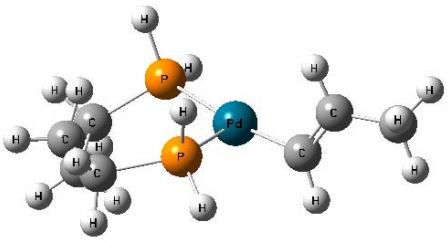

3CT (-14.5 kcal/mol)

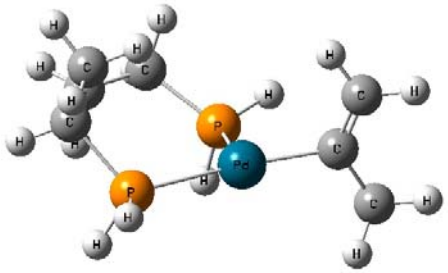

3CG (-15.4 kcal/mol)

Since solvent has a crucial role in determining the regioselectivity of the alkoxycarbonylation reaction, specially the role of acetonitrile solvent in producing the *trans* isomer in higher regioselectivity; we tried to utilize the solvation and coordination properties of acetonitrile in accounting for the interesting regioselectivity of alkoxycarbonylation reaction in this solvent. The calculation of energy profile of the two isomers **3CT** and **3CG** in acetonitrile using PCM resulted in further stability of **3CT** over **3CG** by a 1.5 kcal/mol, while solvent coordination by one molecule of acetonitrile (**3CT-S** and **3CG-S**) resulted in comparable energy of the two isomers in gas phase and slight stability for the *ge*m isomer **3CG-S** in acetonitrile.

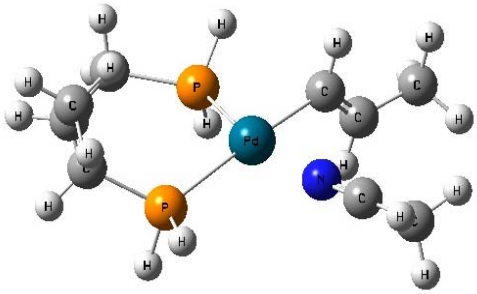

3CT-S (-22.7 kcal/mol)

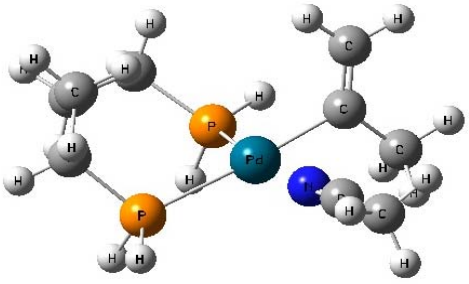

3CG-S (-23.3 kcal/mol)

6.3.1.4 CO addition and insertion. The following step in the catalytic cycle is the CO addition on the coordinatively unsaturated intermediates $(C_3H_5)PdP_2$ (**3CT/3CG**) to produce the 16-electron saturated species $(C_3H_5)PdP_2(CO)$ (**4CT/4CG**), followed by the insertion (carbonylation) process leading to the corresponding acyl complexes $(C_3H_5CO)PdP_2$ (**5CT/5CG**). The two isomers are isoenergetic with energy difference <0.5 kcal/mol, which reveals no contribution of this step in directing the regioselectivity of the alkoxycarbonylation reaction. Its worth to mention here that theoretical calculations on the hydroformylation reaction of propene using $HCo(CO)_3$ catalyst reported in literature (179) accounted for the regioselectivity behavior of the hydroformylation reaction based on energy difference between isomers obtained from CO addition step. This step in our system is exergonic for the two isomers **4CT** and **4CG** and our attempts to locate corresponding transition states (**3CT/4CT-TS** and **3CG/4CG-TS**) have failed due to very low barrier of this step (138).

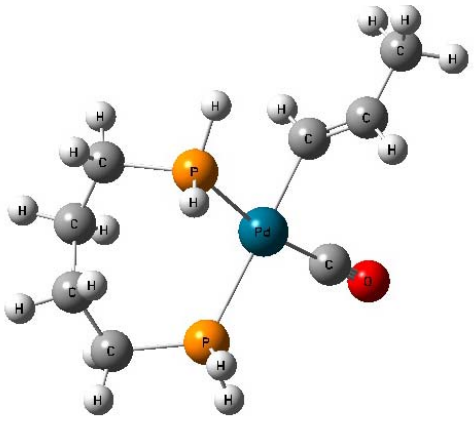

4CT (-19.3 kcal/mol)

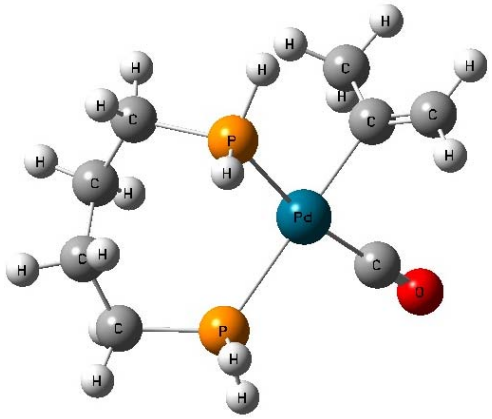

4CG (-19.8 kcal/mol)

The next step is the CO insertion process from the vinyl complexes **4CT**/**4CG** to the acyl complexes **5CT/5CG**. The optimized geometries of the two isomers showed an

interesting rotation of the α,β-unsaturated acyl group to allow η^2-coordination of the double bond to the palladium center. The Pd-CO-C angle in **5CT** and **5CG** is 78 and 74°, respectively, which are much smaller than mono coordinated α,β-unsaturated acyl group (121°). Moreover, the double bond in **5CT** and **5CG** is not coplanar with PdP_2 plane and the distances between Pd and C=C in **5CT** and **5CG** are 2.291/2.436 and 2.240/2.272 Å, respectively. The difference in energy for the two complexes is very small (0.1 kcal/mol), which indicates again no contribution of this step in accounting for the regioselectivity of the alkoxycarbonylation reaction. The insertion of CO on Pd-vinyl bond step is exothermic for the two isomers **5CT** and **5CG** by 7.2 and 7.1 kcal/mol, respectively.

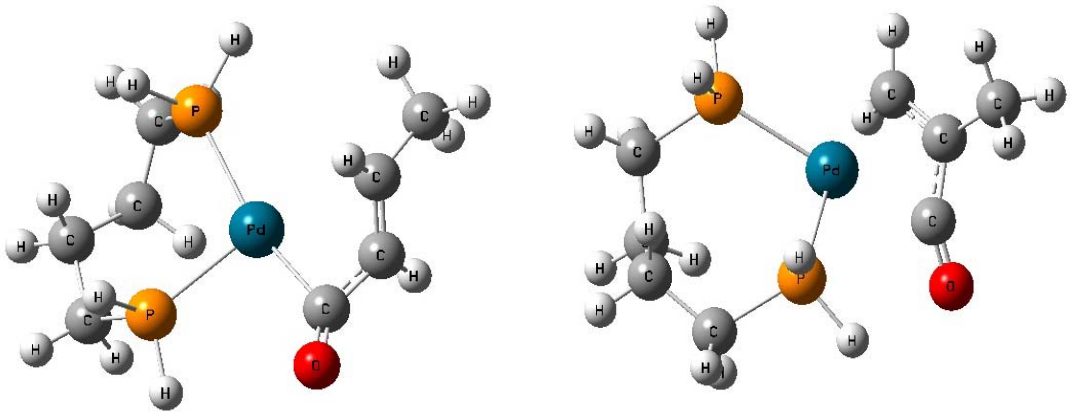

5CT (-26.1 kcal/mol) **5CG (-26.7 kcal/mol)**

In addition to the adducts and products, we have also investigated the corresponding transition states. This process is well studied at various levels of theory (166). The structures of the two authentic transition states, **4CT/5CT-TS** and **4CG/5CG-TS**, are located and characterized by a decrease in the C_3H_5-Pd-CO angle to 57 and 55° in **4CT/5CT-TS** and **4CG/5CG-TS**, respectively. The negative direction modes of the

above transition states (283i and 306i) indicate the right direction of carbonylation. The computed carbonylation barriers for both the *trans* (**4CT**→(**4CT/5CT-TS**)→ **5CT**) and the *gem* routes (**4CG**→(**4CG/5CG-TS**)→ **5CG**) are 5.9 and 8.2 kcal/mol, and they are close to those of corresponding step in propene hydroformylation (167).

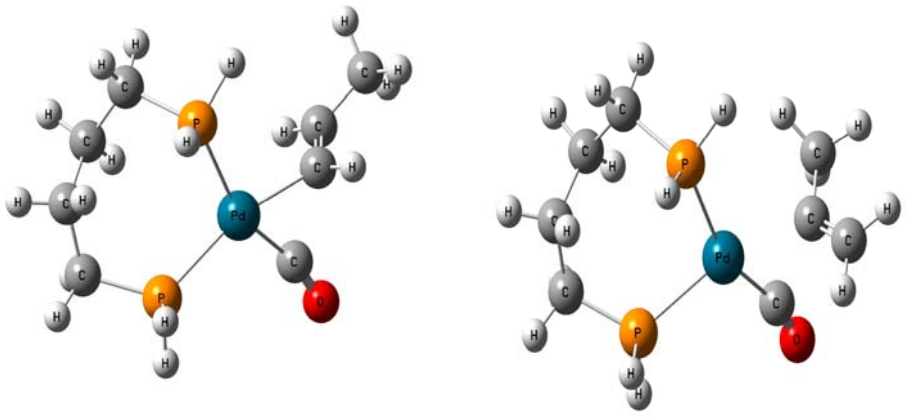

4CT/5CT-TS (5.9 kcal/mol) **4CG/5CG-TS (8.2 kcal/mol)**

6.3.1.5 Solvent coordination. Since acetonitrile solvent showed experimentally an interesting role in directing the alkoxycarbonylation of phenylacetylene reaction to favor the *trans* isomer in high regioselectivity, the coordination of acetonitrile molecule to intermediates **5CT** and **5CG** is studied. The skeleton around the palladium center for the resulted isomers **6CT** and **6CG** is a distorted square planar and the PPdN≡C angle in **6CT** and **6CG** is 171°. The Pd-N distance in **6CT** and **6CG** is 2.160 and 2.163 Å, respectively. Moreover, ACN addition to **5CT** and **5CG** is computed to be highly exothermic by 16.9 and 12.2 kcal/mol, and from thermodynamic stability point of view the difference in the thermodynamic stability of the products from this high exothermic addition (**6CT** and **6CG**) should be responsible for the observed regioselectivity. This

clearly described the alkoxycarbonylation high regioselectivity towards the *trans* ester in acetonitrile solvent (see section 3.2.3).

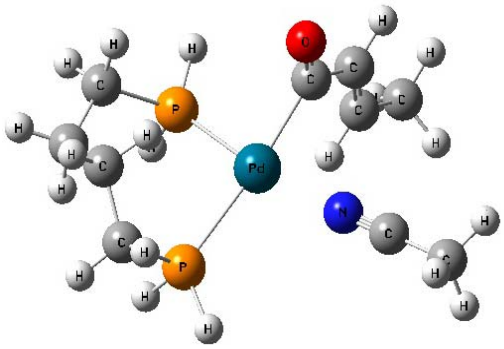

6CT (-16.9 kcal/mol)

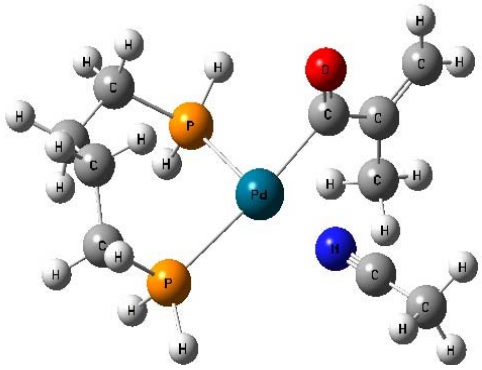

6CG (-12.2 kcal/mol)

The attempts to locate corresponding transition states for solvent coordinated products (**6CT** and **6CG**) have failed.

6.3.1.6 Methanol oxidative addition and α,β-unsaturated ester elimination. The starting points of this step are isomers obtained from the carbonylation and solvent coordination processes (**6CT** and **6CG**). The coordination of methanol leads to the formation of the two isomers **7CT** and **7CG**. Its worth to note here that isomers **7CT** and **7CG** can be obtained directly from coordination of methanol to isomers **5CT** and **5CG**. However, the presence of catalytic amounts of methanol versus large availability of acetonitrile molecules in reaction medium and the interesting regioselectivity of alkoxycarbonylation reaction in this solvent encouraged us to propose the formation of isomers **6CT** and **6CG**. It is interesting to note also that the H–O bonds in **7CT** and **7CG** are parallel to the Pd–C_{acyl} bonds. One reason for this conformation in **7CT** and **7CG** is the attractive electrostatic interaction (H-bonding) between the polar H–O bond and the

acyl C=O bond. The H···O distances in **7CT** and **7CG** are 1.993 and 2.088 Å, while the Pd-O distances are 2.239 and 2.242 Å

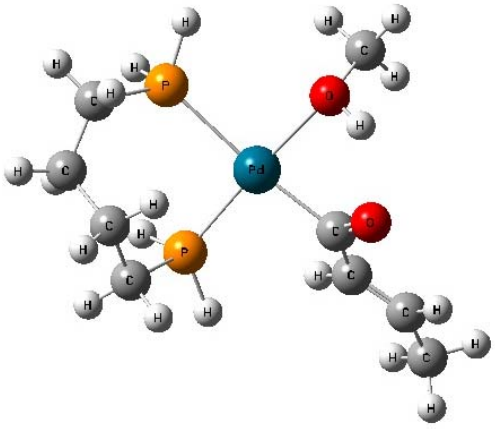

7CT (-11.9 kcal/mol)

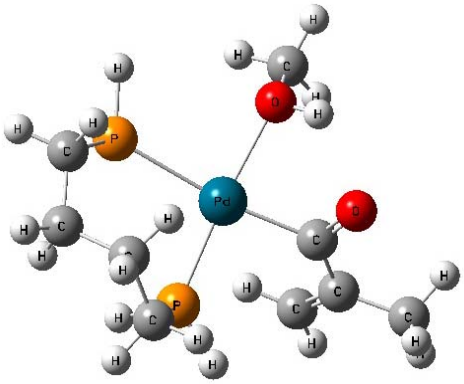

7CG (-8.9 kcal/mol)

For the oxidative addition, the attempts to locate the corresponding intermediates (the hydride and methoxo complex) from the oxidative addition of methanol was unsuccessful and further optimization following the negative vibration modes lead to the formation of intermediates **8CT** and **8CG** directly without any barrier. This indicates that the potential energy surface is flat. The driving force for the simplified reaction might be the attractive electrostatic interaction between the negatively charged oxygen center of the CH_3O ligand and the positively charged carbon center of the acyl ligand; both ligands already have the appropriate orientation, which can facilitate further reaction.

On the basis of the most stable acyl intermediates (**5CT** and **5CG**), the coordination of CH_3OH is exothermic by 11.9 and 8.9 kcal/mol for **7CT** and **7CG**. Since it is not possible to locate the corresponding intermediates of the oxidative addition, and the subsequent transition states for the reductive elimination, no energetic data for these species are available. From the CH_3OH adducts, the formation of the ester complex

8CT/TEP is exothermic by 2.6 kcal/mol and endothermic by 1.3 kcal/mol for **8CG/GEP**. Taking **2C** and (CO + CH_3OH) as the starting point, the formation of the separated product and **1C** are exothermic for the *trans* and *gem* esters by 50.3 and 49.3 kcal/mol, respectively.

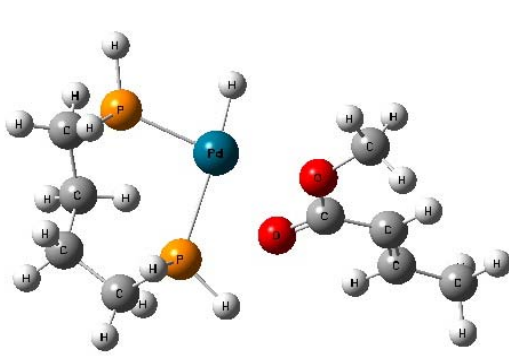

8CT (-2.6 kcal/mol)

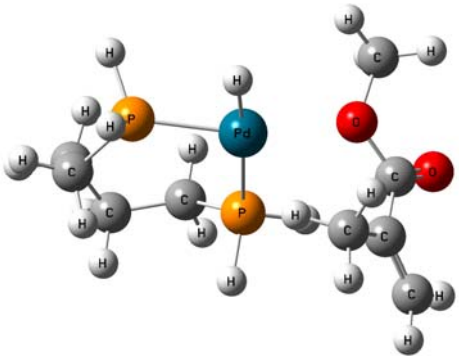

8CG (1.3 kcal/mol)

The calculated relative energies for trans isomer intermediates in the hydroalkoxycarbonylation of propyne in gas phase is shown in Scheme 6.2.

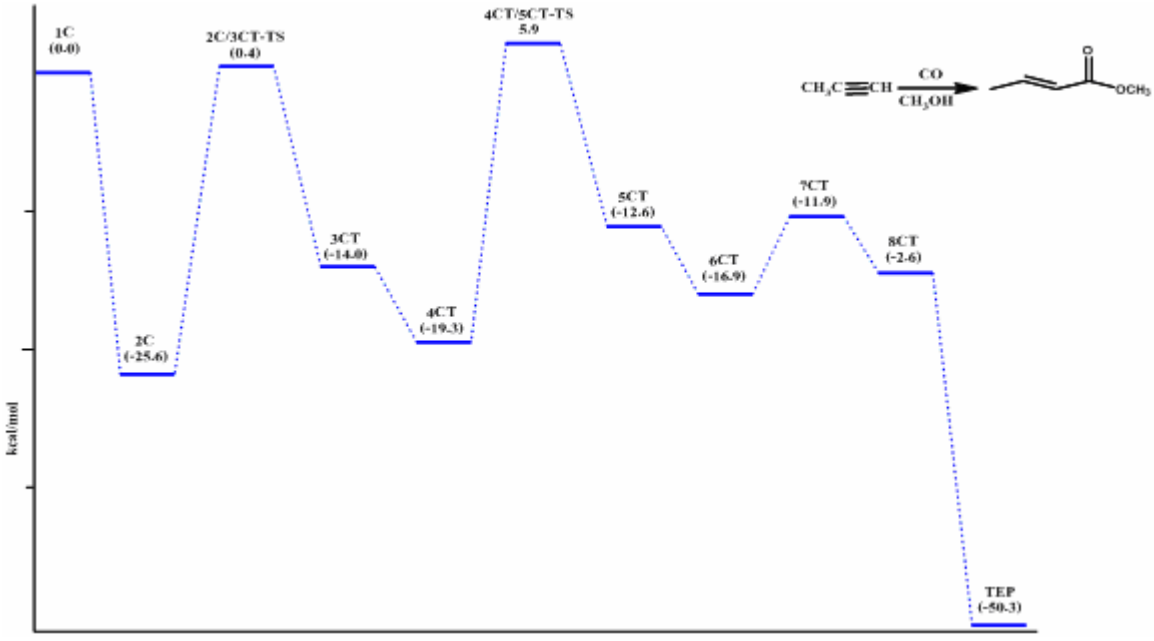

Scheme 6.2. Computed relative energies (kcal/mol) for the *trans* isomer hydride cycle in gas phase obtained via hydroalkoxycarbonylation of propyne.

6.3.1.7. Solvation effect. The effect of acetonitrile, as a solvent, has been taken into account by introducing a polarizable continuum solvent model (PCM). This process yielded results that were similar to those already discussed for the gas phase. Thus, no significant changes in the values of the relative energies do take place and no substantive changes in the energy profiles except for the alkyne coordination step which is now an exothermic process by a 10.2 kcal/mol in acetonitrile. Interestingly, some of the energy barriers are actually higher when the continuum solvent model is applied, the most remarkable corresponding to the change **4CT→4CT/5CT-TS** and **4CG→4CG/5CG-TS**, which are 5.9 and 8.2 kcal/mol in the gas phase versus 6.5 and 9.2 kcal/mol in acetonitrile. The difference in relative energies between trans and gem intermediates have been slightly changed for initial intermediates in the catalytic cycle. The energy difference between intermediates **4CT** and **4CG** increased from a 0.5 kcal/mol in gas phase to a 1.0 kcal/mol in acetonitrile. Interestingly, an opposite case was found with intermediates **7CT** and **7CG** when the energy difference dropped from a 3.0 kcal/mol in gas phase to a 0.7 kcal/mol in acetonitrile. Nevertheless, the regioselectivity profile in acetonitrile still proves energy difference between intermediates **6CT** and **6CG** as key intermediates for accounting the regioselectivity of the alkoxycarbonylation reaction and hence matching the experimental results. The calculated relative energies for *trans* isomer intermediates in the hydroalkoxycarbonylation of propyne in acetonitrile are shown in Scheme 6.3.

The computed energetic data for the whole reactions in hydride-cationic cycle is shown in Table 6.1.

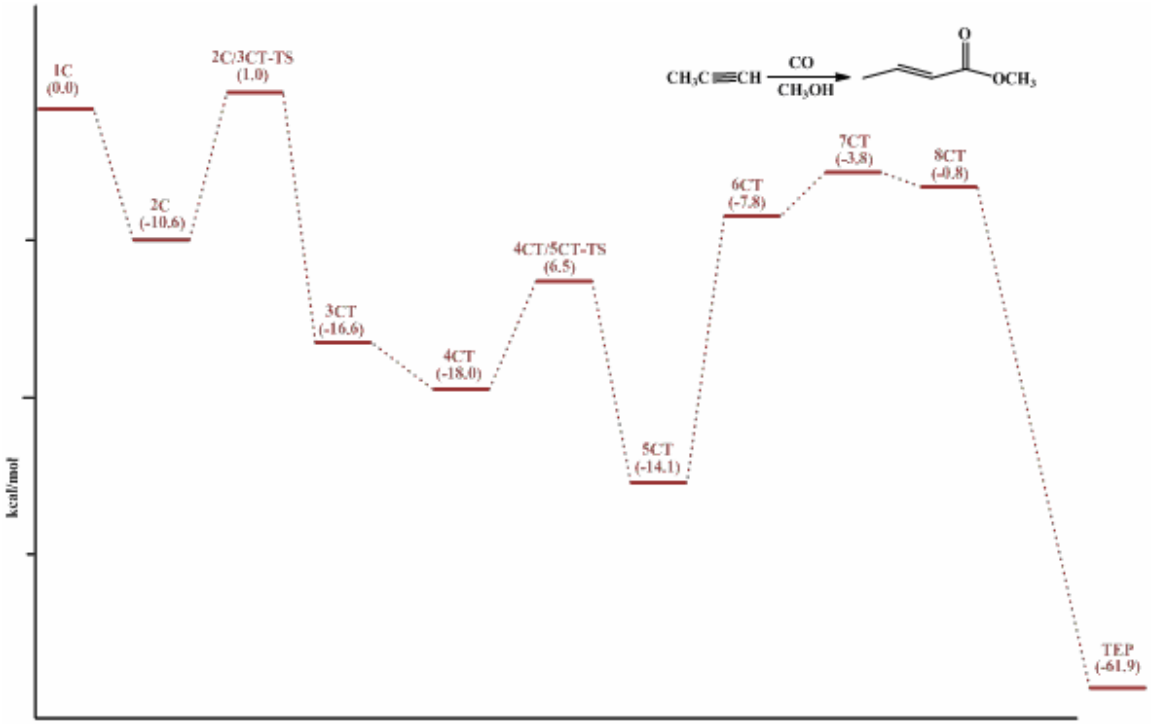

Scheme 6.3. Computed relative energies (kcal/mol) for the *trans* isomer hydride cycle in acetonitrile obtained via hydroalkoxycarbonylation of propyne.

6.3.1.8. Test of validity of ligand simplification. Ligand simplification implied in theoretical calculations is necessary to minimize the time of computation. Successful interpretation of many physical and chemical properties of catalytic species was computationally possible using this simplification. However, since regioselectivity of alkoxycarbonylation and aminocarbonylation of alkynes is affected much by the steric and electronic properties of ligands (see section 3.2.2), we decided to test the validity of ligand simplification in our theoretical calculations. The simplification has been removed from all *trans* intermediates **3CT**, **4CT**, **5CT**, **6CT**, **7CT** and **8CT** and their corresponding *gem* isomer intermediates plus intermediates **1C** and **2C** for accurate comparison with simplified intermediate results.

Table 6.1. B3LYP/LANL2DZp computed total electronic energies (E_{tot}, au) in gas phase, free energies (G_{tot} (298 K), au), zero-point energies (ZPE, kcal/mol) as well as number of imaginary frequencies (N_{Imag}) and (E_{tot}, au) in acetonitrile for cationic cycle.

Compound	E_{tot} (gas phase)	ZPE (N_{Imag})	(G_{tot} (298 K)	E_{tot} (acetonitrile)
Starting materials				
Propyne	-116.653269	34.9653	-116.621778	-116.657379
DHPB	-842.330685	93.8694	-842.216197	-842.335259
CH_3OH	-115.717946	32.3883	-115.689061	-115.726139
CH_3CN	-132.754928	28.6393	-132.732268	-132.763073
CO	-113.309453	3.1574	-113.323561	-113.310525
Alkyne coordination and insertion				
1C	-969.4755620	101.2607	-969.351593	-969.5627760
2C	-1086.171896	137.6996	-1085.995828	-1086.238681
2C/3CT-TS	-1086.170368	137.1627	-1085.993853	-1086.236195
2C/3CG-TS	-1086.168152	137.0219	-1085.992217	-1086.235280
3CT	-1086.199036	140.697	-1086.018135	-1086.268355
3CG	-1086.198043	140.3422	-1086.017689	-1086.265468
3CT-S	-1218.991888	170.4127	-1218.772825	-1219.052975
3CG-S	-1218.992161	170.2673	-1218.771625	-1219.053398
CO coordination and insertion				
4CT	-1199.542174	145.6766	-1199.356820	-1199.610456
4CG	-1199.542167	145.4779	-1199.356724	-1199.609830
4CT/5CT-TS	-1199.532722	145.6173	-1199.346153	-1199.600027
4CG/5CG-TS	-1199.528857	145.2904	-1199.342870	-1199.594928
5CT	-1199.554705	146.7702	-1199.366460	-1199.624292
5CG	-1199.555033	146.6037	-1199.367108	-1199.621110
Solvent Coordination				
6CT	-1332.338087	176.3666	-1332.110134	-1332.401344
6CG	-1332.331349	176.4973	-1332.104547	-1332.393743
Oxidative addition of methanol				
7CT	-1315.295247	181.3947	-1315.057485	-1315.359983
7CG	-1315.290766	181.2596	-1315.053052	-1315.355700
8CT	-1315.297608	180.2338	-1315.061414	-1315.359353
8CG	-1315.286806	180.0826	-1315.050311	-1315.353358
Reaction products				
Trans ester (TEP)	-345.788392	77.8760	-345.697035	-345.795787
Gem ester (GEP)	-345.786659	77.8227	-345.695261	-345.791948

Data shown in Table 6.2 for the energy of non simplified intermediates prove a great effect of ligand simplification on the energy difference between *trans* and *gem* intermediates in the hydride cycle. All *trans* intermediates are now more stable than their corresponding *gem* intermediates in gas phase and this stability was further increased in acetonitrile. These results gave further approval for obtaining *trans* ester regioselectively via hydride cycle. Remarkably, the energy profile of elementary steps involved in the hydride cycle changed significantly for first non-simplified intermediates while the change was less significant for the late intermediates by removing ligand simplification. Based on the above results, we believe that ligand simplification is not valid in theoretical calculations targeting a specific explanation of energy profile of our proposed catalytic cycle or for accounting for the origin of regioselectivity.

Comparison of energy profile of all elementary steps in the hydride cycle between simplified and non-simplified *trans* intermediates in gas phase and acetonitrile is shown in Table 6.3.

6.3.2 Alkoxy cycle

In addition to "hydride" mechanism, alkoxy mechanism based on alkoxy-palladium active species has been proposed for alkoxycarbonylation of alkynes and alkenes (180). In the alkoxy mechanism, the catalytic cycle is initiated by the formation of a Pd-alkoxy complex that reacts with CO, yielding the palladium alkoxycarbonyl intermediate. In both mechanisms the termination step involves the alcohol. A notable difference between these two mechanisms in relation to regioselectivity is that a bulky ligand would promote the selective formation of linear ester in the hydride

Table 6.2. Total energy of *trans* and *gem* intermediates of no ligand simplification in the hydride cycle.

Compound	**E_{tot} (gas phase)**	**Energy difference (kcal/mol)***	**E_{tot} (acetonitrile)**	**Energy difference (kcal/mol)***
1C-LNS	-1893.706345	-	-1893.772332	-
2C-LNS	-2010.386647	-	-2010.444452	-
3CT-LNS	-2010.421273	-0.1	-2010.479785	-1.6
3CG-LNS	-2010.421076		-2010.477266	
4CT-LNS	-2123.760544	-1.4	-2123.818576	-1.6
4CG-LNS	-2123.758234		-2123.816008	
5CT-LNS	-2123.776237	-3.2	-2123.835803	-3.6
5CG-LNS	-2123.771195		-2123.830083	
6CT-LNS	-2256.550432	-1.6	-2256.610706	-2.3
6CG-LNS	-2256.547903		-2256.607062	
7CT-LNS	-2239.506739	-1.8	-2239.566999	-2.3
7CG-LNS	-2239.503874		-2239.563302	
8CT-LNS	-2239.516246	-6.2	-2239.577511	-6.4
8CG-LNS	-2239.506289		-2239.567292	

* Energy difference = E_{tot}(**T**) – E_{tot}(**G**)

Table 6.3. Comparison of energy profile for all elementary steps involved in hydride cycle in case of *trans* simplified and non-simplified intermediates.

	E_{tot} (kcal/mol) ***Simplified intermediates***		***E_{tot} (kcal/mol)*** ***Non-simplified intermediates***	
	Gas phase	***Acetonitrile***	***Gas phase***	***Acetonitrile***
$HPdP_2$	0	0	0	0
Alkyne coordination	-25.6	-10.2	-17.0	-9.3
Alkyne insertion	-14.9	-17.6	-21.7	-22.2
CO coordination	-19.3	-18.0	-18.7	-16.8
CO insertion	-6.7	-7.6	-9.8	-10.8
Solvent coordination	-16.9	-7.8	-12.1	-7.4
Alcohol coordination	-11.9	-3.8	-7.9	-3.2
Alcohol oxidative addition	-2.6	-0.8	-7.8	-6.6
Reductive elimination of product	-50.3	-61.9	-50.6	-49.5

mechanism, while branched ester formation would be preferred in the alkoxy mechanism (181). *cis*-Chelating diphosphines would make the palladium coordination sphere more crowded than monodentate phophine ligands would. Hence, the fact that bidentate phophine ligands dppb and dppf promote selective formation of the linear ester might be taken as the evidence for the hydride mechanism.

It is worth to note here that theoretical calculations based on the alkoxy mechanism have never been reported in literature, which encouraged us to carry out simple computation on simplified proposed alkoxy mechanism for the alkoxycarbonylation of propyne (Scheme 6.4). The mechanism involves (i) formation of an (alkoxycarbonyl)palladium complex generated by the insertion of CO into a Pd-O bond, (ii) migration of the carboalkoxy moiety on a carbon atom of the triple bond of the propyne π-coordinated to the metal center, and (iii) protonoylsis of the resulting vinyl intermediate. Here in this mechanism, regioselectivity of the reaction can be determined by comparison of thermodynamic stability of only one intermediate for each isomer (**5AT** and **5AG**) unlike cationic–hydride mechanism discussed previously in this chapter.

6.3.2.1. Catalyst generation. The first key step in the alkoxy-mechanism of the alkoxycarbonylation of alkyne is the formation of the 14-electron active catalyst $[Pd(II)(P_2)(OMe)]^+$ (**1A**) via reaction of $Pd(OAc)_2$, P_2 and CH_3OH (180). the optimized geometry of this species around palladium center is a distorted triangle with P-Pd-O angles are 96 and 168°, and Pd-P bond distances are 2.265 and 2.370 Å.

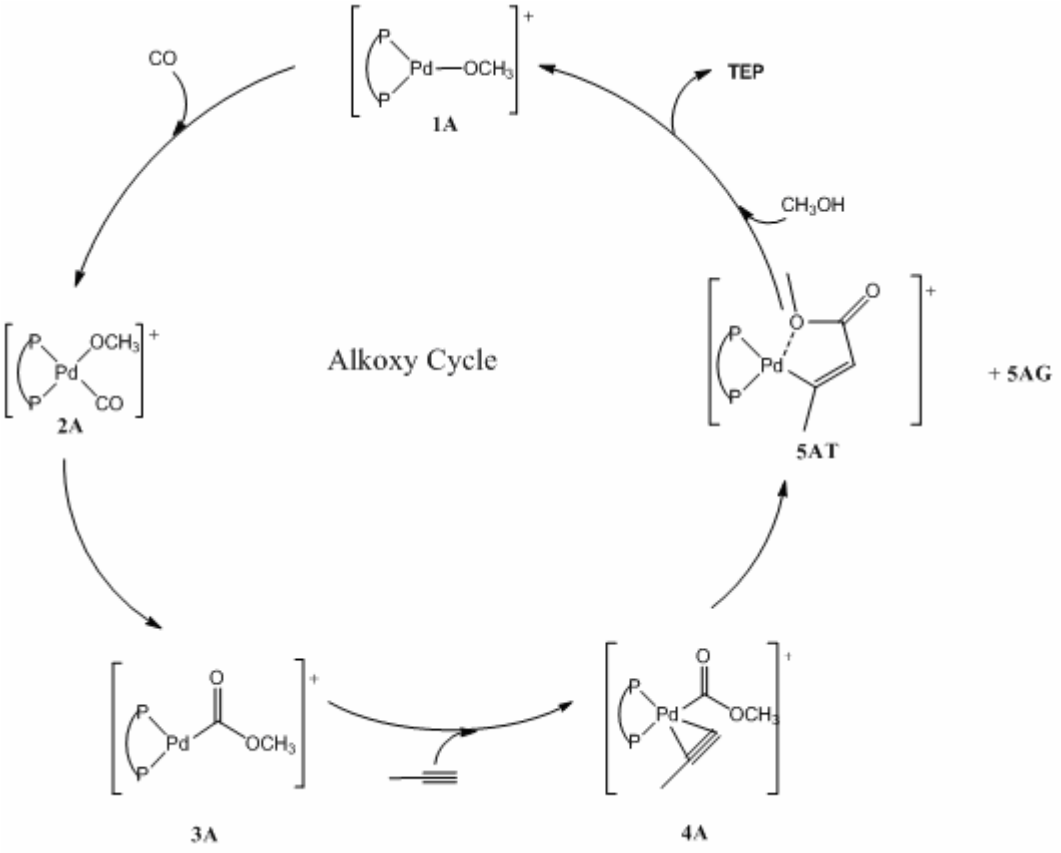

Scheme 6.4. DFT-derived scheme for alkoxycarbonylation of propyne by a cationic Palladium(II) bisphosphine alkoxy complex.

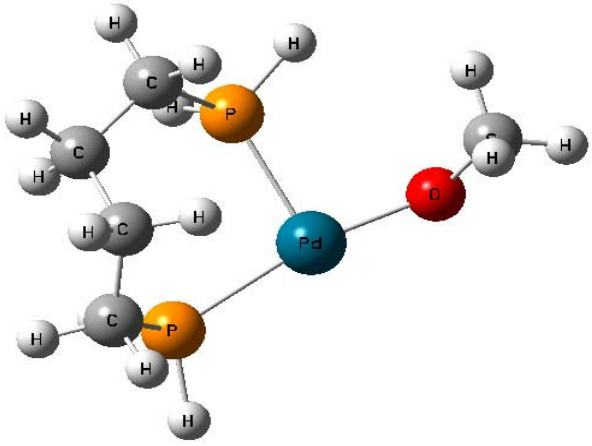

1A (0.0 kcal/mol)

6.3.2.2. CO coordination. The next step is the CO coordination to **1A**. The structure of the resulting optimized geometry **2A** is a square distorted planar conformation around the central palladium with C-Pd-O angle is 92°. The computed relative energy of 2A reveals that this step is exothermic by a 19.1 kcal/mol.

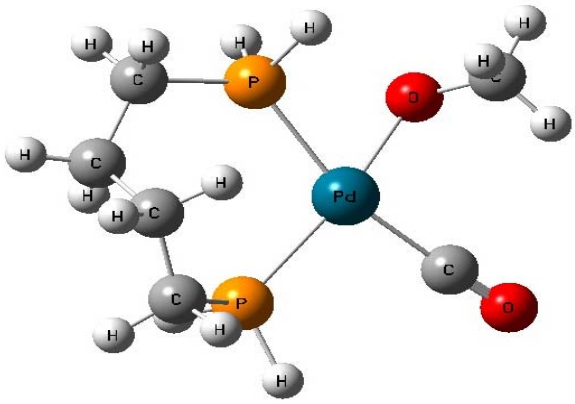

2A (-19.1 kcal/mol)

6.3.2.3. CO insertion. The insertion of CO in intermediate **2A** leads to the formation of carboxy intermediate **3A**. The Pd-C distance is 1.995 Å and the P-Pd-C angle is 111° making the geometry around central palladium approaching a planar triangle shape. The calculated energy for this insertion step is endothermic by a 10.0 kcal/mol which is higher than energy for CO insertion into Pd-C bond in hydride cationic cycle (section 4.3.1.4).

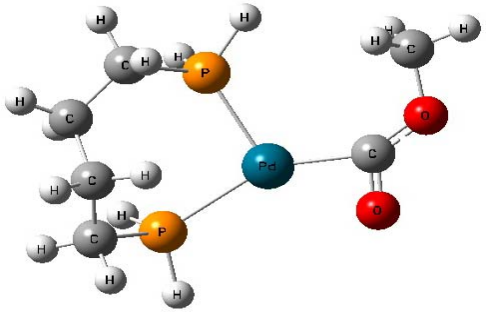

3A (-9.1 kcal/mol)

6.3.2.4. Alkyne coordination and insertion. The coordination of alkyne on palladium central occurs with bidentate coordination of dppb ligand (**4A**) or can be accompanied by dissociation of one phosphine yielding **4A-1**. The energies of the two optimized geometries are much different and the phosphine ligand bidentate fashion in **4A** is more stable than monodentate one in **4A-1** by a 15.7 kcal/mol, and so **4A** will be adopted in this study. However, Pd-C bond distances in **4A-1** (2.238/2.404 Å) are smaller than **4A** (2.316/2.586 Å) which indicates stronger π-interaction of acetylene bond with Pd atom in **4A-1** than **4A**. It is worth to note here that replacing the hydride atom or the carboxy group with amide group resulted in complete favoring of monodentate mode of coordination for the dppb ligand, which indicates an influential role of these coordinating groups on phosphine ligand coordination mode.

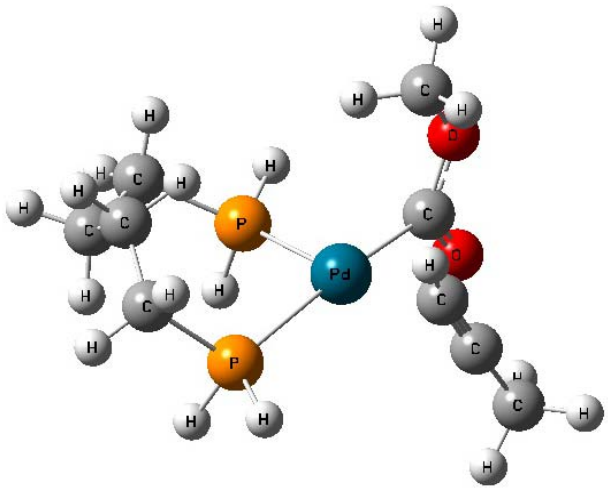

4A (-14.0 kcal/mol)

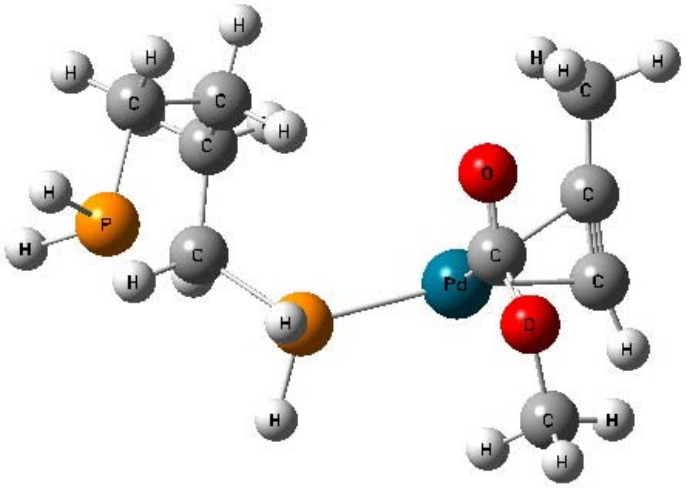

4A-1 (1.7 kcal/mol)

The next step is the migration of the carboalkoxy moiety on a carbon atom of the triple bond of the propyne. Again, migration can occur in two ways, *anti*-Markovnikov and Markovnikov additions yielding *trans* (**5AT**) and *gem* (**5AG**) isomers, respectively. The optimized geometry for the two isomers shows an interesting coordination of lone pair of electrons on alcohol oxygen atom to palladium leading to the formation of planar five-membered ring. The migration step is highly exothermic for the two isomers **5AT** and **5AG** by 27.2 and 29.8 kcal/mol, respectively. This difference in thermodynamic stability for **5AT** over **5AG** can be also used to account for the regioselectivity of the alkoxycarbonylation reaction to produce the *gem* isomer as major product starting from palladium-alkoxy species. Removing ligand simplification from the above two key intermediates increased the stability of **5AG-LNS** over **5AT-LNS by** 7.7 kcal/mol in gas phase and 6.2 kcal/mol in acetonitrile. The above result gives more evidences for the great role of type of solvent and ligand towards the formation palladium-hydride or

palladium-alkoxy species, and hence different regioselectivity of the alkoxycarbonylation reaction.

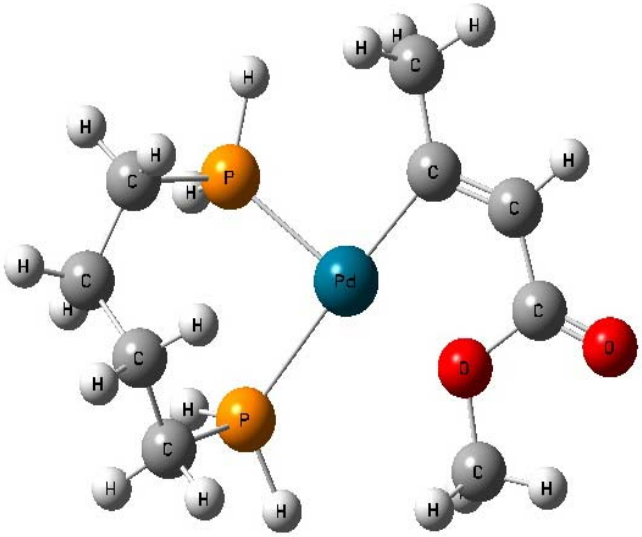

5AT (-27.2 kcal/mol)

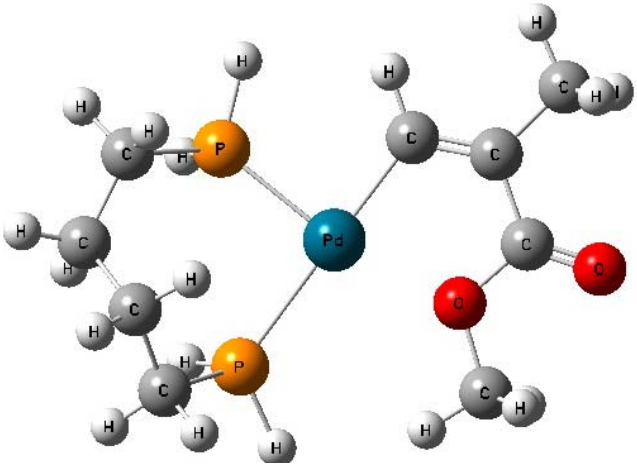

5AG (-29.8 kcal/mol)

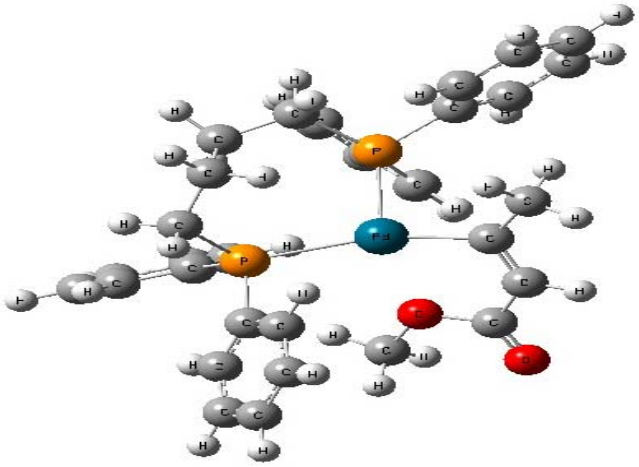

5AT-LNS (E_{tot} = -2238.295595)

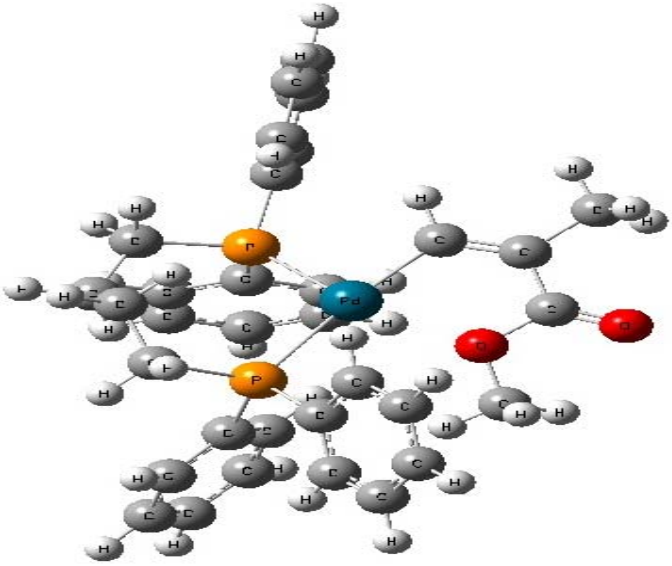

5AG-LNS (E_{tot} = -2238.307815)

It is worth noting that the geometry of the non-simplified regioselectivity key intermediates showed longer Pd-O distance (2.338 Å) than simplified intermediates (2.180 Å) which indicates great effects of ligand simplification on the energy and regioselectivity profile of catalytic cycle intermediates.

The computed energetic data for the whole reactions in alkoxy-cationic cycle is shown in Table 6.4.

Table 6.4. B3LYP/LANL2DZp computed total electronic energies (E_{tot}, au) in gas phase, free energies (G_{tot} (298 K), au), zero-point energies (ZPE, kcal/mol) as well as number of imaginary frequencies (N_{Imag}) and (E_{tot}, au) in acetonitrile for alkoxy cycle.

Compound	**E_{tot} (gas phase)**	**ZPE (N_{Imag})**	**(G_{tot} (298 K)**	**E_{tot} (acetonitrile)**
1A	-1084.000151	122.9892	-1083.845542	-1084.083497
2A	-1197.343125	128.1203	-1197.183277	-1197.416553
3A	-1197.360344	129.8516	-1197.197019	-1197.431763
4A	-1314.036626	165.2548	-1313.824371	-1314.107391
4A-1	-1314.010197	164.3279	-1313.802598	-1314.079041
5AT	-1314.085349	168.6702	-1313.864012	-1314.157035
5AG	-1314.089158	168.4367	-1313.868980	-1314.160118

6.3.2.5. Solvation effect of alkoxy cycle

The solvation effect of acetonitrile has been studied on alkoxy cycle using PCM model. The relative stability of most intermediates involved in the catalytic cycle was lowered in irregular way by introducing this effect. For example, the relative stability of intermediates **2A** and **3A** in acetonitrile was lowered by 6.9 and 1.3 kcal/mol, respectively. However, the regioselectivity profile did not change by introducing this effect and the still intermediate **5AG** is more stable than **5AT** by a 6.2 kcal/mol.

6.3.2.6. Study of the validity of substrate simplification

To test the validity of substrate simplifications, the structure and energy of new regioselectivity key intermediates (with no ligand simplification) in the alkoxy cycle based on phenylacetylene (**5ATLNS-1a** and **5AGLNS-1a**) and 1-heptyne (**5ATLNS-1b** and **5AGLNS-1b**) have been obtained and compared. Results obtained showed no change in the regioselectivity profile of the alkoxycarbonylation reaction based on alkoxy cycle by changing the alkyne substrate. This result confirms the experimental results obtained in chapter 3.

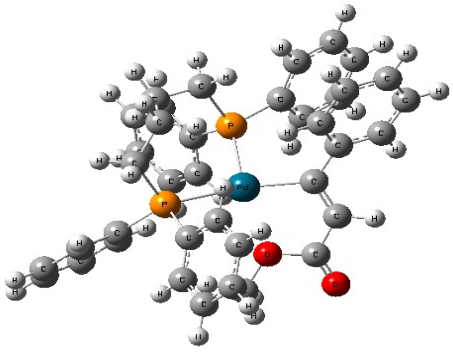

5ATLNS-1a (E_{tot} = -2430.033169)

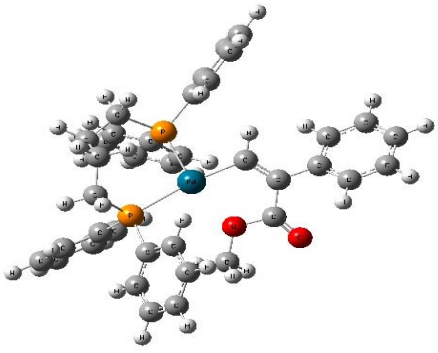

5AGLNS-1a (E_{tot} = -2430.039687)

Energy difference = 4.1 kcal/mol

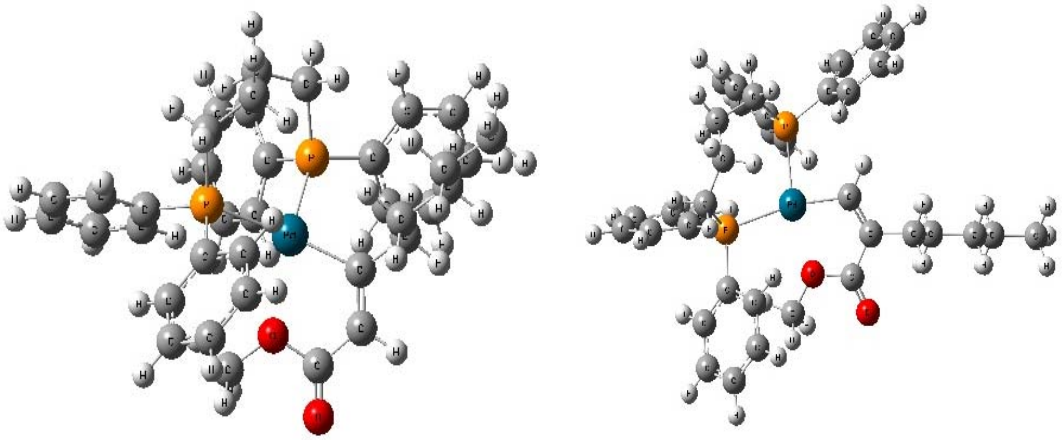

5ATLNS-1b (E_{tot} = -2395.548665) **5AGLNS-1b (E_{tot} = -2395.560839)**

Energy difference = 7.6 kcal/mol

6.4. Regioselectivity profile for aminocarbonylation reaction

The conclusions obtained in the alkoxycarbonylation reaction can be used as basis for the study of regioselectivity profile of *trans* and *gem* amides obtained from aminocarbonylation of alkynes. Using similar strategy, the energy of two different palladium hydride (**7CT-AM** and **7CG-AM**) and palladium-amide (**5AT-AM** and **5AG-AM**) key intermediates (**T** and **G**) were computed and compared.

The stability of regioselectivity key intermediates obtained via hydride cycle is in favor of *trans* amide **7CT-AM** which again supports the formation of *trans* α,β-unsaturated amides starting from active palladium-hydride species. On the other hand, the higher stability of isomer **5AG-AM** relative to **5AT-AM** gives further approval for the palladium-amine cycle we already proposed in chapter 3 to account the regioselectivity of aminocarbonylation reaction towards the formation of *gem* isomer as predominant product.

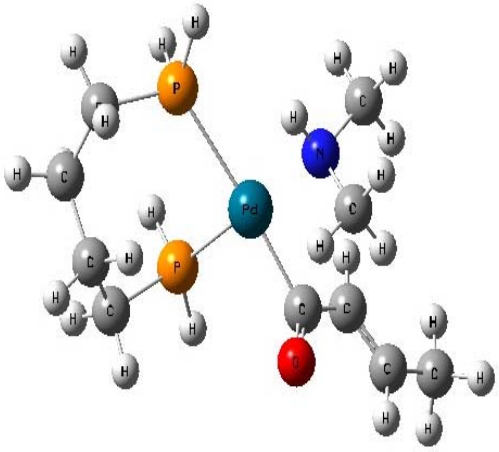

7CT-AM (E_{tot} = -1334.752917)

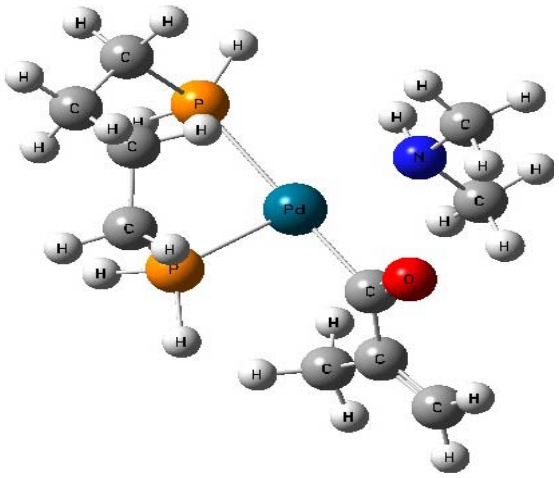

7CG-AM (E_{tot} = -1334.747364)

Energy difference = 3.5 kcal/mol

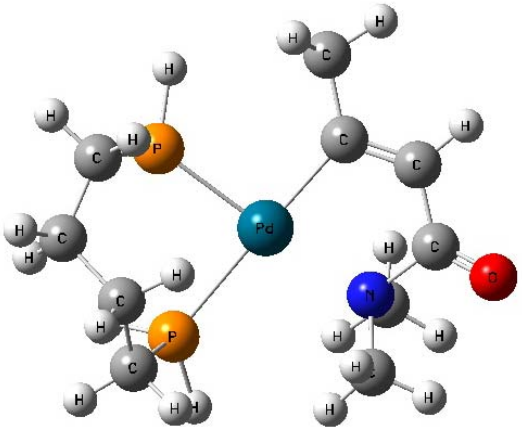

5ATLNS-AM (E_{tot} = -1333.532964)

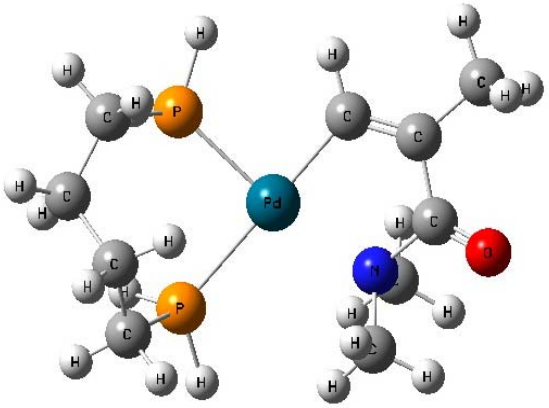

5AGLNS-AM (E_{tot} = -1333.537123)

Energy difference = 2.6 kcal/mol

6.5 Neutral Mechanism

We proposed different catalytic cycles based on active neutral species such as PdP_2 or $HPdP_2X$ and we investigated them computationally using similar strategy to the above studies. However, the results obtained from all proposed intermediates were not useful in

interpretation of experimental results obtained in chapter 3 from the energy and regioselectivity point of views. This mismatching between the computational and the experimental results encouraged us not to consider this mechanism any further in explaining the results obtained for the alkoxycarbonylation and aminocarbonylation reactions.

6.6 Conclusions

A DFT study on the palladium-bisphosphine catalyzed alkoxycarbonylation and aminocarbonylation of alkyne (propyne) is presented. The theoretical study explores the feasibility and regioselectivity control of two independent mechanisms for the alkoxycarbonylation reaction, one based on the active hydride intermediates of the type $[Pd(II)(P_2)(H)]^+$ (where $P_2 = PH_2CH_2CH_2CH_2CH_2PH_2$), and the second based on active palladium-alkoxy species $[Pd(II)(P_2)(OMe)]^+$. The study compares the theoretical results with experimental observations which have already been reported in chapters 2 and 3. The calculations successfully explain the role of solvent in increasing the yield and controlling the selectivity of reaction to produce selectively the *trans* isomer in alkoxycarbonylation reaction (hydride cycle) and the *gem* isomer in alkoxy cycle. In hydride cycle, the regioselectivity is mainly determined by the stability of the ligand simplified complex $[Pd(II)(P_2)(COC_3H_5)(CH_3CN)]^+$ which is formed from the addition of alkyne to the active intermediate, hydride migratory insertion, CO coordination and insertion, and subsequent acetonitrile coordination. When ligand simplification was removed, the regioselectivity is mainly due to the stability of most of *trans* intermediates relative to *gem* intermediates. For the alkoxy cycle, the regioselectivity is mainly

determined by the stability of the complex $[Pd(II)(P_2)(COOMe)(C_3H_5)]^+$. The kinetic data for the formation of the two key complexes in hydride and alkoxy cycles show no difference between the *gem* and *trans* isomers which predict the regioselectivity to be thermodynamically controlled process. The solvation data show good contribution in directing the regioselectivity of the two mechanisms. Using similar strategy, accounting for the regioselectivity of aminocarbonylation catalyst system was possible staring from palladium-hydride and palladium-amine active species. Overall calculations support, for the palladium-bisphosphine systems, a reaction mechanism based on palladium-hydride precursor for alkoxycarbonylation and aminocarbonylation reactions to produce the *trans* isomer regioselectively, and palladium-alkoxy or palladium-amine precursor for producing the *gem* isomer regioselectively.

CHAPTER 7

CONCLUSIONS

1. The results of the study showed clearly that the homogeneous catalytic system including palladium (II), 1,4-bis(diphenylphosphino) butane (dppb) and salicylborate complex in acetonitrile as a solvent is highly active in the alkoxycarbonylation of phenylacetylene. The type of catalyst precursor, the ligand and the solvent are influential on the activity and selectivity of the catalytic reaction. This investigation has allowed us to obtain the largely predominant formation of cinnamate esters with excellent selectivity (90-96 %).
2. The aminocarbonylation and alkoxycarbonylation reactions of terminal alkynes took place smoothly and efficiently using the catalyst system $Pd(OAc)_2$/dppb/*p*-TsOH/CH_3CN/CO under relatively mild experimental conditions. The results showed significant differences in the conversion of **1a** and in the selectivity towards the *gem* or *trans* unsaturated esters or amides with these nucleophiles. With amine nucleophile, excellent regioselectivity towards the 2-acrylamides (*gem* isomer, **3ab**) was almost always observed, while *trans*-α,β-unsaturated esters **4ac** was the predominant product with alcohol nucleophile. This remarkable sensitivity in the selectivity of the reaction indicates two different possible mechanistic pathways for these carbonylation reactions.
3. The alkoxycarbonylation of *gem*-enamides proceeded smoothly and efficiently to give ω-amido esters with complete conversion and total regioselectivity in the presence of the catalyst system: $Pd(PPh_3)_2Cl_2$/MeOH/CO/H_2O. The presence of

phosphine and chloride ligands was essential for the catalytic activity. The reaction was successfully applied to the alkoxycarbonylation of diacrylamides yielding, selectively, the corresponding di-ω-amido esters. These mono and di-ω-amido esters have been used as precursors for the synthesis of *N*-substituted cyclic succinimides in moderate to high yields.

4. Various binuclear palladium(II)-bridged complexes based on chelating diimines and bridging diphosphine or diimine ligands have been synthesized and characterized successfully. The new complexes showed an interesting catalytic activity in the coupling of arylboronic acid derivatives to various olefins under free base or oxidant conditions.

5. Theoretical investigations (DFT/B_3LYP) on palladium-hydride and palladium-alkoxy mechanisms, proposed for the alkoxycarbonylation and aminocarbonylation palladium-catalyzed reaction, were successful in the interpretation of the difference of activity and regioselectivity of the above two reactions. The results obtained indicate the formation of *trans* ester isomer via palladium-hydride cycle, while palladium-alkoxy mechanism is the key for the formation of *gem* isomer. The results prove the ligand simplification protocol to be non-valid in this type of investigation. The role of acetonitrile solvent in enhancing the yield and regioselectivity of the alkoxycarbonylation and aminocarbonylation reactions was improving the stability of the cationic species in the two proposed mechanisms.

REFERENCES

1. Bibhas, R.; Sarkar, Raghunath V. C. *Catalysis Surveys from Asia.* **2005**, 9, 193.

2. Serrano, J. A.; Lledós, A.; Duckett, B. *Organometallics*. **2008**, 27, 43.

3. El Ali, B.; Tijani, J.; El-Ghanam, A. *Appl. Organomet. Chem.* **2002**, 16, 369.

4. Falbe, J.; *New syntheses with carbon Monoxide*, Springer-Verlag Berlin Heidelberg, New York. **1980**, p 31, 274, 304.

5. Pino, P. Wender, I. G; *Organic Syntheses Via Metal Carbonyls*; John Wiley and Sons: New York, **1977,** Vol. 2, p 446, 457, 504.

6. Beller, M.; Cornills, B.; Frohning, C.; D. Kohlpaintner, W. C. *J. Mol. Catal.* **1995**, 104, 17.

7. Waller, F. J; *J. Mol. Catal.* **1985**, 31, 123.

8. Parshall, W. G.; Ittel, D. S; *'The applications and chemistry of catalysis by soluble transition metal complexes'*. (2nd eds). **1992**, p 2, 97, 140.

9. Hardly, D. V. N; *J. Chem. Soc.* **1936**, 358.

10. Koch, H.; Haag, W. *Angew, Chem*. **1958**, 70, 311.

11. Reppe, W.; Kroper, H. *Ger. Pat.* 765 969 & 879 987. **1953**.

12. Reppe, W.; Friederich, H.; Laib, H. *Ger. Pat*. 893,501 ,CAN. 48, 12791d, **1958**.

13. Cornils, B.; Herrmann, W. A. '*Applied Homogeneous Catalysis With Organometallic Compounds'*. VCH Weinhein Germany **1996**; Vol. 1, p 187, 342.

14. Alper, H.; Leonard, D. *Tetrahedron lett.* **1985**, 26, 5639.

15. Falbe, J; Korte, F. *Chem. Ber*. **1962**, 95, 2680.

16. Stille, K. J. '*Comprehensive Organic Synthesis'*, Vol 4, Pergamon Press, Oxford, **1991**, p 913.

17. Sonawane, H. R.; Bellur, N. S.; Ahuja, J. R.; Kulkarni, D. G. *Tetrahedron Asymmetry*, **1992**, 3, 163.

18. Stinson, S. C.; *Chem. Eng. News*, **1992**, Sept. 28, 46.

19. Alper, H.; Hamel, N. *J. Am. Chem. Soc.* **1990**, 112, 2803.

20. Jayasree, S.; Seayad, A.; Gupte, S. P.; Chaudhari, R.V. *Org. Lett.* **1999**, 1, 459.

21. El Ali, B.; Alper, H.; Vasopollo, G. *J. Org. Chem*. **1993**, 58,

22. Consiglio, G.; Nefkens, S. C.; A. Pisano, C.; Wenzinger, F. *Helv. Chim. Acta*, **1991**, 74, 323.

23. El Ali, B.; Alper, H. *J. Mol. Catal*. **1992**, 77, 17.

24. El Ali, B.; Alper, H. *J. Mol. Catal*. **1993**, 80, 377.

25. Ojima, I.; *'Catalytic asymmetric synthesis'* New York, VCH, **1993**; El Ali, B.; Alper, H., in: M. Beller, C. Bolm (eds), *Transition Metals for Organic Synthesis* Vol. 1, Wiley VCH, Weinheim, **1998**, p 57.

26. Cornils, B.; Herrmann, W. A. '*Aqueous phase Organometallic*: *Concept and Application'*. Wiley-VCH, Weinhein, Germany **1998**, p 100.

27. Diab, L.; Gouygou, M.; Manoury, E.; Kalck, P.; Urrutigoïty, M;. *Tetrahedron Lett.* **2008**, 49(35), 5186.

28. Fernando. H. L.; Uzcategui, G. C.; Ortega, M. C.; Alvarez, J.; Pardey, A. J.; Longo, C. *Ciencia (Maracaibo, Venezuela)*. **2007**, 15(1), 85.

29. Tiago, O.; Vieira, M. J.; Green, Alper, H. *Org. Lett*. **2006**, 8(26), 6143.

30. Rangits, G.; Kollár, L. *J. Mol. Cat. A: Chem*. **2005**, 242, 156.

31. Reppe, W. *Ann*, **1948**, 560, 1.

32. Roelen, O. *Angew. Chem.* A.60, **1948**, 3, 213.

33. Jones, E. R.; Shen, T. Y. Whiting, M. C; *J. Chem. Soc.* **1951**, 230.

34. Yamamoto, K. *Bull. Chem. Soc.***1954**, 27, 505.

35. Inoue, S.; Fukumoto, Y.; Chatani, N. *J .Org. Chem*. **2007**, 72(17), 6588.

36. Jacobsen, G.; Spathe, H; *Ger. Patent*, **1962**, 1 138 760.

37. *Chem. Abstr*. **1963**, 58, 6699.

38. Tsuji, J. Nogi, T; *J. Org. Chem*.**1966**, 31, 2641.

39. Tsuji, J.; Nogi, T; *J. Am. Chem. Soc*. **1966**, 88, 1289.

40. Tsuji, J.; Nogi, T; *Tetrahedron Lett*; **1966**, 1801.

41. Tsuji, J.; Nogi, T; *Tetrahedron Lett*; **1969**, 25, 4099.

42. Chiarotto, I.; Carelli, I. *Synth. Communications*. **2002**, 32, 881.

43. Li, J. H.; Tang, S.; Xie, X. *J. Org. Chem.* **2005**, *70*, 477.

44. Dubois, M. R. *Chem. Rev*. **1989**, 89, 1.

45. Kuniyasu, H.; Ogawa, A.; Miyazaki, S.; Ryu, I.; Kambe, N.; Sonoda, N. *J. Am. Chem. Soc*. **1991**, 113, 9796.

46. Ogawa, A.; Kawakami, J.; Mihara, M.; Ryu, I.; Kambe, N.; Sonoda, N. *J. Am. Chem. Soc*. **1995**, 117, 7564.

47. Ogawa, A.; Kawakami, J.; Mihara, M.; Ikeda, T.; Sonoda, N.; Hirao, T. *J. Am. Chem. Soc*. **1997**, 119, 12380.

48. Xiao, J. W.; Alper, H. *J. Org. Chem.*, **1997**, 62, 34222.

49. Xiao, J. W.; Alper, H. *J. Org. Chem.*, **1998**, 63, 7939.

50. Xiao, J. W.; Vasapollo, G.; Alper, H. *J. Org. Chem*., **1997**, 62, 34222.

51. Xiao, J. W.; Vasapollo, G.; Alper, H. *J. Org. Chem*., **1999**, 64, 2084.

52. El Ali, B.; Tijani, J.; El-Ghanam, A.; Fettouhi, M; *Tetrahedron Lett.* **2001**, 42(8), 1567.

53. Reppe, W; *Ann*., **1953**, 1, 582.

54. Ferbenindustris, A. G.; Ludwigshafen, BIOS *Final Report* No. **1947**, 37, 1811.

55. Neher, H. T.; Specht, E. H.; Newman, A. *U.S. Pat*. 2 773 063, **1956**.

56. Pino, P.; Paleari, C. *Gazz. Chim. Ital*. **1951**, 81, 646.

57. Torii, S.; Okumoto, H.; Sadakane, M. He Xu, L. *Chem. Lett*. **1991**, 1673.

58. Murahashi, S.; Imada, Y.; Nishimura, K. *Tetrahedron*, **1994**, 50, 2 453.

59. Imada, Y.; Alper, H. *J. Org. Chem*. **1996**, 61, 6799.

60. Imada, Y.; Vasopollo, G.; Alper, H. *J. Org. Chem*. **1996**, 61, 7982.

61. El Ali, B.; Tijani J.; El-Ghanam, A. *J. Mol. Cat. A: Chemical*. **2002**, 187, 17.

62. El Ali, B.; Tijani J. *Applied Organometallic Chem.* **2003**, 17(12), 921.

63. Matteoli, U.; Scrivanti, A.; Beghetto V. *J. Mol. Cat. A: Chemical*, **2004**, 213 (2), 183.

64. Park, J. H.; Kim, S. Y.; Kim, S. M.; Chung. Y. K. *Org.Lett*. **2007**, 9, 2465.

65. Li, Y.; Alper, H.; Yu, Z. *Org. Lett.* **2006**, 8, 5199.

66. Sternberg, W.; H. Markby, R.; Wender, I. *J. Org. Chem*. **1960**, 82, 3638.

67. Periasamy, M.; Radhakrishnan, U.; Rameshkumar, C.; Brunet, J. *Tetrahedron Letters*. **1997**, 38(9), 1623.

68. Bird, C.; W. Briggs, E. M. *J. Chem. Soc*. **1967**, 1265.

69. Rosenthal, W. R.; Schwartzman, H. L. *J. Org. Chem*. **1959**, 24, 836.

70. El Ali, B.; Alper, H. *Synlett*. **2000**, 2, 161.

71. Huo, Z.; Patil, N. T.; Jin, T.; Pahadi, N. K.; Yamamoto, Y. *Advanced Synthesis & Catalysis*. **2007**, 349 (4+5), 680.

72. Akao, M.; Sugawara, S.; Amino, K.; Inoue. Y. *J. Mol. Cat.* **2000**, 157, 117.

73. Mori, K.; Mizoroki, T.; Ozaki, A. *Chem. Lett*. **1975**, 39.

74. El Ali, B.; Alper, H. *J. Mol. Cat.* **1991**, 67, 29.

75. Itoh, K.; Miura, M.; Nomura, M. *Tetrahedron Lett*. **1992**, 33, 5369.

76. Kushino, Y.; Itoh, K.; Miura, M.; Nomura, M. *J. Mol. Cat.* **1994**, 89, 151.

77. El Ali, B.; Alper, H. *J. Mol. Cat.* **1995**, 96, 197.

78. Drent, E.; Budzelaar, M.; H. P. *J. Organomet. Chem*. **1993**, 455, 247.

79. Knifton, F. *J. Mol. Cat.* **1977**, 2, 293.

80. Alper, H.; Maldonado, M. S.; Lin, I. J. B; *J. Mol. Cat.* **1988**, 49, L27.

81. Scrivanti, A.; Menchi, G.; Matteoli, U. *J. Mol. Cat.* **1995**, 96, 223. Scrivanti, A.; Chinellato, R. G.; Matteoli, U. *J. Mol. Cat.* **1993**, 84, L141.

82. El Ali, B.; Tijani, J.; El-Ghanam, A. *Tetrahedron Lett.* **2001**, 42(12), 2385.

83. Simon, K.; Julian G.; Betham, M. *Chem. Comm.* **2006**, 108.

84. Zurakowska, O. J. *Polymer*, **1978**, 19, 720.

85. Shiohara, K.; Habaue, S.; Okamoto, Y. *Polymer J*. **1998**, 30, 3, 249.

86. Zurakowska, O. J., *Polymer Sci. part C*, **1968**, 16, 3291.

87. Trippet, S.; Walker, M. D. *J. Chem. Soc.* **1961**, 1266.

88. Tsuji, J. *Organic Synthesis with Palladium Compounds*. Springler-Verlag: Berlin, **1980**, p159.

89. Beller, M.; Bolm C. *Transition Metals for Organic Synthesis*, vol. I-II. Wiley-VCH: Weiheim, **1998**.

90. Bianchini, C.; Mantovani, G.; Meli, A.; Oberhauser, W.; Bruggeller, P.; Stampfl, T. *J. Chem. Soc., Dalton Trans.* **2001**; 690.

91. Mats, L.; Mikael, M.; Sivaprasad, S. *Organic Process Research & Development* **2004**, 8(6), 838.

92. Hongzhou, G.; Jinling Z.; Qinglei, M. *Xueyuan Xuebao.* **2005**, 24(5), 116.

93. Heck, R. F. *J. Am. Chem. Soc*. **1969**, 91, 6707.

94. Patrick, P.; Marc, F.; Yves, C.; Andre, M.; Francis, P. *Applied Catalysis A: General*. **1996**, 135(2)**,** 329.

95. Usaji, T.; Isamu, S.; Yoshihiro, Y.; Retsu, H. *(Mitsui Toatsu Chemicals, Inc., Japan). Jpn. Kokai Tokyo Koho* 1987: JP 62123151.

96. Izawa, Y.; Shimizu, I.; Yamamoto, A. *Bull. Chem. Soc. Jap.* **2004**, 77, 2033.

97. James, D. E.; Hines, L. F.; Stille, J. K. *J. Am. Chem. Soc.* **1976**, 98**,** 1806.

98. Vieira, T. O.; Green, M. J.; Alper H. *Org. Lett.* **2006**, 8, 6143.

99. Seayad, A.; Kelkar, A. A.; Toniolo, L.; Chaudhari, R. V. *J. Mol. Cat.* **2000**, 151, 47.

100. Jayasree, S.; Seayad, A.; Gupte, S. P.; Chaudhari, R. V. *Cat. Lett.* **1999**, 58, 213.

101. Del Rio, I.; Ruiz, N.; Claver, C.; vanVeen, L. A.; van Leeuwen PWNM. *J. Mol. Cat.* **2000**, 161, 39.

102. Dekker, G. C.; Elsevier, J. C.; Vrieze, K.; van Leeuwen, PWNM. *Organonometallic* **1992**, 11, 1598.

103. Paviglianiti, A. K.; Minn, D. J.; Fultz, W. C.; Burmeister, J. L. *Inorg. Chim. Acta.* **1989**, 159, 65.

104. Nobuaki, K.; Keiji, M. *J. Am. Chem. Soc.* **1985**, 107, 7230.

105. Koga, N.; Morokuma, K. *J. Am. Chem. Soc.* **1986**, 108, 6136.

106. Peter, D.; van Leeuwen, PWNM. *J. Chem. Soc., Dalton Trans.* **1999**, 10, 1519.

107. Kayaki, Y.; Shimizu, I.; Yamamoto, A. *Chem. Lett.* **1995**, 1089.

108. El Ali, B.; Alper, H. *J. Org. Chem.* **1991**, 56, 5357.

109. El Ali, B.; Okuro, K.; Vasapolo, G.; Alper, H. *J. Am. Chem. Soc.* **1996**, 118, 4264.

110. Tezuka, K.; Ishizaki, Y.; Inuoue, Y. *J. Mol. Cat.* **1998**, 129, 199.

111. Rivetti, F.; Romano, U. *J. Organomet. Chem.* 1978; **154**: 323.

112. Bertani, R.; Cavinato, G.; Toniolo, L.; Vasapollo, G. *J. Mol. Cat.* 1993; **84**: 165.

113. Zudin, V. N.; Chinakov, V. D.; Nikipelov, V. M.; Rogov, V. A.; Likholobov, V. A.; Ermakov, Y. I. *J. Mol. Catal.* **1989**, 52, 27.

114. Zargarian, D. *Ph.D. Thesis*, *University of Ottawa*. **1992**.

115. Oshima, M.; Shimizu, I.; Yamamoto, A.; Ozawa, F. *Organometallics.* **1991**, 10, 1221.

116. Cooper, D. G.; Powel, J. *Can. J. Chem.* **1973**, 51, 1634.

117. Davies, J. A.; Hartley, F. R.; Murray, S. G. *J. Chem. Soc., Dalton Trans.* **1980**, 2246.

118. Leone, A.; Gischig, S.; Consiglio, G. *J. Organomet. Chem.* **2006**, 691, 4816.

119. Sperrle, M.; Consiglio, G. *J. Mol. Cat.* **1999**, 143, 263.

120. Pino, P.; Wender, I. G. *Organic Syntheses Via Metal Carbonyls*, John Wiley and Sons: New York. **1977**, 2, 178.

121. Zargarian, D.; Alper, H. *Organometallics.* **1993**, 12, 712.

122. Kiss, G. *Chem. Rev.* **2001**, 101, 3435.

123. Marc, A.; Klingshirn, R. D.; Rogers, K. H. Shaughnessy *J. Organomet. Chem.* **2005**, 690, 3620.

124. Nozaki, K.; Sato, N.; Tonomura, Y.; Yasutomi, M.; Takaya, H.; Hiyama, T.; Matsubara, T.; Koga, N. *J. Am. Chem. Soc*. **1997**, 119, 12779.

125. Skoda-Földes, R.; Kollár, L. *Curr. Org. Chem.***2002**, 6, 1097.

126. (a) Tatee, T.; Narita, K.; Kurashige, S.; Ito, S.; Miyazaki, H.; Yamanaka, H.; Mizugaki, M.; Sakamoto, T.; Fukuda, H. *Chem. Pharm. ull.* **1986**, 34, 1643. (b) Kitagawa, O.; Aoki, K.; Inoue, T.; Taguchi, T. *Tetrahedron Lett.* **1995**, 36, 593. (c) Andres, C.; Duque-Soladana, J. P.; Pedrosa, R. *J. Org. Chem.* **1999**; 64, 4282.

127. Caulfield, M. J.; Qiao, G. G.; Solomon, D. H. *Chem.Rev.* **2002**, 102, 3067.

128. Ouerfelli, O.; Isida, M.; Shinozaki, H.; Nakanishi, K.; Ohfune, Y., *Synlett* **1993**, 6, 409.

129. Konishi, M.; Kumada, V.; Hayashi., T., *Tetrahedron Lett*. **1979**, 21, 1871.

130. El Ali, B.; Tijani, J.; El-Ghanam, A.; Fettouhi, M., *Tetrahedron Lett.* **2000**, 41, 5761.

131. Wen, R., Luo, Xin-xiang, Yu.; Shan-xin, Zhang Lu-xi. *Hecheng Huaxue*. **2001**, 9, 269.

132. Takayama, C.; Fujinami, A. *Pestic. Biochem. Physiol*. **1979**, 12, 163.

133. Nargund, K. S.; Nemlekar, S. G.; Dabholkar, R. D. *Indian Drugs*. **1984**, 22, 121.

134. Barman, G.; Roy, M.; Jayanta. K. Ray. *Tetrahedron Lett*. **2008**, 49, 1405.

135. Nakao, Y.; Chen, J.; Imanaka, H.; Hiyama, T.; Ichikawa, Y.; Duan, W.; Shintani, R.; Hayashi, T. *J. Am. Chem. Soc*, **2007**, 129(29), 9137.

136. Shintani, R.; Duan, W.; Nagano, T.; Okada, A.; Hayashi, T. *Angewandte Chemie International Edition*. **2005**, 44, 4611.

137. Becker, Y.; Eisenstadt, A.; Stille, J. K. *J. Org. Chem*. **1980**, 45, 2145.

138. Klaus, S.; Neumann, H.; Jiao, H.; Jacobi von Wangelin, A.; Gördes, D.; Strübing, D.; Hübner, S.; Hateley, M.; Weckbecker, C.; Huthmacher, K.; Riermeier, T.; Beller, M. *J. Organometal. Chem*. **2004**, 689, 3685.

139. Zhu, B. C.; Jiang, X. Z. *Appl. Organometal. Chem*. **2006**, 20, 277.

140. Ojima, I.; Zhang, Z. *Organometallics* **1990**, 9, 3122.

141. Cesa, M. C.; Burrington, J.D. United States Patent, **1987**, PN 4,710,574.

142. Ruan, Z; Lawrence, R. M.; Cooper, C. B. *Tetrahedron Letters*. **2006**, 47(43), 7649.

143. Amir, Mohammad; Singh, Era. *Pharmazie*. **1991**, 46(10), 705.

144. Sangeeta, V. J.; Deshpande, R. M. *Catalysis Today*. **2008**, 131, 353.

145. Zhao, B.; Lu, X. *Organomettallics*. **2006**, 8, 5987.

146. Ishii, H.; Goyal, M.; Ueda, M.; Takeuchi, K.; Asai, M. *Applied Catalysis A: General*. **2000**, 201, 101.

147. Tian, G.; Boone, H. W.; Novak, B. M. *Macromolecules*. **2001**, 34 (22), 7656.

148. Fujita, M.; Ogura, K. *Coord. Chem. Rev*. **1996**, 148, 249.

149. Bianchini, C.; Lee, H. M.; Barbaro, P.; Meli, A.; Moneti, S. *New J. Chem*., **1999**, 23, 929.

150. Janka, M.; Anderson, G.; Rath, N. *Inorg. Chim. Acta*. **2004**, 357,2339.

151. Milani, B.; Alessio, E.; Mestroni, G.; Sommazzi, A.; Garbassi, A.; Sangrando, E.; Pahor, N. B.; Randaccio, L. *J. Chem. Soc. Dalton. Trans.* **1994**, 1903.

152. Durig, J.; Mitchell, B. R.; Sink, D. W.; Willis, Jr. N.; Wilson, A. S. *Spectrochimica acta*. 23A, **1967**, 1121.

153. Lu, X.; Lin, S. *J. Org. Chem*. **2005**, 70 (23), 9651.

154. Rossiter, B. E.; Swingle, N. *Chem. Rev*. **1992**, 92, 771.

155. Dieck, H. A.; Heck, R. F. *J. Org. Chem.* **1975**, 40, 1083.

156. Cho, C. S.; Uemura, S. *J. Organomet. Chem*. **1994**, 465, 85.

157. Du, X.; Suguro, M.; Hirabayashi, K.; Mori, A. *Org. Lett*. **2001**, 3, 3313.

158. (a) Crowley, J. D.; Hänni, K. D.; Lee, A.-L.; Leigh, D. A. *J. Am. Chem. Soc*. **2007**, 129, 12092. (b) Lindh, J.; Enquist, P.-A.; Pilotti, Å.; Nilsson, P.; Larhed, M. *J. Org. Chem.* **2007**, 72, 7957. (c) Yoo, K. S.; Park, C. P.; Yoon, C. H.; Sakaguchi, S.; O'Neill, J.; Jung, K. W. *Org. Lett.* **2007**, 9, 3933. (d) Yoo, K. S.; Yoon, C. H.; Mishra, R. K.; Jung, Y. C.; Yi, S. W.; Jung, K. W. *J. Am. Chem. Soc*. **2006**, 128, 16384. (e) Enquist, P.-A.; Lindh, J.; Nilsson, P.; Larhed, M. *Green Chem*. **2006**, 8, 338. (f) Farrington, E. J.; Barnard, C. F. J.; Rowsell, E.; Brown, J. M. *Adv. Synth. Catal.* **2005**, 347, 185. (g) Akiyama, K.; Wakabayashi, K.; Mikami, K. *Adv. Synth. Catal*. **2005**, 347, 1569. (h) Andappan, M. M. S.; Nilsson, P.; Larhed, M. *Chem. Commun*. **2004**, 218. (i) Andappan, M. M. S.; Nilsson, P.; von Schenck, H.; Larhed, M. *J. Org. Chem.* **2004**, 69, 5212. (j) Lautens, M.; Mancuso, J.; Grover, H. *Synthesis* **2004**, 2006. (k) Kabalka, G. W.; Guchhait, S. K.; Naravane, A. *Tetrahedron Lett.* **2004**, 45, 4685. (l) Andappan, M. M. S.; Nilsson, P.; Larhed, M. *Mol. Diversity* **2003**, 7, 97. (m) Jung, Y. C.; Mishra, R. K.; Yoon, C. H.; Jung, K. W. *Org. Lett*. **2003**, 5, 2231.

159. Nathan, C.; Gianneschi, M. S.; Masar, C. A.; Mirkin. *Acc. Chem. Res.*, **2005**, 38 (11), 825.

160. Ruan, J.; Li, X.; Saidi, O.; Xiao, J. *J. Am. Chem. Soc.* **2008**, 130, 2424.

161. Miyaura, N. *Synlett*. **2009**, 13, 2039.

162. Braga, A. A. C.; Morgen, N. H.; Ujaque, G.; Maseras, F. *J. Am. Chem. Soc.* **2005**, 127, 9298.

163. Nishikata, T.; Yamamoto, Y; Gridnev, I. D.; Miyaura, N. *Organometallics.* **2005**, *24*, 5025.

164. Albéniz, A. C.; Catalina, N. M.; Espinet, P.; Redón, R. *Organometallics.* **1999**, 18, 5571.

165. Barder, T. E.; Biscoe, M. R.; Buchwald, S. L. *Organometallics.* **2007,** 26, 2183.

166. Niu, S.; Hall, M. B. *Chem. Rev*. **2000**, 100, 353.

167. Huo, C.; Li, Y. W.; Beller, M.; Jiao, H. *Organometallics* **2003,** *22*, 4665.

168. Lukas, J.; Goossen, D. K.; Hermann, H. L.; Thiel, W. *J. Am. Chem. Soc*. **2005**, 127, 11102.

169. Frisch, M. J.; Trucks, G. W.; Schlegel, H. B.; Scuseria, G. E.; Robb, M. A.; Cheeseman, J. R.; Montgomery, J. A., Jr.; Vreven, T.; Kudin, K. N.; Burant, J. C.; Millam, J. M.; Iyengar, S. S.; Tomasi, J.; Barone, V.; Mennucci, B.; Cossi, M.; Scalmani, G.; Rega, N.; Petersson, G. A.; Nakatsuji, H.; Hada, M.; Ehara, M.; Toyota, K.; Fukuda, R.; Hasegawa, J.; Ishida, M.; Nakajima, T.; Honda, Y.; Kitao, O.; Nakai, H.; Klene, M.; Li, X.; Knox, J. E.; Hratchian, H. P.; Cross, J. B.; Bakken, V.; Adamo, C.; Jaramillo, J.; Gomperts, R.; Stratmann, R. E.; Yazyev, O.; Austin, A. J.; Cammi, R.; Pomelli, C.; Ochterski, J. W.; Ayala, P. Y.; Morokuma, K.; Voth, G. A.; Salvador, P.; Dannenberg, J. J.; Zakrzewski, V. G.; Dapprich, S.; Daniels, A. D.; Strain, M. C.; Farkas, O.; Mallick, D. K.; Rabuck, A. D.; Raghavachari, K.; Foresman, J. B.; Ortiz, J. V.; Cui, Q.; Baboul, A. G.; Clifford, S.; Cioslowski, J.; Stefanov, B. B.; Liu, G.; Liashenko, A.; Piskorz, P.; Komaroni, I.; Martin, R. L.; Fox, D. J.; Keith, T.; Al-Laham, M. A.;

Peng, C. Y.; Nanayakkara, A.; Challacombe, M.; Gill, P. M. W.; Johnson, B.; Chen, W.; Wong, M. W.; Gonzalez, C.; Pople, J. A. *Gaussian 03, Revision D.01*; Gaussian, Inc.: Wallingford, CT, **2004**.

170. Becke, A. D. *J. Chem. Phys.* **1993**, 98, 5648.
171. Lee, C.; Yang, W.; Parr, R. G. *Phys. Re*v. *B: Condens. Matter Mater. Phys.* **1988**, 37, 785.
172. Hay, P. J.; Wadt, W. R. *J. Chem. Phys.* **1985**, 82, 299.
173. Höllwart, A.; Böhme, M.; Dapprich, S.; Ehlers, A. W.; Gobbi, A.; Jonas, V.; Köhler, K. F.; Stegmann, R.; Veldkamp, A.; Frenking, G. *Chem. Phys. Lett.* **1993**, 208, 237.
174. Hehre, W. J.; Ditchfield, R.; Pople, J. A. *J. Chem. Phys.* **1972**, 56, 2257.
175. Hariharan, P. C.; Pople, J. A. *Theor. Chim. Acta.* **1973**, 28, 213.
176. Francl, M. M.; Pietro, W. J.; Hehre, W. J.; Binkley, J. S.; Gordon, M. S.; DeFrees, D. J.; Pople, J. A. *J. Chem. Phys.* **1982**, 77, 3654.
177. Tomasi, J.; Persico, M. *Chem. Rev.* **1994**, 94, 2027.
178. Amovilli, C.; Barone, V.; Cammi, R.; Cancès, E.; Cossi, M.; Mennucci, B.; Pomelli, C. S.; Tomasi, J. *J. Ad*v. *Quantum Chem.* **1999**, 32, 227.
179. Hong, F. E.; Chang, Y. C. *Organometallics*. **2004**, 23, 718.
180. Fenton, D. M. *J. Org. Chem.* **1973**, 38, 3192.
181. Yun, H. S.; Lee, K. H.; Lee, J. S. *J. Mol. Catal. A: Chem.* **1995**, 95, 11.

APPENDICES

AI. Setup for the Catalytic Reactions.

The experimental setup of the catalytic reaction is shown hereafter (Figure AI-1). The first system includes the carbonylation system that involves a carbon monoxide cylinder, hydrogen cylinder, high pressure houses, carbon monoxide detector, and high pressure autoclaves. Hotplate stirrers with oil baths are used to heat the high pressure vessels. The second system includes a gas chromatography equipped with computer and printer to analyze the sample collected from high-pressure system after cooling down and releasing of gases.

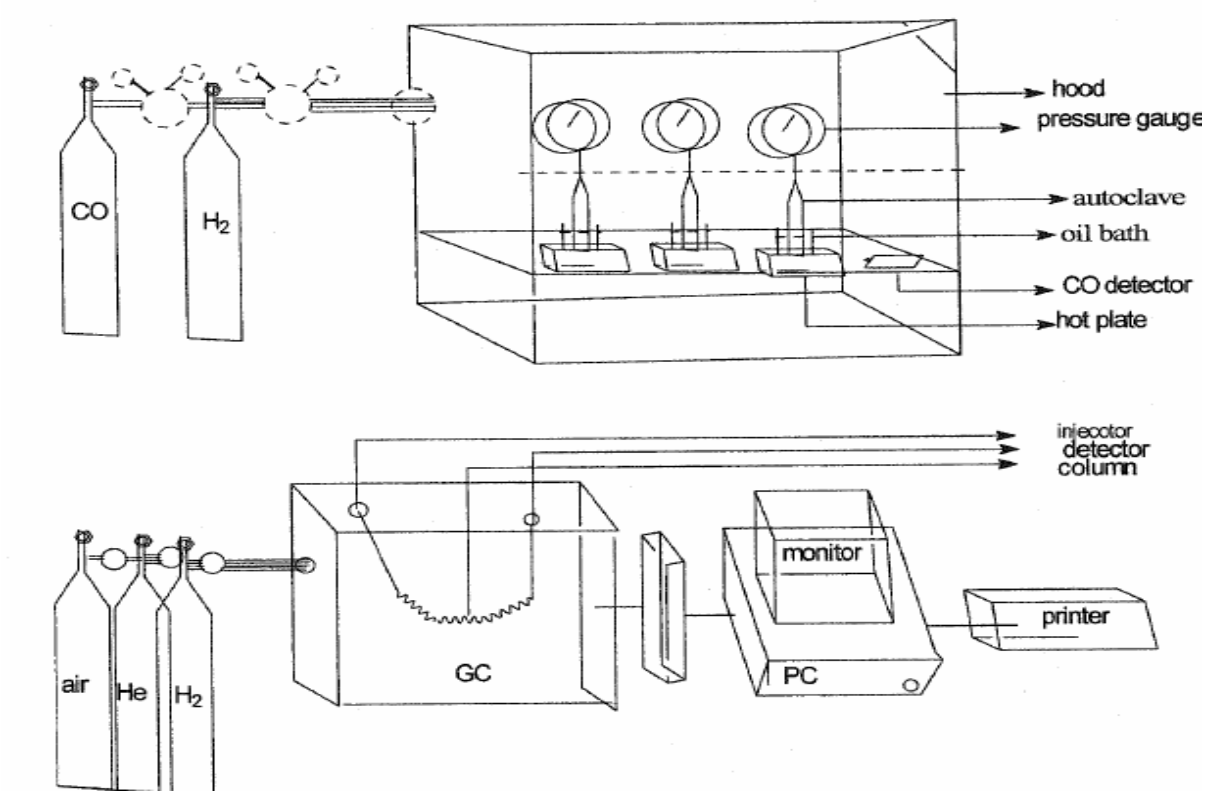

Figure AI-1. Setup for catalytic reactions and GC analysis

AII. NMR spectra of some enamides, amidoesters and cyclic scuccinimides

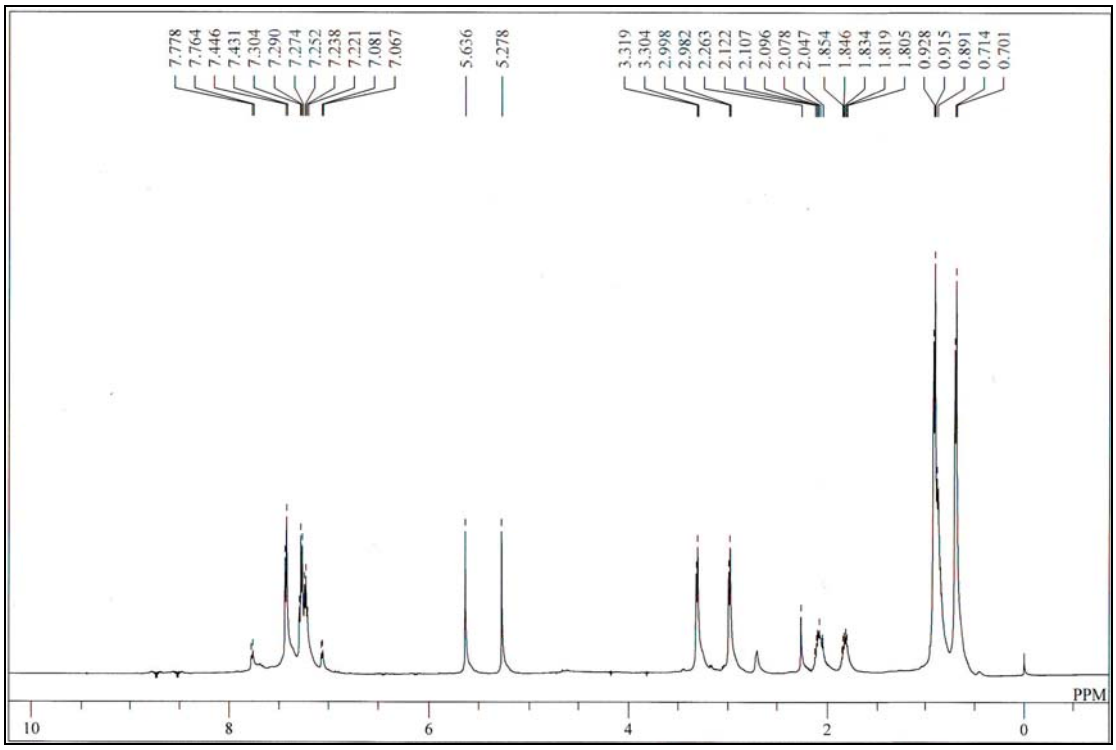

Figure AII-1. ^{1}H NMR spectrum of compound **3ab$_1$**.

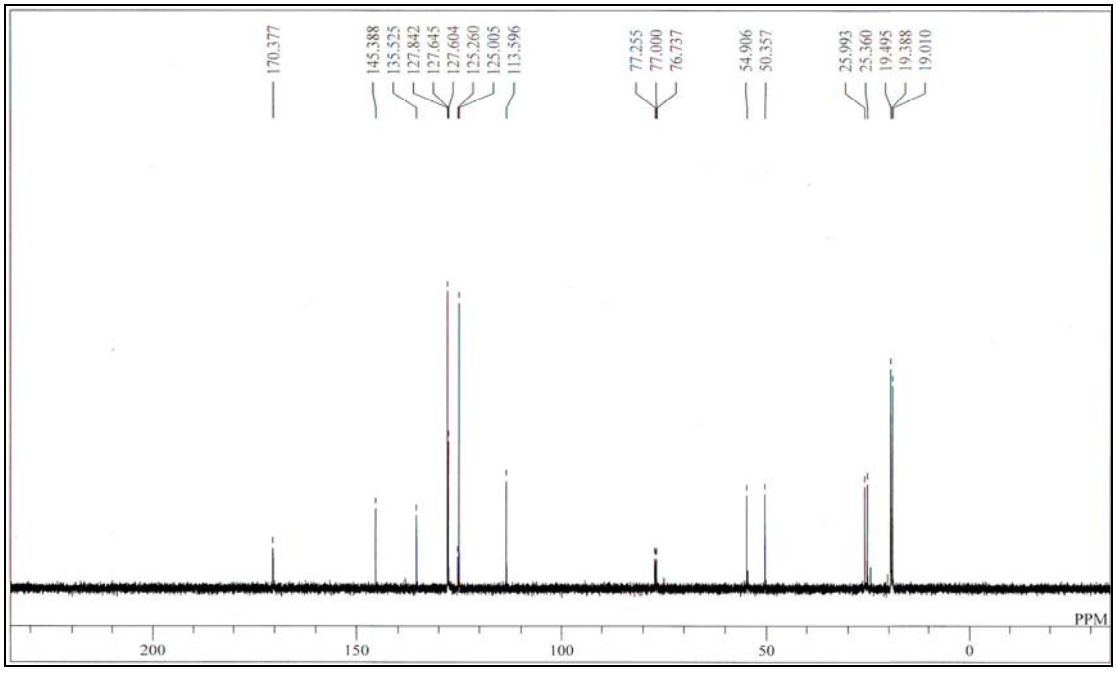

Figure AII-2. ^{13}C NMR spectrum of compound **3ab$_1$**.

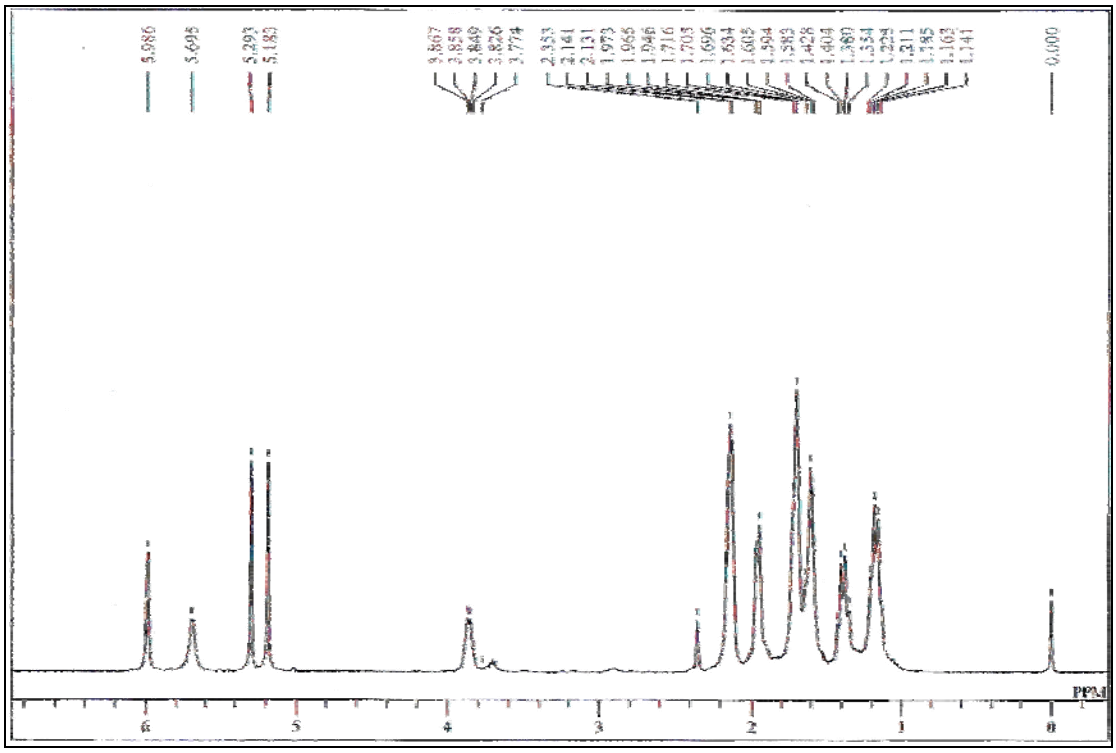

Figure AII-3. ^{1}H NMR spectrum of compound **3ab$_8$**.

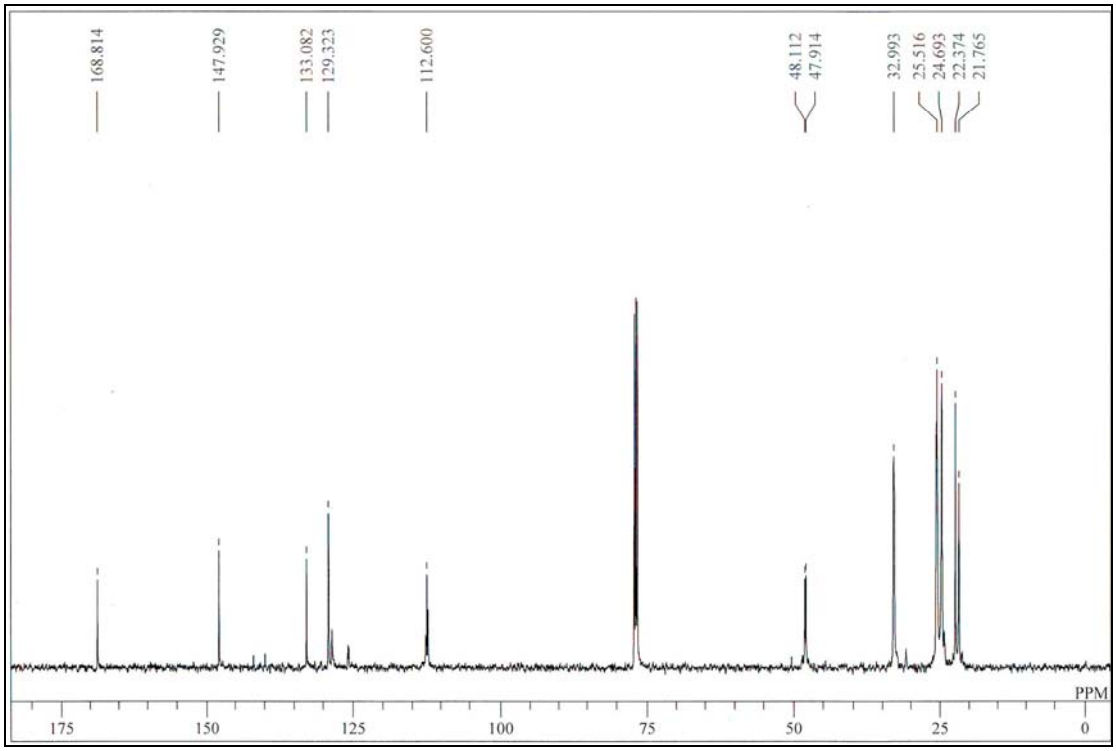

Figure AII-4. ^{13}C NMR spectrum of compound **3ab$_8$**.

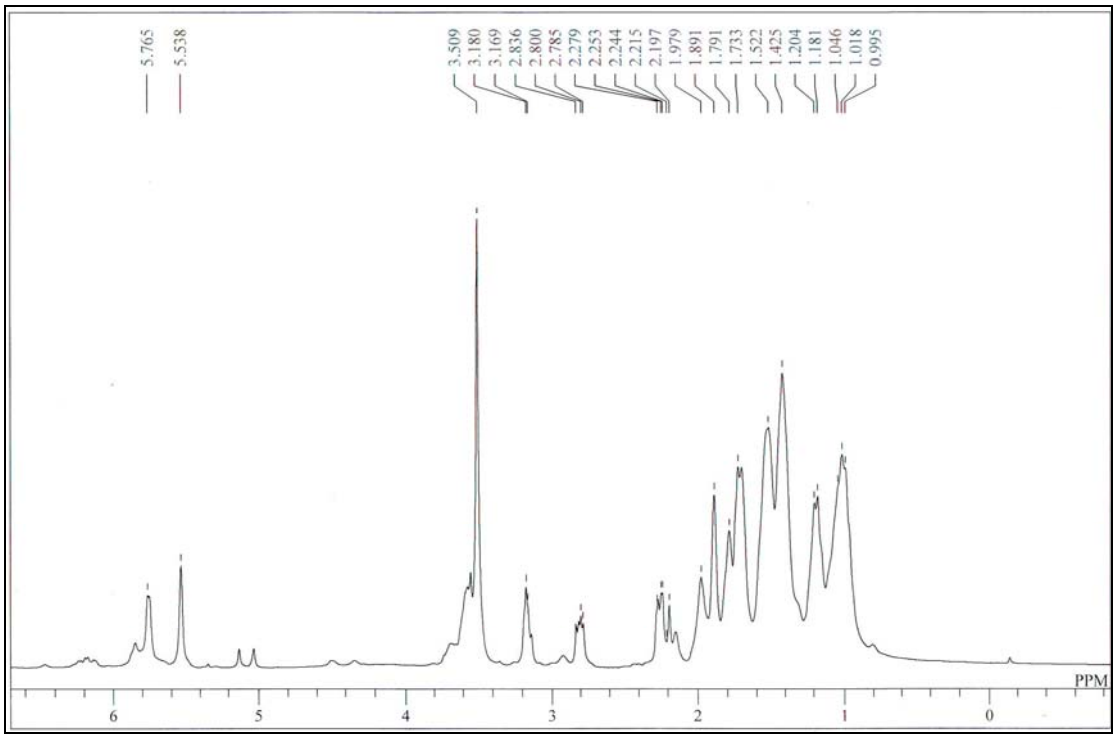

Figure AII-5. ^{1}H NMR spectrum of compound **6b$_8$c$_1$**.

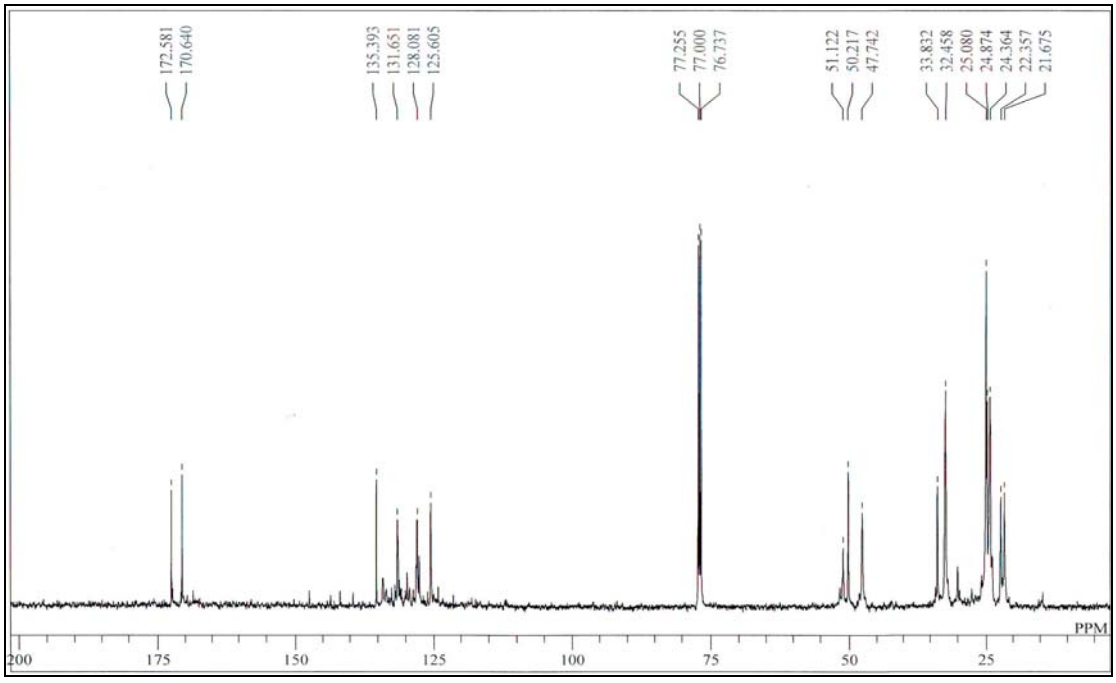

Figure AII-6. ^{13}C NMR spectrum of compound **6b$_8$c$_1$**.

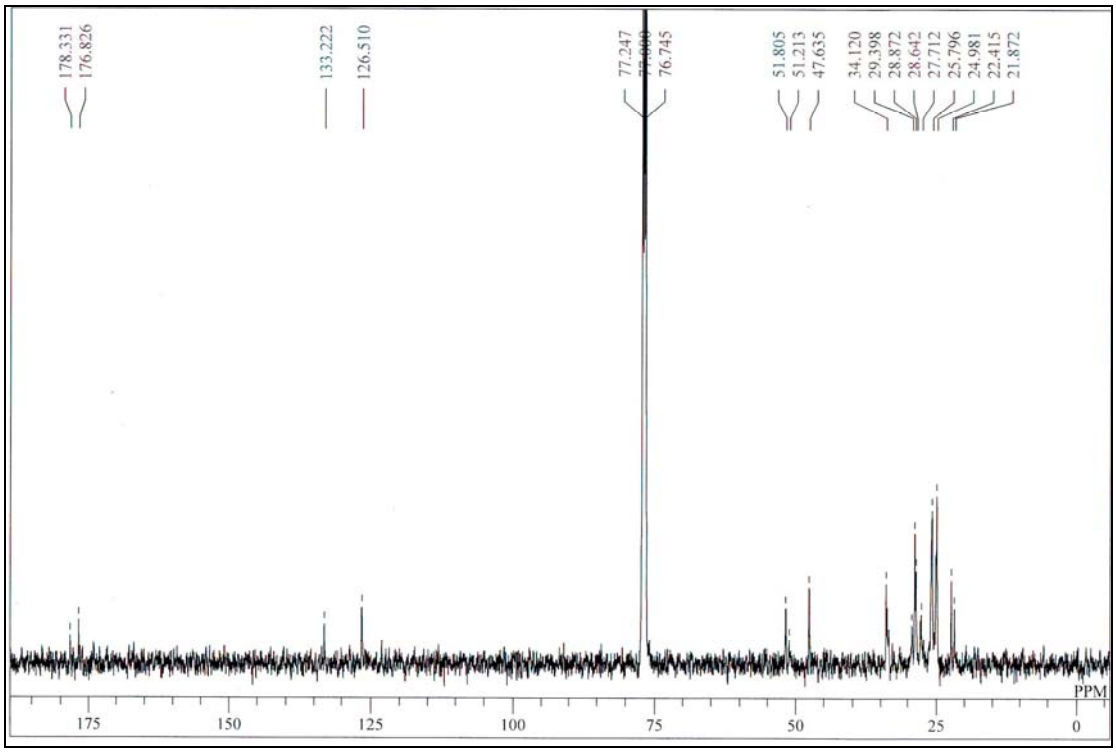

Figure AII-7. ^{13}C NMR spectrum of compound **7b$_8$**.

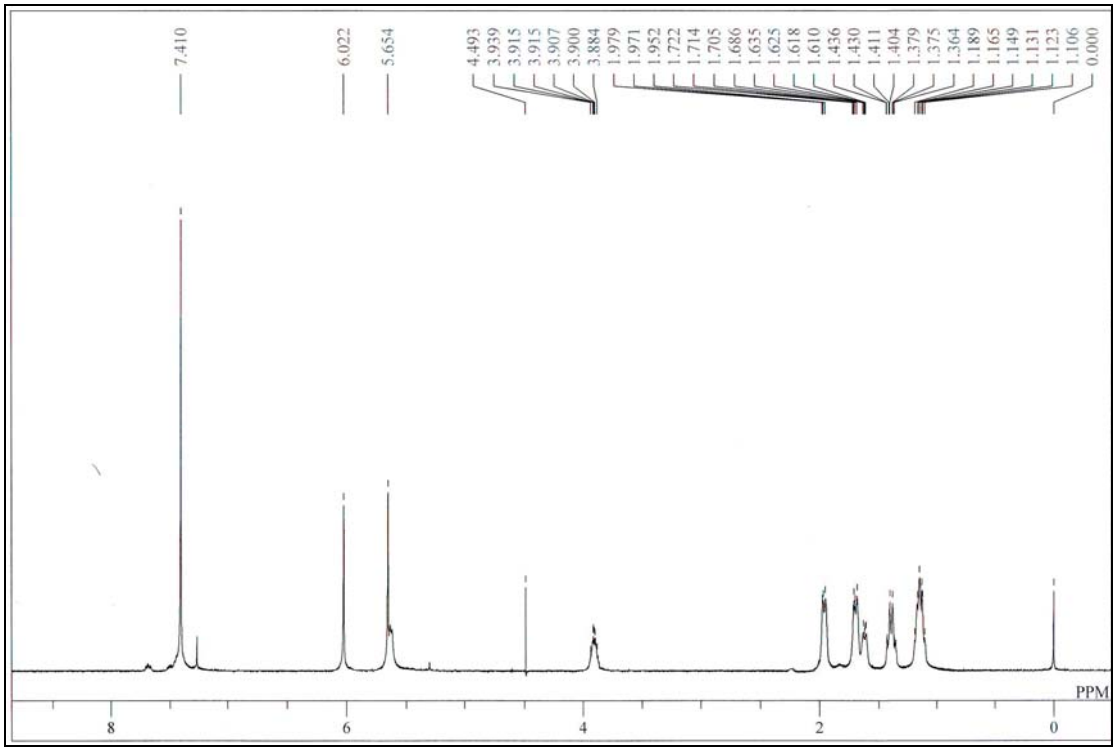

Figure AII-8. ^{1}H NMR spectrum of compound **9ab$_3$**.

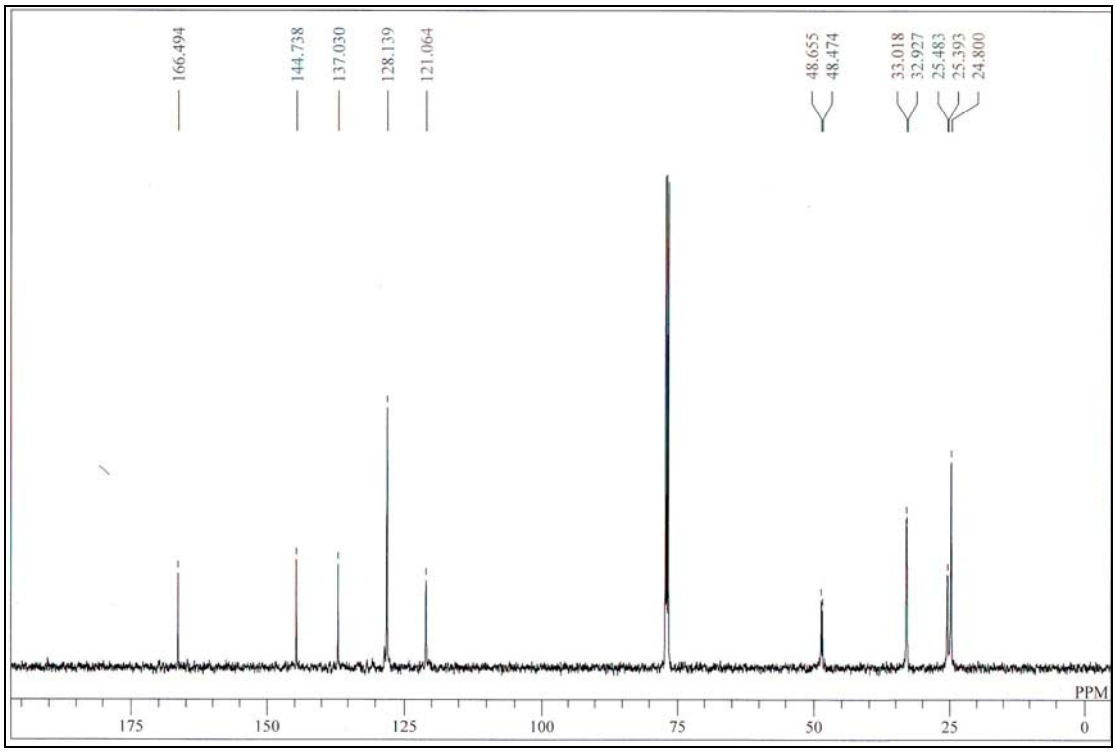

Figure AII-9. ^{13}C NMR spectrum of compound **9ab$_3$**.

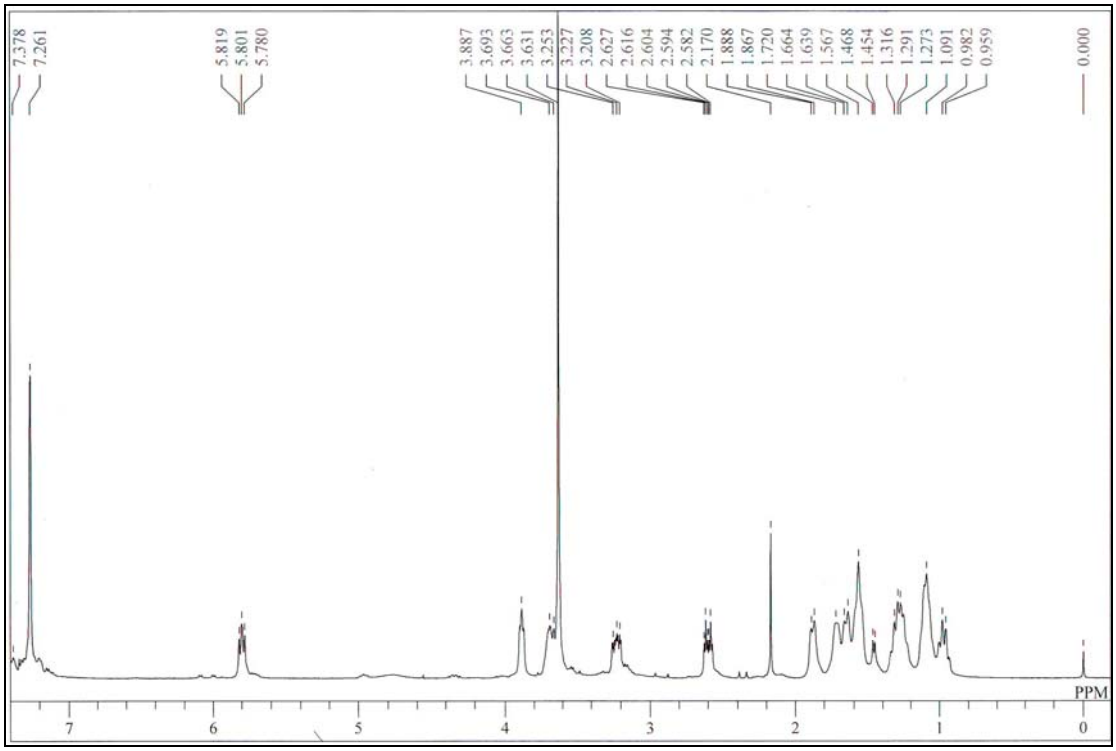

Figure AII-10. ^{1}H NMR spectrum of compound **10ab$_3$c$_1$**.

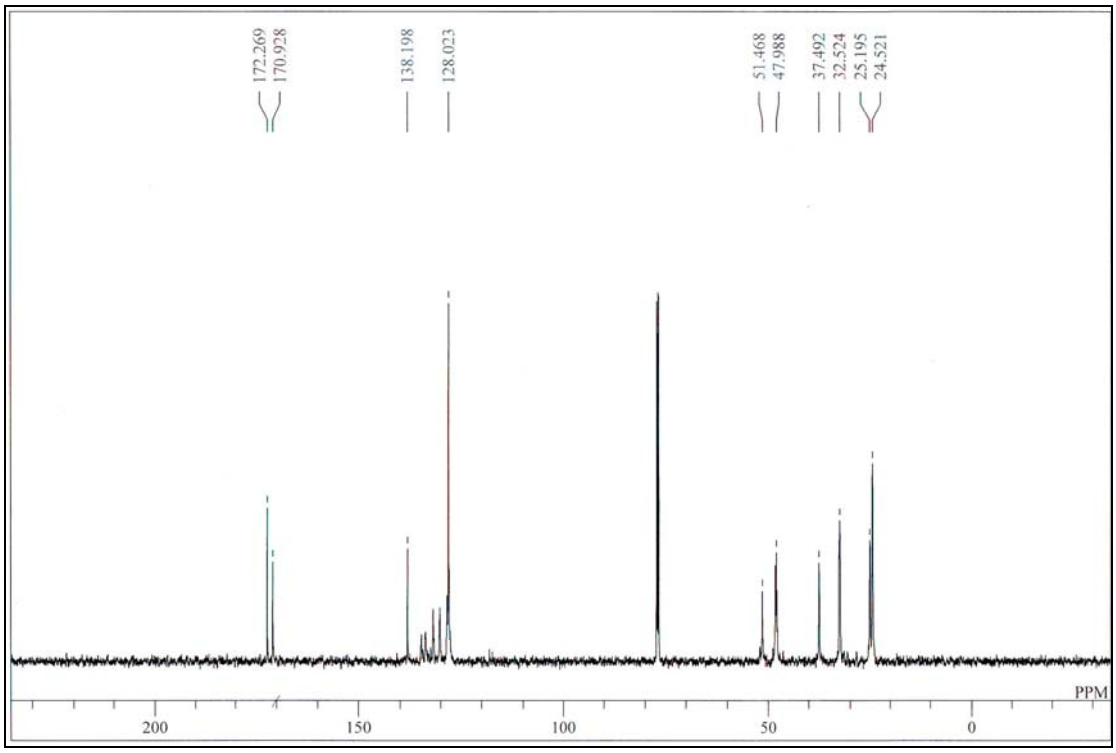

Figure AII-11. ^{13}C NMR spectrum of compound **10ab$_3$c$_1$**.

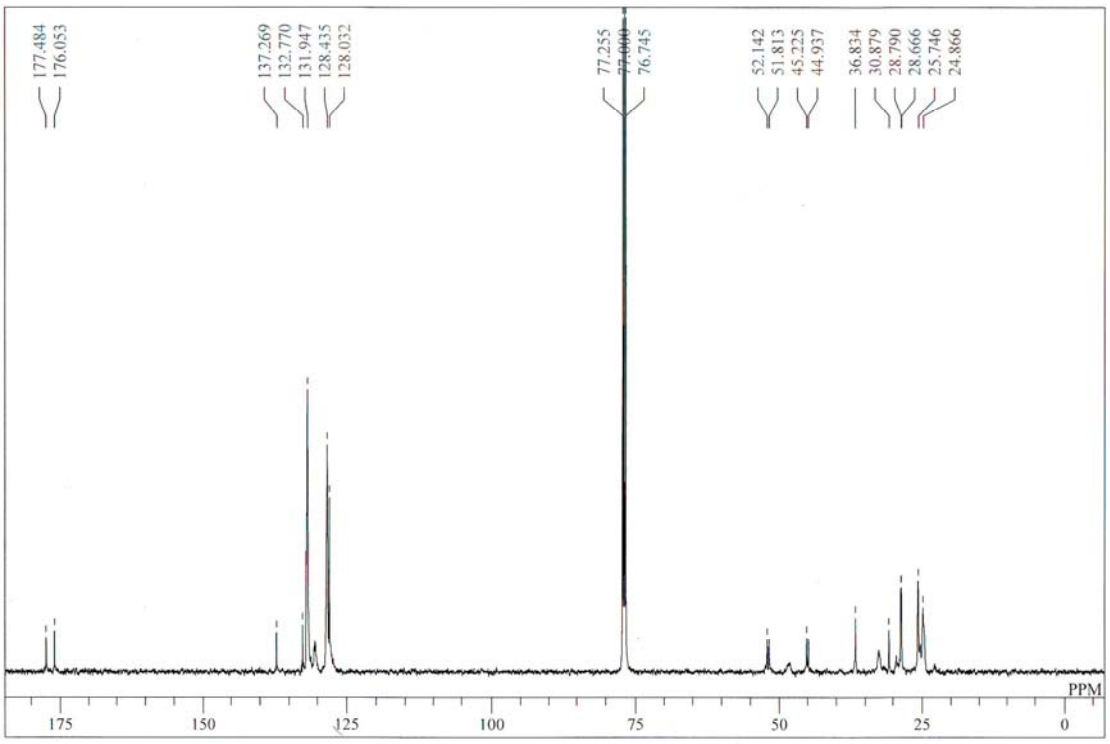

Figure AII-12. ^{13}C NMR spectrum of compound **11ab$_3$**.

AIII. IR spectra of free ligands and new binuclear palladium(II) complexes

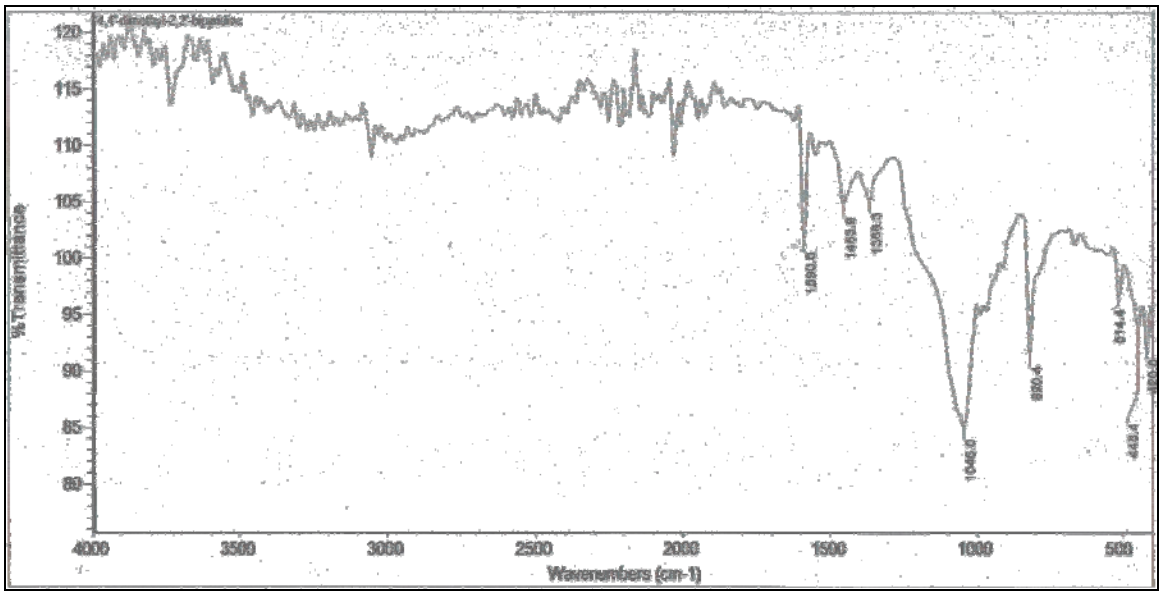

Figure AIII-1. IR spectrum of 4,4'-dimethyl-2,2'-bipyridine.

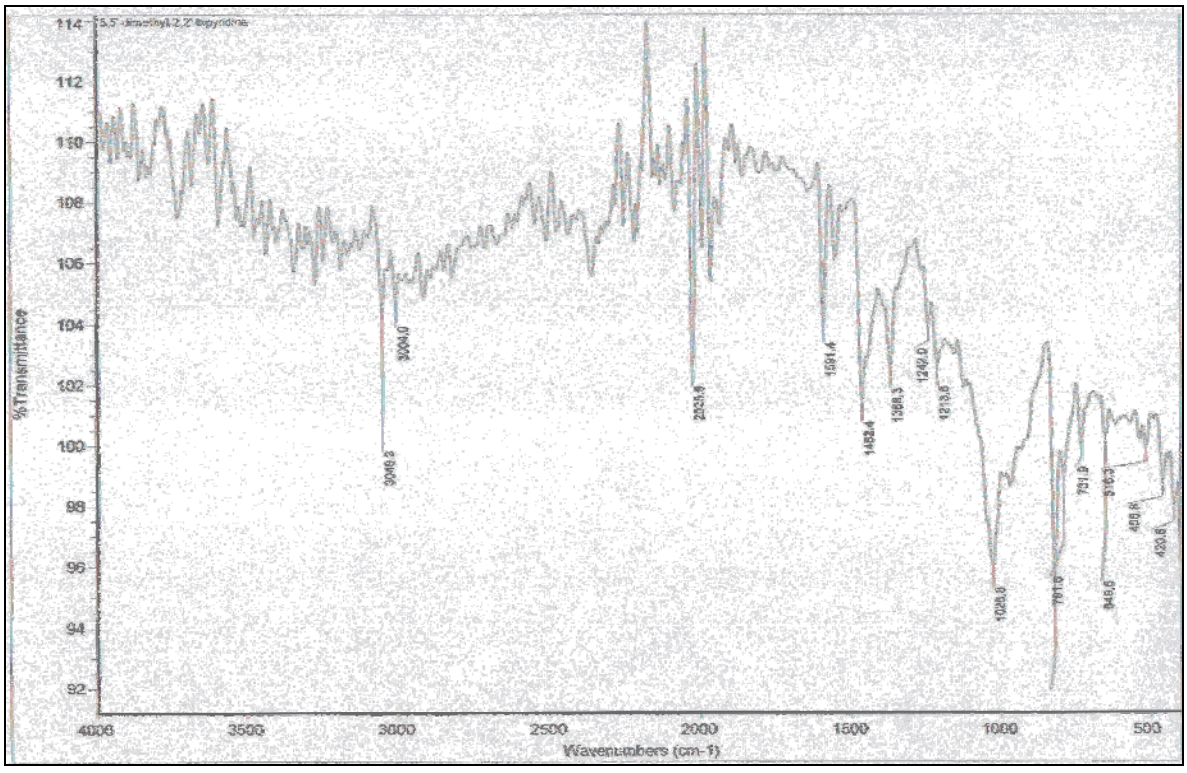

Figure AIII-2. IR spectrum of 5,5'-dimethyl-2,2'-bipyridine.

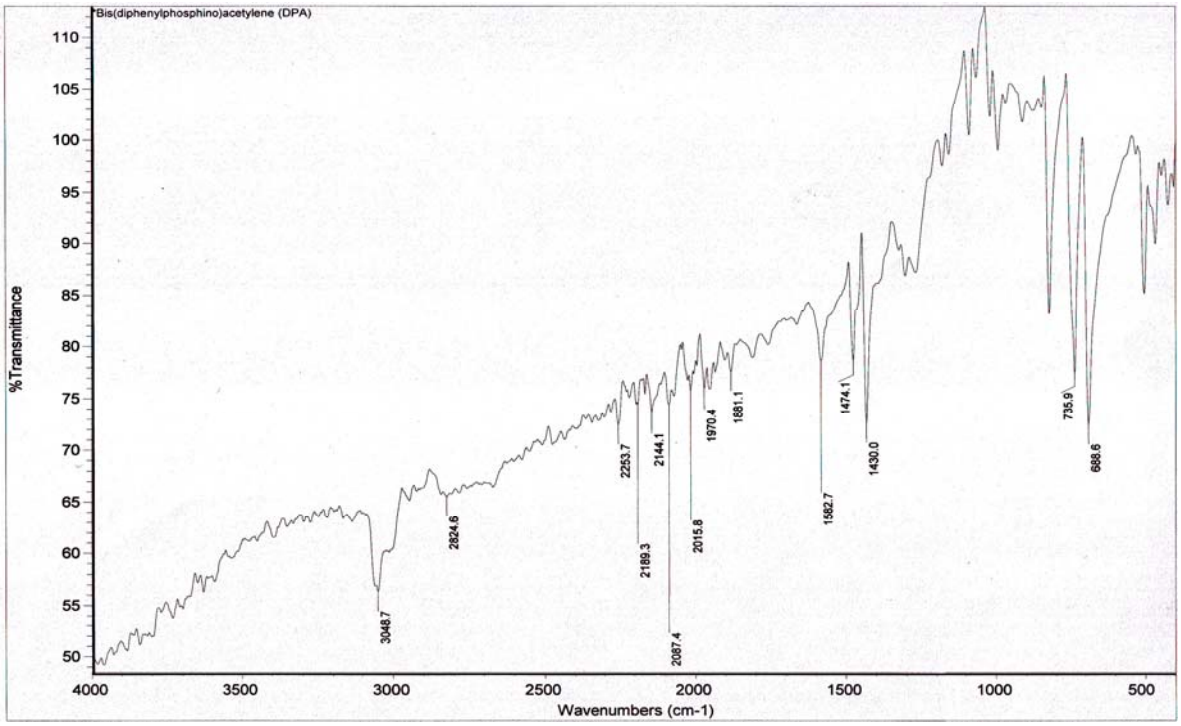

Figure AIII-3. IR spectrum of DPA.

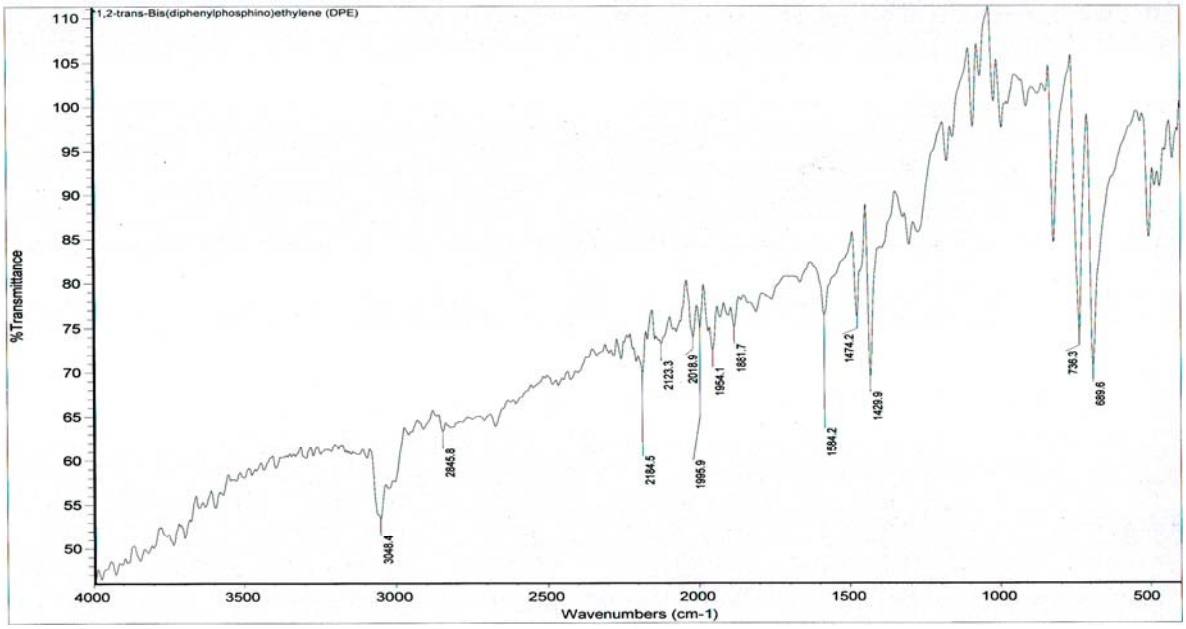

Figure AIII-4. IR spectrum of DPE.

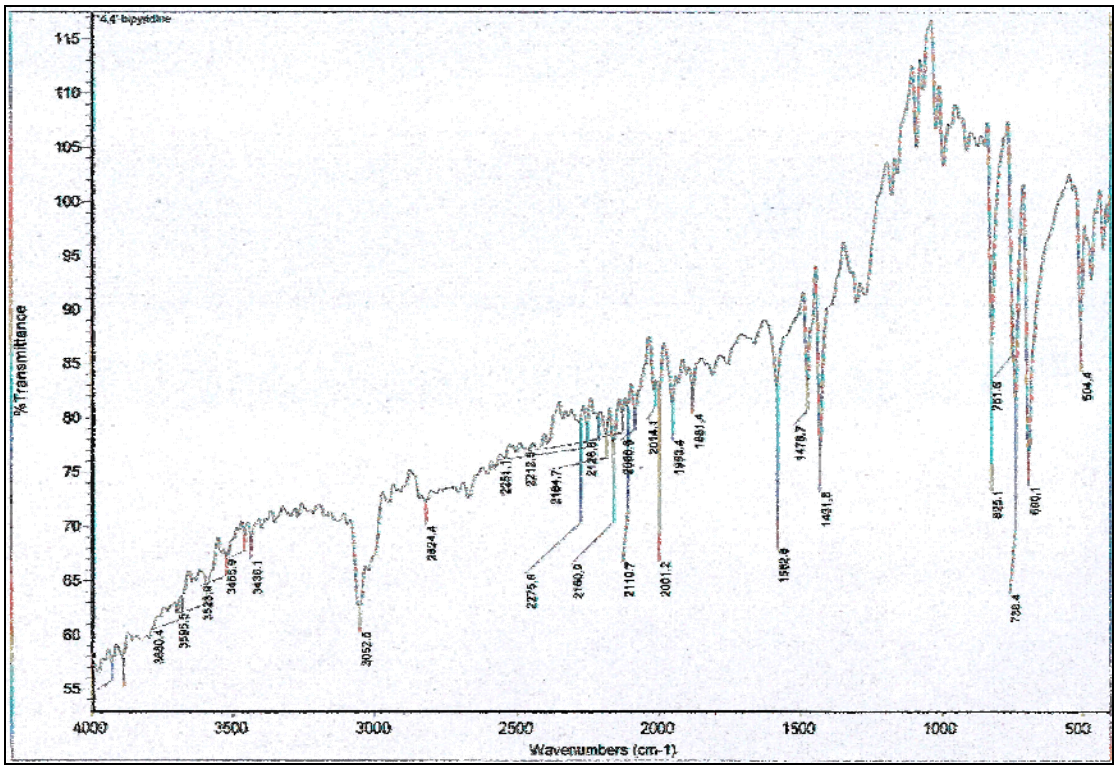

Figure AIII-5. IR spectrum of 4,4'-bipyridine.

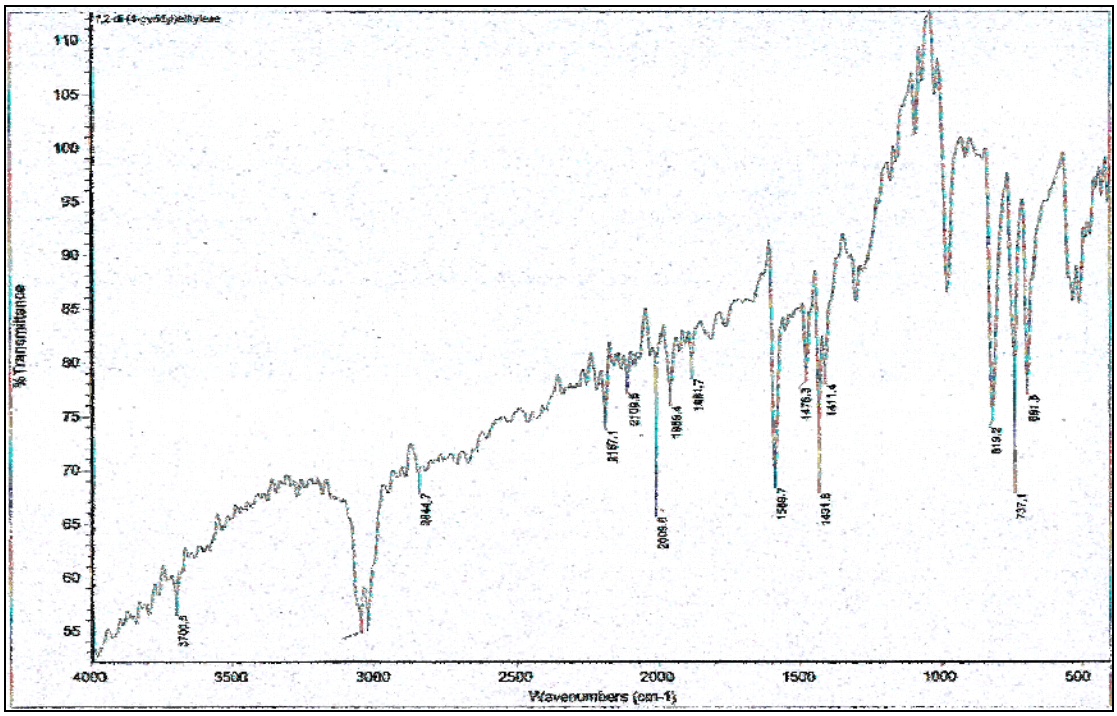

Figure AIII-6. IR spectrum of 1,2-bis(4-pyridyl)ethylene.

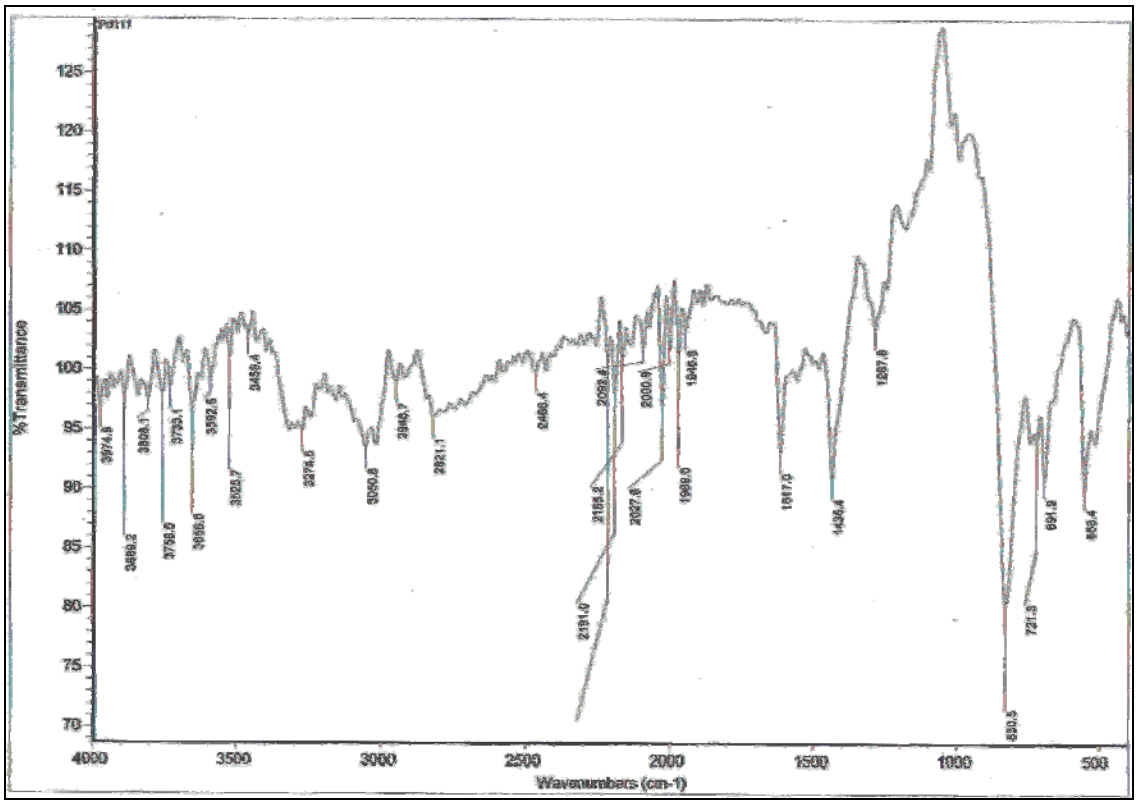

Figure AIII-7. IR spectrum of Pd111.

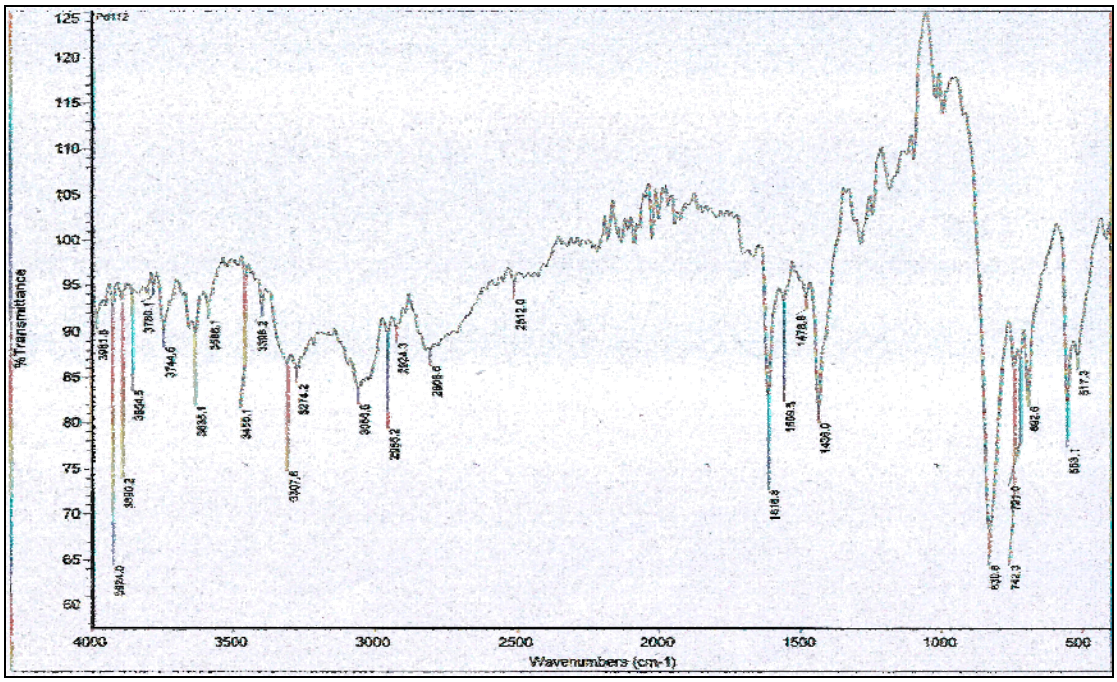

Figure AIII-8. IR spectrum of Pd112.

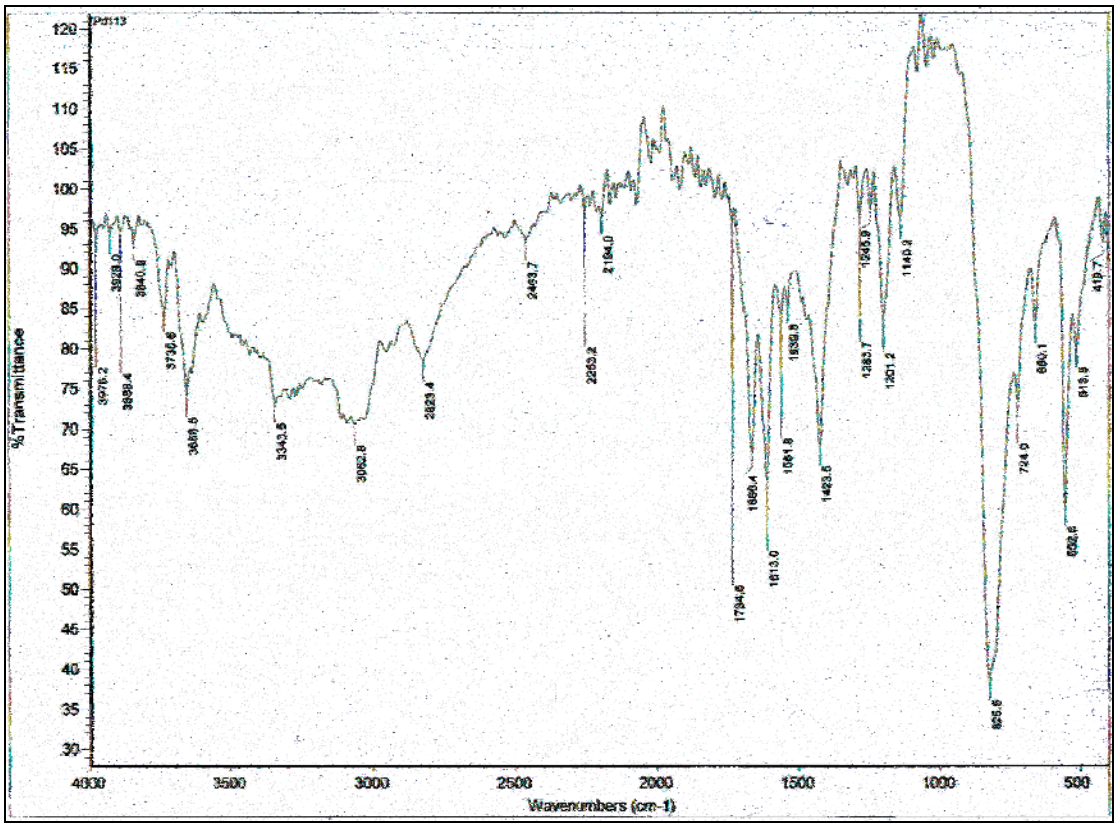

Figure AIII-9. IR spectrum of Pd113.

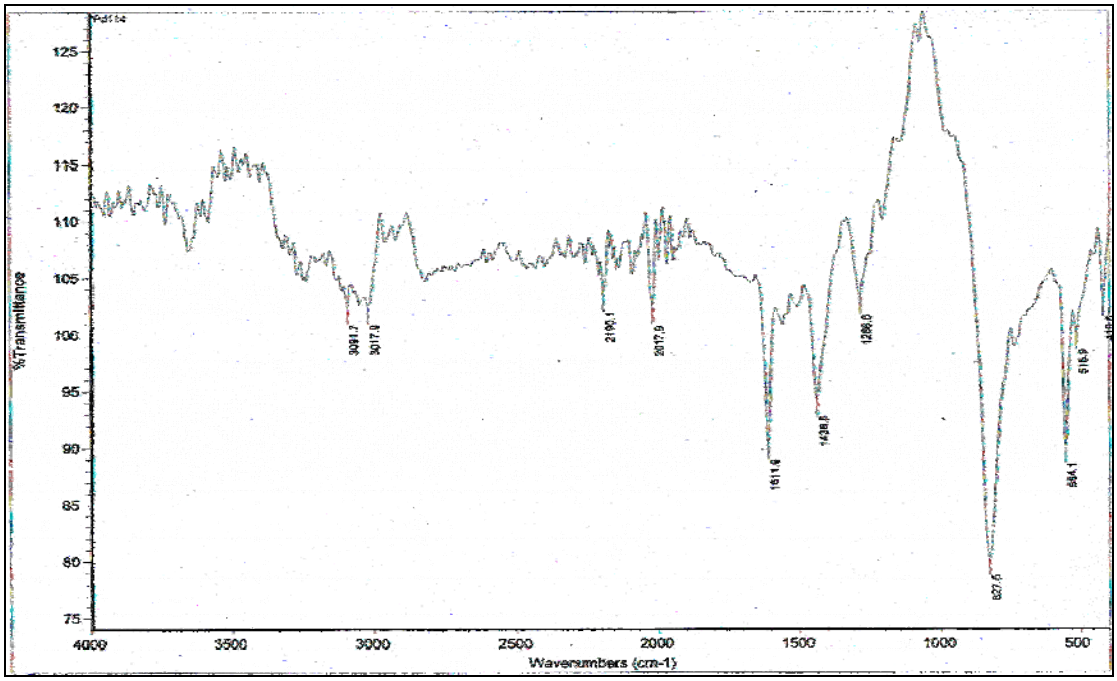

Figure AIII-10. IR spectrum of Pd114.

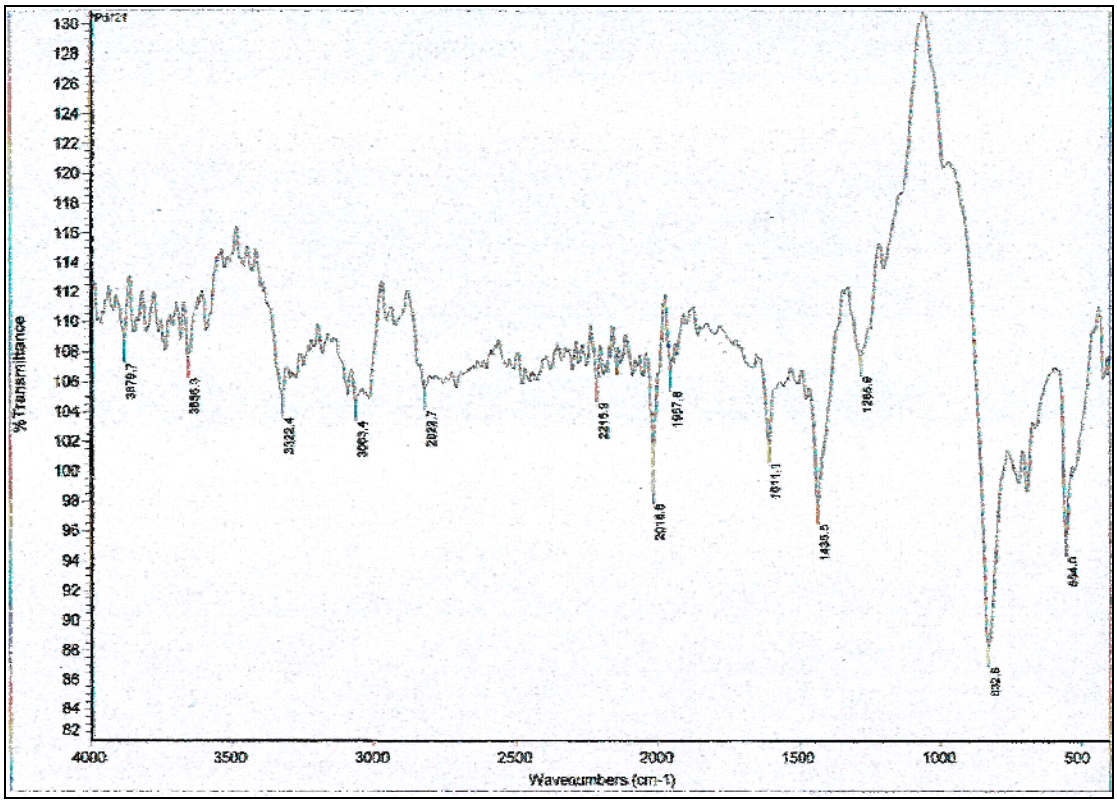

Figure AIII-11. IR spectrum of Pd121.

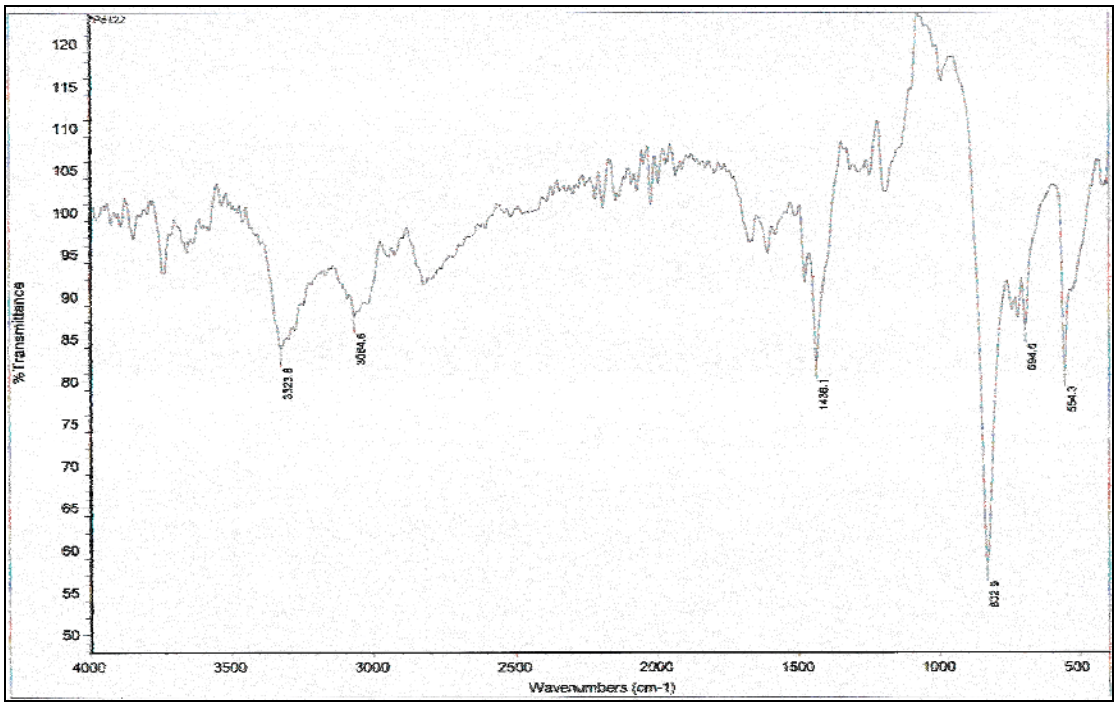

Figure AIII-12. IR spectrum of Pd122.

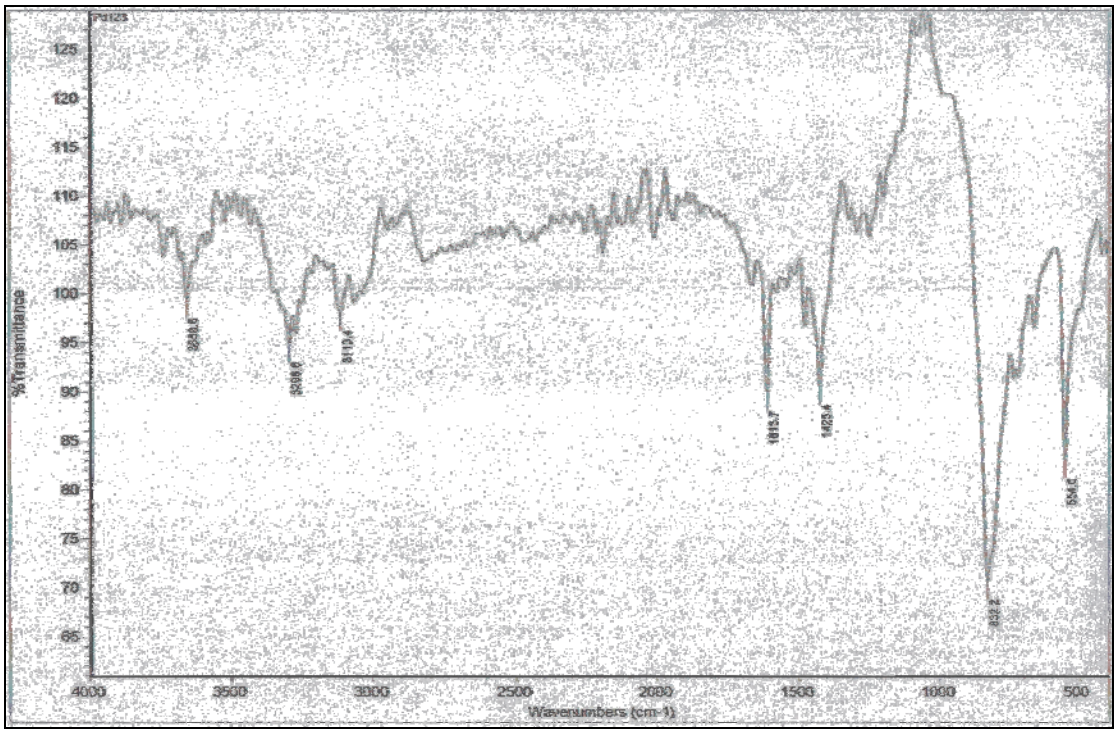

Figure AIII-13. IR spectrum of Pd123.

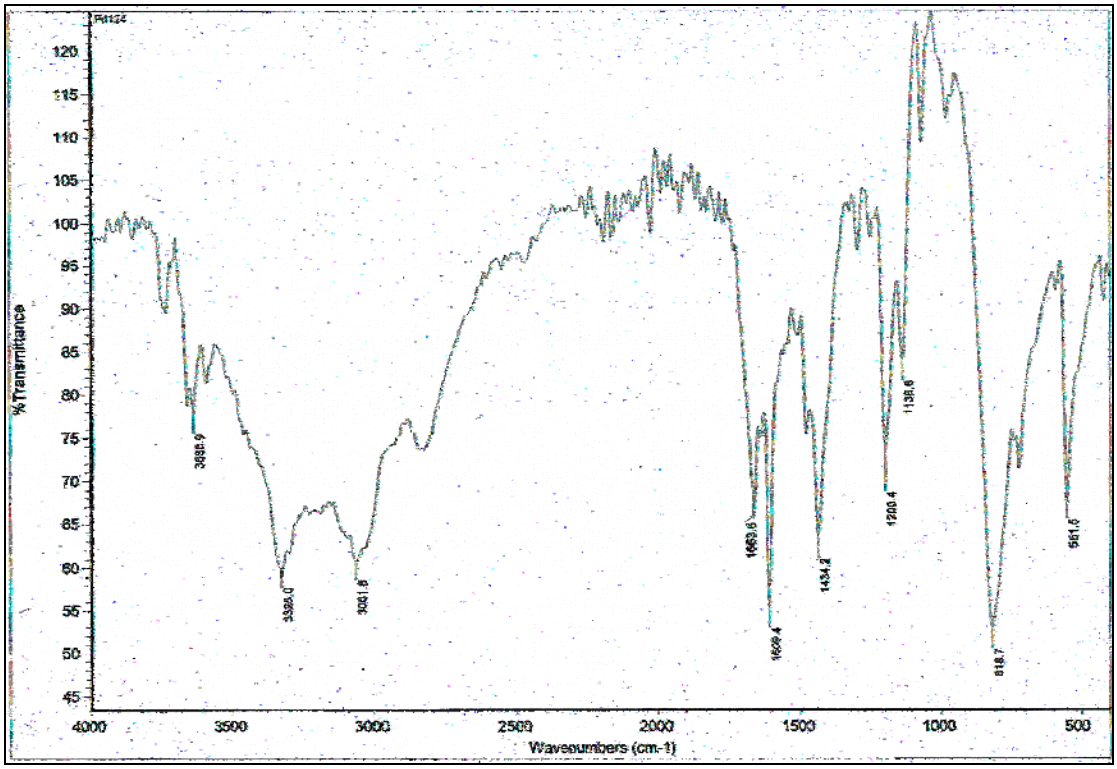

Figure AIII-14. IR spectrum of Pd134.

AIV. UV-Vis spectra of free ligands and new binuclear palladium(II) complexes

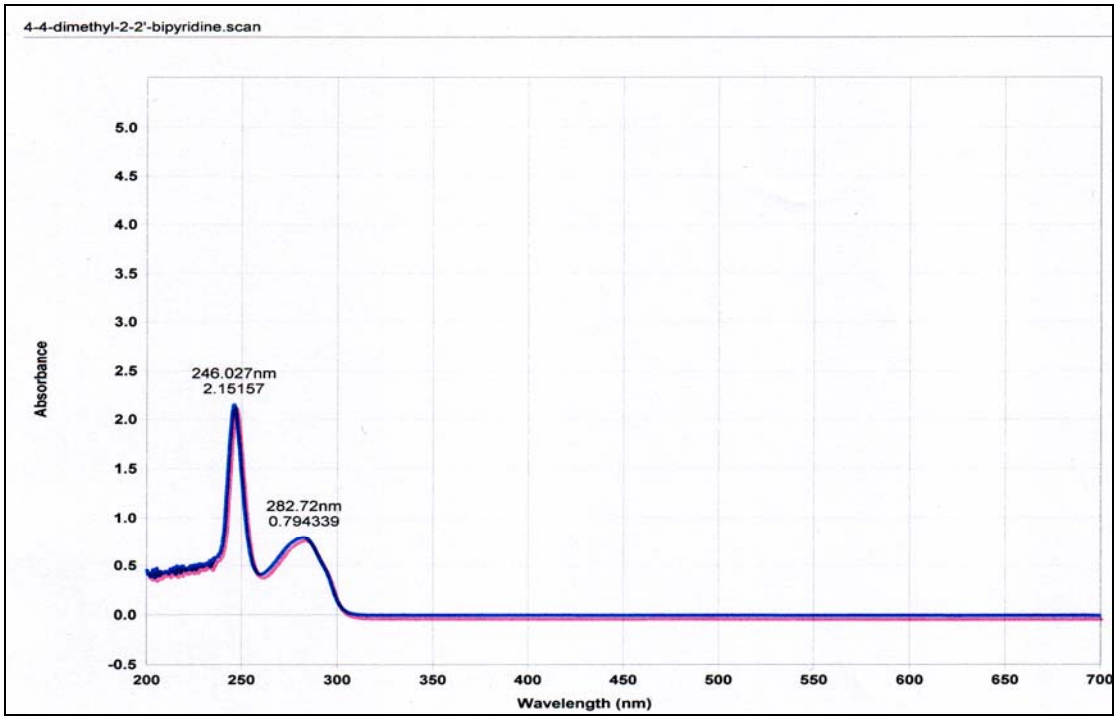

Figure AIV-1. UV-Vis spectrum of 4,4'-dimethyl-2,2'-bipyridine.

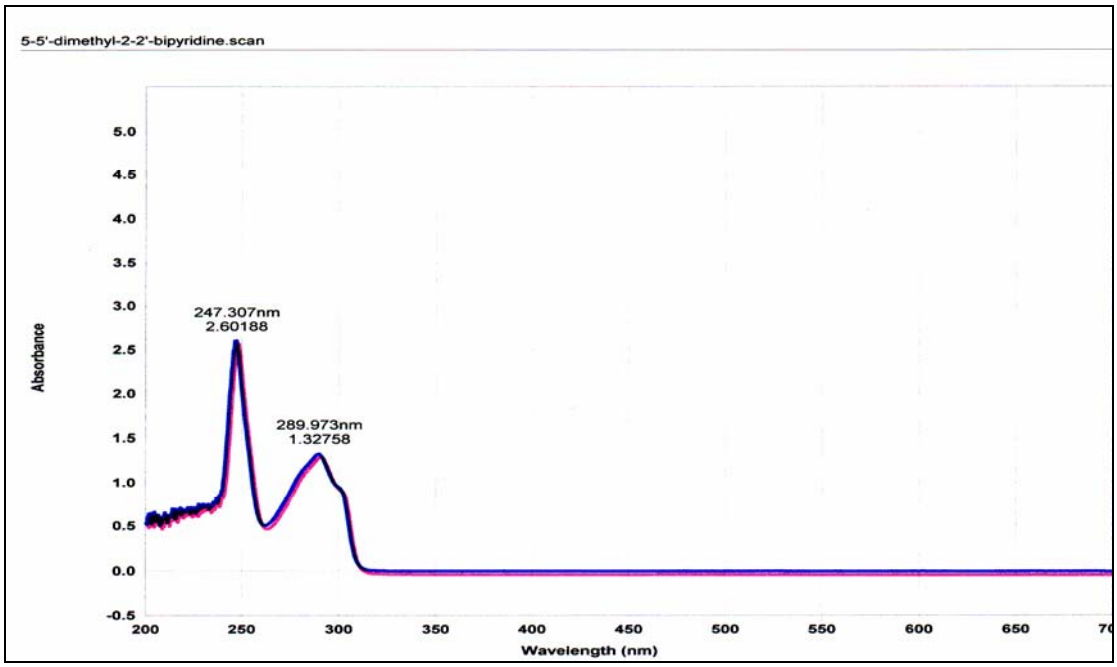

Figure AIV-2. UV-Vis spectrum of 5,5'-dimethyl-2,2'-bipyridine.

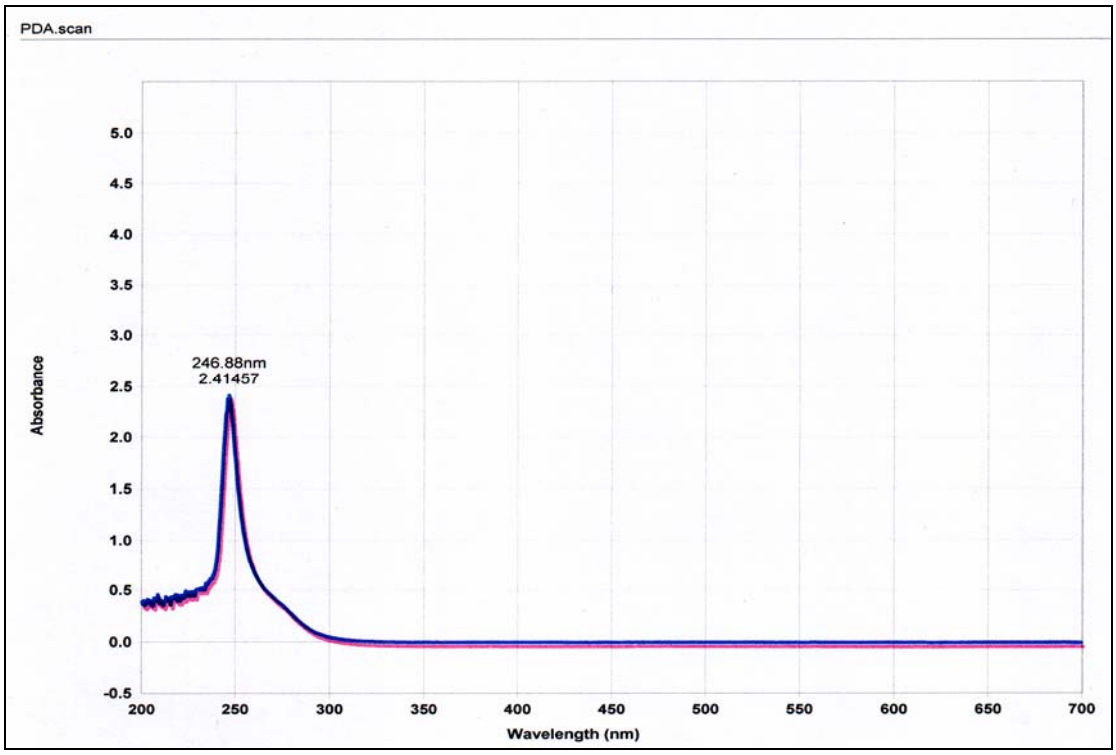

Figure AIV-3. UV-Vis spectrum of DPA.

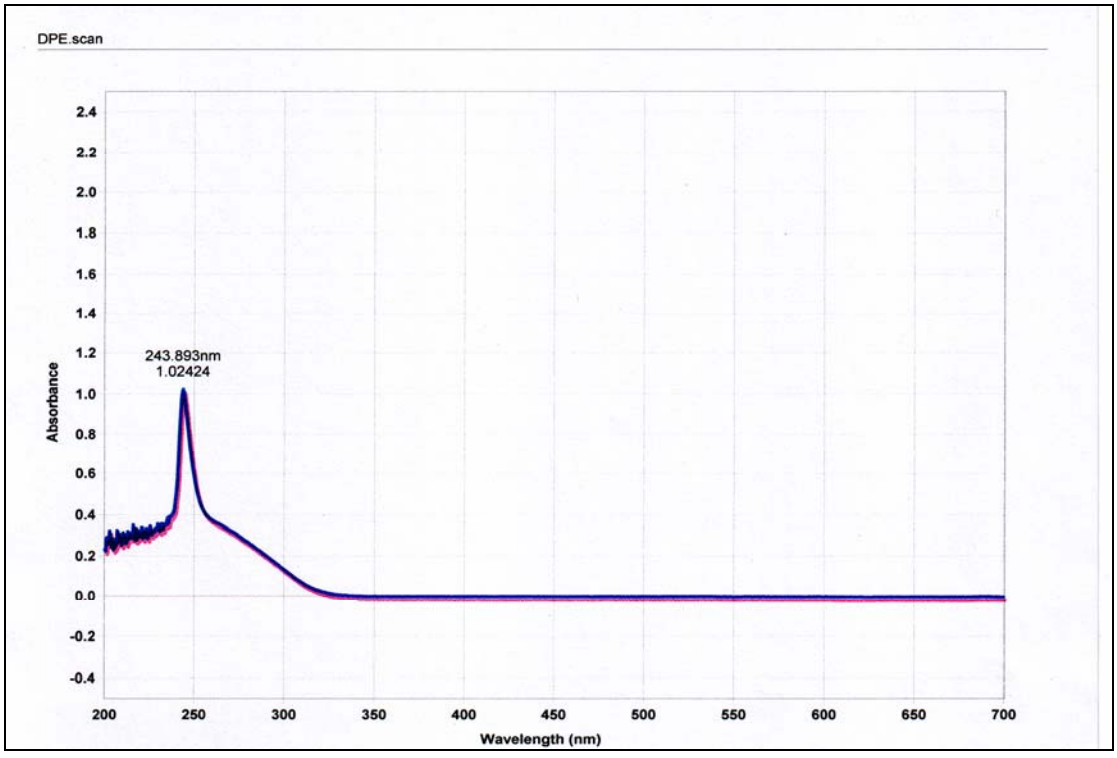

Figure AIV-4. UV-Vis spectrum of DPE.

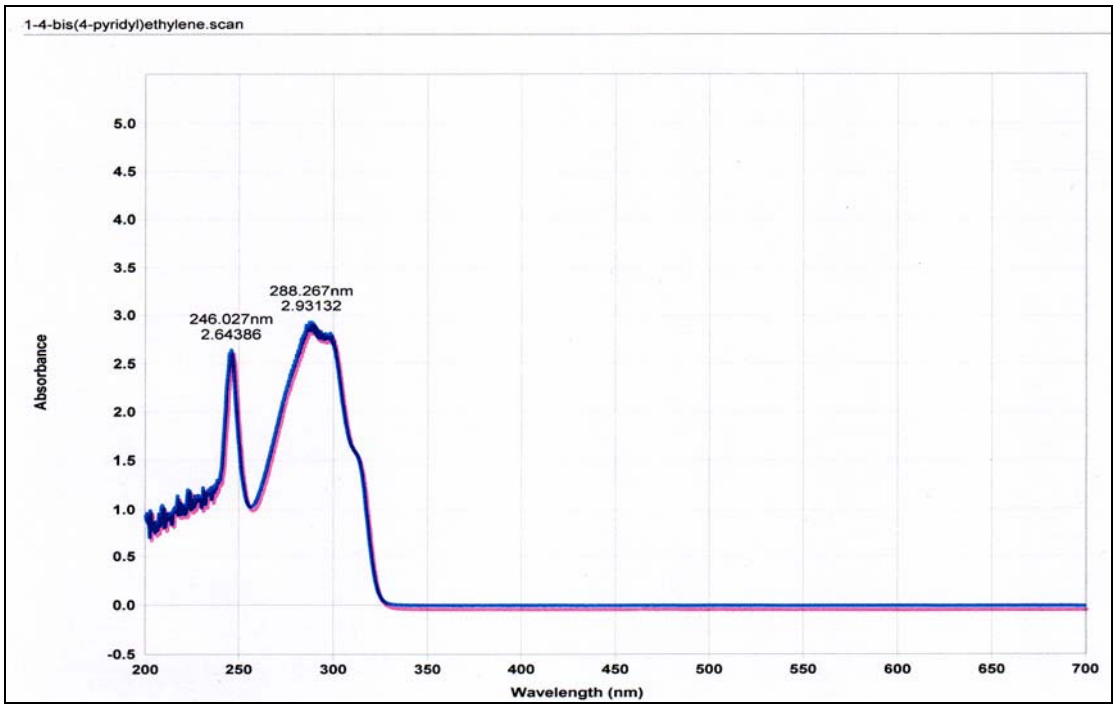

Figure AIV-5. UV-Vis spectrum of 1,2-bis(4-pyridyl)ethylene.

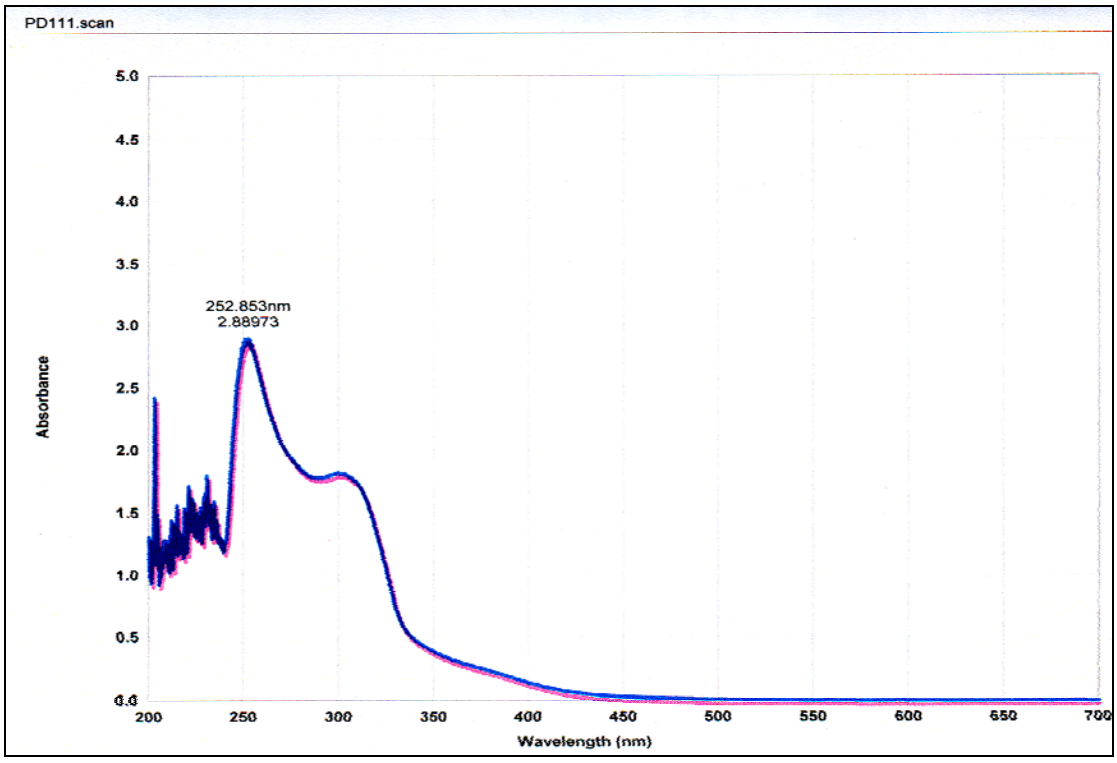

Figure AIV-6. UV-Vis spectrum of Pd111.

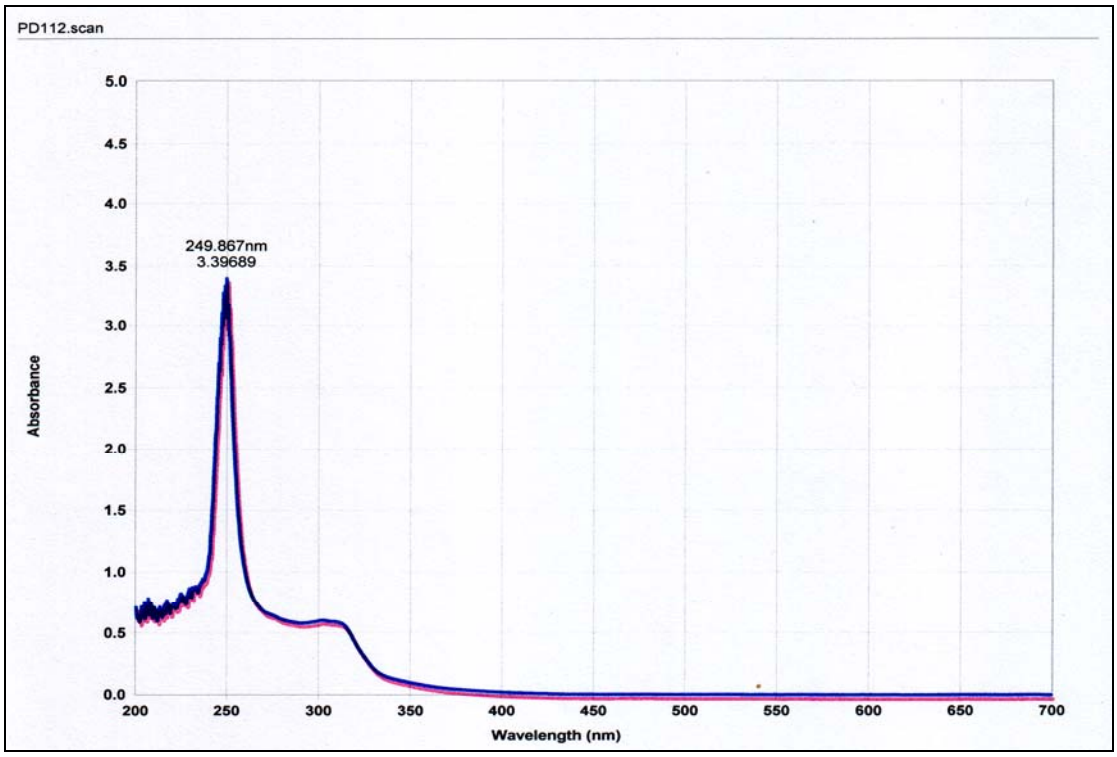

Figure AIV-7. UV-Vis spectrum of Pd112.

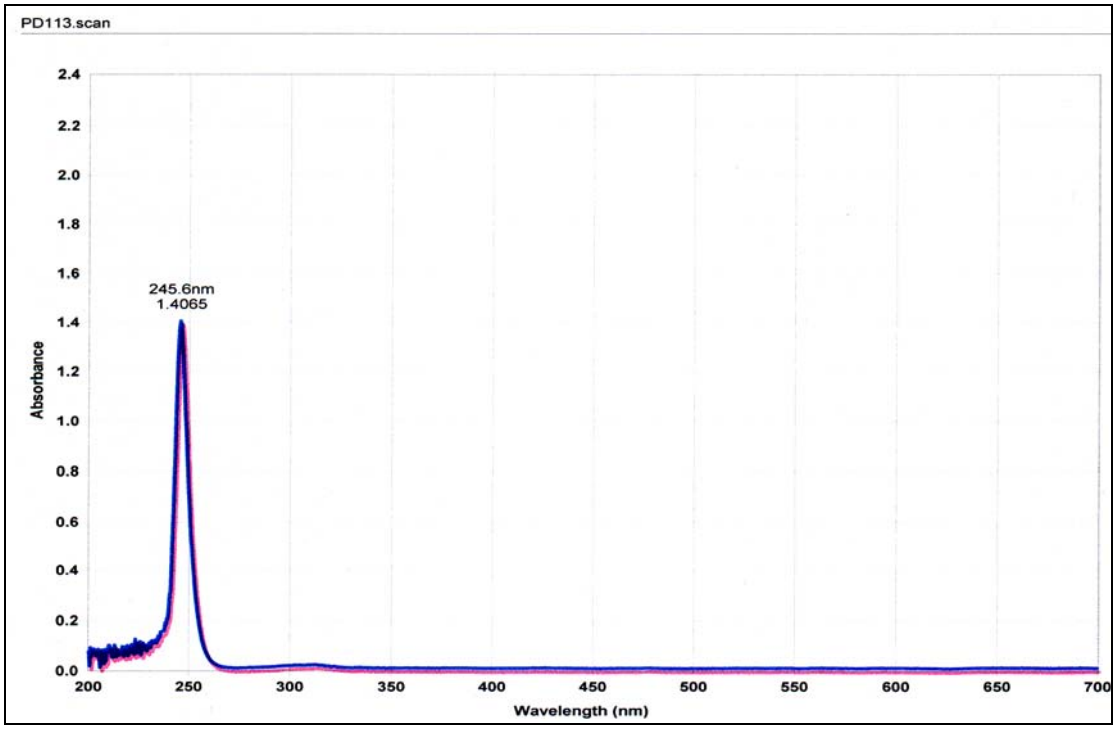

Figure AIV-8. UV-Vis spectrum of Pd113.

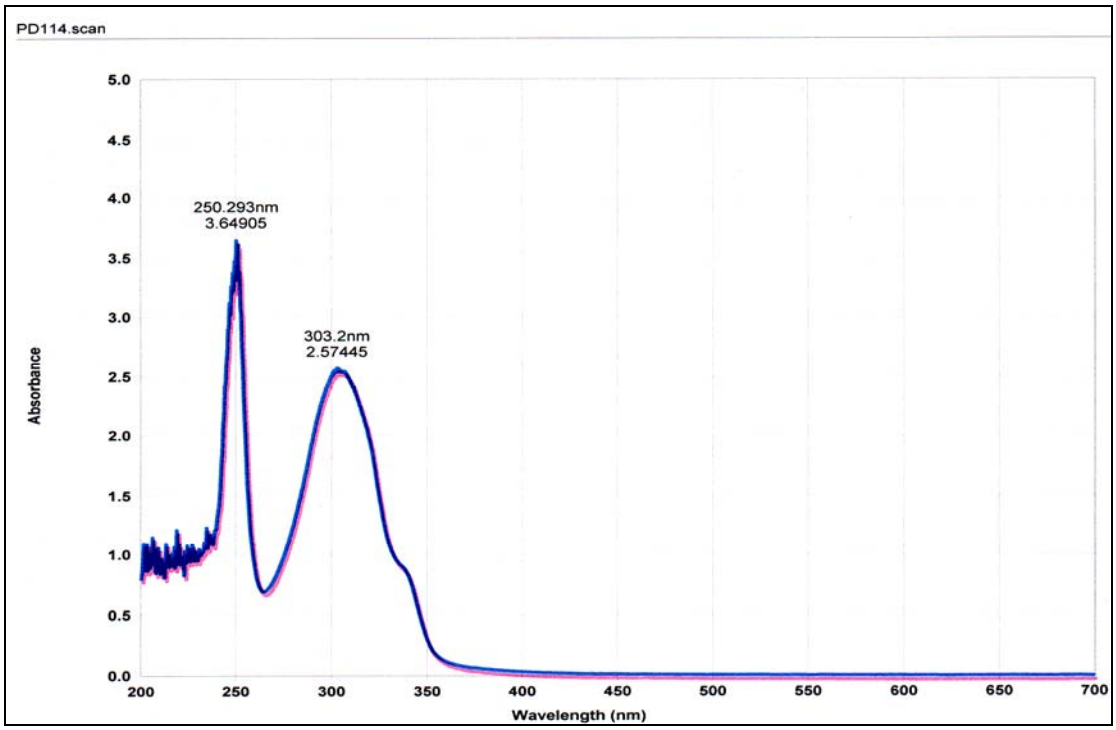

Figure AIV-9. UV-Vis spectrum of Pd114.

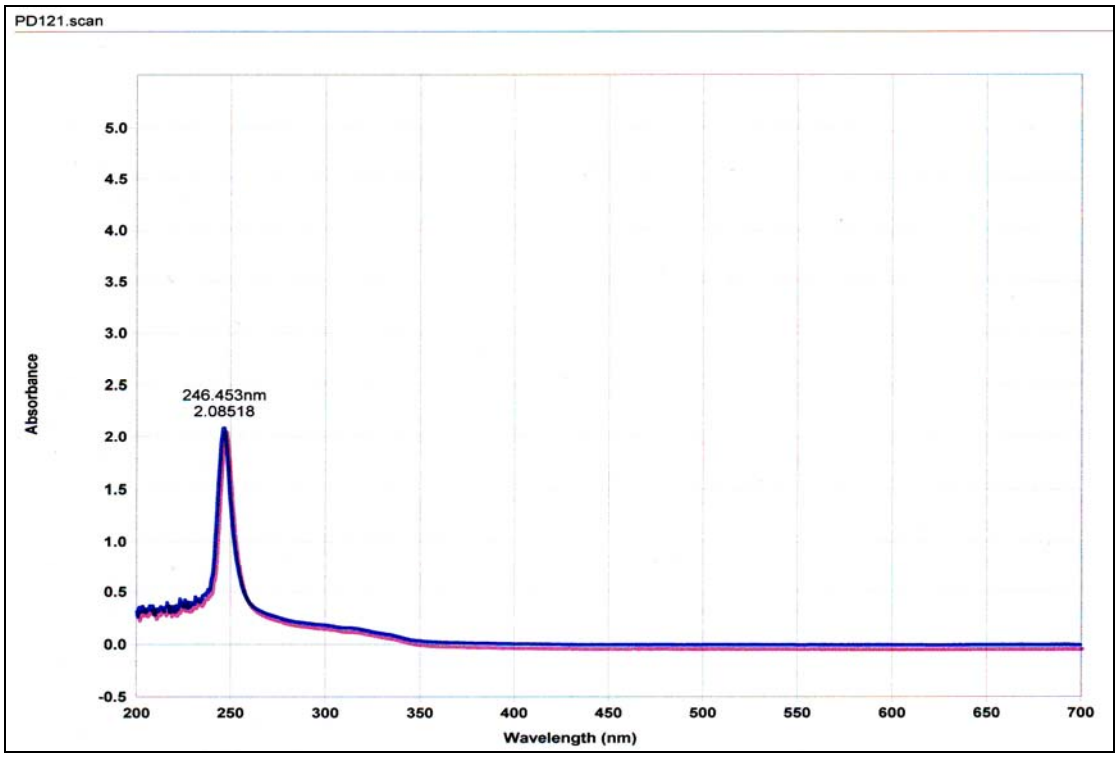

Figure AIV-10. UV-Vis spectrum of Pd121.

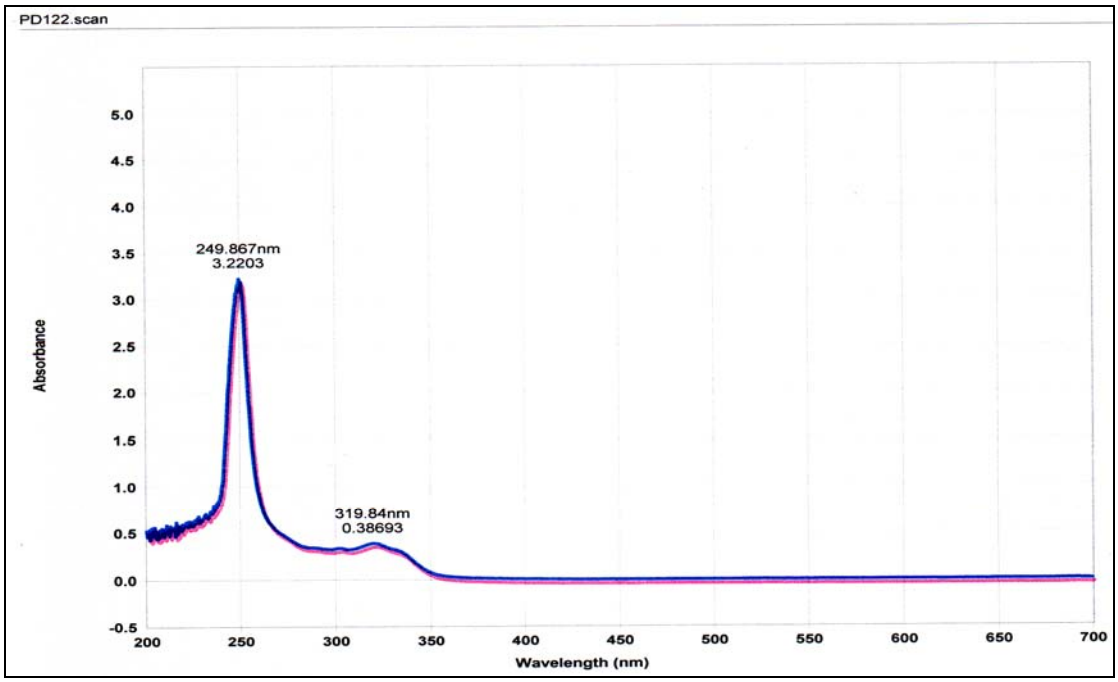

Figure AIV-11. UV-Vis spectrum of Pd122.

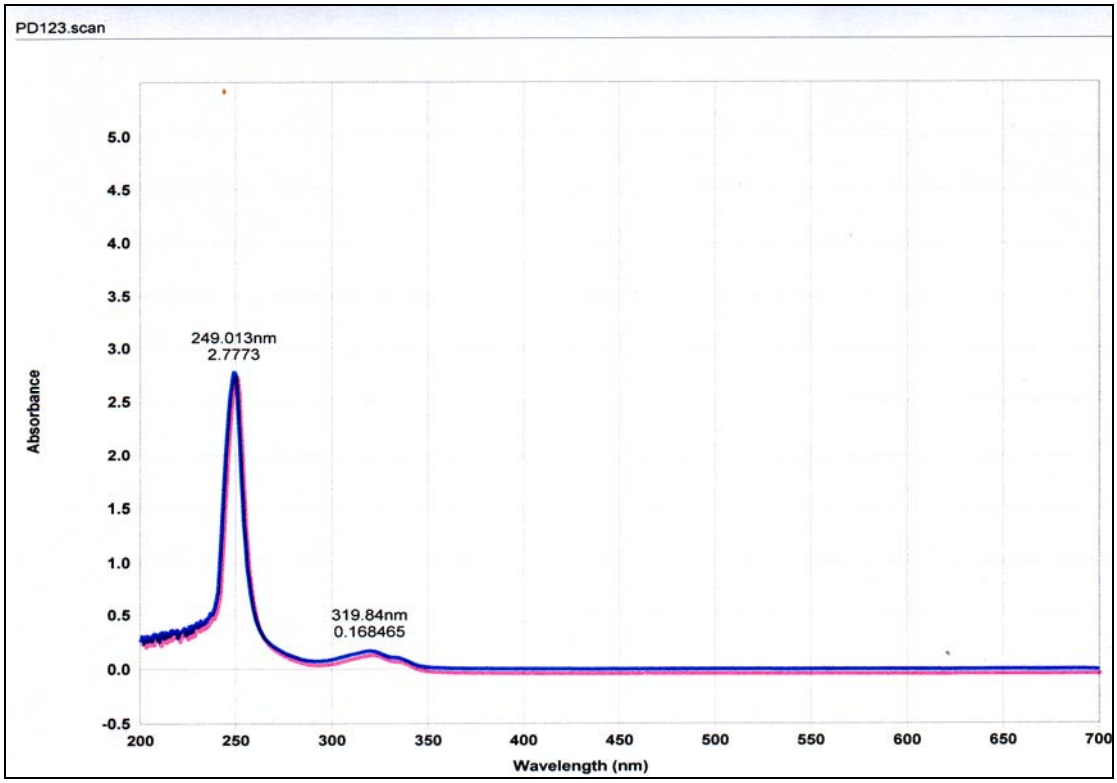

Figure AIV-12. UV-Vis spectrum of Pd123.

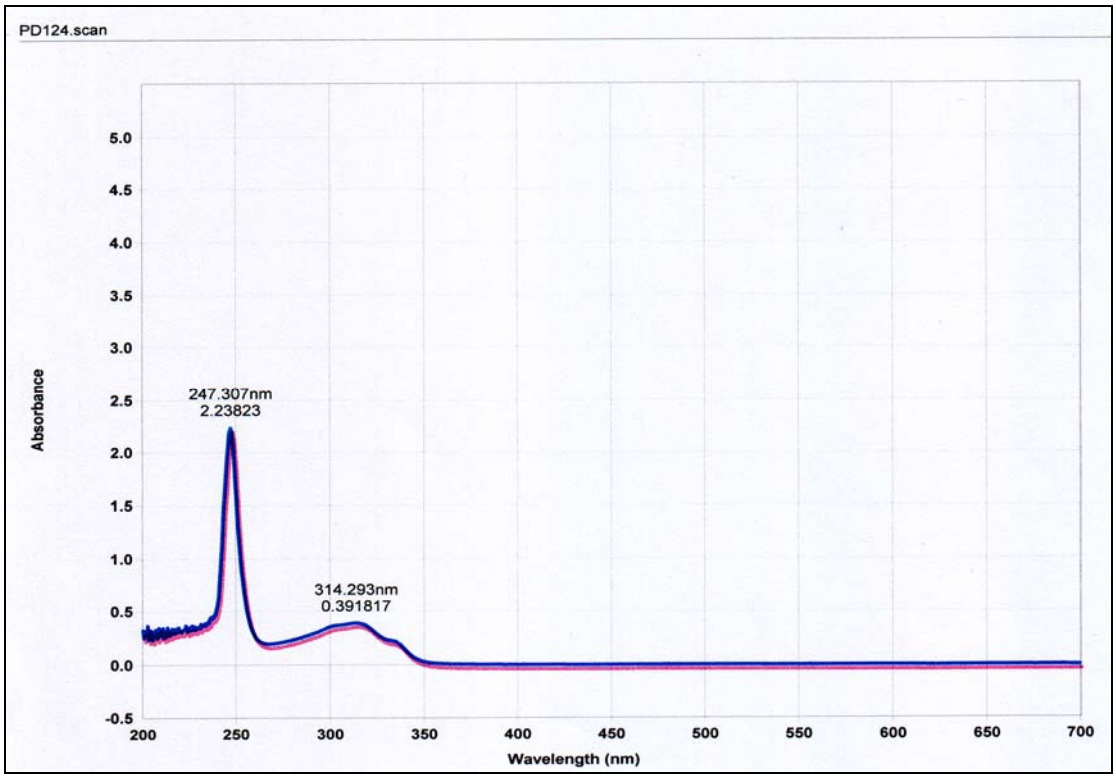

Figure AIV-13. UV-Vis spectrum of Pd124.

AV. ^{1}H NMR spectra of free ligands and new binuclear palladium(II) complexes

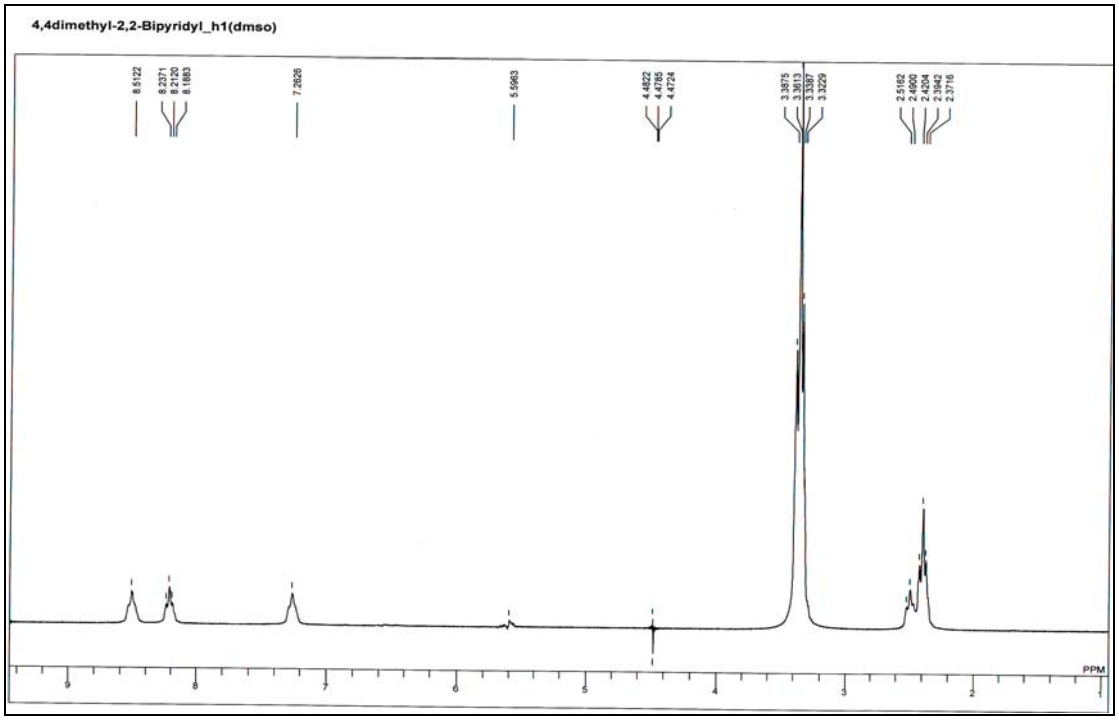

Figure AV-1. ^{1}H NMR spectrum of 4,4'-dimethyl-2,2'-bipyridine.

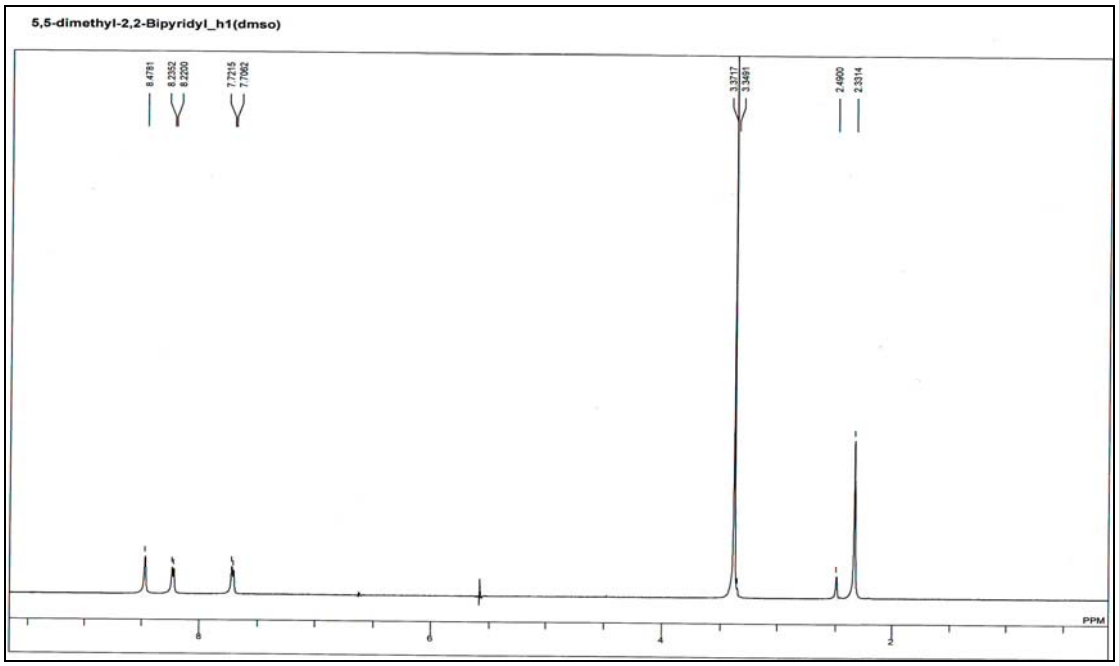

Figure AV-2. ^{1}H NMR spectrum of 5,5'-dimethyl-2,2'-bipyridine.

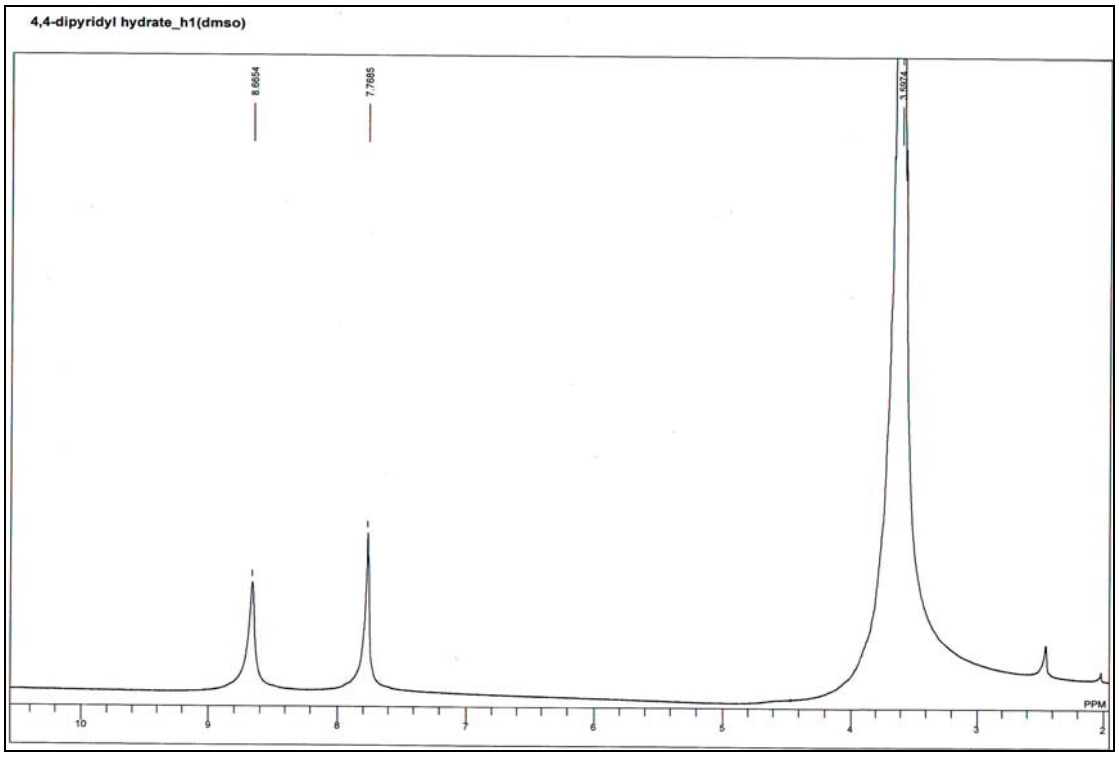

Figure AV-3. ^{1}H NMR spectrum of 4,4'-bipyridine.

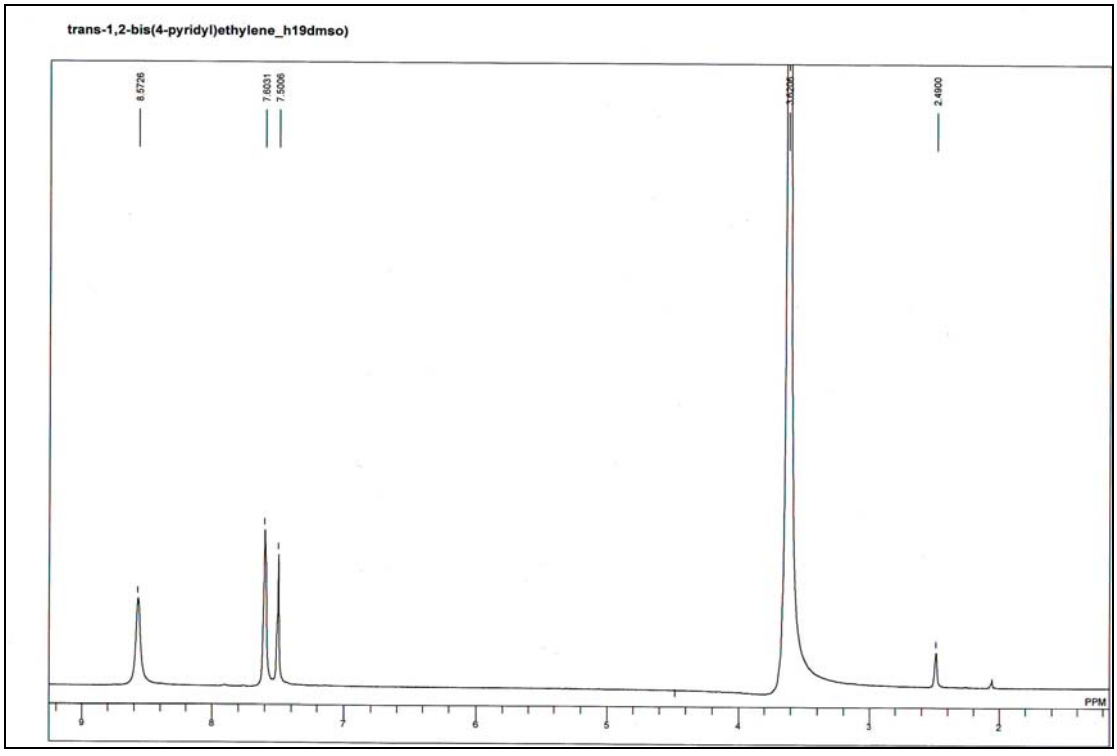

Figure AV-4. ^{1}H NMR spectrum of 1,2-bis(4-pyridyl)ethylene.

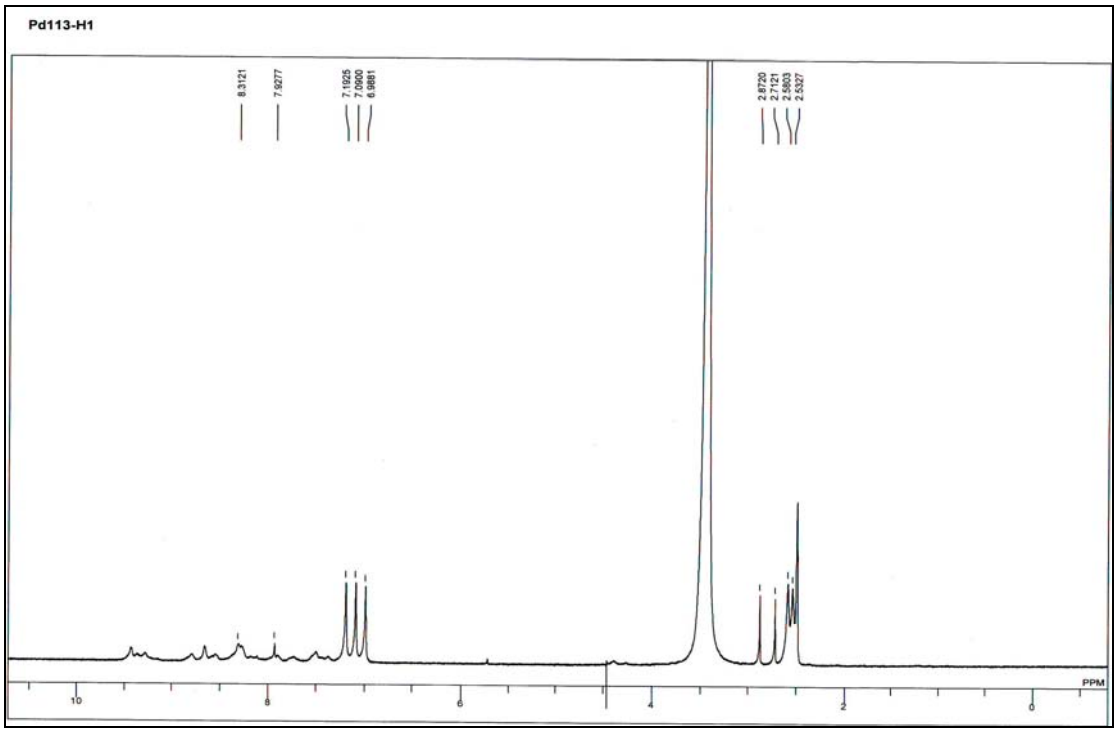

Figure AV-5. ^{1}H NMR spectrum of Pd113.

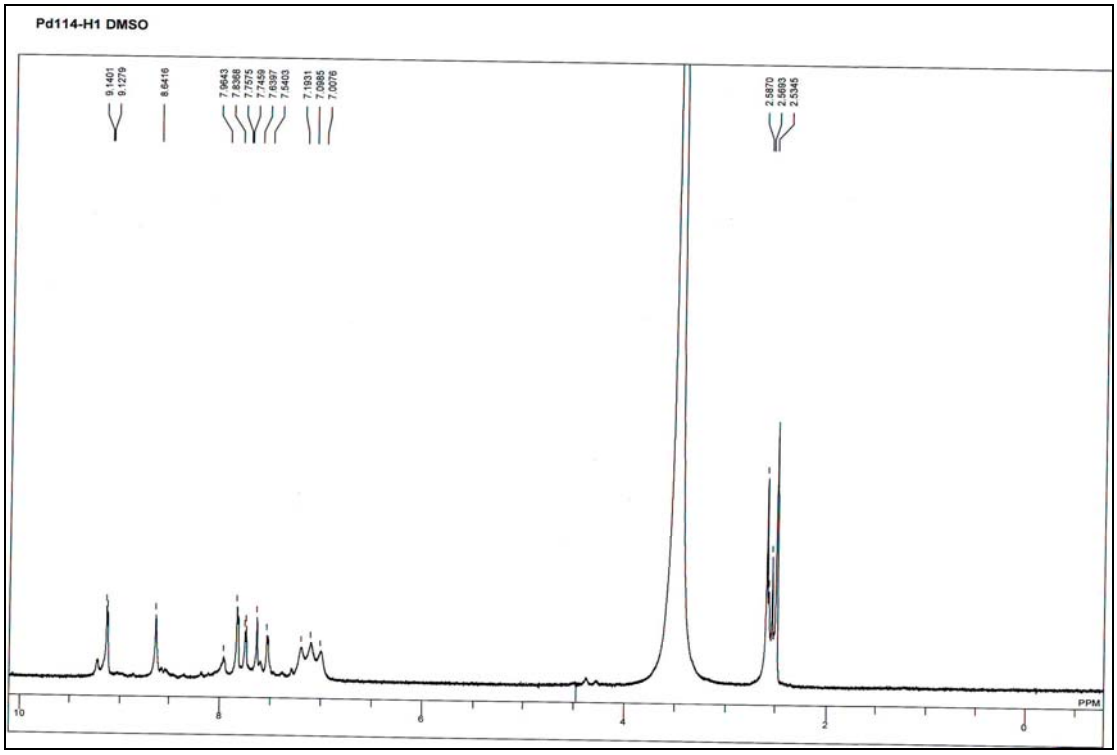

Figure AV-6. ^{1}H NMR spectrum of Pd114.

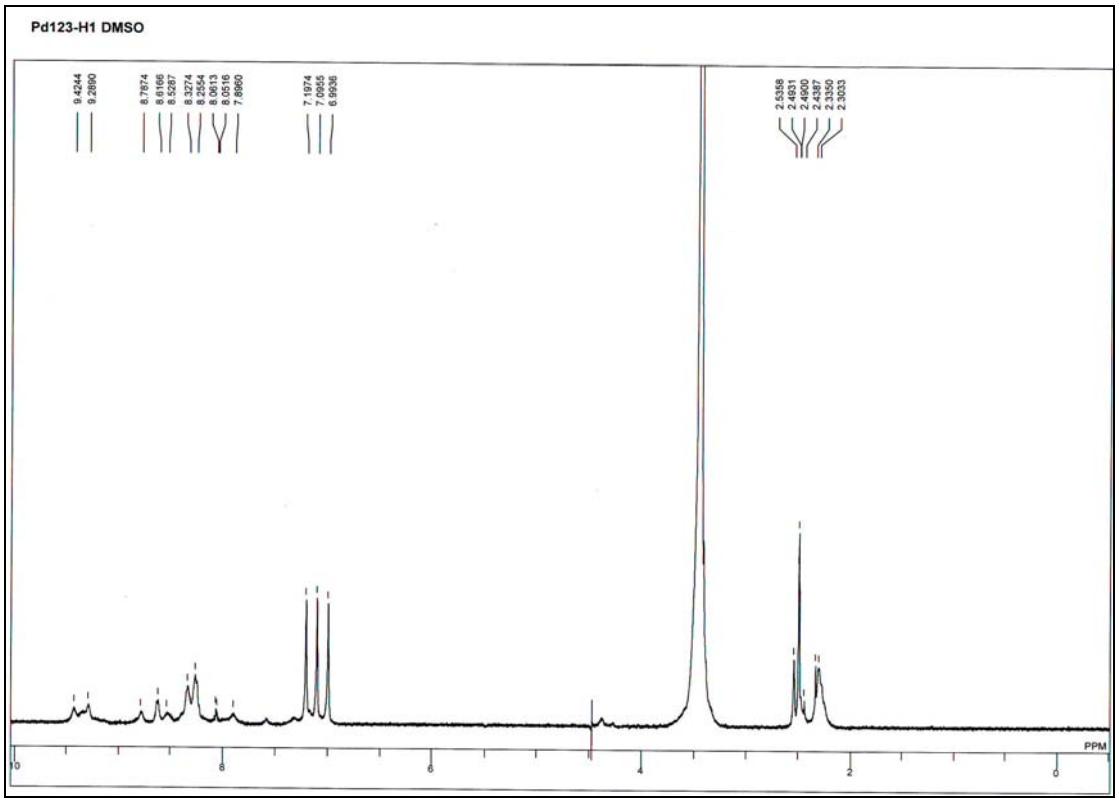

Figure AV-7. ^{1}H NMR spectrum of Pd123.

Abbreviations

ar aromatic

atm atmosphere

B branched

Binap 2,2’-bis(diphenylphosphino)-1,1’-binaphthyl

Binaphos (2-(diphenylphosphino)-1,1’-binaphthalene-2’-yl)-(1,1’-binaphthalene-2,2’-yl)phosphate

Br broad

Cat catalyst

COD 1,5-cyclooctadiene

d doublet

Dba dibenzylidene acetone

DIOP 2,3-*O*-Isopropylidene-2,3-dihydroxy-1,4-bis(diphenylphosphino)butane

DME dimethyl ether

Dppb 1,4-bis(diphenylphosphino)butane

Dppe 1,2-bis(diphenylphosphino)ethane

Dppf bis(diphenylphosphino)ferrocene

Dppp 1,3-bis(diphenylphosphino)propane

Dpppt 1,5- bis(diphenylphosphino)pentane

Dppm bis(diphenylphosphino)methane

DMA dimethyl acetamide

DMF dimethyl formamide

DMSO dimethyl sulfoxide

Et ethyl

Eq equation

FT Fourier transform

GC Gas chromatography

GC-MS Gas chromatography mass spectroscopy

h hour

i iso

Hz hertz, cycle per seconds

IR infrared

J coupling constant, in Hz

L linear

m multiplet

Me methyl

med medium

n normal

NMR nuclear magnetic resonance

OAc^- acetate ion

PBD Polybutadiene

Pd Palladium

Ph phenyl

PPh_3 triphenylphosphine

ppm part per million

psi pounds per square inch

q quartet

Rh Rhodium

r.t room temperature

s singlet

sh sharp

t triplet

T Trans

THF Tetrahydrofuran

TLC Thin Layer Chromatography

TMS tetramethylsilane

UV Ultraviolet

VIS Visible

δ chemical shift

Vita

- Rami Suleiman (*Jordanian*)
- Born in Syria in august 23th, 1977.
- Married with two children.
- Received B.Sc. in Chemistry from The University of Jordan, Amman in June 1999.
- Awarded M.S degree in Organic Chemistry from The University of Jordan in March 2002.
- Worked as QC analyst at RAM PHARMA Amman, Jordan from 2002-2005.
- Worked as Lecturer in the college of pharmacy at Al-Isra University Amman, Jordan from 2005-2006.
- Joined King Fahd University of Petroleum and Minerals in February 2006 as lecturer B and started Ph.D. program in Chemistry.
- Awarded Ph.D. degree in Organic Chemistry from KFUPM in March 2010.
- Participated in several funded research projects and short courses.
- A co-author in 5 publications in international journals.
- A co-author in 1 conference paper.
- Current address: KFUPM, Chemistry Department, Tel. (Work): +96638602187, Cell phone: +966561325537, Dhahran, 31261, Box 8112. E-mail: ramismob@kfupm.edu.sa.
- Permanent address: KFUPM, Chemistry Department, Tel. (Work): +96638602187, Cell phone: +966561325537, Dhahran, 31261, Box 8112. E-mail: ramisamarah@hotmail.com.